istituto nazionale di fisica nucleare
laboratori nazionali di frascati

2003 ANNUAL REPORT

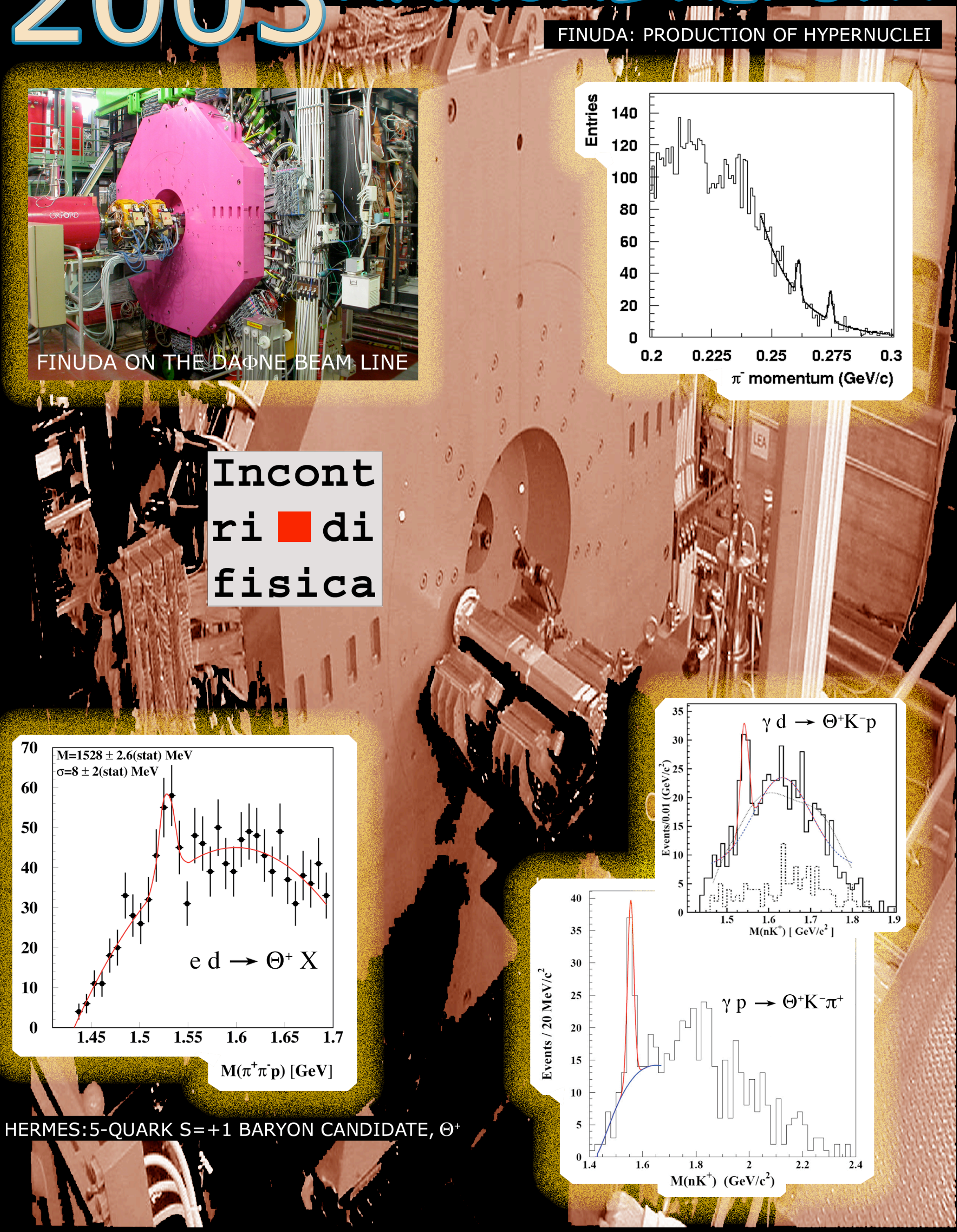

AIACE:5-QUARK S=+1 BARYON CANDIDATE, Θ⁺

Cover

The top left photo shows the FINUDA detector at the end of its installation on the DAΦNE beam line. The production of hypernuclei observed by FINUDA is reported in the top right graph (see the FINUDA report).
The bottom left plot shows the 5-quark baryon candidate signal published by the HERMES experiment (see the HERMES report). The two bottom right plots describe the 5-quark baryon candidate signals observed by AIACE in two different production reactions (see the AIACE report).

Background: *the FINUDA detector during its its roll-in at DAΦNE.*

Cover artwork by: Claudio Federici
Photos by: Roberto Baldini and Claudio Federici

istituto nazionale di fisica nucleare

laboratori nazionali di frascati

2003

ANNUAL REPORT

LNF-04/08 (IR)
April, 2004

Editor
Simone Dell'Agnello

Technical Editor
Luigina Invidia

Published by
SIS-Pubblicazioni
P.O.Box 13 – I–00044 Frascati (Italia)

Available at www.lnf.infn.it/rapatt

Sergio Bertolucci
LNF Director

Lucia Votano
Head, Research Division

Pantaleo Raimondi
Head, Accelerator Division

LNF Scientific Coordinators

Maria Curatolo
Particle Physics

Marco Ricci
Astroparticle Physics

Valeria Muccifora
Nuclear Physics

Calogero Natoli
Theory and Phenomenology

Francesco Celani
Techn. and Interdisciplinary Research

FOREWORD

Looking in retrospective to a year life of a Lab represents for any observer (directors included) a very stimulating exercise: the description of the present and future activities, the obtained results and even the delays in the programs contribute as a whole to the formation of a sort of global rating of the year, pretty much as for wine vintages.

Allowing for the uncontrollable factors (like the climate for the wines), it is also a valuable source of guidelines for the short and long term planning.

As it can be inferred by the report cover, last year highlights are in the field of nuclear physics: for the internal activities, the commissioning and the first physics run of the FINUDA experiment, which has come swiftly to operation and has immediately started to produce excellent results in the field of the hypernuclei; for the external activities, the discovery of a possible pentaquark state by the CLAS and HERMES experiments, where strong groups of LNF are active since long time.

Year 2003 has also seen a very important shutdown of DAΦNE, where major upgrades and fixes have been implemented, to cure long known problems, to increase operation flexibility with two magnetic detectors, to eventually continue the so far successful hunt for higher luminosities. Also the other projects of the Accelerator Division (SPARC, CTF3, CNAO) have progressed very satisfactorily and the Test Beam Facility (BTF) has hosted (with a very high grade of customers' satisfaction) a dense program of detector tests and even a small experiment (RAP).

KLOE and DEAR have largely profited of the pause of data taking, to concentrate on the analysis of the collected data and/or to study substantial upgrades.

The outward-bound programs have also progressed briskly, with ATLAS approaching the end of the construction of the MDT chambers and LHCb starting mass production, closely followed by the other big LNF commitment, OPERA, which has succeeded to stay on the installation trail, despite the difficulties which LNGS is presently experiencing.

The ultracryogenic detector NAUTILUS has resumed data taking, with the community eagerly awaiting for confirmation of the tantalizing 2001 results and PAMELA is progressing to the launch date.

For the first time, it is also nice to see an account of the excellent initiatives that LNF has staged in the past years in the field of the formation and outreach. The quality and the consistency along the years of these programs have greatly enhanced the lab visibility for the general public and have contributed to attract the young generations to fundamental research.

Finally, a special rank in the achievement list is held by the successful participation of LNF in the calls of the EU Sixth Framework Program "Structuring the European Research Area" (FP6).

In particular, the Integrated Infrastructure Initiative "Hadron Physics", representing more than 2000 researchers of 140 European Institutes, ranked first for Physics among all the Research Infrastructure projects.

This is a prestigious achievement for INFN and LNF, since the lab is coordinating the whole initiative, through the consummate skills and the relentless dedication of Carlo Guaraldo.

Many more activities, which have reached substantial results during 2003, are described in the report, conveying to the reader the image of a lively laboratory, involved in a number of good projects and able to keep the pace with them.

This being undoubtedly a source of pride, is by no means a reason to "lull on laurels": the lab has started to reason on its future, by staging a very participated workshop in Alghero on the future of DAΦNE and more in general by the creation of a strategy group, whose first written report is expected to be available by summer 2004.

Sergio Bertolucci
Director

ACKNOWLEDGMENTS

I would like to thank Luigina Invidia, for her hard work and her relentless effort to complete the project within the planned yearly deadline. Many thanks also to Claudio Federici, who created the cover page, for his graphics skills. I am also grateful to Sergio Bertolucci and Stefano Bianco for their many helpful suggestions and encouragments.

Finally, I want to thank the authors of the reports included in this book, for the interesting scientific contributions they gave to INFN.

Simone Dell'Agnello
Editor

Laboratori Nazionali di Frascati dell'INFN

2003 ANNUAL REPORT

CONTENTS

5 — Technological and Interdisciplinary Research

6 — Accelerator Physics

COMMUNICATION AND OUTREACH

R. Centioni, L. Sabatini, S. Vannucci (Resp.)
Office of Education and Public Relations
Scientific Information Service

The “Laboratori Nazionali di Frascati dell’INFN” (LNF) provide basic education in Physics for the general public, students and teachers. The LNF Educational and Public Relation programmes are made possible by the enthusiastic involvement of the laboratory graduate students, postdocs, researchers, engineers and technicians. This report describes the 2003 activity.

1 LNF guided tours, “Scientific Week” and “Open Day”

`http : //www.lnf.infn.it/edu/`

A well established laboratory tradition: 4000 people/year for general public, students and teachers.
Scientific coordinators: L. Benussi, P. Gianotti, G. Mazzitelli, C. Petrascu, B. Sciascia.
57 volounteers have received 147 groups. A typical visit consists of:

- history of the laboratory;
- presentation of INFN-LNF activities on site and abroad;
- visit to the “en plain air museum”;
- visit to experimental areas.

LNF Scientific Week and Open day: 2000 visitors.
Most of LNF employees are in action to present their research center, answer questions and care for their guests. Since 1990 this is organized as:

- guided tours;
- conferences and public lectures;
- scientific videos;
- exhibitions of students’ projects;
- Open Day.

2 Outreach: Scientific Itineraries

The aim is to offer a more complete view of the scientific institutions operating in the area and improve the communication with the general public. In collaboration with:

- CNR Tor Vergata;
- ENEA Frascati;
- ESA-ESRIN Frascati;

Figure 1: *LNF Tutors Luigi Benussi, Danilo Babusci, Mauro Iannarelli and Ennio Turri with summer stagists (photo by Roberto Baldini)*

- INAF Astronomical Observatory of Rome, Monte Porzio Catone;
- COPIT, Rome;
- Frascati Municipality;
- International non-government organizations;
- University of Rome Tor Vergata.

3 High school students' programme

`http://www.lnf.infn.it/edu/stagelnf/`

Scientific Coordinator: L. Votano.
Goal: enable students to acquire the knowledge and understanding of INFN research activities.

- Winter stages, 2-4 weeks: 8 students with 4 tutors;
- Spring stages, 2-4 weeks: 28 students with 13 tutors;
- Summer stages, 1 week: 20 students with 6 tutors;
- INFN research and university course orientation, 2-3 days: 375 students with 6 tutors.

Figure 2: *LNF Tutor Barbara Sciascia, working for the QUASAR project (photo by Claudio Federici).*

New Special Program for Primary School: QUASAR

`http://www.lnf.infn.it/edu/quasar/`

Care of F. Murtas and B. Sciascia.
Age: 8 - 14.
First meeting with the children at their school to introduce the world of research and some concepts of modern physics. Then, visit to the Frascati National Laboratories by small groups. Total of children and teachers in visit = 213.

4 High school teachers' programme

"Incontri di Fisica"

`http://www.lnf.infn.it/edu/incontri/`

Organizing Committee: S. Bertolucci, L. Votano (chair), D. Babusci, S. Bianco, L. E. Casano, R. Centioni, G. Isidori, S. Miozzi, L. Sabatini, S. Vannucci.

- Lectures and Experiments for high-school science teachers and scientific journalists.
- Goal: stimulate teachers' professional training and provide an occasion for interactive and hands-on contact with the latest developments in physics.

September 5 - 7, 2001; September 16 - 18, 2002; October 2 - 4, 2003.

Figure 3: *Scientific journalist Franco Foresta Martin during his talk at LNF (photo by Roberto Baldini).*

The participants in 2003 were: 150 teachers and scientific journalists; 60 LNF Tutors (researchers, engineers and technicians).

5 General public programme

Seminars

`http://www.lnf.infn.it/edu/seminaridivulgativi/seminari.html`

Upon request, LNF researchers give seminars to high school students and the general public on:

- INFN Activities and Elementary Particles;
- Modern Physics;
- Synchrotron Light;
- Gravitational waves.

Incontri con l'Autore
Scientific coordinators: D. Babusci and C. Petrascu.
To disseminate the scientific culture by inviting an author presenting his recent book.
Franco Foresta Martin, "Dall'Atomo al Cosmo", LNF April 2, 2003.

Figure 4: *Nobel Prize winner Prof. Rita Levi-Montalcini received by the Lab Director, Dr. Sergio Bertolucci (photo by Roberto Baldini).*

Events

1. Conference given by Nobel Prize winner Prof. Rita Levi Montalcini, Frascati April 1, 2003;
2. "Terzo Forum Ricerca Scientifica e Diffusione dell'Innovazione", Monte Porzio Catone April 5, 2003;
3. "La Ricerca come sviluppo del territorio", Prize for high school students, Frascati May 30, 2003;
4. "Scienza per Tutti", Premio Frascati Città della Scienza, Frascati October 30, 2003;
5. Christmas Concert, LNF December 18, 2003.

Conferences

International conferences, workshops and schools hosted and organized by the LNF:

1. I3HP Meeting, LNF 14-15 January, 2003;
2. "Advances in experimental and theoretical methods for biological applications", LNF Feb 27 - March 1, 2003;
3. I3HP Meeting, LNF March 31, 2003;
4. "Les Rencontres de Physique de la Vallée d'Aoste", La Thuile, ITALY, 9-15 March, 2003;
5. "International Conference on the Structure and Interactions of the Photon", LNF 7-11 April 2003
6. "Le Emergenze Radiologiche", LNF May 13, 2003;
7. LNF Spring School, LNF 19-23 May, 2003;
8. TESLA Collaboration Meeting, LNF 26 - 28 May, 2003;
9. "Frontier Science. A Non-Linear World: the Real World", Pavia, ITALY, 8-12 September, 2003;
10. "e^+e^- in the 1-2 GeV range: Physics and Accelerator Prospects", Alghero (SS),ITALY, 10-13 September, 2003;
11. "Nanotubes & Nanostructures", LNF 15 -19 September, 2003.

ATLAS

A. Antonelli, M. Antonelli, M. Barone, M. Beretta, S. Bertolucci, H. Bilokon, S. Braccini, E. Capitolo (Tecn.), F. Cerutti, V. Chiarella, M. Curatolo, B. Dulach, B. Esposito (Resp.), G. Felici, M.L. Ferrer, P. Laurelli, W. Liu, G. Maccarrone, A. Martini, W.Mei, G. Nicoletti, G. Pileggi (Tecn.), B. Ponzio (Tecn.), V. Russo (Tecn.), A. Sansoni, T. Vassilieva (Tecn.)

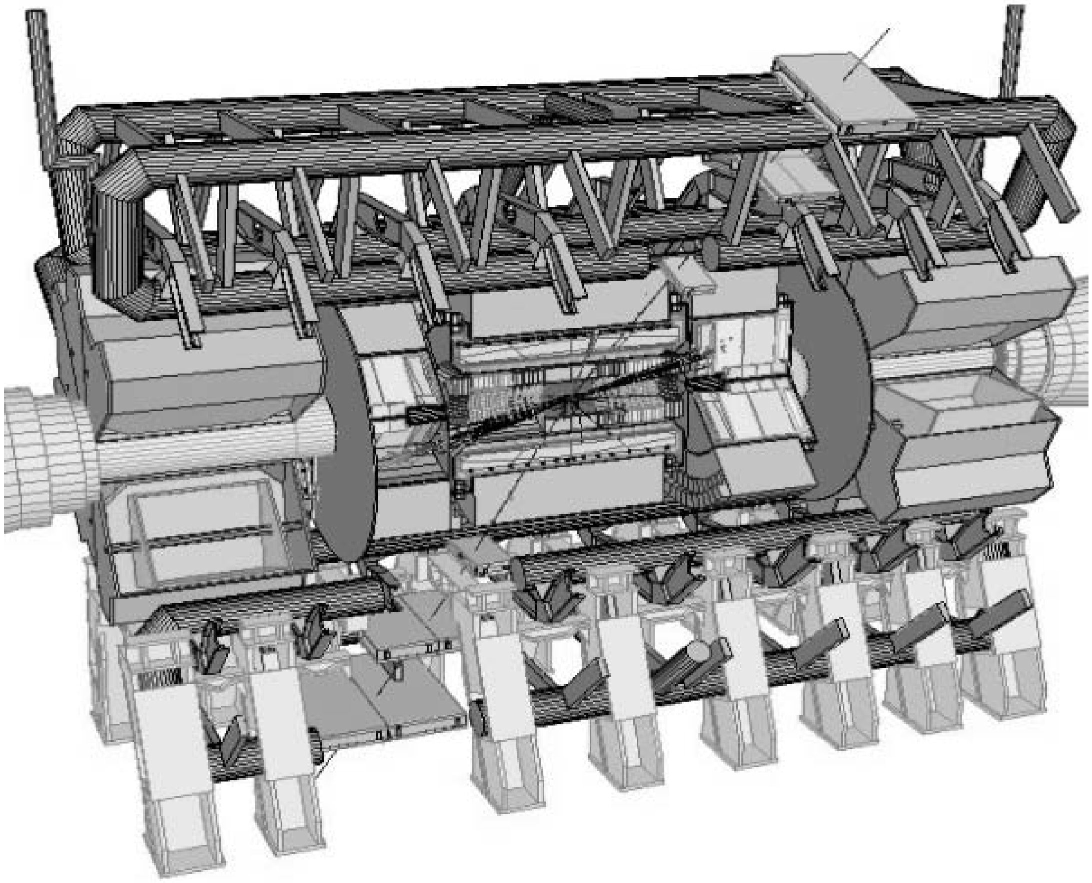

1 Introduction

ATLAS is one of the two general purpose experiments at the Large Hadron Collider (LHC) at CERN.

The detector is in a well advanced phase of construction in the many production sites spread all over the world.

The responsibility of the LNF group is the construction of all the muon precision tracking chambers of the middle stations in between the coils of the air toroidal magnet, that is 94 chambers of dimensions ranging from 1.2m x 3.6m to 1.7m x 3.6m.

The chambers, called MDT (Monitored Drift Tube) chambers, are made of an assembly of high pressure drift tubes, operated at 3 bars. Both the mechanical precision of the assembly and the individual tube intrinsic performances are very tight and have required research and developments to which the Frascati group has significantly contributed.

The mechanical precision of the chambers is checked with an X-ray tomograph at Cern and the verification of the performances is based on test beam and cosmic ray studies.

In this report the status of the production at LNF and the studies made by the LNF group are summarized.

The Frascati group has also been involved in the software work, namely in the Data Challenge-1 (DC1) event production and validation, in the studies of physics channels with simulated events, and in the DAQ software developments.

2 MDT chamber production in the year 2003

The chamber construction is a complex process which requires different phases:

a) tube wiring
b) tube quality assurance/quality control (QA/QC)
c) chamber assembling
d) installation of services on chambers
e) chamber QA/QC

The phases from a) to c) produce the so-called bare chambers.

The phases d), e) produce equipped chambers.

2.1 Bare chamber production

In the year 2003 the production of bare chambers (fig. 1) has advanced according to the schedule, actually even faster.

During the year 2003 the production of the chambers of the size 1680 mm, corresponding to 56 tubes/layer was completed. The assembly jig was modified to be adapted to the chamber size 960 mm, corresponding to 32 tubes/layer and 4 chambers were produced. Then the jig was modified again to adapt it to the production of chambers of size 1200 mm, corresponding to 40 tubes/layer and the production was resumed.

Although some time had to be spent to adapt the jig to different chamber size twice in the year, the chamber production went on very well, and the total number of chambers produced in the year 2003 is 34. At the end of 2003 87 chambers were built, that is more than 90% of the total. The wiring of the tubes and the relative QA/QC tests were following the chamber production rate, as needed, with about 8000 tubes fabricated in 2003, and a total of 27000 tubes since the start of the production.

2.2 X-ray tomograph measurement

The X-ray tomograph at Cern performs a scanning of the chambers with two X-ray beams and from the position of the absorption peaks provides a 2D measurement of the wire positions with a resolution of a few microns. The measured wire positions are compared to the nominal grid. The figures of merit are the rms values of the deviations from the grid, in the two coordinates perpendicular to the tube direction.

Four chambers produced at LNF in the year 2003 were measured at the X-ray tomograph, particularly to check the effect of the modifications to the jig, performed to adapt it to build different size chambers.

For all the measured chambers the rms values of the deviations of the wire positions were found to be well below the 20μm specification (fig. 2).

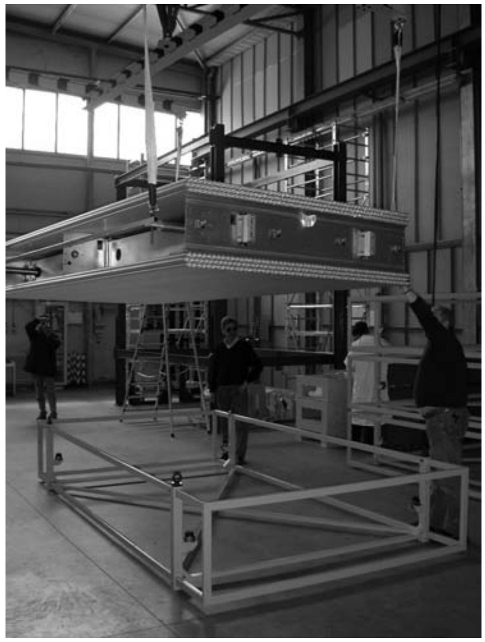

Figure 1: *A MDT chamber being inserted in the storage frame.*

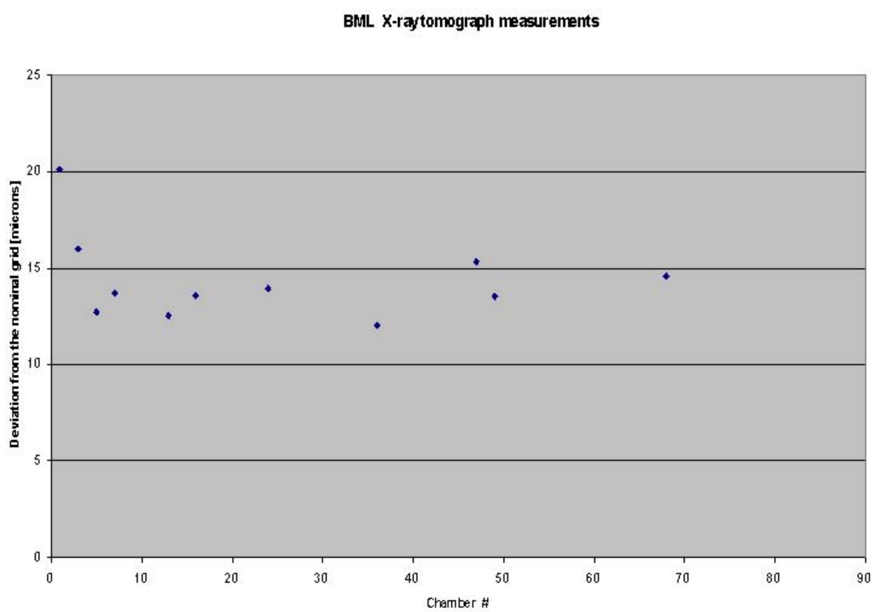

Figure 2: *The results of the Cern X-tomograph for all the measured BML chambers .*

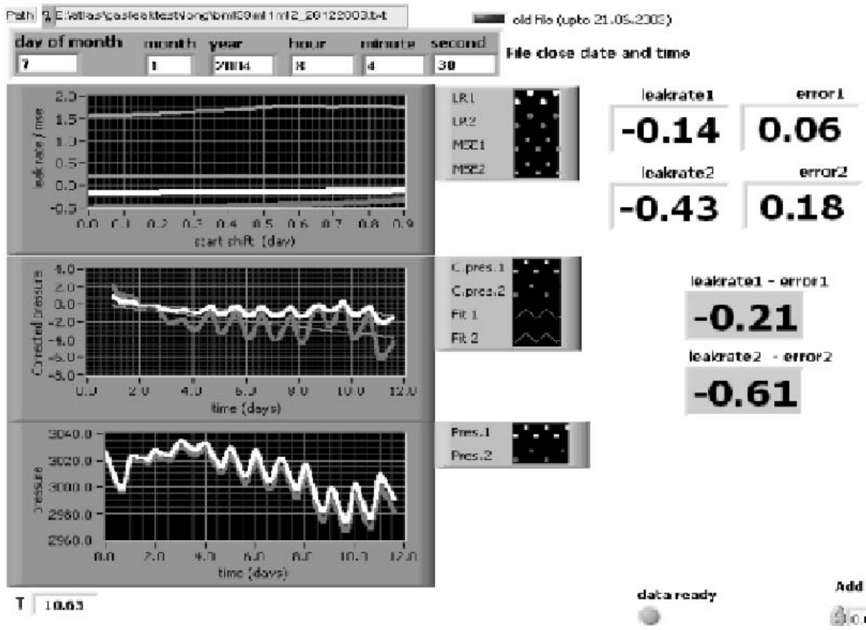

Figure 3: *A view of the monitor with the result of a measurement for the gas tightness certification of a chamber BML .*

2.3 Chamber equipment and QA/QC test

Once the bare chambers have been produced, they have to be equipped with the gas distribution system and then certified to be tight according to the Atlas specifications, that is 2 x 10^{-8}bar l/s per tube. Such a high level of tightness corresponds to less than 1 mbar/day pressure drop, with the chamber operated at 3 bars. In order to comply with this specification, great care is needed in the assembly of the gas components as well as the use of a very sensitive leak detector instrumentation, as the spectrometer leak detector to search for leaks over all the connection points. Once no leaks are found, the chamber is finally certified by the measurement of the pressure drop over a period of 2 days. The temperature is monitored and its effect is carefully corrected in the data. A typical measurement is shown in fig. 3. The slope with time of the pressure, corrected for temperature changes, is estimated.

The work of installation of the gas system could only take place after July 2003 because of the late availability of the stainless steel tubelets which were needed to replace the brass tubelets initially chosen, which were demonstrated to develop cracks with time.

In the period from July to end 2003, 36 chambers were equipped, tested and certified to be within the Atlas specifications. The results of the measurements are shown in fig. 4.

2.4 MDT and RPC integration

The Resistive Plate Chambers (RPC) are used in the Atlas muon spectrometer for triggering and for the determination of the second coordinate. They are to be coupled to the MDT chamber in a MDT+RPC station, and such a station is mounted as a whole on the apparatus.

The MDT chambers built by the Frascati group are to be sandwiched between two RPC chambers, forming a MDT+RPC station (fig. 5).

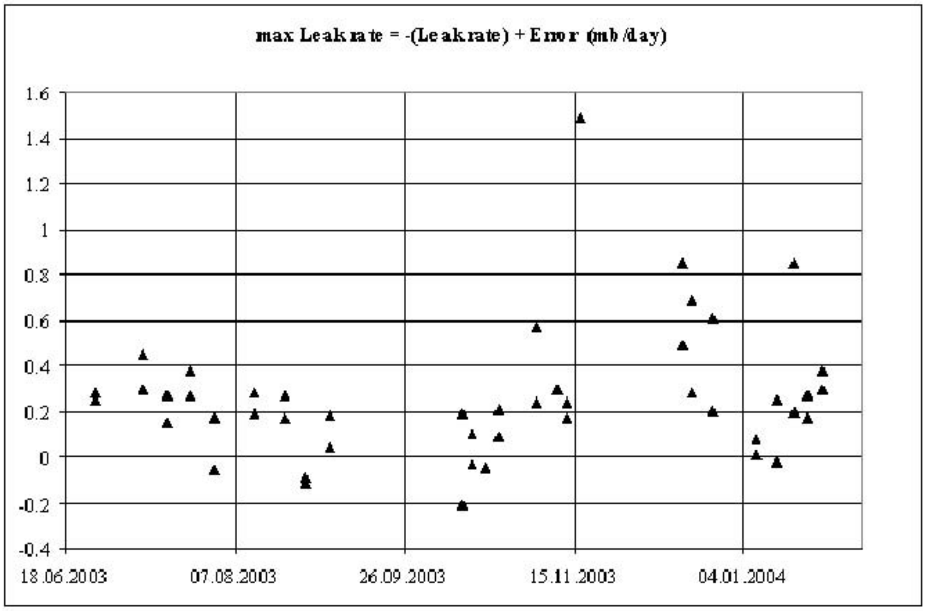

Figure 4: *The results of the measurements of all the certified BML chambers.*

Figure 5: *A MDT chamber being assembled with the RPC trigger chambers.*

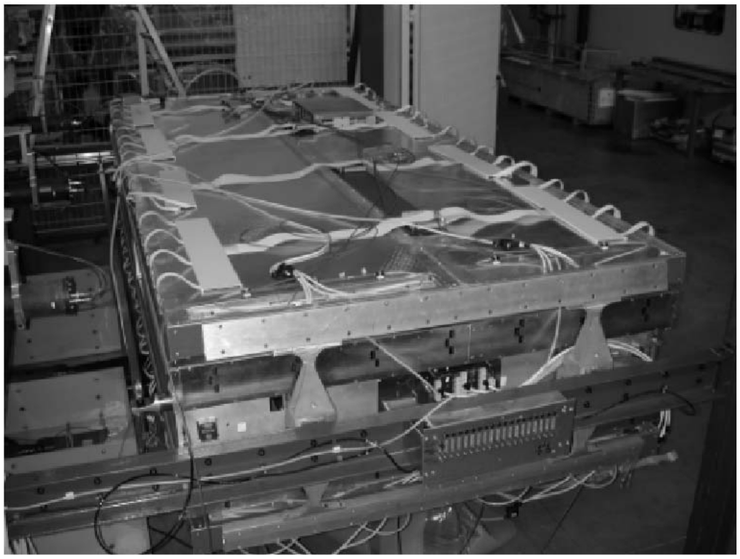

Figure 6: *The MDT+RPC station used for RPC cabling studies.*

The mechanical supports to hold together the MDT and RPC chambers, have been designed by Frascati, in contact with the Lecce RPC group. Prototypes of the common supports have been realized and used to assemble two stations at Cern, which have been part of the muon spectrometer sector tested on the H8 beam at Cern. After the test, the full production of the supports by Al casting has been made.

A very delicate aspect is the one of the integration of the services on MDT and RPC, and possible interferences, not just from the mechanical point of view, but also from the electromagnetic point of view. First studies of the RPC cabling have been made by the RPC groups in Frascati and the effect on the noise induced on the MDT have been studied in the test setup at Frascati A photograph of a MDT+RPC station used for RPC cabling studies at LNF is shown in fig. 6.

2.5 Detector studies with cosmic rays and beam tests

Detector performance studies and system tests are done with beam tests at Cern and with cosmic ray stations in the various construction sites. The Frascati group has been actively involved in both lines of activities.

At LNF a cosmic ray stand has been built (fig. 7) to test the produced MDT chambers. Due to the unavailability of F.E. electronics in the period of the chamber construction, as a matter of fact it has not been possible to perform systematic tests of all the produced chambers. Now this test is foreseen to take place at Cern, once the MDT are assembled with the RPC chambers.

The cosmic ray stand has allowed, with the test of a limited number of chambers, to study the chamber performances following the work done with the beam tests with further studies on specific aspects. The cosmic ray stand has also allowed to install and test the online software being developed for the Atlas DAQ. In particular, in the year 2003, the effect of the serial gas distribution on the tube response, which was seen in the results of the beam tests performed in the year 2002, was carefully studied and found to be negligible (fig. 8).

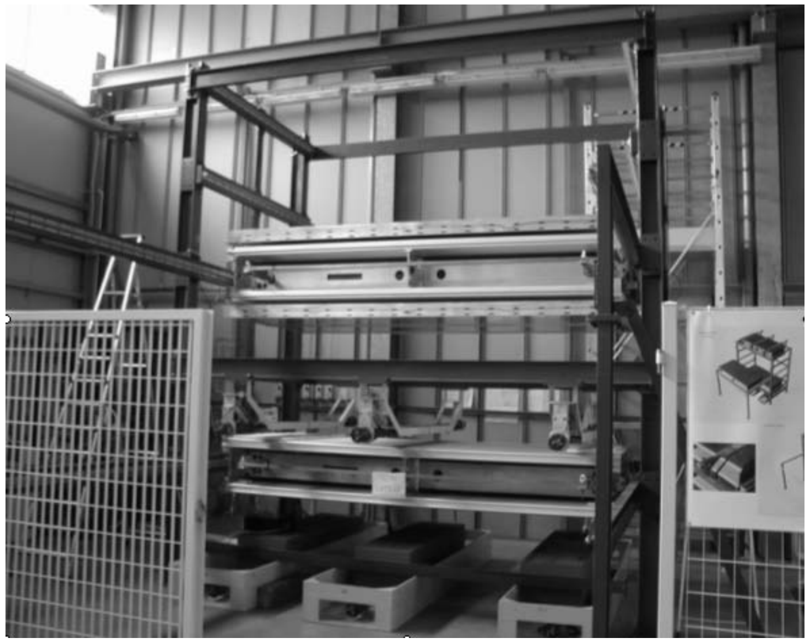

Figure 7: *A view of the cosmic ray stand used for BML chamber performance studies at LNF.*

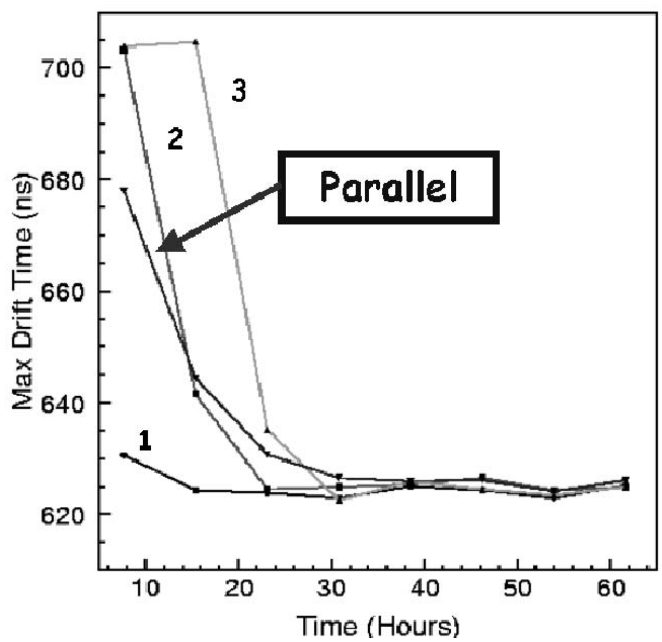

Figure 8: *The evolution of the tube drift times for the 'serial' gas system .*

For the 2003 beam test the Frascati group has provided two BML chambers assembled with RPC and has taken care of their installation on the beam and their setting-up. The overall coordination of the test beam activity has been responsibility of a member of the Frascati group, and there has been a very active participation in the data analysis. In particular the issue of the stability and uniformity of the MDT chamber response was the object of a careful study, based on data taken over one month period in stable conditions (fig. 9).

The Frascati group has performed the data analysis, has investigated with quantitative estimations the causes of possible gas contaminations, has evaluated the effects on the chamber resolutions. The results are satisfactory for the MDT performances [1].

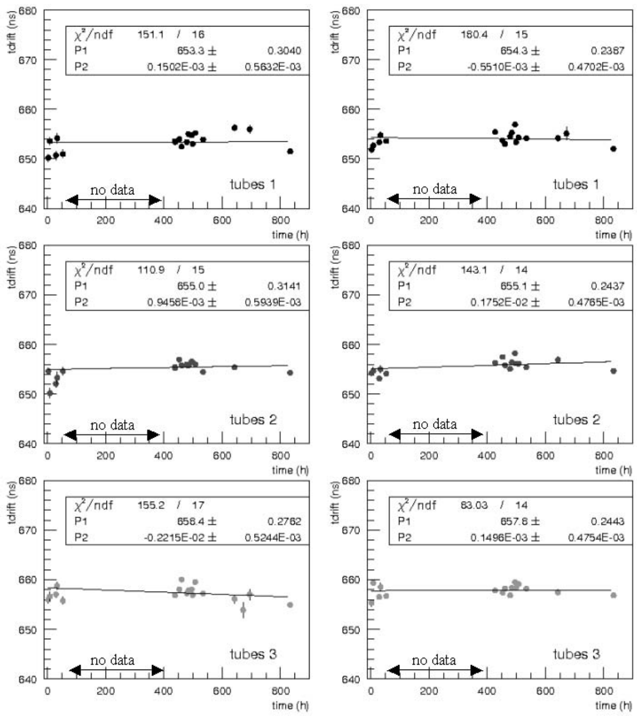

Figure 9: *Study of the MDT chamber performance stability with 2003 test beam data: drift time versus data taking period for two multilayers of the BML chamber.*

2.6 DAQ activity

The activity in the data acquisition field has been devoted to the following items: a) design and implementation of a monitor system that allows the distribution of built events to the monitoring tasks asking for un-filtering the complete events during the run; b) collaboration with the 2003 test beam team, mainly during the first phase dedicated to software installation and test.

In order to align the present cosmic ray test stand in Frascati with the official software/hardware versions that will be used in the test beam 2004 at CERN, the required hardware has been ordered. The final installation is programmed for March 2004.

2.7 MC event production and physics simulation studies

The activity in this field has consisted in the study of discovery decay channels and in the participation in the event production DC1. In particular, studies have been performed on the detection of Higgs to 4 muons, applying a neural network analysis in addition to a simple cut-based analysis, in order to find the optimal selection criteria (fig. 10).

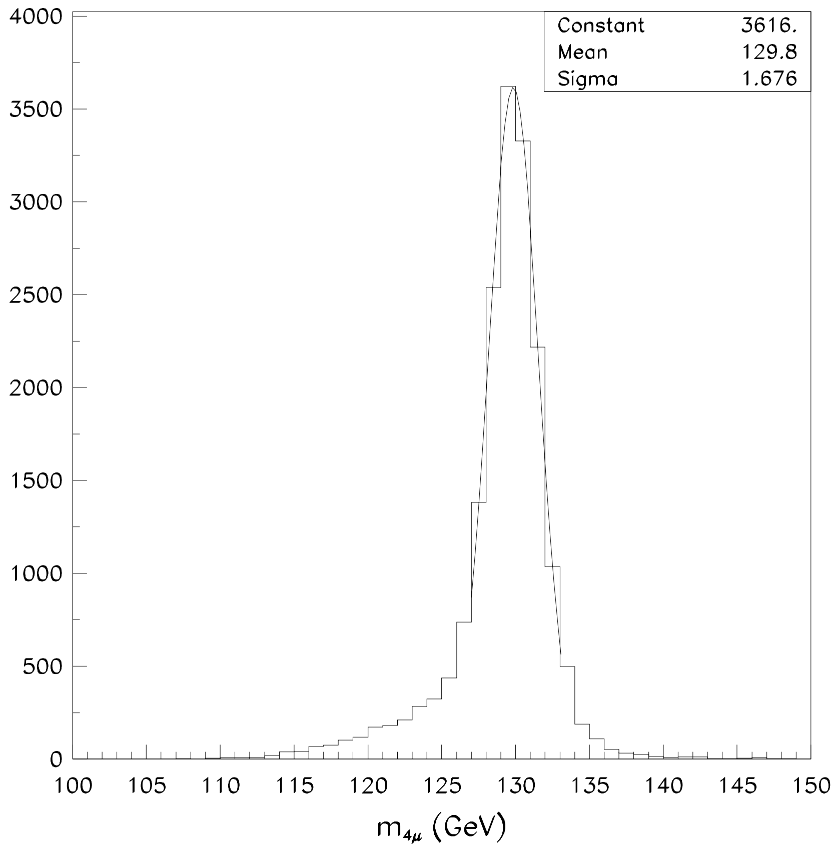

Figure 10: *Higgs mass resolution for the reaction $H \to \mu^+\mu^-\mu^+\mu^-$ in the low mass region.*

The overall coordination of the Higgs working group has also been responsibility of a Frascati group member.

In the framework of the Atlas DC1, the production and validation of B-physics events and also the production of pile-up events has been made.

A new activity was started in the field of computing resources dedicated to the ATLAS Data Challenge programs and local data analysis. The installation in Frascati of a TIER 2 was accepted and financed by INFN during 2003.

3 Program for the year 2004

In the year 2004 the chamber production will be completed and the chamber commissioning at Cern will start.

The PC farm, funded by INFN in view of the realization of an Atlas TIER2 at LNF, will be installed and will be used for the participation to the Atlas Data Challenge-2.

The work on the on-line and off-line software will continue, as well as the detector and system tests on the H8 muon test beam at Cern.

References

1. M. Antonelli *et al*, ATL-COM-MUON-2003-035, December 2003.

BaBar

F. Anulli(Ass.), R. Baldini Ferroli, A. Calcaterra, L. Daniello(Tecn.), R. de Sangro
G. Finocchiaro, P. Patteri, I. Peruzzi(Resp.), M. Piccolo, A. Zallo

1 Introduction

BaBar (in fig. 1) is the experiment running at the SLAC asymmetric B-factory PEP-II; the physics program is centered on, but not limited to, the study of the CP violation effects in the decay of neutral B mesons. The B system is the best suited to study CP violation because the expected effects are large, should appear in many final states and, most importantly, can be directly related to the Standard Model parameters. The large data sample now being collected has already allowed significant advances in a large number of topics in B, charm and top quark physics.

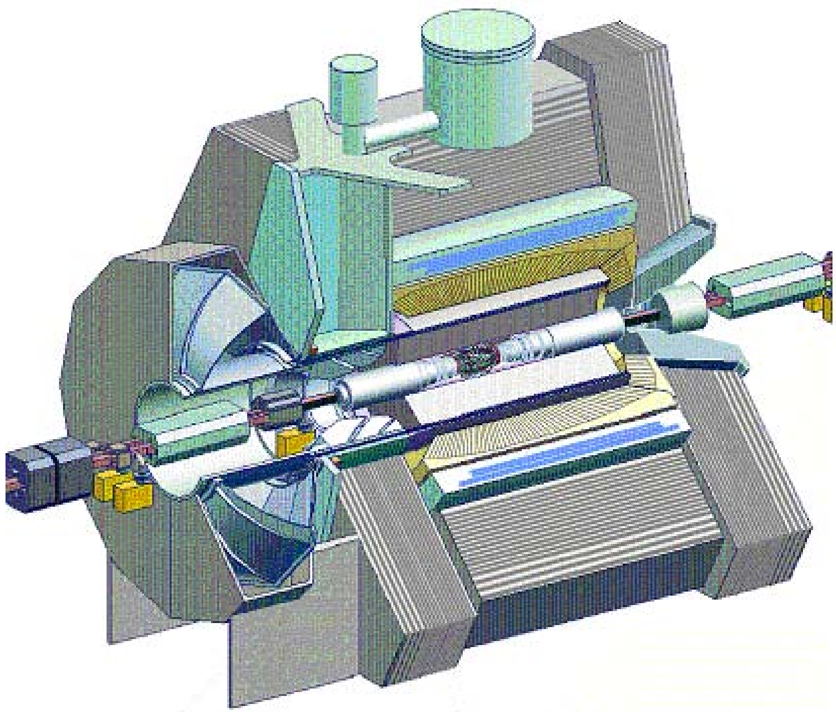

Figure 1: The BaBar Detector.

PEP-II is a two-ring e^+e^- storage ring, colliding 9 GeV electrons with 3.1 GeV positrons, energies chosen to maximize the production of B mesons. The c.m. energy corresponds to the mass of the $\Upsilon(4S)$ resonance which decays 50% to B^+B^-, 50% to $B^0\ \overline{B}^0$. The energy asymmetry is necessary in order to boost the B meson momentum, so that the decay length can be measured with the accuracy needed to prove the CP violation effects.

The BaBar Collaboration includes about 560 physicists, with contributions from about 80 Institutions in 10 countries in North America, Europe, and Asia. Approximately half of the group are physicists from U.S. Universities and Laboratories, with the largest foreign contribution coming from Italy, with 12 INFN Institutions and more than 90 people.

The BaBar detector has been designed primarily for CP studies, but it is also serving well for the other physics objectives of the experiment. The asymmetry of the beam energies is reflected in the detector design: the apparatus is centered 37 cm ahead of the collision point, along the direction of the high-energy beam, to increase forward acceptance. All services are placed on the opposite side of the detector, in order to minimize multiple scattering in the forward direction.

The momentum of the charged tracks is obtained from the curvature in a solenoidal field of 1.5 T and is measured in a low mass Drift Chamber. Different species of hadrons are identified in the DIRC, a dedicated device of a novel kind, based on the detection of Čerenkov light. Excellent photon detection and electron identification is provided by a CsI crystal e.m. calorimeter.

Muons and neutral hadrons are identified in the iron magnet's yoke, where a total thickness of 65 cm of Fe plates has been segmented in 18 slabs of graded thickness (from 2 to 10 cm) and instrumented with Resistive Plate Counters. This system, made of a 6-sided barrel, 2 endcaps and a double cylindrical layer inside the magnet coil, is called Instrumented Flux Return, or IFR. The final ingredient in the CP asymmetry measurements, the distance between the two decay vertices, is measured by a state of the art vertex detector, with five layers of double sided silicon strips.

2 Activity

During the year 2003 additional 60 fb^{-1} have been delivered by PEP-II (see fig. 2), bringing the total data sample recorded by BaBar to 160 fb^{-1}. Data taking was suspended for a 2-month period during the Summer for detector maintenance. In May PEP-II luminosity reached

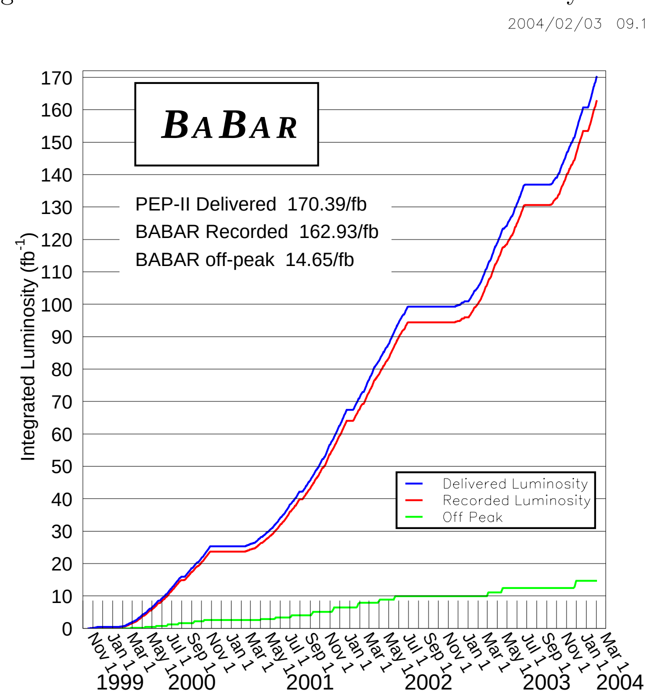

Figure 2: The BaBar Detector.

$6.5 \times 10^{33}\ cm^{-2}\ s^{-1}$, a factor of 2 above the design value, and by the end of the year 2003 the attempts to run the machine in continuous-injection mode for the Low Energy Ring (the positron ring) have been successful, so that a daily integrated luminosity of $\sim 400\ pb^{-1}$ has been achieved.

Among the most important results published by BaBar in 2003 is the discovery of a new narrow ($\leq$ 10 MeV/c^2, consistent with experimental resolution) meson decaying to $D_s^{\pm}\pi^0$ at a mass of 2.32 GeV/c^2. Other results include the measurements of CP-violation in channels other than the "golden mode" $J/\psi K^0$, the measurement of the B^0 decay to $\pi^0\pi^0$ and the measurements of B decays into rare decay channels like $K^{(*)}\ell^+\ell^-$. In the next sections the items of analysis in which the Frascati group is more directly involved are shortly described.

3 Measurement of sin(2β) with partial reconstruction of B mesons to the $D^{*+}D^{*-}$ final state

In 2003 the Monte Carlo optimization of the event selection and background characterization started last year has been completed, and a first look at the data from RUN 1 and 2 was taken.

The work has then progressed in two other main areas: 1- the definition of a fitting procedure for the simultaneous determination of the various background fractions and sin(2β); 2- the construction of a Fisher discriminant to reduce the background from continuum (uds and $c\bar{c}$) events. The contributions of charged and neutral B backgrounds and continuum can be extracted from the recoil mass and Fisher distributions, while sin(2β) is extracted from the time difference distribution between the CP-side and tag-side vertices.

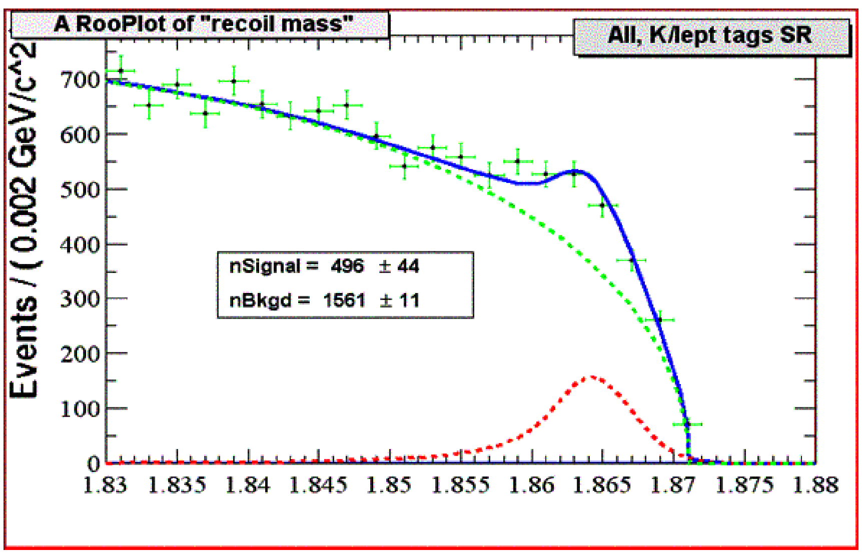

Figure 3: Missing mass for $B \to D^{*\pm}\pi^{\mp}(X)$.

In fig. 3 we show the recoil mass distribution of real data from RUN 1 and 2 (solid histogram), $\approx$ 80 fb^{-1} of integrated luminosity. The presence of an excess of events in the signal region is evident, and a very preliminary fit to the data with a probability distribution function (blue curve) made of a signal component (red) plus a background component (green) has shown that the statistical power of this measurement is somewhat higher than that of the analysis made with the fully reconstructed sample. This is a very encouraging result, as the two measurements of sin(2β) can be regarded as almost independent of each other.

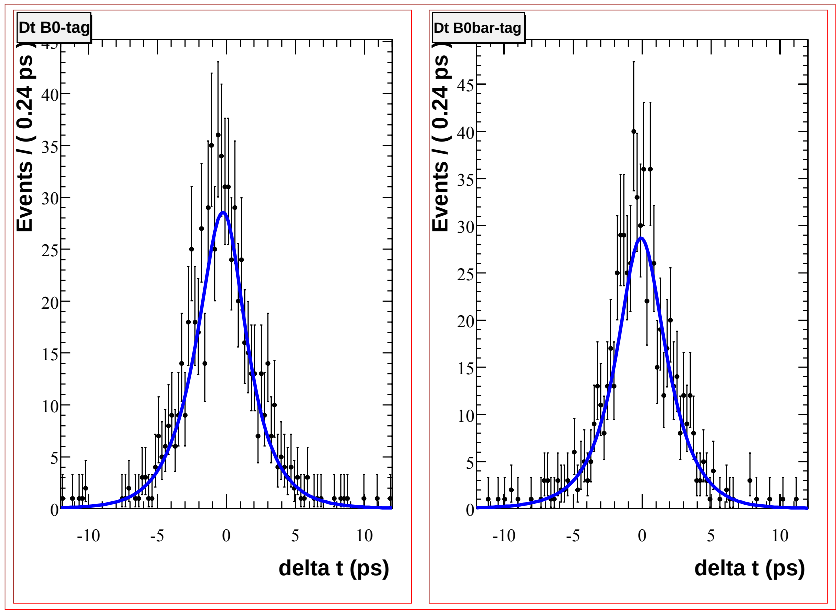

Figure 4: Δt fit to Monte Carlo signal data.

We did not attempt to fit the time distribution in the data, but in fig. 4 we show a fit to the time difference distribution of $\approx$ 1400 signal Monte Carlo events without background, corresponding to $\approx 113\ fb^{-1}$ luminosity (this is equivalent to RUN1, 2 and 3). The fit returns the generated values for $\sin(2\beta)$ with an error of $\delta(\sin(2\beta))\approx 0.25$, which can be compared to the ≈ 0.07 from the "golden modes" average and ≈ 0.43 of the exclusive measurement.

4 Measurement of the $B^0 \to D_s^{*+} D^{*-}$ and $D_s^+ \to \phi\pi^+$ branching fractions with partial reconstruction of B mesons to the $D_s^{*+} D^{*-}$ final state

The $B^0 \to D^{*+} D_s^{*-} \to D^0 \pi^+ D_s^- \gamma$ process is studied with a partial reconstruction technique, combining a completely reconstructed D^* meson with a soft photon. A preliminary analysis based on $20 fb^{-1}$ of data was presented as a contribution to the XXIst International Symposium on Lepton and Photon Interactions at High Energies [1]. The analysis has then been updated to include $80 fb^{-1}$ worth of data. Distributions of the recoil mass separately for different data taking periods are shown in figure 5 and 6. This analysis improves by a factor three on the previous most precise measurement of the $B^0 \to D^{*+} D_s^{*-}$ branching fraction. We are at present in the process of writing the final paper, which will be submitted for publication before Spring 2004.

In the same paper, we also present an analysis with full reconstruction of the D_s^+ in the $D_s^+ \to \phi\pi^+$ mode. Combining the results from these analyses allows us to measure the $D_s^+ \to \phi\pi^+$ branching fraction, improving on the existing result by about a factor two.

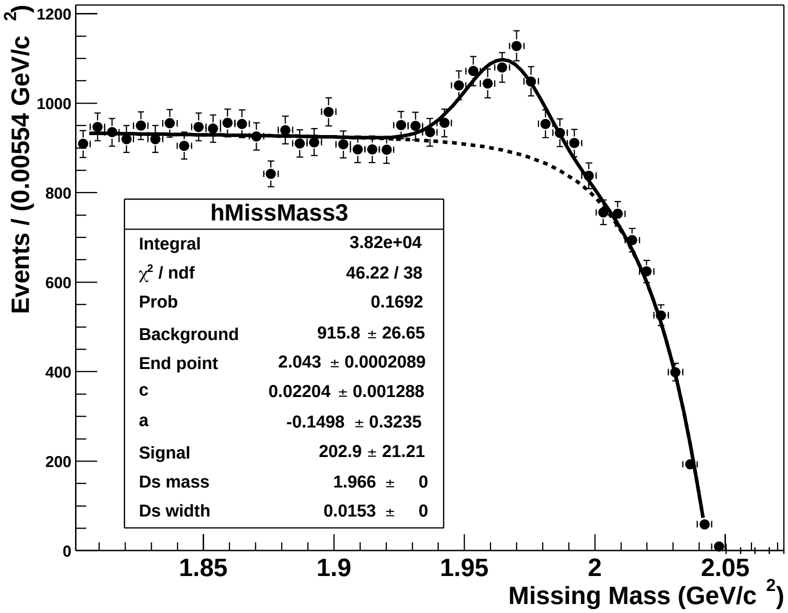

Figure 5: Missing mass of $D^*D_s^*$ candidates in different data samples (2000 data).

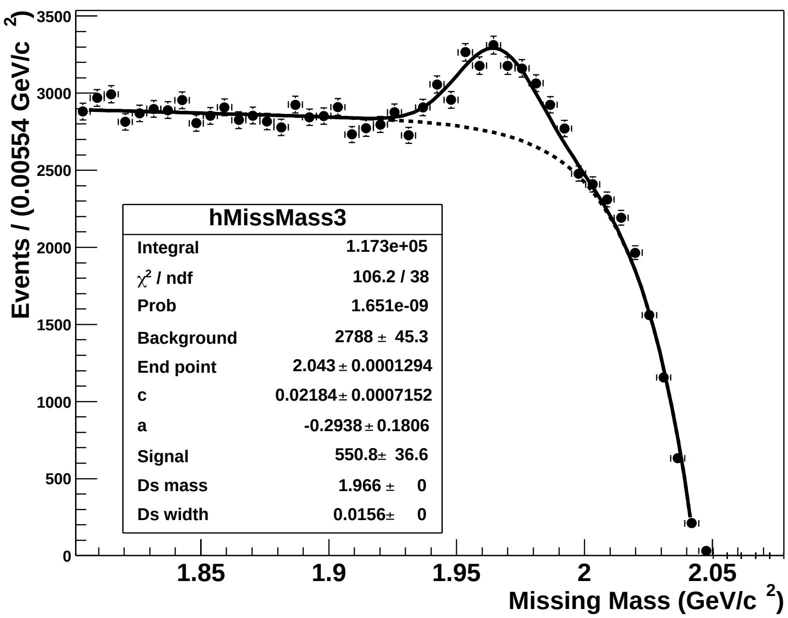

Figure 6: Missing mass of $D^*D_s^*$ candidates in different data samples (2001-02 data).

5 Analytic continuation of the transition form factor $\phi\eta$

A general procedure was determined, to establish a link between the amplitudes for the processes $\phi \to M\gamma$ and $\phi \to Me^+e^-$, (where M is a generic light meson) measurable at DAΦNE-Frascati and VEPP-2M-Novosibirsk to the measurement of the cross section for the process $e^+e^- \to \phi M$, measurable at BaBar using initial state radiation events.

In this work, the cross section for $e^+e^- \to \phi\eta$ measured by the LNF group [2] was used to extract the modulus of the transition form factor (TFF) $F_{\phi\eta}(q^2)$, an analytic function in the complex plane of q^2 (4-momentum of the virtual photon) featuring a cut on the real axis from $q^2 = (2M_K)^2$ to ∞. From the cross section one can extract $|F_{\phi\eta}(q^2)|$, where $q^2 \geq (M_\phi + M_\eta)^2$. As can be seen in fig.7, the data show a remarkable growth in proximity of the physical threshold $q^2 = (M_\phi + M_\eta)^2$.

The other data in the physical region are obtained from the radiative decay $\phi \to \eta\gamma$ for the point at $q^2 = 0$ (red square [5]), and from the decay $\phi \to \eta e^+e^-$ for the data in $[(2m_e)^2, (M_\phi - M_\eta)^2]$ (empty squares). In the unphysical region $[(M_\phi - M_\eta)^2, (M_\phi + M_\eta)^2]$ the TFF cannot be measured, but the analiticity of the function $F_{\phi\eta}(q^2)$ allows the low energy points to be connected to the high energy measurements, using logarithmic dispersion relations. The procedure [3] searches for a very general function that has the correct behavior for $q^2 \to \infty$, correctly represents the data both above and below the unphysical region, and describes the ϕ resonance. Once the TFF modulus is achieved on both, physical and unphysical region, the phase is obtained by means of the same dispersion relation. The Argand plot supports the existence of a resonance near the $\phi\eta$ threshold.

In Fig.7 the plot of this function shows how the growth of the data right after the unphysical region may be taken as a hint of a possible wide resonance, slightly below threshold, with $M = (1600 \pm 60)\ MeV/c^2$ and $\Gamma = (140 \pm 70)\ MeV/c^2$.

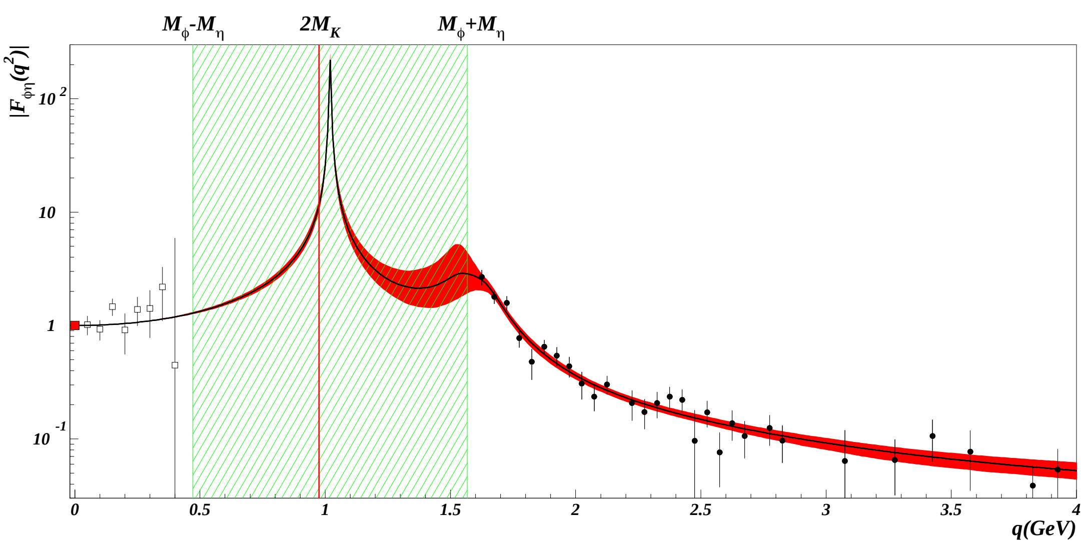

Figure 7: Data and TFF fit with BaBar (black dots) and VEPP-2M [4] data (empty squares). The red line is the threshold $q^2 = (2M_K^2)$. The black line is the calculation, with its error band in red.

6 BaBar publications in 2003

- B. Aubert *et al.*, “Measurement of the Branching Fraction for Inclusive Semileptonic B Meson Decay” Phys. Rev. D **67**, 031101 (2003).
- B. Aubert *et al.*, “Study of Inclusive Production of Charmonium Mesons in B Decay” Phys. Rev. D **67**, 032002 (2003).
- B. Aubert *et al.*, “Measurement of the B^0 Meson Lifetime with Partial Reconstruction of $B^0 \to D^{*-}\pi^+$ and $D^{*-}\rho^+$ Decays” Phys. Rev. D **67**, 091101 (2003).
- B. Aubert *et al.*, “Simultaneous Measurement of the B^0 Meson Lifetime and Mixing Frequency with $B^0 \to D^{*-}\ell^+\nu_\ell$ Decays” Phys. Rev. D **67**, 072002 (2003).
- B. Aubert *et al.*, “Measurement of $B^0 \to D_s^{(*)+}D^{*-}$ branching fractions and $B^0 \to D_s^{*+}D^{*-}$ polarization with a partial reconstruction technique” Phys. Rev. D **67**, 092003 (2003).
- B. Aubert *et al.*, “Measurement of the branching fractions for the exclusive decays of B^0 and B^+ to $\bar{D}^{(*)}D^{(*)}K$” Phys. Rev. D **68**, 092001 (2003).
- B. Aubert *et al.*, “Measurement of the $B^0 \to J/\psi\pi^+\pi^-$ Branching Fraction” Phys. Rev. Lett. **90**, 091801 (2003)
- B. Aubert *et al.*, “Study of the Rare Decays $B^0 \to D_s^{(*)+}\pi^-$ and $D_s^{(*)-}K^+$” Phys. Rev. Lett. **90**, 181803 (2003)
- B. Aubert *et al.*, “Measurement of the Cabbibo-Kobayashi-Maskawa Matrix Element $|V_{ub}|$ with $B \to \rho e\nu$ Decays” Phys. Rev. Lett. **90**, 181801 (2003)
- B. Aubert *et al.*, “Measurement of the Branching Fraction, and Bounds on the CP-violating Asymmetries in neutral B Decays to $D^{*\pm}D^{\mp}$” Phys. Rev. Lett. **90**, 221801 (2003)
- B. Aubert *et al.*, “Evidence for $B^+ \to J/\psi p\bar{\Lambda}$ and Search for $B^0 \to J/\psi p\bar{p}$” Phys. Rev. Lett. **90**, 231801 (2003)
- B. Aubert *et al.*, “Observation of a Narrow Meson State Decaying to $D_s^+\pi^0$ at a Mass of 2.32 GeV/c^2” Phys. Rev. Lett. **90**, 242001 (2003)
- B. Aubert *et al.*, “Observation of the Decay $B^\pm \to \pi^\pm\pi^0$, Study of $B^\pm \to K^\pm\pi^0$ and Search for $B^0 \to \pi^0\pi^0$” Phys. Rev. Lett. **91**, 021801 (2003)
- B. Aubert *et al.*, “Study of Time-Dependent CP Asymmetry in Neutral B Decays to $J\psi\pi^0$” Phys. Rev. Lett. **91**, 061802 (2003)
- B. Aubert *et al.*, “Measurements of the Branching Fractions and Bounds on the Charge Asymmetries of Charmless Three-Body Charged B Decays” Phys. Rev. Lett. **91**, 051801 (2003)
- B. Aubert *et al.*, “Rare B Decays into States Containing a J/ψMeson and a Meson with $s\bar{s}$ Quark Content” Phys. Rev. Lett. **91**, 071801 (2003)
- B. Aubert *et al.*, “Measurements of CP-Violating Asymmetries and Branching Fractions in B Meson Decays to $\eta\prime K$” Phys. Rev. Lett. **91**, 161801 (2003)
- B. Aubert *et al.*, “Search for $D^0 - \bar{D}^0$ mixing and a measurement of the Doubly Cabbibo-Suppressed Decay Rate in $D^0 \to K\pi$ Decays” Phys. Rev. Lett. **91**, 171801 (2003)

- B. Aubert *et al.*, "Limits on $D^0 - \bar{D}^0$ Mixing and CP-Violation from the Ratio of Lifetimes for Decay to $K^-\pi^+$, K^-K^+, and $\pi^-\pi^+$" Phys. Rev. Lett. **91**, 121801 (2003)
- B. Aubert *et al.*, "Measurements of Branching Fractions and CP-Violating Asymmetries in $B^0 \to \rho^\pm h^\mp$ Decays" Phys. Rev. Lett. **91**, 201802 (2003)
- B. Aubert *et al.*, "Measurement of Time-Dependent CP Asymmetries and the CP-Odd Fraction in the Decay $B^0 \to D^{*+}D^{*-}$" Phys. Rev. Lett. **91**, 131801 (2003)
- B. Aubert *et al.*, "Rates, Polarizations, and Asymmetries in Charmless Vector-Vector B Meson Decays" Phys. Rev. Lett. **91**, 171802 (2003)
- B. Aubert *et al.*, "Observation of a Significant Excess of $\pi^0\pi^0$ Events in B Meson Decays" Phys. Rev. Lett. **91**, 241801 (2003)
- B. Aubert *et al.*, "Evidence for the Rare Decay $B \to K^*\ell^+\ell^-$ and Measurement of the $B \to K\ell^+\ell^-$ Branching Fraction" Phys. Rev. Lett. **91**, 221802 (2003)

References

1. B. Aubert *et al.*, Partial Reconstruction of $B^0 \to D^{*+}D_s^{*-}$ Decays and Determination of the $D_s^+ \to \phi\pi^+$ Branching Fraction, hep-ex/0308017
2. For a description of this measurement see the BaBar section in the 2002 LNF Activity Report.
3. R. Baldini *et al.*, Eur. Phys. J. **C11** (1999) 709
4. "Conversion Decays of $\phi(1020)$ Decays into $\pi^0 e^+e^-$, $\eta(550)$ e^+e^- and $\eta(550)$ e^+e^- from SND Detector at VEPP-2M", by T. V. Dimova et al. Jul 2001. 5pp. Prepared for International Europhysics Conference on High-Energy Physics (HEP 2001), Budapest, Hungary, Jul 2001. Published in *Budapest 2001, High energy physics* hep2001/172
5. PDG 2003

BTeV

E. Basile[2] (Ass.), F. Bellucci[3] (Ass.), M. Bertani, S. Bianco,
M.A. Caponero[1] (Ass.), F. Di Falco[2] (Ass.), F.L.Fabbri (Resp.), F. Felli[2] (Ass.),
M. Giardoni, G. Mensitieri[3] (Ass.), A. La Monaca, B. Ortenzi,
M. Pallotta, A. Paolozzi[2] (Ass.), L. Passamonti (Tecn.), D. Pierluigi (Tecn.), S. Tomassini
permanent address: [1]ENEA Centro Ricerche Frascati
[2]La Sapienza University Rome
[3]Federico II University Naples

The BTeV experiment is designed to challenge the Standard Model explanation of CP violation, mixing and rare decays of beauty and charm quark states. The Standard Model has been the baseline particle physics theory for several decades and BTeV aims to find out what lies beyond the Standard Model. In doing so, the BTeV results will also shed light on phenomena associated with the early universe such as why the universe is made up of matter and not anti-matter.

The BTeV Collaboration is a group of about 170 physicists drawn from more than 30 universities and physics institutes from Belarussia, Canada, China, Italy, Russia, and the United States of America. The Italian collaboration is composed about 40 physicists from Laboratori Nazionali di Frascati, University of Milan, INFN-Milan and University of Bergamo.

The BTeV experiment will utilize the Fermilab Tevatron proton-antiproton collider (USA). The experiment is still being developed; installation is scheduled to start in 2006, followed by commissioning in 2008.

1 The experiment

The Standard Model has been the backdrop of particle physics theory for more than a quarter of a century. It is a combination of three of the four known fundamental forces - electromagnetism, strong nuclear force, and weak nuclear force (gravity is the fourth). It also contains the fundamental particles which make up the universe which are the six quarks (up, down, charm, strange, top, beauty) and six leptons (electron, muon, tau, electron neutrino, muon neutrino, tau neutrino). All of these particles are partnered with antiparticles with opposite charge but the same mass. This Model is very unsatisfactory, however, because it asks more questions than it answers. The Model does not tell us why there are three generations of quark doublets and three generation of lepton doublets. The Model also fails to predict the masses of these particles. It is believed by many that a more fundamental theory will be able to predict many of the parameters of the Standard Model, which today must be measured by experiments. Physicists hope this more fundamental theory will also include the gravitational force which is not in the Standard Model.

BTeV is an experiment which is designed to deeply probe several aspects of the Standard Model. At the very least, BTeV will make very precise measurements of many Standard Model parameters. It is hoped that these precise measurements will reveal weaknesses in the Standard Model which will point the way to a more fundamental theory.

One of BTeV's main goals is to precisely measure CP violation in the beauty quark system. CP violation was first observed in strange quarks in 1963 and recently in beauty quarks at BaBar and Belle. CP violation causes particles and antiparticles to behave differently. There are two main reasons to study CP violation. The first reason is that many theories which provide extensions or replacements for the Standard Model predict effects in this realm. The second reason is that one of the big mysteries of the universe is why the universe is composed of matter instead of antimatter. The prevalance of matter over antimatter appears to require a large CP violating process sometime during the early formation of the universe. Although the levels of CP violation in the Standard

Model are not large enough to explain this effect, it is the only place where CP violation has been observed and is therefore a natural place to look for more answers.

The BTeV detector is shown in Fig.1: it is composed of a charged particle tracker, em calorimetry, Čerenkov particle identification detector, muon detection and data acquisition triggering. The charged particle tracker is composed of a pixel vertex detector and a forward magnetic spectrometer. The forward spectrometer is made of six stations of straw tubes and silicon microstrips.

The Frascati group has responsability of the small-angle straw tube modules which hold the silicon microstrips. The Frascati group is also responsible of providing detector position monitoring of pixels, microstrips and straw-tubes by means of Fiber Bragg Grating sensors.

2 Activity during year 2003

The activity of the Frascati group related to the straws-microstrip interface took a relevant step forward during 2003 with the design of a first protoype of small-angle strawtube module able to hold the microstrip system. The baseline idea of such a *Module 0* is based on a straw-rohacell sandwich which is surrounded by a Carbon-Fiber Reinforced Plastic (CFRP) shell. Straws in Module 0 are kept in place with no mechanical tension. The conceptual design was finalized, and test of grooving process of rohacell were performed (Fig.2). A detailed study was setup to investigate the effect of gas mixture composition on straws mechanical tension, which was recently shown to be affected in the case of kapton straws.

The monitoring of sensitive components of pixels, microstrips and straws will be performed by position detectors using Fiber Bragg Grating (FBG) sensors as active components(Fig.2 b). FBG's are optical strain gauges with μ-strain sensitivity. During 2003 the long term test of FBG's was completed, spanning a 9-month period. Radiation hardness was investigated at the ENEA neutron source in Frascati, reaching a 6-month-maximum BTeV dose level. A detailed campaign of measurements was carried out on the pixel carbon fiber mockup structure, in order to characterize its thermal and stress behaviour, and to validate the Finite Element Model simulations developed.

3 Outlook

In 2004 we plan to assemble the first prototype of Module 0, to instrument it and to test its response to particles. In parallel we shall proceed with the second prototype which will clarify the problems related to the integration with the microstrip detector. The second prototype will be exposed to test beams at Fermilab, possibly with the first microstrip protoype. The activity on FBG sensors will be centered on the full characterization of sensor displacements along the final pixel support structure, as well as on the proof-of-principle for the repositioning device to be used for replacing the pixel detector on the beams after each accelerator store.

References

1. BTeV-doc-1564-v2 Status of project on straw-rohacell integration A. Paolozzi 02 May 2003

2. BTeV-doc-1338-v1 Manufacturing procedure for central straw module A. Paolozzi 10 Oct 2003

3. BTeV-doc-1337-v1 Mechanical tests on straw tubes A. Paolozzi 10 Oct 2003

4. BTeV-doc-1297-v1 Use of Fiber Bragg Grating Sensors for detector position monitoring Stefano Bianco 29 Sep 2003

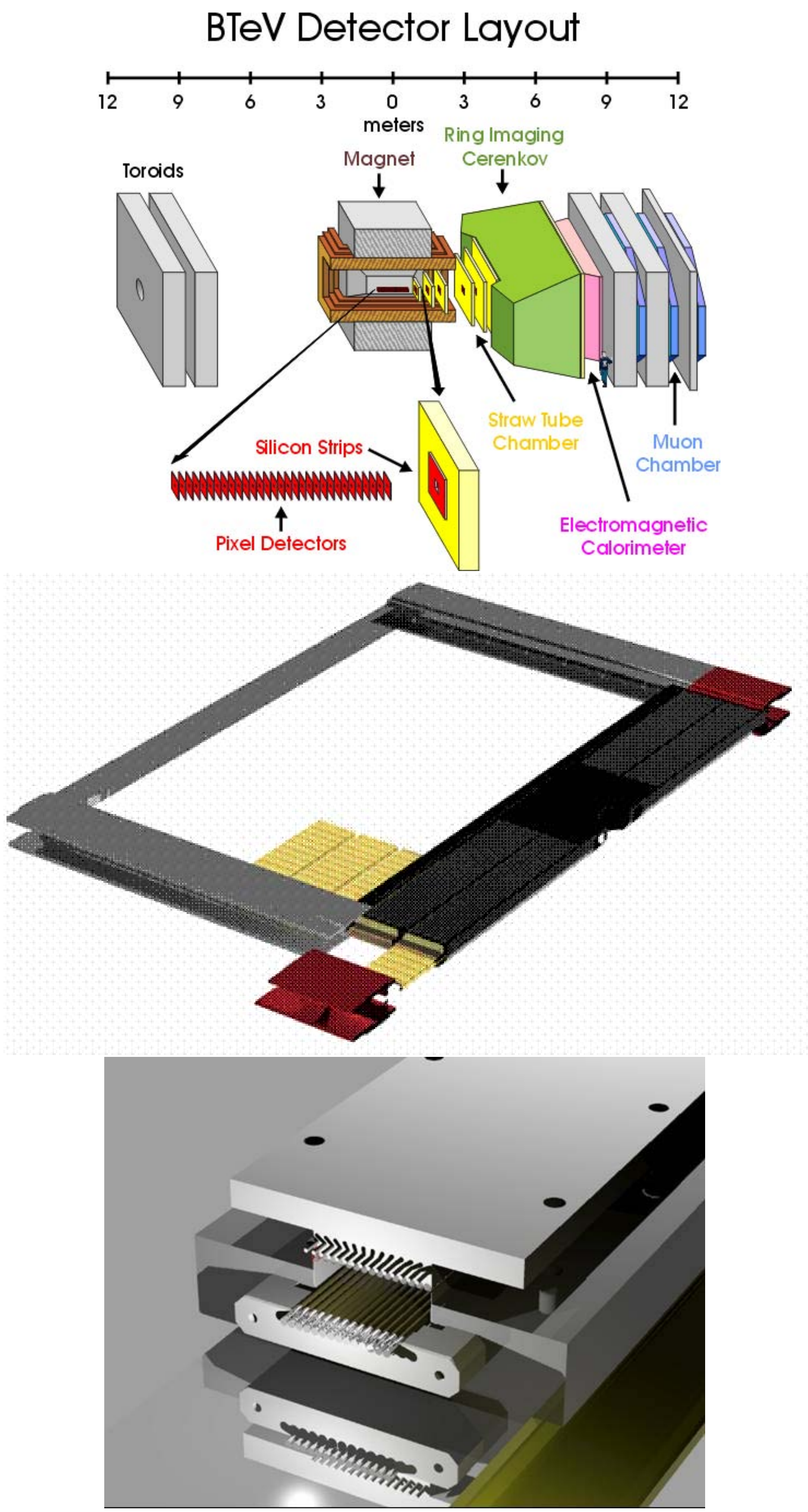

Figure 1: The BTeV detector (top). Conceptual design of one half straw tube station, including the CFRP Module 0 (middle). Exploded view of Module 0 (bottom).

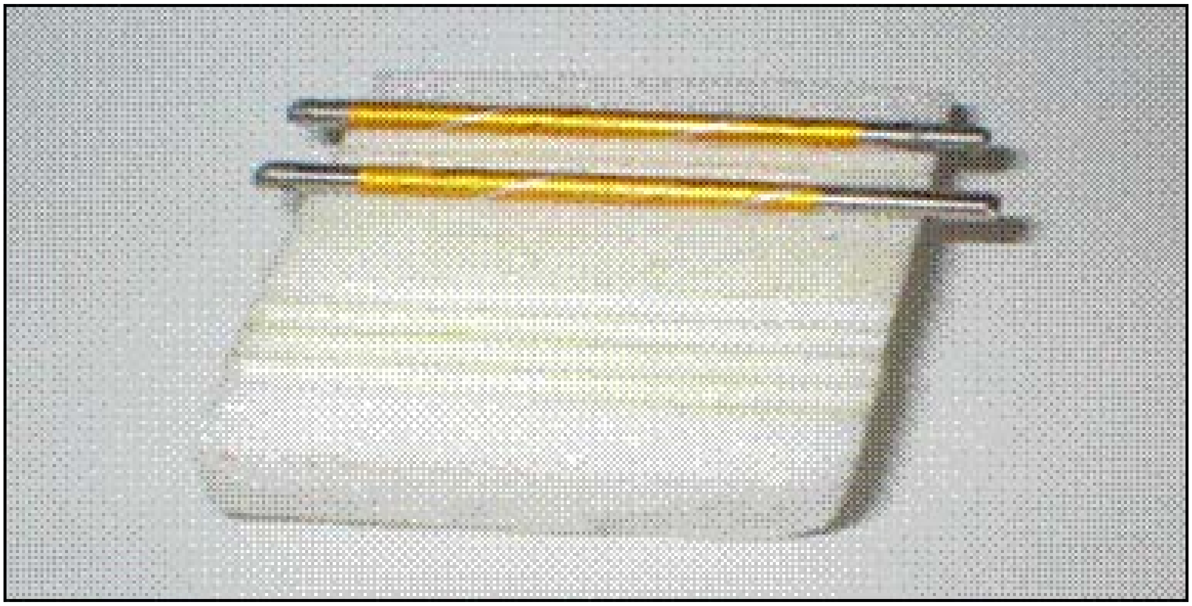

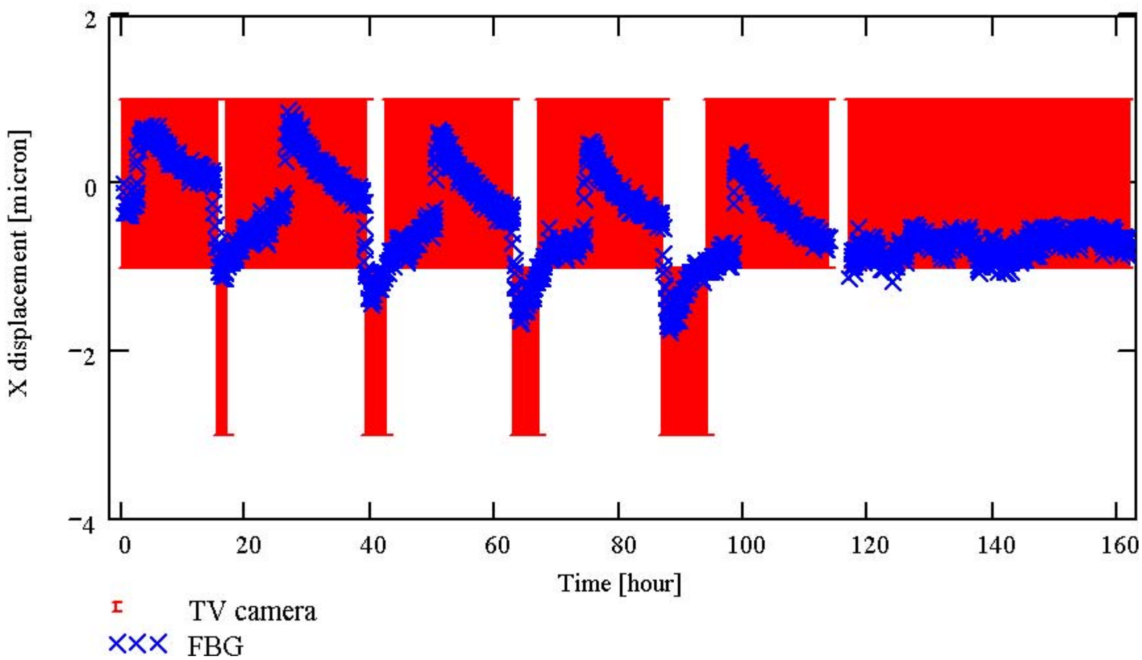

Figure 2: Test of assembly for the straw-rohacell Module 0 (top); Monitoring mechanical deformations due to thermal cycling via Fiber Bragg Grating sensors (bottom).

5. BTeV-doc-1067-v2 Use of Fiber Bragg Grating sensors in BTeV - Long-term and real-time monitoring detector position M. A. Caponero 30 Aug 2003

6. BTeV-doc-177-v1 Smart materials in BTeV? A. Paolozzi 29 Aug 2003

7. BTeV-doc-1066-v1 On the use of Fiber Bragg Grating Sensors for position monitoring in BTeV Stefano Bianco 29 Aug 2003

8. BTeV-doc-1065-v1 Use of Fiber Bragg Grating sensors for BTeV M. A. Caponero 29 Aug 2003

9. BTeV-doc-1064-v1 Composite materials for FBG A. Paolozzi 29 Aug 2003

10. BTeV-doc-922-v1 Microstrip-Straw Tube Interface A. Paolozzi 18 Jul 2003

11. LNF-03/15(IR) E. Basile et al. Results of Long-Term Position Monitoring by Means of Fiber Bragg Grating Sensors for the BTeV Detector

12. S.Berardis, M.Bertani, S.Bianco, M.A.Caponero, D.Colonna, F.L.Fabbri, F.Felli, M.Giardoni, A.La Monaca, B.Ortenzi, E.Pace, M.Pallotta, A.Paolozzi, S. Tomassini, "Fiber optic sensors for space missions" 2003 IEEE Aerospace Conference Proceedings, Big Sky Montana, March 8-15, 2003, CD 5.0101, pp. 1661-1668.

CDF II

M. Barone (Ass.), M. Cordelli (Resp.), S. Dell'Agnello, F. Happacher (Ass. Ric.), S. Miscetti, A. Sansoni, I. Sfiligoi (Art. 23)

1 Introduction

The Tevatron runs at a $p\bar{p}$ collision energy of 1.96 TeV in the centre of mass system. In 2003 it has delivered to CDF II and D0 a maximum instantaneous luminosity, L, of 5×10^{31} $cm^{-2}s^{-1}$, still below the designed value of 2×10^{32} $cm^{-2}s^{-1}$ ($L \sim 1.5 \times 10^{31}$ in Run I). During Run IIa CDF II has collected on tape $\sim$ 270 pb^{-1} at the end of 2003. During Run I CDF collected $\sim$ 109 pb^{-1}. The goal for 2004 is to run at $\sim 8 \times 10^{31}$ $cm^{-2}s^{-1}$ and deliver 300 pb^{-1} to each experiment. To reach these high values of L it has been necessary to increase the number of p and $\bar{p}$ bunches (N_b), thus shortening the time interval between consecutive bunch crossings to 132 $n$sec (3.5 μs in Run I). This has imposed a substantial upgrade of the CDF II detector. The central calorimeters, electromagnetic and hadronic, could work properly in the new Run after the renewal of the Front-End electronics (FEE).

The Frascati CDF II group is responsible for the hardware maintenance and for the energy scale calibration of the two iron-scintillator hadronic calorimeters covering $|\eta| < 1.35$ (the "central" or CHA for $|\eta| < 1.0$ and the "endwall" or WHA for $0.7 < |\eta| < 1.35$).

To calibrate the calorimeter we use the following techniques, some inherited from the past and some developed for the new run:

1. the system of the ^{137}Cs sources provides the bulk of the absolute energy scale determination; this procedure relies on the 1983-85 test beam with π's with energy greater than 10 GeV;

2. in Run II we use for the first time MIP energy deposition from $J/\Psi \to \mu\mu$ decays to cross-calibrate the calorimeter towers;

3. the N_2 laser system is run periodically to track the photomultiplier (PM) gains and to quickly check the functionality of the PM-ADC readout chain (CHA PM gains are stable within $\sim 2\%$, while for WHA they drift a bit more).

Stricly related to the above, INFN-Frascati has the responsibility of the slow control of the HV common to CHA, WHA and to the central electromagnetic (e.m.) calorimeter. The slow control system has been significantly improved with respect to Run I: (i) the PM HV is readout much more often; (iii) the HV data are used online to monitor the detectors; (iii) the HV bulk power supplies are monitored at a faster rate ($\sim$ 1 Hz), to stop the trigger and data acquisition in case the HV drifts out of the tolerance range. The slow control was commissioned in 2000 and has performed with no problems ever since.

The group is also involved in the calorimeter timing project, both for the hadronic and electromagnetic compartments. The timing system in the hadronic calorimeters (CHA, WHA, PHA) is fully working since the end of the experiment commissioning (end of 2001). Our responsibility consisted in the design and realization of the fast VME discriminator boards (HADASDs), the realization of the transition boards (TBs) that connect the PM signal cables to the backplane of the VME crates, and in the debugging and calibration of the system. We completed successfully the installation of the boards, the calibration of the t_0s, of the discriminator thresholds and of the slewing corrections (the dependence of the timing on the energy pulse-height). These calibration constants, taken every ~ 10 pb^{-1}, are stored into database tables and are used during the offline reconstruction.

Adding the time information to the electromagnetic calorimeters is a Run IIb project. However, since it does not require a long shut-down and the production of the components is well advanced, we plan to do it in Run IIa. The Frascati group designed and built the e.m. discriminator and transition boards. During the shut-down of September 2003, we cabled the PMs and installed the VME boards for the forward e.m.calorimeter. This system is working well and is being calibrated. Only 8% of the central e.m was instrumented and this part is working properly. The rest will be installed during the next long shut-down.

2 Determining the Energy Scale

The most important activity carried on during 2003 has been the refinement of the setting of the absolute calorimeter energy scale. An accurate determination of the calorimeter energy scale is essential as a starting point for the absolute jet energy corrections. A correct jet energy scale improves the invariant mass resolution and reduces the systematic uncertainty in the reconstruction of top quark decays and of the hadronic decays of W and Z bosons. To reach this goal we profit of all the available techniques.

2.1 ^{137}Cs Sources

In order to correct for light yield losses of the scintillator due to aging, we have acquired the current output (I) from the PMs when the moveable ^{137}Cs sources are run in front of the scintillator planes located around the maximum of the hadronic shower. Since a few of the scintillator/absorber layers are irradiated, we can monitor in this way the aging of the scintillator together with PM gain variations. We compute the Linear Energy Response

$$LER = \frac{^{137}Cs(test\ beam)e^{-\Delta t/\tau}}{^{137}Cs(today)}$$

for the CHA and WHA calorimeter towers and we correct for these factors the raw ADC counts.

Unlike previous years, in 2003 it was not possible to run sources for CHA towers due to mechanical problems. For the WHA, instead, the source system has been completely refurbished, all sources were run and we measured an average drop in the WHA energy response of ~ 8 %. The tower-by-tower LER has been derived and downloaded in the FEE.

2.2 Minimum Ionizing Particles

We looked at the energy deposition of MIPs (HadE) to monitor the energy response of the hadronic calorimeter. At the Tevatron energies muons are MIPs, so that for our studies clean samples of μ's from J/Ψ decays are used. By exploiting the ~ 80 pb^{-1} dimuon trigger sample collected in Run Ib, we foud that the tower-by-tower peak is determined with a precision of $\sim 1.5\%$.

At the beginning of Run II, the comparison of Run I and Run II MIP peaks showed a $\sim 10\%$ difference. We applied this additional correction to the raw ADC output of the PMs into the FEE. In this way the mean HadE of Run II has been restored to the ~ 1.70 GeV we had in Run I.

After correcting for this overall factor and with the increase of the available statistics, we performed a detailed analysis of the muon hadronic energy release on a tower-by-tower basis. In Figure 1 we show the HadE distribution for J/Ψ muons impinging the $\eta = 0$ towers of the west side of CHA. Comparing Run I and Run II, we have noticed that the overall $\sim 10\%$ correction was not homogeneous across all towers: towers at high rapidities were overcorrected. A further correction factor was derived by normalizing every tower to the Run I MIP response. Figure 2 shows the

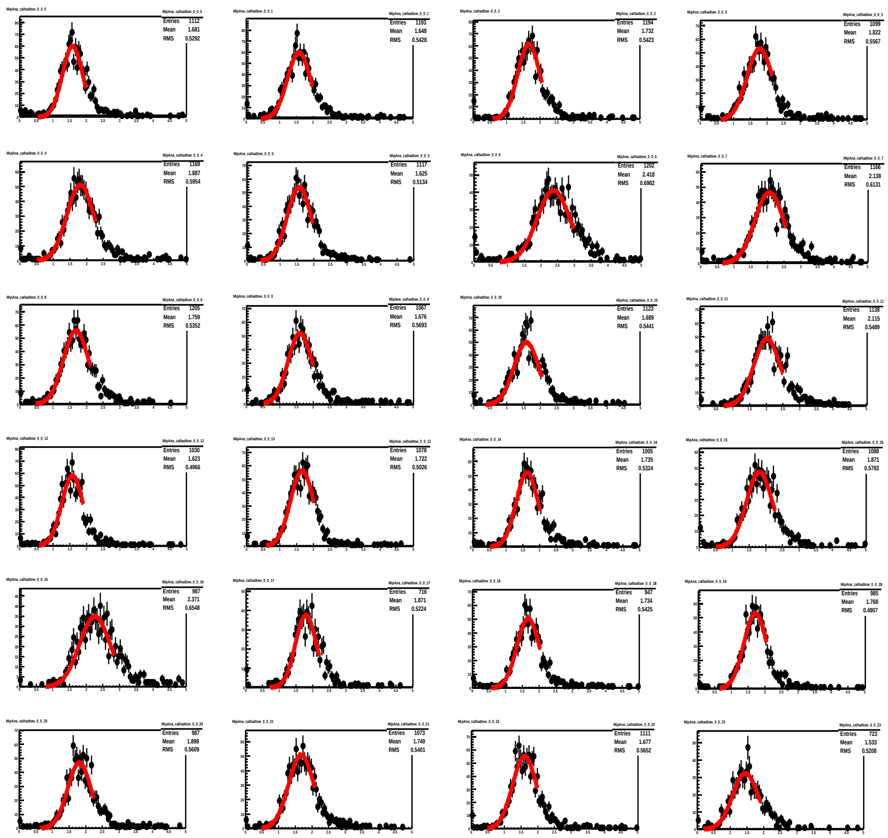

Figure 1: *Run II μ's from J/Ψ. Hadronic energy deposition for the $\eta = 0$ towers of west CHA.*

comparison of the MIP peaks of Run I (green points) and Run II (blue triangles) for the $\eta = 0, 1$ rings of towers of west CHA (24 towers at different ϕ's and the same η). These distributions are similar and are not flat. This is to be expected, because the hadronic calorimeter was calibrated and equalized using test beams of 50 GeV pions. The behavior of figure 2 is due to differences in the shower shape and sampling fractions of the calorimeter to pions and muons and it was already measured at the test beam to be $\sim 4.5\%$. The red triangles in the same figure represent an attempt of equalizing the MIP response for each η ring. This approach was immediately dropped because of the consideration above.

In order to check whether the MIPs track properly the degradation of the calorimeter we studied the correlation between the MIP peaks and the Cs source response for the subset of CHA towers ($\sim 8\%$) for which 2003 source data were available. If this were the case we could determine the new LERs using the following formula:

$$LER = LER^{03}_{Cs} \times \frac{MIP(RunI)}{MIP(03)}$$

i.e. multiplying the LER values used in 2003 (determined with Cs sources in 2002), by the ratio of the MIP peaks between the latest $30pb^{-1}$ period of 2003 data and Run I data. Figure 3 shows the correlation between the LERs calculated in the two different methods: the MIPs track pretty well the degradation of the CHA response. Therefore, in the future only MIPs will be used to maintain the energy calibration, due to the mechanical problems encountered in running the sources. This is a fundamental difference compared to Run I, when this was done exclusively with Cs sources.

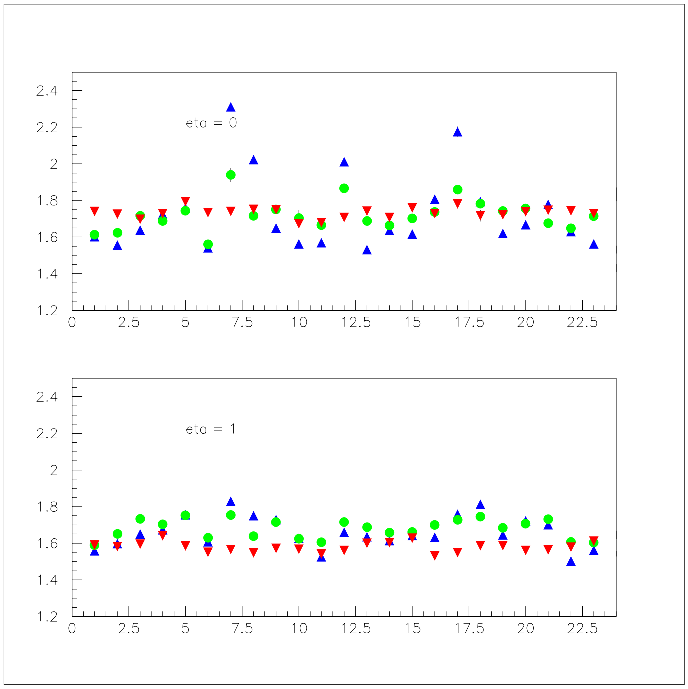

Figure 2: *Run II vs Run I HadE deposition in* $\eta = 0, 1$ *towers of west CHA, see text.*

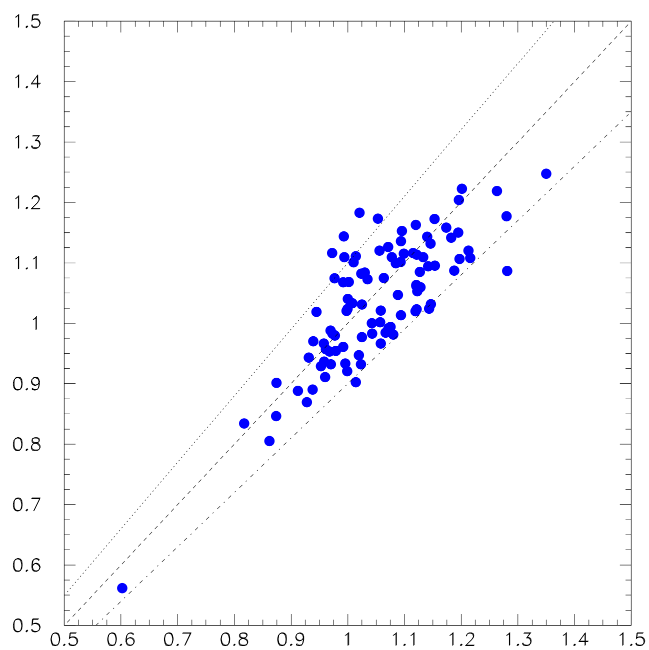

Figure 3: *Correlation between the energy response measured with Cs sources and MIPs.*

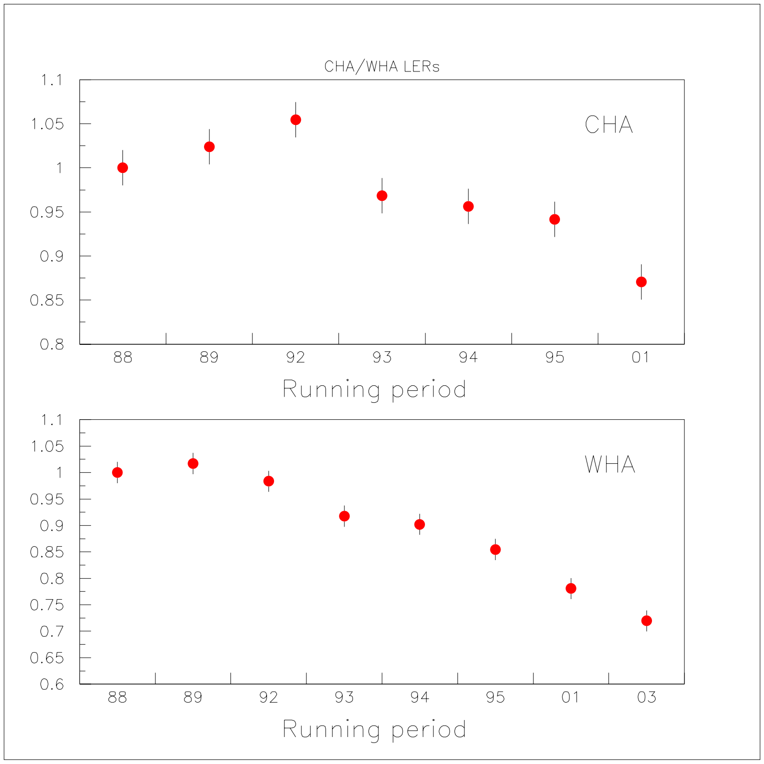

Figure 4: *Variation of the energy response of the central and endwall hadron calorimeters.*

Figure 4 shows the 15 year old tale of the energy response of CHA and WHA. Note that the construction of these calorimeters started about 20 years ago.

2.3 N_2 Laser

The laser system has been used periodically in 2003 as a quick tool to follow the trend of the PM gains. For CHA the mean value of the PM gains are stable within $\sim 2\%$, while for WHA they drift a bit more (see Figure 5 and 6).

3 Check of the jet energy scale

To check the raw hadronic energy scale of jets we have compared the so-called (transverse momentum) $\gamma-$jet balancing between Run I and Run II data. We build the variable$f_b = (p_T(jet) - p_T(\gamma))/p_T(\gamma)$ and compare it to Run I data. This study shows that there is still a 5.5% discrepancy. Out of this 5.5%, 1% is due to extra material in the tracking volume in front of the calorimer, 1.9% is known to come from different electromagnetic energy scale determination between Run I and Run II jets, while the shorter integration gate is responsible for 0.6% of the disagreement. The remaining 2 % disagreement still needs to be understood and is due to the hadronic AND the e.m. calorimeter energy scale. This implies that the hadronic energy scale is correct at the 1% level.

4 CAF

The Frascati group is also contributing to the development the CDF II Central Analysis Facility (CAF). The CAF system is composed of ~ 300 computing nodes for user analysis. A simple-to-use graphical interface that allows the submission of jobs from any desktop inside or outside Fermilab

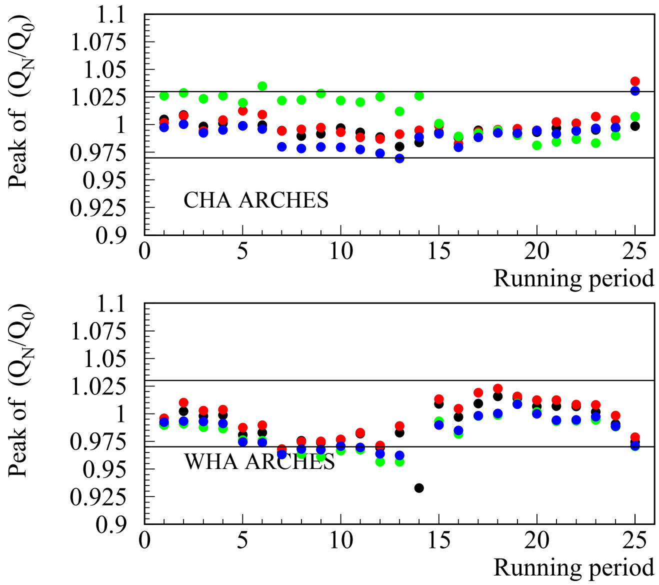

Figure 5: *Mean value of the PM gains normalized to a reference run (in %) vs time, as determined using the laser during year 2003. Each arch is a quarter of each detector.*

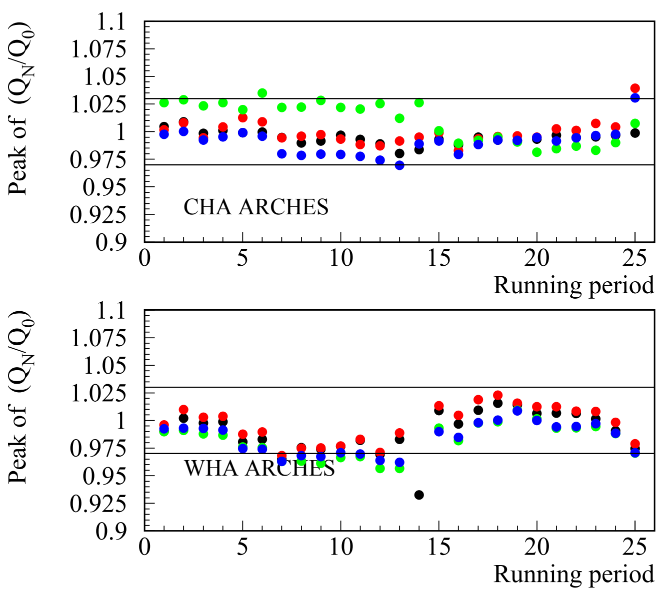

Figure 6: *Width of the PM gains normalized to a reference run (in %) vs time, as determined using the laser during year 2003. Each arch is a quarter of each detector.*

has been developed. The output of the jobs is then written to a central disk pool and can be retrieved upon the user's request. This interface also provides the user with a *quasi*-interactive access to the running job.

The current *production* version of the CAF is based on the FBSNG batch manager. The problem with the current software is that it was written with a centralized framework scheme in mind; moving to a distributed structure is not a trivial task. The CAF group is therefore considering the Condor batch manager instead of FBSNG's. The first prototype system has been developed in autumn 2003 and an early 'beta' stage has been started at the beginning of 2004. The Frascati group has the responsibility for the development this new Condor-based CAF in close connection to the Condor development team, since the needs for a Condor-based CAF are close to the current limitations of the Condor software itself.

The Fermilab CAF is not the only user batch pool available at CDF II. Several contributing institutions (including INFN) are building their own pools and are trying to use the CAF infrastructure.

Talks at Conferences 2003

1. "Properties of jets with heavy flavor produced in $\sqrt(s) = 1.8$ TeV $p\bar{p}$ collisions at the Tevatron", presented by F. Happacher at IFAE Lecce, Italy, 2003.
2. "The CDF II Central Analysis Farm", T.H.Kim, M.Neubauer, I.Sfiligoi, L.Weems, F.Würthwein, presented by I. Sfiligoi at the NSS IEEE2003, Portland OR, USA. Submitted to Transactions on Nuclear Science (ref. TNS-00316-2003).

Publications 2003

1. CDF II Collaboration, "Observation of the narrow state X(3872) → J/psi pi+ pi- in anti-p p collisions at s**(1/2) = 1.96-TeV," arXiv:hep-ex/0312021.
2. CDF Collaboration, "Heavy flavor properties of jets produced in p anti-p interactions at s**(1/2) = 1.8-TeV," arXiv:hep-ex/0311051.
3. CDF Collaboration, "Measurement of the polar-angle distribution of leptons from W boson decay as a function of the W transverse momentum in p anti-p collisions at s**(1/2) = 1.8-TeV," arXiv:hep-ex/0311050.
4. CDF Collaboration, "Inclusive double pomeron exchange at the Fermilab Tevatron anti-p p collider," arXiv:hep-ex/0311023.
5. CDF Collaboration, "Measurement of the average time-integrated mixing probability of b-flavored hadrons produced at the Tevatron," arXiv:hep-ex/0309030.
6. CDF II Collaboration, "Search for the flavor-changing neutral current decay D0 → mu+ mu- in p anti-p collisions at s**(1/2) = 1.96-TeV," Phys. Rev. D **68**, 091101 (2003) [arXiv:hep-ex/0308059].
7. CDF II Collaboration, "Measurement of the mass difference m(D/s+) - m(D+) at CDF II," Phys. Rev. D **68**, 072004 (2003) [arXiv:hep-ex/0310043].
8. CDF II Collaboration, "Measurement of prompt charm meson production cross sections in p anti-p collisions at s**(1/2) = 1.96-TeV," Phys. Rev. Lett. **91**, 241804 (2003) [arXiv:hep-ex/0307080].
9. CDF Collaboration, "Search For Associated Production Of Upsilon And Vector Boson In P Anti-P Collisions At S**(1/2) = 1.8-Tev," Phys. Rev. Lett. **90**, 221803 (2003).
10. CDF Collaboration, "Search for pair production of scalar top quarks in R-parity violating decay modes in p anti-p collisions at s**(1/2) = 1.8-TeV," arXiv:hep-ex/0305010.
11. CDF Collaboration, "Central pseudorapidity gaps in events with a leading antiproton at the Fermilab Tevatron anti-p p collider," Phys. Rev. Lett. **91**, 011802 (2003) [arXiv:hep-ex/0303011].
12. CDF Collaboration, "Search for the supersymmetric partner of the top quark in dilepton events from p anti-p collisions at s**(1/2) = 1.8-TeV," Phys. Rev. Lett. **90**, 251801 (2003) [arXiv:hep-ex/0302009].

E831

R. Baldini-Ferroli, L. Benussi (Ass.), M. Bertani, S. Bianco (Resp.)
F.L. Fabbri, M. Giardoni, S. Pacetti (Ass.), A. Zallo

FOCUS (Experiment 831 at Fermilab, www-focus.fnal.gov) studies photoproduction and decays of charm mesons and baryons at Fermilab. In FOCUS, a forward multi-particle spectrometer is used to measure the interactions of high energy photons on a segmented BeO target. The FOCUS detector is a large aperture, fixed-target spectrometer with excellent vertexing, particle identification, and reconstruction capabilities for photons and π^0's. FOCUS is a considerably upgraded version of a previous experiment, E687, and it amply surpassed the goal of collecting ten times the E687 sample of fully reconstructed charm decays, i.e. a sample of over 1 million fully reconstructed charm particles in the three major decay modes: $D^0 \rightarrow K^-\pi^+$, $K^-\pi^+\pi^-\pi^+$ and $D^+ \rightarrow K^-\pi^+\pi^+$. The FOCUS Italian groups (Milano, Pavia and Frascati) hold full responsibility for the μ-strip detector, the Hadron calorimetry, and the Outer em calorimetry respectively, and coordinate about half of the software-related projects. The Frascati group also coordinates the calorimetry working group, and is responsible for the first level selection process in physics analyses utilizing em calorimetry.

1 Activity during year 2003

The activity of the Frascati FOCUS group in 2003 was concentrated on the data analysis and presentation of results at conferences. The data analysis studies of the group were centered on spectroscopy. Along with the traditional ensemble of studies on the spectroscopy of orbitally and radially excited charm mesons, a new line of research was opened, regarding the spectroscopy of light quark mesons diffractively photoproduced.

Heavy Quark Symmetry and Heavy Quark Effective Theory predict a rich spectrum for the excited charm mesons. In 2003 FOCUS published the analysis carried on by the Frascati group on the precise new measurements of D_2^* masses and widths (with errors less than or equal to PDG2003 averages). Evidence was found for new broad states in both isospin channels $D^0\pi^+$ and $D^+\pi^-$ (Ref. [1)]). Mass peaks in both distributions are shown in Fig.1.

Light quark diffractive physics is a surprise for a heavy quark experiment. Thanks to a dedicated trigger FOCUS has collected a very significant sample of diffractive events, thus starting studies of interest in hadronic physics and predictions of χQCD. During 2003, the Frascati group published a follow-up study of the evidence found in 2001 for a narrow dip structure in diffractive photoproduction of the 6π final state. When interpreted as a new resonance interfering with the diffractive continuum, the structure has $1.911 \pm 0.004\,\mathrm{Gev/c^2}$ mass and $29 \pm 11\,\mathrm{Mev/c^2}$ width.

In 2002 we showed preliminary evidence for a confirmation signal in FOCUS data, at a mass and width compatible with the E687 published result.

We also showed evidence for diffractively photoproduced $\phi\eta$, $\phi\eta'$, ϕf_0 events, studied the q^2 evolution, and investigated a relationship via dispersion relations to the debated value of the branching ratio $\Gamma(\phi \rightarrow f_0\gamma)$. Results were presented at Alghero 2003 and SIF 2003.

1.1 Conference Organization and IAC Memberships

During 2003, members of the FOCUS Frascati group have participated in the organization of the conference *DAΦNE 2004* , Frascati, Italy, May 2004. Members of the Frascati group served in International Advisory Committees of the following conferences: 12th Conference On Calorimetry

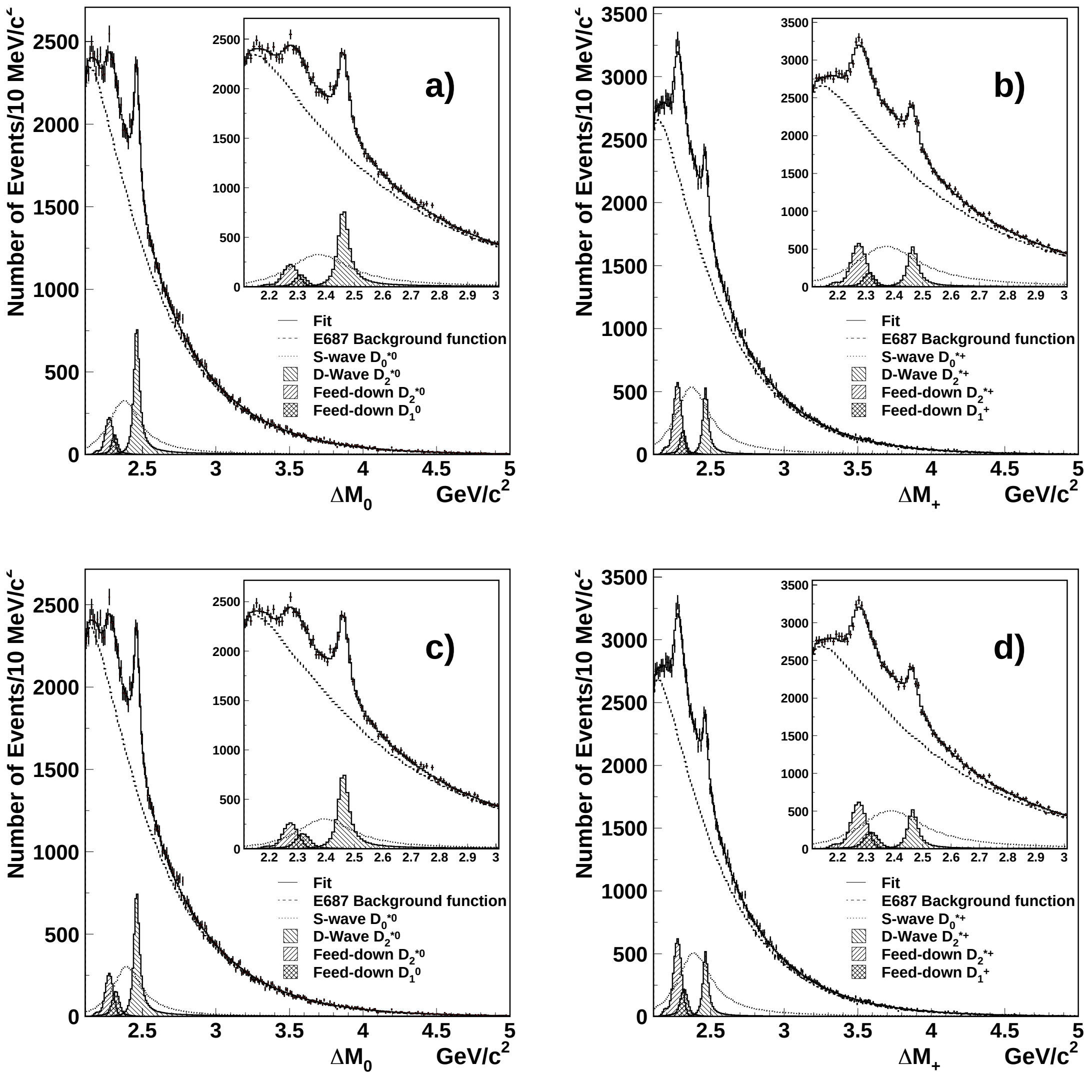

Figure 1: The fit to the $D^+\pi^-$ and $D^0\pi^+$ mass spectra including a term for an S-wave resonance. The case with the mass and width for the $D_1(3/2)$ and D_2^* feed-downs fixed to the PDG values is shown in a) and b). The case with the mass and width for the $D_1(3/2)$ feed-down fixed to the PDG values and for the D_2^* feed-down determined by fits in a) and b) is shown in c) and d). Notice the excellent agreement when the broad resonance is included.

In High Energy Physics (CALOR 2003), 2nd Int. Conf. on Heavy Quarks and Leptons (HQL04), 23rd Physics In Collision Conference (PIC03).

2 Outlook

The activity in 2004 will be focussed in finalizing the ongoing analysis of the $D^*\pi$ final state, and in searching for radial excitations, including channels with γ and π^0 in the final state. In the light quark sector, we plan to continue the study to seek confirmation of the six pion structure and to finalize the study f_0 production and $\eta - \eta'$ mixing from our diffractive sample.

3 Conference Talks in 2003

1. NARROW STRUCTURES IN HIGH STATISTICS DIFFRACTIVE PHOTOPRODUCTION by S.Pacetti, prepared for "e+e- in the 1-2 GeV range: Physics and Accelerator Prospects", 10-13 September 2003, Alghero (SS), Italy. To be published in eConf, LNF Preprint LNF-03/24(P).
2. NUOVI RISULTATI IN SPETTROSCOPIA DEI QUARK LEGGERI DA E831-FOCUS by S.Pacetti [FOCUS Coll.], prepared for "LXXXIX Congresso Nazionale Societa‘ Italiana di Fisica", 17-22 September 2003, Parma, Italy.

References

1. J. M. Link *et al.* [FOCUS Coll.], accepted by Phys. Lett. B arXiv:hep-ex/0312060.
2. J. M. Link *et al.* [FOCUS Coll.], accepted by Phys. Lett. B arXiv:hep-ex/0312040.
3. J. M. Link *et al.* [FOCUS Coll.], Phys. Lett. B **581**, 39 (2004) [arXiv:hep-ex/0311022].
4. J. M. Link *et al.* [FOCUS Coll.], accepted by Phys. Lett. B arXiv:hep-ex/0310051.
5. P. L. Frabetti *et al.*, Phys. Lett. B **578**, 290 (2004) [arXiv:hep-ex/0310041].
6. S. Bianco, F. L. Fabbri, D. Benson and I. Bigi, "A cicerone for the physics of charm," accepted by Riv. Nuovo Cim. arXiv:hep-ex/0309021.
7. J. M. Link *et al.* [FOCUS Coll.], Phys. Lett. B **575**, 190 (2003) [arXiv:hep-ex/0308054].
8. J. M. Link *et al.* [FOCUS Coll.], Phys. Lett. B **572**, 21 (2003) [arXiv:hep-ex/0306049].
9. J. M. Link *et al.* [FOCUS Coll.], Phys. Lett. B **571**, 139 (2003) [arXiv:hep-ex/0305038].
10. J. M. Link *et al.* [FOCUS Coll.], Phys. Lett. B **566**, 51 (2003) [arXiv:hep-ex/0305018].
11. J. M. Link *et al.* [FOCUS Coll.], Phys. Lett. B **561**, 41 (2003) [arXiv:hep-ex/0302033].

KLOE

The KLOE-LNF collaboration:
A. Antonelli, M. Antonelli, G. Bencivenni, S. Bertolucci, C. Bloise, F. Bossi,
P. Campana (Resp), G. Capon, P. Ciambrone, P. De Simone, S. Dell'Agnello,
M. Dreucci (Ass), G. Felici, M. L. Ferrer, G. Finocchiaro, C. Forti, A. Franceschi,
C. Gatti (Ass. Ric.), S. Giovannella (Art. 23), G. Lanfranchi, J. Lee-Franzini (Art. 23),
M. Martini (Laur), W. Mei (Art. 23), S. Miscetti, M. Moulson (Art. 23), F. Murtas,
M. Palutan (Art 23), L. Passalacqua, V. Patera (Ass), P. Santangelo, B. Sciascia (Ass. Ric),
A. Sciubba (Ass), I. Sfiligoi (Art 23), T. Spadaro (Ass. Ric.), P. Valente (Art. 23)

The KLOE-LNF Technical Staff:
M. Anelli, A. Balla, A. Ceccarelli, G. Fortugno, G. Paoluzi,
G. Papalino, R. Rosellini, M. Santoni, A. Saputi

1 Introduction

After a first engineering run in 1999, the KLOE experiment has taken physics data for three consecutive years (2000-2002) at DAΦNE the Frascati ϕ factory. During the year 2002 run, DAΦNE has reached the record luminosity of $7.7 \cdot 10^{31}$ cm^{-2}s^{-1}. The integrated luminosity has been continuously increasing during time as shown by fig. 1. At present, a total of $\sim$450 pb^{-1} have been collected by KLOE.

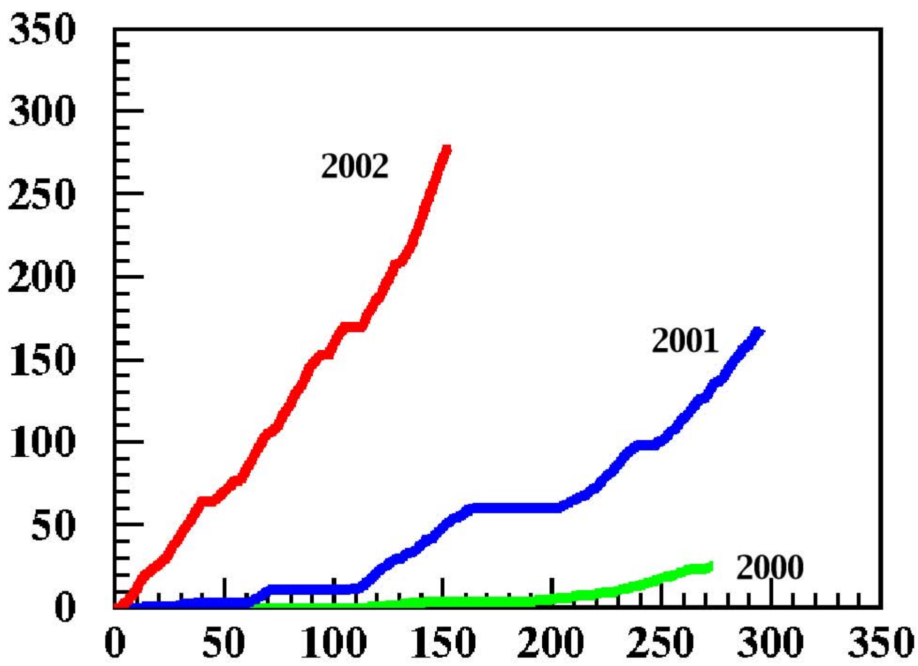

Figure 1: The luminosity integrated by KLOE in the years 2000-2002

KLOE has been designed and built to perform a wide variety of physics measurements, with emphasis on the neutral kaon decays, and most notably on the issue of CP violation. The detector (see fig. 2) consists of a large drift chamber [1] (DC), 3.5 m long, 2 m radius, surrounded by a lead-scintillating fibres electromagnetic calorimeter [2] (EmC). It operates in a solenoidal magnetic field of ∼5.2 T intensity. In order to maximise the coverage for photon detection, the low-β quadrupoles of DAΦNE, which are placed well inside the detector's acceptance are instrumented with special tile calorimeters [3] (QCALs).

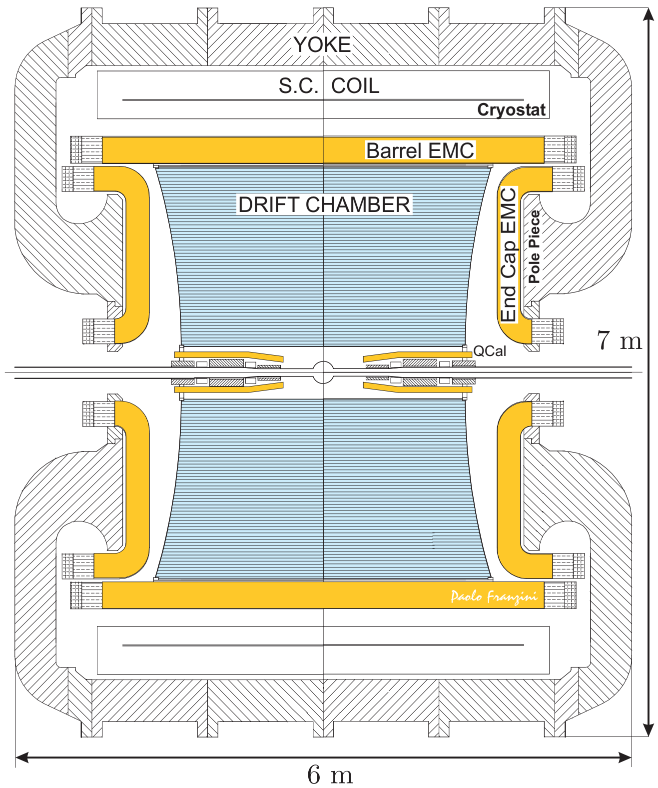

Figure 2: The KLOE detector

Data taken in year 2000 (~ 20 pb^{-1}) have been analysed to produce the first physics results, as reported in the previous editions of this report. Due to the much larger statistics collected in the following years, a deeper attention to systematics studies had to be devoted in the extention to the entire data set of the previous analyses, as well as in the study of new channels. Particular attention has been paid in a massive production of Monte Carlo (MC) events, for which a complete revision of the simulation of all the known detector effects has been carried out. Moreover, the need for effectively handling such a large data sample has imposed the development of new software tools for data management and the definition of a new, more compact format for the reconstructed data (DSTs).

Therefore the main activity in year 2003 has focussed onto the solution of the aforementioned problems, profiting of the machine stop during the main part of the year. In the same period some improvements on the detector hardware have also been performed, as reported in the next section.

2 Modification of the interaction region and QCALs

In the first half of the year the existing interaction region has been replaced by a new one, with a different design of the low-β quadrupoles. These modifications have the goal of improving the control on the machine optics in the KLOE interaction region, with a beneficial effect on the luminosity delivered to the experiment.

The extraction of the interaction region has also allowed to perform some upgrade work on the quadrupoles calorimeters. During the 2001 and 2002 runs, it was observed a channel by channel variation of the QCAL efficiency on MIPs, due to a similar variation in the related PMT's signal. It was also observed a relatively high level of noise induced by the DAΦNE radiofrequency, which affected both energy and time measurements. The upgrade work consisted in the following:

- improved shielding and grounding of the PMTs;
- shortening from 60 cm to 10 cm of the coaxial cables connecting the PMTs and the preamplifiers;
- replacement of the old preamps with newer ones with a factor 4 higher gain;
- insertion of receivers at input in the FEE and replacement of the coaxial cables connecting the preamps to the FEE.

Complete functionality tests on the improved QCAL have been performed by the end of November. The expected increase in the signal gain has been observed.

3 Data reconstruction and Monte Carlo

Data acquired during year 2002 were processed by an improved version of the reconstruction program with respect to that used in year 2001. In order to guarantee the consistency of the selection algorithms over the entire data sample, the 164 pb^{-1} of good data taken during year 2001 have been therefore re-reconstructed.

All the DSTs relative to the entire 2001-2002 data set were produced already during year 2002, except those needed for the analysis of the charged kaons. K^+K^- events had to be re-reconstructed anyway, because of the low velocity of the produced $K^\pm$ which highly affects the treatment of multiple scattering and energy loss in this particular case. Therefore a dedicated software had to be developed, which also includes the calculation of the dE/dx of the tracks based on the measurement of the ADCs installed during year 2002. The entire DST set amounts to 4.1 TB, to be compared to the 27 TB of the input data.

Since November 2002 a large effort has been undertaken by the Collaboration to improve the the reliability of the simulation program. This work included:

- implementation of new generators; particular attention has been paid to the addition of the radiative corrections to kaon decays;
- a revised and more refined geometrical description of the detector, including effects such as the gravitational sags of the drift chamber wires;
- each run individually simulated on the basis of its fundamental physics variables ($\sqrt{s}$, position of the luminous point, trigger thresholds, dead channels etc.);
- insertion of the accidental activity in the detector, extracted from real data;
- production of DSTs for MC events

4 Physics analysis

4.1 Improvements on previously published results

Most of the previously published anlyses refer to data taken in year 2000 ($\sim$20 pb^{-1}). In the following the status of the same analyses repeated on the entire data set is reported.

- $\Gamma(K_S \to \pi^+\pi^-(\gamma))/\Gamma(K_S \to \pi^0\pi^0)$. The published result [4] quotes the most precise value ever obtained on this ratio (total relative error 0.7%). The relevance of this measurement is twofold. First, it is the K_S part of the *double ratio* measurement, i.e. it is needed to determine the value of the CP violating parameter $\mathrm{Re}\,(\epsilon'/\epsilon)$; under this respect one needs to improve the precision of the measurement to $\sim 0.1\%$. Second, from this one can extract the difference between the phase of the amplitudes of the $\pi - \pi$ final state with isospin 0 and 2 ($\delta_0 - \delta_2$). The determinations of this phase shift from previous measurements of kaon decays and from $\pi - \pi$ scattering data [5] show some inconsistency; the present KLOE measurement, $\delta_0 - \delta_2 = 47.8 \pm 0.8°$, is now in agreement with $\pi - \pi$ scattering data.

  The present error is dominantly systematic; preliminary studies show that it is possible to keep these contribution down to the requested level of 0.1%.

- $K_S \to \pi e \nu$. The previous analysis [6] has been repeated on 170 pb^{-1} of 2001 data. A separation between the two states of different leptonic charge has been obtained, providing:

$$\begin{array}{ll} (3.46 \pm 0.09 \pm 0.06) \times 10^{-4} & (K_S \to \pi^- e^+ \nu) \\ (3.33 \pm 0.08 \pm 0.05) \times 10^{-4} & (K_S \to \pi^+ e^- \nu) \\ (6.81 \pm 0.12 \pm 0.10) \times 10^{-4} & (\textit{combined}) \end{array}$$

  From here, the first measurement to date of the leptonic asymmetry has been obtained: $A_S = (19 \pm 17 \pm 6) \times 10^{-3}$. From the same result one can also determine the value $\mathrm{Re}\,x_+ = (3.3 \pm 5.2 \pm 3.5) \times 10^{-3}$ which parameterize the violation of the $\Delta S = \Delta Q$ rule when CPT is conserved.

  Before the inclusion of the 2002 data, further corrections to the time response of the calorimeter have been implemented, together with new MC generators for radiative decays. An accurate treatment of radiative corrections is relevant here, as in the parent charged kaon mode, for the extraction from the measured branching ratio of the CKM parameter V_{us} (see charged kaon section for a more detailed discussion of this issue).

  At present, 23336 ± 253 signal events have been extracted from the entire data set, to be compared with the 624 ± 30 obtained in the 2000 data (see fig.3).

- $\phi \to \eta'\gamma$. From the previously published result $\mathrm{BR}(\phi \to \eta'\gamma)/\mathrm{BR}(\phi \to \eta\gamma) = (6.10 \pm 0.61 \pm 0.43) \times 10^{-5}$ the best evaluation to date of the pseudoscalar mixing angle could be obtained: $\theta_P = (-12.9\,^{+1.9}_{-1.6})°$ [7]. Performing the same analysis on 100 pb^{-1} of the 2001 data, the number of signal event candidates increases from 120 to $\sim$700.

- $\phi \to \pi^0\pi^0\gamma$ ($f_0\gamma$) and $\phi \to \eta\pi^0\gamma$ ($a_0\gamma$). KLOE has published results on this important decay channels, based on the 2000 data [8, 9]. These measurements are crucial to shed light on the nature of the scalar mesons, a_0 and f_0; consequently, the above mentioned results have been matter of lively discussion in the physics community, especially in the case of the $\pi^0\pi^0\gamma$ channel [10] [11] [12]. It is of particular interest, therefore, to use the entire data set to repeat both analyses.

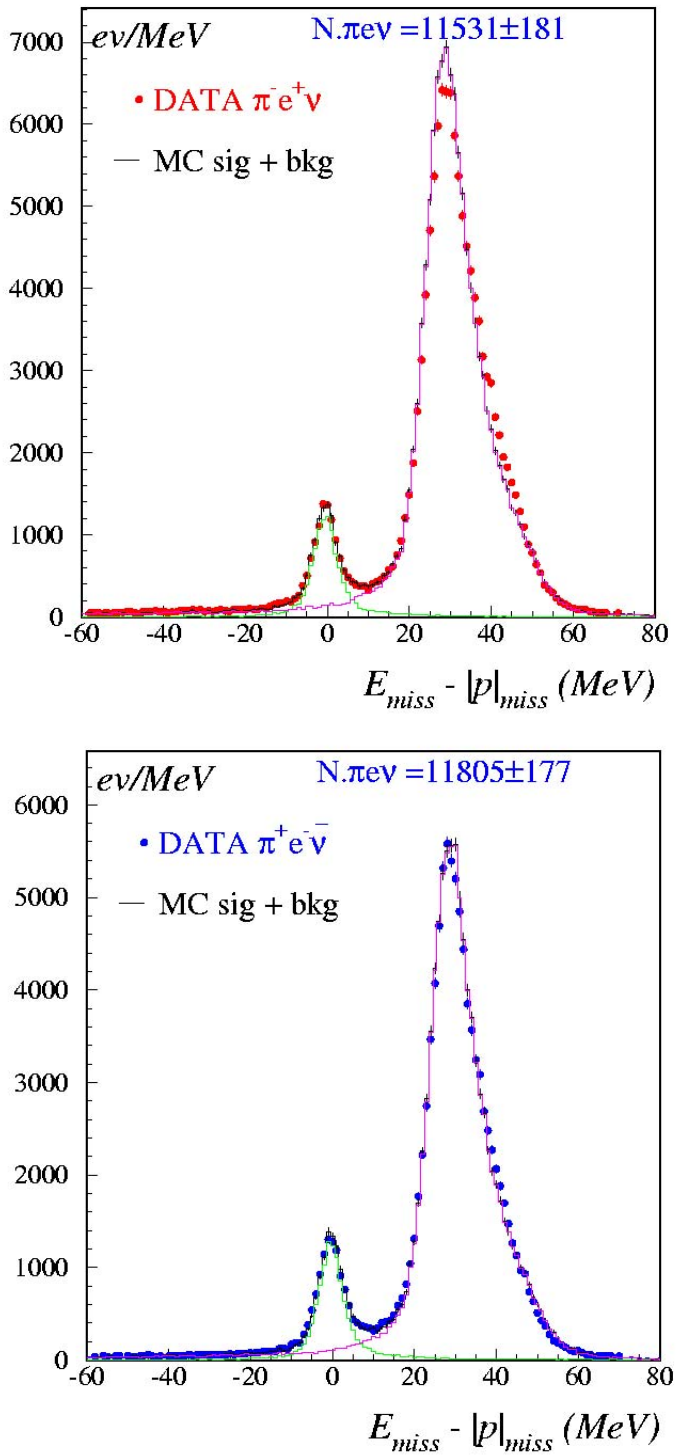

Figure 3: $K_S \to \pi^{\pm} e^{\mp} \nu$ signal (peak at 0) and background (mostly π decays in flight) in $\sim$0.45fb^{-1}.

Due to the increased statistics the analysis strategy has to be refined; in particular, in the study of the $\phi \to \pi^0\pi^0\gamma$ channel the various contribution to the final state $(f_0\gamma, \omega\pi^0, \rho\pi^0)$ and their interference terms are taken into account. In addition, a search for the $\phi \to f_0\gamma \to \pi^+\pi^-\gamma$ decay has been performed, with the purpose of comparing the parameters describing the mass spectrum of this decay to those of the previous one.

4.2 Status of advanced analyses

Other analyses, started during year 2002, have progressed in the following year such to be ready, or almost ready for publication.

- $\Gamma(K_L \to \gamma\gamma)/\Gamma(K_L \to 3\pi^0)$. This is the first published paper based on the entire data set [13]. The KLOE value $(2.793 \pm 0.022 \pm 0.024) \times 10^{-3}$ has the same precision of the measurement of the NA48 experiment at CERN. Ancillary to this analysis is the study of the time distribution of the $K_L \to 3\pi^0$ decays; this will provide a measurement of the K_L lifetime with a statistical error at the level of 0.2%.

- $K^\pm \to \pi^\pm\pi^0\pi^0$ (τ'). The branching ratio of this decay mode has been measured, using 187 pb^{-1} of data for the event counting and the rest of the acquired statistics for the determination of the signal efficiency and other systematics studies. The preliminary result, BR(τ') $=(1.810 \pm 0.013 \pm 0.017)\%$, has been contributed to the summer conferences and is now in the process of being submitted for publication. In an extension of the same analysis the Dalitz plot parameters g, h e k have also been measured, obtaining preliminary values significantly more precise than those reported in the literature.

- $\eta \to 3\gamma$: In the Standard Model, this C violating process is calculated to occur with a branching ratio of $\sim 10^{-12}$; a discovery of a larger decay rate would be therefore a clear indication of new physics. The best published result to date is that of the GAMS2000 experiment which obtained an upper limit of 5×10^{-4} at 90% C.L. [16].

  At DAΦNE, η mesons are produced in the decay $\phi \to \eta\gamma$ with a branching ratio of $\sim$1.3%; therefore more than 10^7 η decays can be observed in the entire 2001-2002 data sample. The energy of the radiative photon ($E_{rad} \sim 363 MeV$) is used to tag the event; three other prompt photons are then searched to kinematically close the event. The most relevant backgrounds come from the 4-photon events $e^+e^- \to \omega\gamma$ with $\omega \to \pi^0\gamma$, and from other decays with more (or less) than four photons with accidental losses (or additions) of photons in the detector. This backgrounds are removed either requiring a minimal photon energy of 50 MeV, or rejecting events with a detected π^0.

  KLOE obtains BR$(\eta \to 3\gamma) \leq 1.6 \times 10^{-5}$, at 95% CL. This result has been contributed to the summer conferences, and the corresponding paper is in the process of being submitted for publication.

- $\sigma(e^+e^- \to \text{hadrons})$. This particularly relevant and delicate analysis has progressed a lot since last year, thanks to the implementation of more refined generators (Phokara, v3.0 and later) and to a careful treatment of correlation effects between the various theoretical corrections to be applied to the raw result. More attention has also been paid to the effects of the experimental resolution on the $M_{\pi\pi}$ spectrum (see fig. 4) and to the determination of the integrated luminosity.

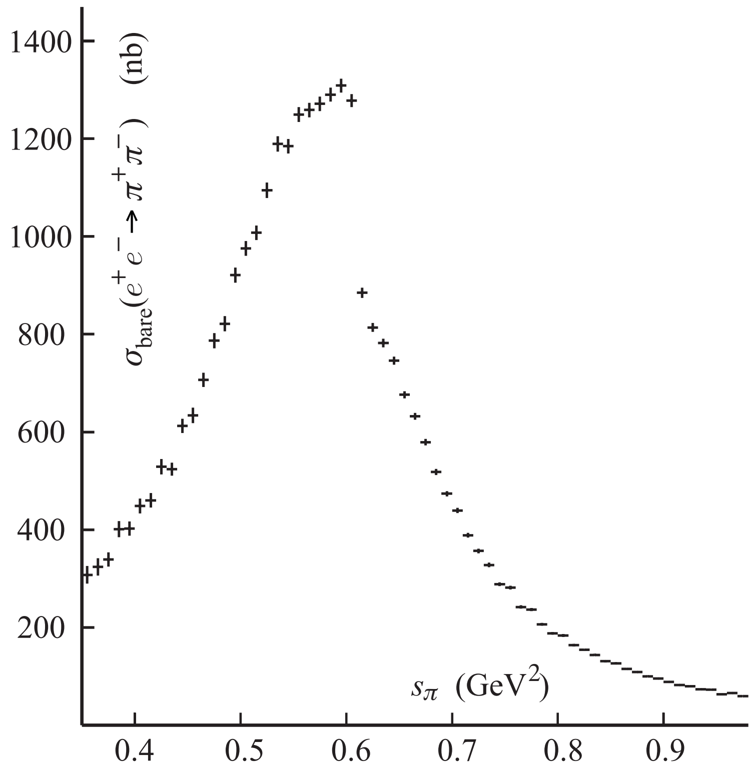

Figure 4: The measured $e^+e^- \to \pi^+\pi^-$ cross section after subtraction of the radiation emission effect.

The first KLOE result on the hadronic contribution to a_μ in the interval $0.37 < M^2_{\pi\pi} < 0.93$ GeV^2, based on the analysis of 2001 data has been presented to the summer conferences [18]:

$$a_\mu \times 10^{10} \; (0.37 < M^2_{\pi\pi} < 0.92 \text{ GeV}^2) = 378.4 \pm 0.8_{\text{stat}} \pm 4.9_{\text{syst}} \pm 3.0_{\text{th}} \pm 3.8_{\text{FSR}}.$$

This result, obtained with a cut on the direction of emission of the photon of 15°, is well compatible with what obtained by the CMD2 experiment at Novosibirsk. In the final result, the uncertainty on the effect of the treatment of the final state radiation (FSR) should disappear; the experimental systematics should also be reduced by about 20%.

- $K_S \to \pi^0\pi^0\pi^0$. The observation of this transition is evidence for CP violation in the $K^0 - \overline{K^0}$ mixing matrix. Its branching ratio can be easily deduced by the known transition rate of the CP-allowed $K_L \to \pi^0\pi^0\pi^0$, by the ratio of the K_S and K_L lifetimes and the value of the CP violation parameter ϵ: the SM theoretical prediction is $\text{BR}_{TH} \sim 2{\times}10^{-9}$. The present experimental limit is: $< 1.4{\times}10^{-5}$ at 90% C.L [19].

A search for this decay has been performed in KLOE, using a sample of K_S decays *tagged* by the observation of the interaction of the accompanying K_L on the EmC (the so called *KCRASH*). Six prompt photons generated at the interaction point are the signature for the signal.

Five events have been found in 450 pb^{-1} of data with an expected background of 3.0 ± 1.3. The preliminary limit on the branching ratio is thus BR $< 3. \times 10^{-7}$ at 90% CL, which is the best limit on this important decay to date.

4.3 Charged Kaons

Although copiously produced at DAΦNE charged kaons are difficult to study because of several effects, such as spiralization of low momentum charged particles in the DC, nuclear interactions on the DC walls, effects of variation of the tracking efficiency inside the DC volume, etc ... The previously mentioned improvements on the simulation of the detector response, are therefore of particular relevance in this case. For this reason, all the results concerning charged kaon decays produced up to now, and listed in the following, have to be considered preliminary.

The decays $K \to \mu\nu$ and $K \to \pi\pi^0$ have been studied using the entire data set. The selection of the events is based on a *tagging* technique by which the presence of one of the two K is inferred by the reconstruction of the decay of the other. The $\mu\nu$ final state is then selected by cutting on the momentum of the secondary particle in the K rest frame (p^*). For both charge states, the total error is of order 0.1%. Systematic errors are still under study. At present, a difference of order 1% is observed between the two charge states, most likely due to nuclear interaction on the DC walls. The effect of final state radiation has to be still taken into consideration.

Also in the case of the $\pi\pi^0$ events, the selection is based on the value of the p^* of the secondary particle. In this case, however, subtracting some background due to $\mu\nu$ and three-body decays is needed. Tracking and vertex efficiencies are still under study.

The various contributions to the p^* spectrum have been studied in detail, using both data and Monte Carlo. A by-product of these studies is the preliminary determination of the ratio BR($K \to \pi\pi^0$)/BR($K \to \mu\nu$): $0.3346 \pm 0.0003 \pm 0022$. This result is obtained by the analysis of $\sim$280 pb^{-1} taken in the year 2002; the quoted error is sizeably smaller than that found in the PDG.

The decay $K \to \pi^0\ e\ \nu$ is particularly relevant for the extraction of the CKM matrix element V_{us}. Actually, the most precise test of unitarity for the CKM matrix can be obtained using the measured values of the elements of its first row; since V_{ub} is small, the relevant parameters are V_{ud}, which is determined by nuclear transitions measurements, and V_{us}, which can be determined by semileptonic kaon decays (both charged and neutral) or by hyperon decays. At present, the experimental situation is controversial, since the values of V_{us} extracted from different decay modes do not agree with each other, and those obtained by kaon decays deviate from the unitarity condition by $\sim$3 sigmas [20]. KLOE can determine V_{us} by using both neutral (as discussed before) and charged kaons.

$K \to \pi^0\ e\ \nu$ decays are searched in events with a π^0 and a charged track originating from a K decay vertex. After removal of the two body decays, good events are selected by a fit on the squared mass of the charged particle, which is obtained from the difference of the time of flight of the electron and the π^0 (see fig. 5). At present, detailed studies are being performed to evaluate from data the selection efficiencies and contaminations. Preliminary results on this important topic are expected for the summer 2004.

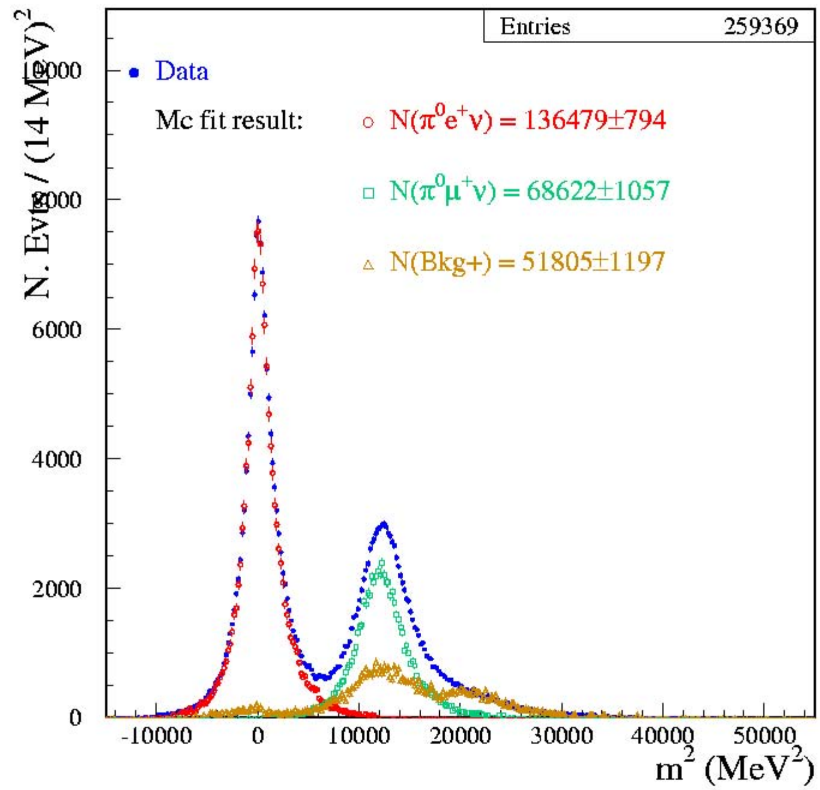

Figure 5: The squared mass of the charged particle in $K^{\pm}$ decays into a charged particle and a π^0.

4.4 Status of recent analyses

- K_SK_L interferometry. It is a well established fact that at a ϕ-factory one can determine all the parameters describing the neutral kaon system via quantum interferometry experiments, i.e. by measuring the decay intensity of the two kaons into well determined final states as a function of the decay time [21]. However, in order to extract these parameters competitively with other techniques, integrated luminosities of order of several fb^{-1} are required.

  A preliminary study on the decay time distribution of the two kaons in $\phi \to K_SK_L \to \pi^+\pi^-\pi^+\pi^-$ events, has been performed on $\sim$340 pb^{-1} of data. The expected dip in the distribution for $\Delta t < 5\tau_S$, due to the initial state being antisymmetric, is clearly observed (see fig. 6). This is the first observation of quantum interference in the decay distribution of a coherent K_SK_L state.

- $K_L \to$ charged particles. K_L decays to charged patrticles have been selected using $\sim$78 pb^{-1} of 2001 data. The momentum spectra of the secondary particles in the K_L reference frame have been analysed, providing preliminary values of the absolute branching ratios of the decays $K_L \to \pi^+\pi^-\pi^0$, $K_L \to \pi\mu\nu$ and $K_L \to \pi e\nu$ with statistical accuracies of order 1%. Systematic effects are presently under study, including those deriving by the proper treatment of the radiation in the determination of the detection efficiencies.

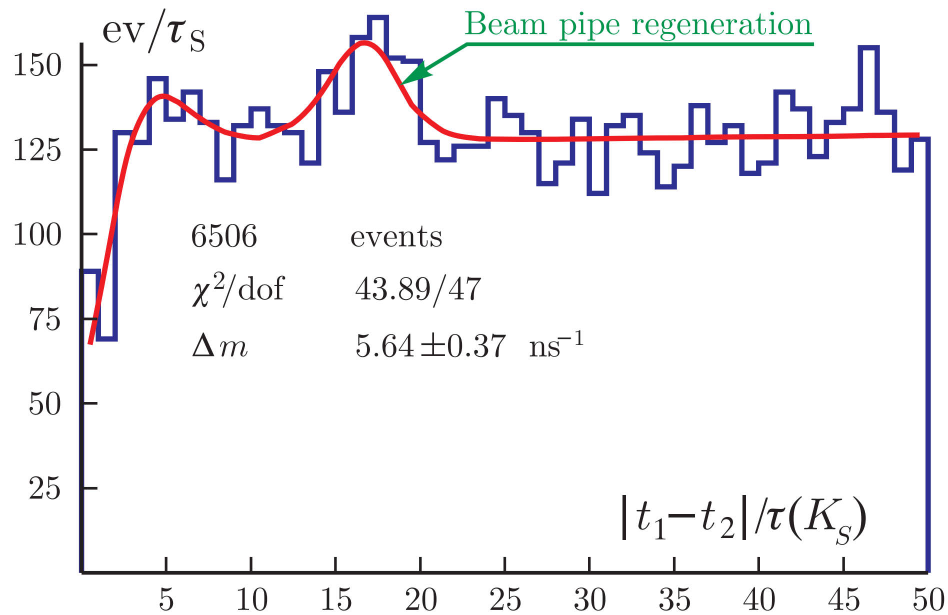

Figure 6: The decay time difference distribution of events with two $\pi^+\pi^-$ pairs in the final state.

As in the case of the charged kaon and of the K_S, the semileptonic K_L decays are relevant for the extraction of the CKM matrix parameter V_{us}.

- Study of the ϕ meson parameters. During year 2002, a set of dedicated runs have been acquired at different values of $\sqrt{s}$: 1017, 1019.5 e 1022 MeV. Each of these samples consisted of about 7 pb^{-1}. With these data, the ϕ production cross section has been measured using all of the four main decay channels, K^+K^-, K_SK_L, 3π and $\eta\gamma$. A precise determination of the width of the resonance has been obtained: $\Gamma_\phi = 4.19 \pm 0.04$ MeV. Moreover, by measuring the forward-backward asymmetry of the reaction $e^+e^- \to e^+e^-$, $\Gamma(\phi \to e^+e^-) = (1.32 \pm 0.05 \pm 0.02)$ keV has been obtained. This is the first direct measurement of $\Gamma(\phi \to e^+e^-)$ to date.

- $\eta \to \pi^+\pi^-\pi^0$. The Dalitz plot of this decay mode has been studied using $\sim$100 pb^{-1} of 2001 data. The values obtained for the parameters describing C-violating effects are consistent with zero within the errors, while the precisions obtained on the other parameters are of the same order of the average PDG values.

- $\eta \to \pi^+\pi^-\gamma$. The preliminary branching ratio BR $= (4.56 \pm 0.04 \pm 0.09)\%$ has been obtained. The total error is a factor about two smaller than that obtained by averaging previous experimental results. The asymmetry between the momenta of the two charged pions has also been measured, obtaining preliminarly $(0.8 \pm 0.4) \times 10^{-2}$

5 Talks by LNF authors in year 2003

L. Passalacqua, Recent results from KLOE, La Thuile Workshop, La Thuile Italy, March 2003.
B. Sciascia, KLOE prospects on $K_{\ell 3}$, 2nd Workshop on CKM, Durham UK, April 2003 (hep-ex/0307016).
P. de Simone, Vus at KLOE, IFAE, Lecce Italy, April 2003.
M. Antonelli, Recent results from KLOE, Capri Italy, May 2003.
M. Moulson, Recent results from KLOE, CIPANP, New York USA, May 2003 (hep-ex/0308023).
C. Gatti, Scalar mesons and $\delta_0 - \delta_2$ at KLOE, International Workshop on QCD, Conversano Italy, June 2003 (hep-ex/0310031).
C. Bloise, Results from KLOE at DAΦNE, HADRON 03, Aschaffenburg Germany, September 2003.
P. Valente, Risultati da KLOE, SIF, Parma Italy, September 2003.
S. Dell'Agnello, KLOE results on neutral kaons, Alghero Workshop, Alghero Italy, September 2003 (hep-ex/0402030).
L. Passalacqua, KLOE results on charged kaons, Alghero Workshop, Alghero Italy, September 2003.
F. Bossi, Searches for $K_L \to \pi^0 \nu \bar{\nu}$ at a Φ-factory, Alghero Workshop, Alghero Italy, September 2003.
F. Bossi, Recent results from KLOE, WIN03, Lake Geneva USA, October 2003.
M. Moulson, The KLOE Computing environment, Portland USA, October 2003.

6 KLOE papers in year 2003

1. KLOE Collaboration *Study of the decay $\phi \to \pi^+\pi^-\pi^0$ with the KLOE detector*, Phys. Lett. **B561**, 55 (2003)
2. KLOE Collaboration *Measurement of the ratio $\Gamma(K_L \to \gamma\gamma)/\Gamma(K_L \to 3\pi^0)$ with the KLOE detector*, Phys. Lett. **B566**, 61 (2003)

References

1. KLOE Collaboration *Nucl. Inst. Meth.* **A488**, 1 (2002).
2. KLOE Collaboration *Nucl. Inst. Meth.* **A482**, 363 (2002).
3. KLOE Collaboration *Nucl. Inst. Meth.* **A483**, 649 (2002).
4. KLOE Collaboration, *Phys. Lett.*, **B538**, 21 (2002).
5. V. Cirigliano, J.F. Donoghue, E. Golowitch, *Eur. Phys. J.*, **C18**, 83 (2000).
6. KLOE Collaboration, *Phys. Lett.*, **B535**, 37 (2002).
7. KLOE Collaboration, *Phys. Lett.*, **B541**, 45 (2002).
8. KLOE Collaboration, *Phys. Lett.*, **B537**, 21 (2002).
9. KLOE Collaboration, *Phys. Lett.*, **B536**, 209 (2002).
10. N.N. Achasov and A.V. Kiselev, *hep-ph/0212153*, (2002)
11. M. Boglione and M.R. Pennington, *hep-ph/0303200* (2003)

12. J.A. Oller, *hep-ph/0205121* (2002)

13. KLOE Collaboration, *Phys. Lett.*, **B566**, 61 (2003).

14. KLOE Collaboration, hep-ex/0307054 (2003), submitted to *International Europhysics Conference on High-Energy Physics (HEP 2003)*, Aachen, Germany, 17–23 July 2003, and to *21st International Symposium on Lepton and Photon Interactions at High Energies (LP 03)*, Batavia IL, USA, 11–16 August 2003.

15. KLOE Collaboration, *Phys. Lett.*, **B561**, 55 (2003).

16. D.M. Alde et al. *Z. Phys* **C25** 255 (1984)

17. KLOE Collaboration, hep-ex/0307042 (2003), submitted to*International Europhysics Conference on High-Energy Physics (HEP 2003)*, Aachen, Germany, 17–23 July 2003, and to *21st International Symposium on Lepton and Photon Interactions at High Energies (LP 03)*, Batavia IL, USA, 11–16 August 2003.

18. KLOE Collaboration, hep-ex/0307051 (2003), submitted to *International Europhysics Conference on High-Energy Physics (HEP 2003)*, Aachen, Germany, 17–23 July 2003, and to *21st International Symposium on Lepton and Photon Interactions at High Energies (LP 03)*, Batavia IL, USA, 11–16 August 2003.

19. M.N. Achasov et al. *Phys. Lett.*, **B459** 674 (1999)

20. see for instance G. Isidori, in *2nd Workshop on the CKM Unitarity Triangle*, P. Ball, J.M. Flynn, P. Kluit, A. Stocchi eds. (2003)

21. G. D'Ambrosio, G. Isisdori, A. Pugliese in *The second DAΦNE Physics Handbook*, L. Maiani, G. Pancheri, N. Paver eds. (1995).

LHCb

M. Alfonsi (Bors.), M. Anelli (Tecn.), G. Bencivenni, C. Bloise, F. Bossi, P. Campana,
G. Capon, M. Carletti (Tecn.), P. Ciambrone, P. de Simone, C. Forti, A. Franceschi, G. Lanfranchi,
F. Murtas, L. Passalacqua, V. Patera (Ass.), M. Poli Lener (Dott.), R. Rosellini (Tecn.),
M. Santoni (Tecn.), A. Saputi (Tecn.), A. Sciubba (Resp.Ass.)

In collaboration with:
"Servizio di Automazione":
U. Denni, M.A. Frani
"Servizio di Elettronica":
A. Balla, F. Bertino, G. Corradi, G. Felici, G. Paoluzzi, G. Papalino.
"Servizio di Sviluppo e Costruzione Rivelatori":
G. Bisogni, A. Ceccarelli

1 Introduction

The LNF group of LHCb operates on the **muon subdetector** with responsibilities on detectors (WPC and GEM), electronics and mechanics. The detector production started at the end of 2003 and is expected to be completed within two years. The electronics production will start in 2004.

2 Multiwire Proportional Chambers

LHCb-LNF has the responsibility for the construction of $\sim 1/4$ of the MWPCs of the muon detector. Depending on the position inside the detector, there are different chamber dimensions with different readout: anode pads, cathode pads, anode & cathode pads.

We designed, collaborating with the Ferrara group, all the details of 10 different chambers types (with active dimensions ranging from 29×35 cm^2 to 31×151 cm^2). With these characteristics 292 chambers will be assembled and tested in LNF. The same design is applied to the remaining 1170 chambers that will be built in Ferrara, Firenze, CERN and S.Petersbourg.

2.1 Brief description of MWPC

The MWPC chambers of the LHCb muon detector must fulfill stringent requirements on time response: for triggering purpose $\sim 99\%$ minimum efficiency must be exploited in 20 ns. Each chamber is constituted by 4 layers assembled as two independent bigaps with hardwired-OR of the readout. In each 5 mm gap there are 30 microns gold plated tungsten wires stretched at about 65 grams with a pitch of 2 mm. The filling mixture is $Ar/CO_2/CF_4$ (40/40/20).

2.2 Main goals reached in 2003

STATUS OF PRODUCTION SITE
In August 2003, the set up of the clean room (transfer and set up of tooling) has been completed. In September-November we started the production of M3R3 chambers with final design. Six of these chambers are completed and two of them have been tested at CERN PS (see below).

Several upgrades of the tooling have been done: automatic gluing of HV bars and of wires, precise setup of the wiring and soldering machines and of the device for wire tension measurement (by Rome-I group). The automatic measurement of the chamber gas leakage has been set up. The device for the measurement of the chamber gap uniformity with a radioactive source (built by Rome-I) is completed and operating.

A lot of effort has been adressed to finalize quality control tests and optimize the work flow.

PANELS

The chamber panels are obtained injecting a rigid polyurethanic foam (ESADUR 120) between two FR4 printed circuit boards. The panel planarity must guarantee the gap uniformity within $\pm$ 90 μm over 95 % of the gap area.

Over a total number of $\sim$ 130 panels produced ($\sim 140 \times 35\ cm^2$) we manually measured the thickness of the last 50 panels and found all thickness values within $\pm$ 40 μm with $\sigma = 21\mu m$.

The Rome-II group has designed and realised a device based on inductive sensors for the automatic measurement of the panel thickness. The tests performed up to now prove that the device can be precisely calibrated. This device is being installed at the production company.

Two new moulds are under construction for M2-3 and M4-5 detector regions. The final set up (with 3 moulds) foresees 20 panels/day. For a total number of 5360 panels, 270 working days are needed, well within our requirements.

CHAMBER TESTS AT CERN PS BEAM

We have tested 2 M3R3 chambers, one with double cathode readout (DC), the other one with single cathode readout (SC). The DC doubles the charge collected on cathode pads, so that we can reach the same efficiency as for SC with a gas gain amplification about a factor 2 smaller. The advantages are that aging is reduced (important for M1) and that chambers can operate at a lower voltage. The main disadvantage is the increase of the capacitive crosstalk, as consequence of a larger pad-pad capacitance ($C_{pp}(DC) \sim 2C_{pp}(SC)$). Capacitive crosstalk is detrimental for P_t evaluation, because it is “in time” (within 20 ns time window) and is independent from the track position in the pad. The requirement fixed in TDR [5, 6] is to have for each station working at $> 99\%$ efficiency in 20 ns time window an “in-time” pad cluster size (i.e. number of adjacent pads fired) less than 1.2.

For double gap chambers the starting point of the efficiency plateau is set by the request to have efficiency 95%. Our measurements show that the plateau for double cathode begins $\sim$ 100 V earlier with respect to single cathode (at 2.45 kV for DC, at 2.55 kV for SC) but also that the cluster size is much more critical for DC (see Fig. 1, left).

We combined the two double gaps to calculate the efficiency and cluster size of the quadrigap. Assuming that plateau begins where efficiency is 99 % and ends where cluster size is 1.2 we found that: DC has a plateau length of $\sim$ 50 V while SC has a plateau length $>$ 100 V (see Fig. 1, right). Taking into account all considerations above, the single cathode readout is the preferred solution for stations M2-5.

Tests with the final front-end electronics have been carried out. Four boards of CARIOCA10 [1] (8 chan. each) have been tested on both (SC and DC) M3R3 chambers. They showed a stable behavior and performances comparable to ASDQ++ [2, 3] ones. We expected an increase of capacitive crosstalk with respect to ASDQ++ due to the increase of input impedance (from 25 to 50 Ohm) but the effect is marginal in particular for SC readout. Results are shown in Fig. 2.

AGING TEST OF CHAMBER PROTOTYPES

An aging test has been performed on a small chamber quadrigap prototype (with active area $\sim 1200\ cm^2$). The test was carried out with the ^{60}Co source of the Calliope gamma facility at ENEA-Casaccia Research Center, near Rome [4]. The source is characterised by a cylindrical geometry with the ^{60}Co pencils placed in the rack circumference . The emitted radiation consists of two photons with energy of 1.17 MeV and 1.32 MeV, mean energy being 1.25 MeV. The maximum

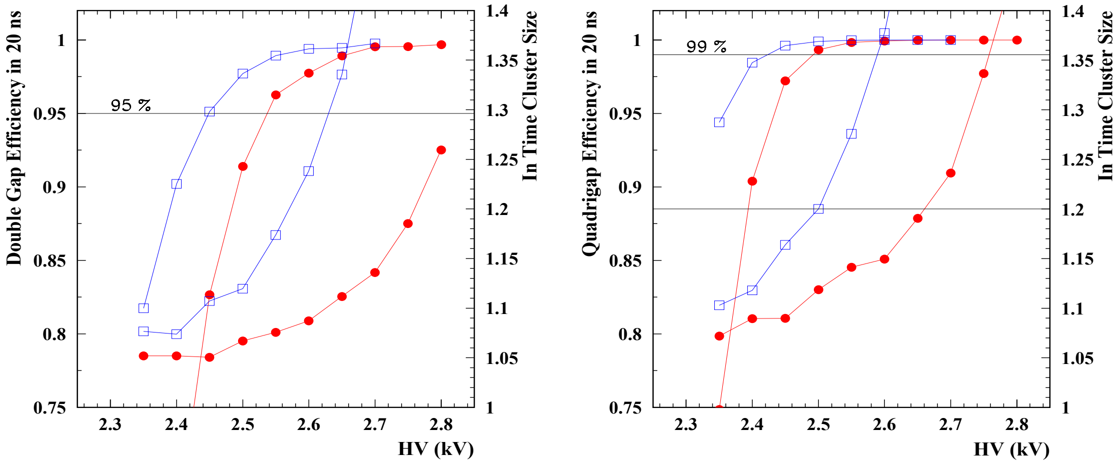

Figure 1: Efficiency and cluster size as function of high voltage for double cathode pad readout (squares) and single cathode pad readout (dots). LEFT: double gap (required efficiency > 95%) RIGHT: quadrigap (required efficiency > 99%).

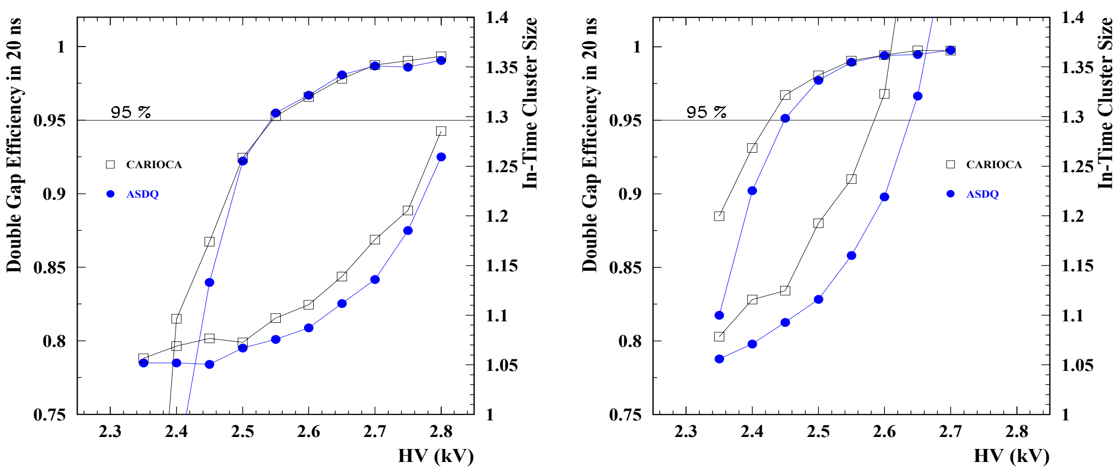

Figure 2: Double gap efficiency and cluster size as function of high voltage for CARIOCA (squares) and ASDQ (dots) boards. LEFT: single cathode pad readout (Threshold ∼ 6.8 fC); RIGHT: double cathode pad readout (Threshold ∼ 8.1 fC).

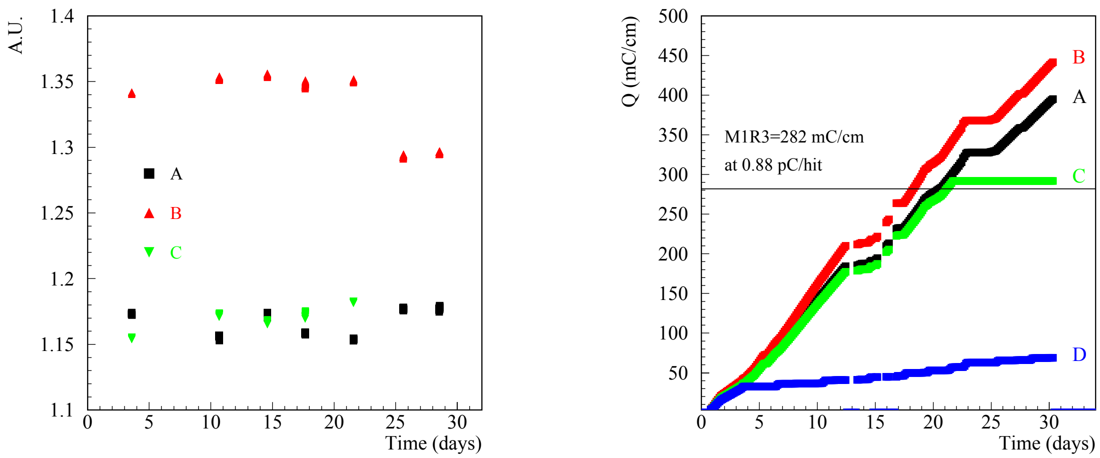

Figure 3: Aging test of a MWPC prototype quadrigap. LEFT: ratio of currents in gaps A,B,C over current in reference gap D; RIGHT: integrated charges in gaps A,B,C,D.

licensed activity is 3.7 10^{15} Bq and the present activity is 7.98 10^{14} Bq (June, 15th, 2003). The gas mixture was $Ar/CO_2/CF_4$ with percentages 40/40/20. We monitored the current in the 4 gaps (A,B,C,D) of the test chamber. The gaps A,B,C were permanently on (at 2.75 kV) while the gap D was used as a reference (was switched on only for few hours every 2-3 days). In Fig. 3 we show the ratios of the currents in test gaps A,B,C over the current in reference gap D. Over $\sim$ 30 days of test, corresponding to $\sim$ 440 mC/cm, we observed no variation in the chamber gain (within $\sim$ 4%). In Fig. 3 we also show the integrated charges. The test is equivalent to $\sim$ 10 years of LHC at luminosity L = 2 10^{32}cm^{-2}s^{-2}, in region M1R2.

3 GEM

4 Triple GEM detectors for M1R1

For the innermost part (regions R1, $\sim$ 0.6m^2 area) of the first muon station (M1) of the LHCb experiment the LNF group, in collaboration with INFN-Cagliari, proposes a detector based on Gas Electron Multiplier (GEM) technology. The requirements [5] for detectors in M1R1 are: a rate capability of $\sim$ 500 kHz/cm^2; each station must have an efficiency of $\sim$ 96% in a 20 ns time window (two independent detector layers per station, logically OR-ed, are foreseen); a cluster size, i.e. the number of adjacent deetctor pads fired when a track crosses the detector, should not be larger than 1.2, for a 10$\times$25 mm^2 pad size. In addition the detector must tolerate, without damages or large performance losses, an integrated charge of $\sim$ 0.88 C/cm^2 in 10 years of operation at a gain of $\sim$6$\times$10^3 and an average particle flux of 184 kHz/cm^2, for an average machine luminosity of 2$\times$10^{32} $cm^{-2}s^{-1}$.
The GEM [7] consists of a thin (50 μm) kapton foil, copper clad on each side, chemically perforated by a high density of holes having bi-conical structure, with external (internal) diameter of 70 μm

(50 μm) and a pitch of 140 μm. In safe condition, gains up to $10^4 \div 10^5$ are reachable using multiple structures, realized assembling more than one GEM at close distance one to each other.
The first part of the R&D, performed with small size prototypes (see the activity report of the 2003 and [8, 9, 10]) was mainly devoted to the optimization of the gas mixture in terms of time resolution. After the gas mixture choice a full size prototype (hereafter module-0), composed by two 20×24 cm^2 triple-GEM detectors, has been built. The module-0, operated with the Ar/CO_2/CF_4(45/15/40) gas mixture and equipped with front-end electronics based on the ASDQ++ chip [2, 3], has been tested at the electron beam facility (BTF) of the Laboratori Nazionali di Frascati.
A global aging test has been successively performed irradiating the whole surface of the two full size chambers of the module-0 with a high intensity 1.25 MeV γ ray flux from the ^{60}Co source of the Calliope facility at ENEA-Casaccia. The two chambers were exposed for about one month to a dose rate of ∼16 Gray/hour, while a third one, used as a monitor chamber was exposed for the same period to a dose rate of ∼0.5 Gray/hour.

4.1 The full size prototype: construction and performance

The full size triple-GEM prototype has an active area of 20×24 cm^2. The intrinsic parameters of the GEM foils are the same of those used for the small size prototypes. The GEM foils are manufactured by the CERN-EST-DEM workshop following our global geometrical design. The main difference with respect to the small size GEM foil is that, in order to reduce the energy stored on the GEM and the discharge propagation, one side of the GEM foil has been divided in six sectors of about 66×240 mm^2. The separation between sectors is 200 μm. The other side of the GEM foil is not segmented.

A detailed description of the detector mechanics and the assembly tools is reported in [11]. The module-0 was realized by coupling two of such 20×24 cm^2 triple-GEM prototypes. The front-end electronics boards, based on the ASDQ++ chip, are mounted on the four side of the module. Taking into account the pad size of 10×25 mm^2, 384 electronic channels are needed to readout the whole module-0.
The module-0 has been tested at the BTF of the Laboratori Nazionali di Frascati. The results [11], shown in Fig. 4, are in good agreement with those obtained with the small prototypes. A large and safe working region (defined as the HV range between the onset of the efficiency plateau and the voltage at which the cluster size is 1.2) of about 90 Volts, is found at electronic thresholds corresponding to 2-3 fC.

4.2 Global aging test of the module-0

Local aging tests, either with a high intensity X-ray beam or with the πM1 hadron beam at the Paul Scherrer Institute (PSI), were performed on small size 10×10 cm^2 triple-GEM prototypes. In both cases, after an integrated charge equivalent to several years of operation at LHCb, negligible aging effects were observed with all the gas mixtures used [11].
Anyway, due to the unprecedented large amount of CF_4 (40%) presents in the gas mixture, in order to check the compatibility between the construction materials (for detectors and gas system) and the gas mixture, a global irradiation test of the final chamber is required.
For this reason we performed a test at the Calliope facility of the ENEA-Casaccia with an intense 1.25 MeV γ ray flux ^{60}Co source. Three full scale prototypes were irradiated on the whole active area at different gamma rates from $\sim$ 1MHz/cm^2 up to $\sim$ 15-20MHz/cm^2. The gas flow rate was 350 cm^3/min, to be compared with the single detector volume of $\sim$ 350 cm^3.

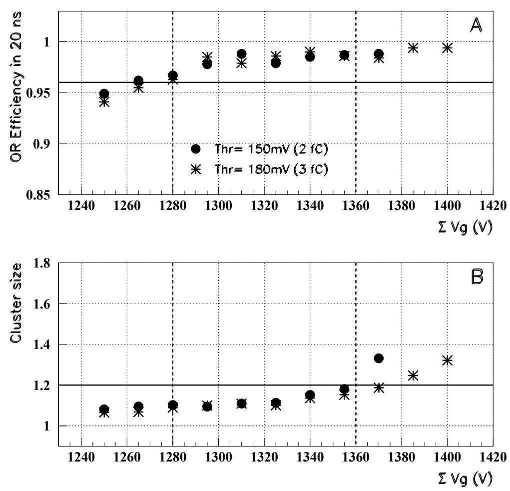

Figure 4: Results obtained with the module-0 at BTF beam test: efficiency in 20 ns time window (A) and cluster size (B) as a function of the sum the voltages applied to the three GEM foil (ΣV_g).

The lowest irradiated detector was used as reference chamber and installed upstream in the same gas line of the high irradiated detectors. The whole gas inlet line was made of stainless-steel tubes, while the exhaust gas line was made of polypropilene tubes (not hygroscopic). A probe was directly installed on the gas line, downstream the test chambers, in order to monitor the temperature and humidity of the gas mixture.

The water content in the gas mixture was substantially kept under few ppm during the whole test. An additional probe supplied the monitor of the atmospheric pressure.

The total accumulated charges on the three prototypes were ~ 0.08 C/cm^2 for the lowest irradiated detector, ~ 0.8 C/cm^2 and ~ 1.1 C/cm^2 for the highest irradiated ones, corresponding respectively to about 1 (chamber C), 8.5 (chamber B) and 11.5 (chamber A) years of operation at LHCb. At the end of the test the chamber C shows no aging, while current drops of ∼89% and ∼80% were observed respectively for chamber A and B.

The negative result obtained in the global aging test can be attributed to the insufficient gas flow rate (350 cm^3/min, the maximum flow reachable with our mass-flowmeters) with respect to the very high gamma rate ($\sim$ 15-20MHz/cm^2 equivalent m.i.p. on the whole detector area, corresponding to a pad current of the order of 400-500 μA) at which chambers were exposed during the irradiation test. On the contrary local tests were perfomed in completely different experimental conditions: a gas flow rate of 100 cm^3/min for a global detector current of 0.2-0.4 μA (over an irradiated area of the order of $1mm^2$).

In this framework we believe that the Casaccia test has been performed in strong gas pollution conditions and then should be considered pessimistic and misleading. Infact, in such test conditions chambers were probably submitted to a strong plasma etching by fluorine, produced in the fragmentation of the CF_4 , and not quickly removed by the gas flow. As a consequence, permanent changes should be found on the GEM foil, in particular on the GEM holes diameter and probably also on the holes shape, especially on the third GEM foil, where the global amplification is larger. Several checks and measurements successively done on the aged chambers support such hypothesis.

4.2.1 *Beam test results on aged chambers*

The two chambers, A and B, were measured before the Casaccia test at the electron beam facility (BTF) of the Frascati Laboratory. After the aging test both chambers have been tested at the PS beam facility at CERN. We thus have the possibility to compare the performances of the aged chambers with those of the same chambers before their irradiation. The results show that aged chambers exhibit practically the same performances (in terms of global efficiency, efficiency in 20 ns time window and pad cluster size) as before their irradiation, except for moderate shifts, at higher voltages, in their working points. Indeed, as shown in Fig. 5, the effect of etching processes seems to be the shift of the operating voltage of the detectors, of about 25 V, without reducing the range of stable operation, 90-100 V, of detectors.
A possible explanation of this behaviour could be that fluorine etching results in GEM holes widening, especially on the third GEM foil, thus decreasing the global gas gain of the detector.

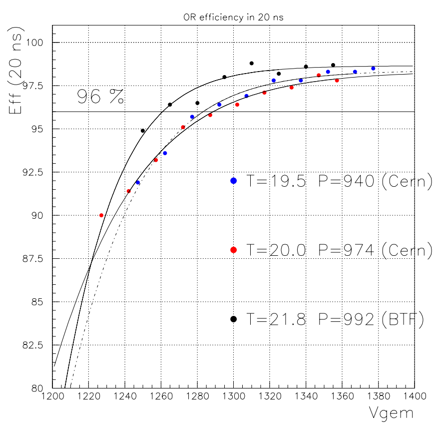

Figure 5: Comparison between the OR-efficiency in 20 ns measured before (at BTF-LNF) and after (at CERN) the aging test at ENEA-Casaccia.

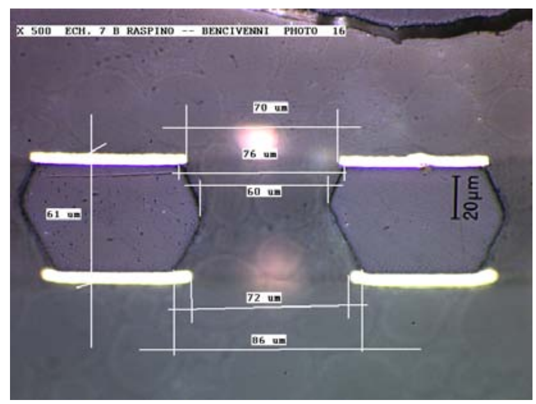

Figure 6: Cross section of the third GEM foil of the aged chamber A. It is clearly visible the etching of the kapton on the bottom part of the hole.

4.2.2 *SEM analysis and X-rays test results on aged chambers*

In order to understand the etching mechanism occurred during the Casaccia test, a scanning electron microscope (SEM) analysis has been performed on various samples of the aged chambers. The results obtained are clearly compatible with a fluorine etching: no polymerization deposits (typical of the so called classical aging) have been observed on the surfaces. As expected the etching effects are larger on the third GEM foil, minor effects are found on the second GEM, while the first GEM does not present any appreciable etching effects. The cathode (drift electrode) and the anode (the pad PCB) are perfectly clean. On both third and second GEMs the observed effect consists in a appreciable widening of the external (copper) holes diameter, from the standard 70 μm up to 80 μm. On the third GEM, where the etching processes were clearly larger, also the kapton inside holes has been etched: the effective holes diameter from the standard 45-50 μm becomes 60-65 μm Fig. 6.

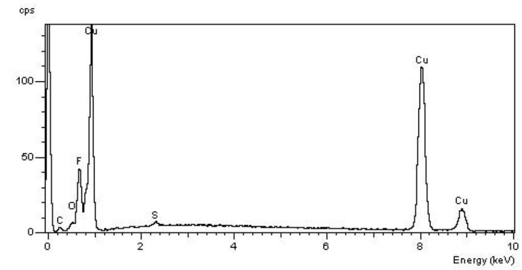

Figure 7: X-ray spectroscopy of the bottom surface of the third GEM foil near the hole edge. The analysis clearly indicates a presence of fluorine.

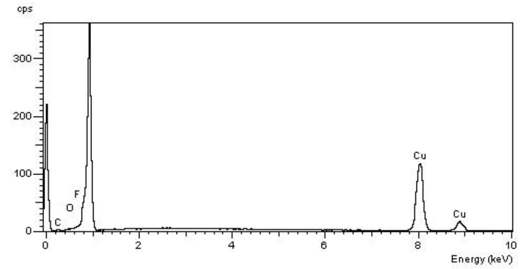

Figure 8: X-ray spectroscopy of the top surface of the third GEM foil near the hole edge. No fluorine has been found in this case.

Fluorine has been found only on the bottom surface of the third and second GEM, being larger on the third GEM and smaller on the second one. Fluorine is mostly located on the copper near the holes edge, leading to the formation of a thin non conductive layer (a fluorine-copper compound) in proximity of the holes, Fig. 7 and Fig. 8. The enlargement of GEM holes leads to a decrease of the gas gain [12], while the etching of the kapton inside the holes and the non conductive layer on the copper near the hole edge, enhancing charging-up effects, reduce the rate capability of the detector (at very high rate). For chamber A the gas gain reduction measured with X-rays (at relatively low particle rate, $\sim$ 1.6MHz/cm^2) is of the order of 50-55% Fig. 9, while the lost in terms of rate capability, Fig. 10, is at a level of 30% at particle rate of $\sim$ 15MHz/cm^2 (the rate capability is fine up to 3-4 MHz/cm^2, well above the LHCb requirements for M1R1, $\sim$500 kHz/cm^2). These results are compatible with the current drop of 89% observed at the Casaccia test.

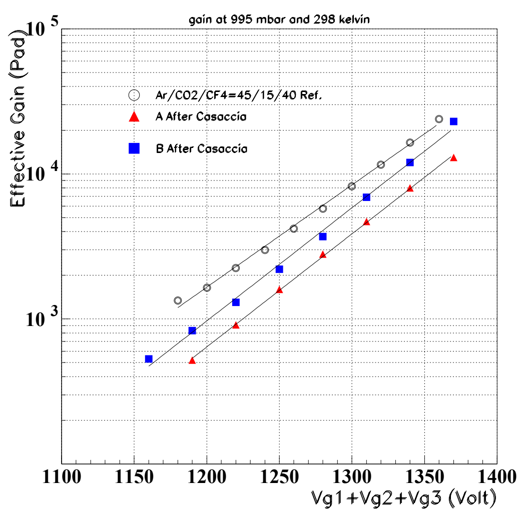

Figure 9: Comparison between the gain measured on a new GEM detector and the gain measured on chamber A and B after the Casaccia aging test.

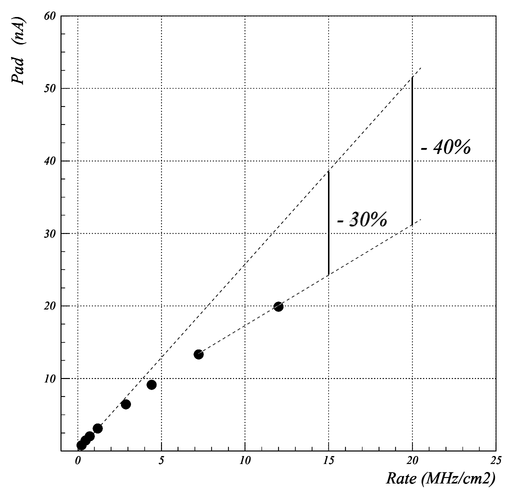

Figure 10: Rate capability of chamber A, measured after the Casaccia test. The measurement has been performed with an X-ray tube.

Finally, in order to demonstrate that the etching observed at the Casaccia test was essentially due to an insufficient gas flow rate compared with the high irradiation level, we reproduced such conditions irradiating with a high intensity X-rays beam a 10×10 cm^2 prototype, flushed with a reduced gas flow, Fig. 11. The current drawn by the chamber was about 1 μA on a $1cm^2$ irradiated area, while the gas flow was $\sim$ 20 cm^3/min . In such conditions we observe a gain drop of about 40% in ∼3 LHCb equivalent years. The test, repeated with a gas flow of $\sim$ 200 cm^3/min and with a current of 0.5μA on a $1cm^2$ irradiated area, gave a result compatible with no aging in about 10 LHCb equivalent years. The results of the severe and systematic tests performed on triple-GEM detectors, indicate that the detector is robust and can tolerate the radiation dose foreseen in 10 years of operation in the region M1R1 of the LHCb experiment: detectors, even after a severe irradiation in very bad conditions, exhibit good time and efficiency (in 20 ns) performances, except for a shift of about 20-25 V on the working point, with practically unaffected working ranges.
In addition the results of the Casaccia test, apparently in disagreement with the other aging tests previously performed, have been understood. We have demonstrated that the etching observed during this test is clearly correlated with bad gas flow rate conditions. No aging occur if the gas flow is properly set. In the LHCb running conditions, where the average current collected on pads by one full size chamber will be of the order of 5μA, a safe gas flow rate could be $\sim$ 100 cm^3/min.

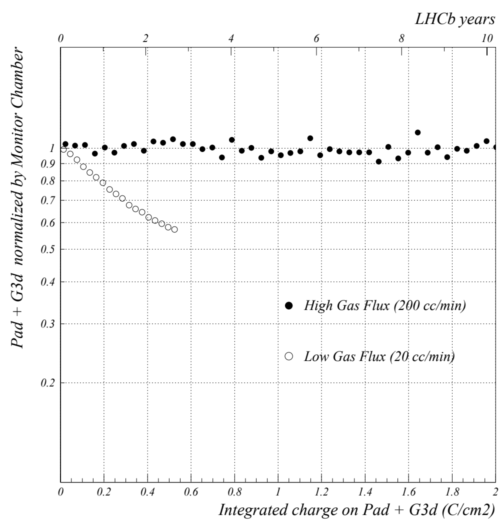

Figure 11: Comparison between the aging measured on a small prototype with low gas flow ($\sim$ 20 cm^3/min) and high gas flow ($\sim$ 200 cm^3/min).

5 Electronics

The LHCb muon trigger architecture relays on 1248 *Trigger Sector* (TS) built by the first stage of the front-end electronic chain.

About 120.000 *physical channels* are firstly merged to generate $\sim$ 26.000 *logical channels* both in the chamber front-end and in the *Intermediate Boards* (IB) system. Then, in the *Off Detector Electronics* (ODE) boards, the logical channels are synchronized to the bunch crossing, arranged to implement the required TS, and, finally sent to the *Level-0* (L0) trigger logic through 1248 optical links at 1.6 Gbit/s.

The ODE board provides also a measure of the signal arrival times with a 1.5 ns time resolution and implements the L0-pipelines, the DAQ interface via a 1.6 Gbit/s optical link and the ECS interface.

As a consequence of the huge number of input channels per boards (192 LVDS) and of the very strict requirements on timing performances for optical link connections (less than 100 ps peak to peak on clock jitter) the design of this board has been very challenging. Over 140 boards will be used to fully instrument the muon detector. A first prototype of ODE has already been realized.

The IB system [13] is used to merge part of the *physical channels* and is made of about 160 boards. Each IB board can manage up to 192 LVDS input signals and 60 LVDS output signals.

To minimize the number of boards (because the chamber/TS geometries we have 5 different IB I/O configurations) the logic functions have been implemented using programmable devices. That choice allowed us to design a single PCB to fit the whole detector geometry. Both for IB and for TB, a first prototype has been realized.

The use of anti-fuse technology for programmable devices (we have used ACTEL devices) gives also an intrinsic robustness in moderate radiation environment (like the levels foreseen near the LHCb detector).

A big effort was devoted to match the skew requirements, due to the huge number of I/O managed by the board. IB and ODE system use a passive Transition Board (TB) to arrange the different topologies of input *logical channels* and are hosted in a mechanical standard 6U VME crate with custom backplane. The backplane allows to interconnect IB and TB boards and to distribute low voltage (+ 2.5V and + 3.3V) to the IB boards. The crate can hold up to 16 boards (5 slots have been reserved for crate power supply).

Both IB and ODE systems are localized close to the detector to minimize the cables length, then the boards must be implemented using radiation tolerant components.

Besides the IB and ODE system the LNF group is also in charge for the low voltage system layout and for the on-chamber low voltage generation.

6 Chamber supporting structure

LHCb-LNF has the responsibility for the construction of the 10 movable walls that will support the chambers in between the iron absorbers of the muon filter. The feasibility of the project was demonstrated in 2002 by building and mounting at LNF a full scale ($4.5 \times 7{,}5$ m^2) light aluminum structure with the dimensions of the second station (M2).

Since then new constraints were put to the structure: the irregularity of the iron blocks of the filter was underestimated by CERN and new earthquake protection rules require a belt system to avoid/reduce shifting of the iron blocks. This enlargement of the iron wall envelope obliged to reduce the thickness of the aluminium wall from 4,4 cm to 2,4 cm. The LNF staff was able to redo the project without changing the building procedure and the related tools. The redrawing process started at the end of last year and will finish soon in order to start bids in 2004.

In the meanwhile it is going on, together with the CERN group, the optimization of the platforms needed to install the racks for the electronics around the detector. The central issue is the moving system that must enable the extraction of the detector walls without de- connecting the electronics and without interfere with closest elements of the cryogenics and the RICH. The adopted solution sees a unique structure per side that will move together the walls of stations M2 to M5. M1 electronics will be housed in the tunnel under the RICH.

7 List of Conference Talks by LNF Authors in Year 2003

- **The Muon Detector FE Trigger Electronics** 9th Workshop on Electronics for LHC esperiments, Holland, September 29 - October 3, 2003;

The results of the R&D on triple-GEM detectors have been presented at the following conferences:

- Frontier Detectors for Frontier Physics, 9^{th} Pisa meeting on advanced detectors, La Biodola, Isola d'Elba, Italy, May 25-31, 2003.
- 23^{rd} International Conference On Photonic, Electronic And Atomic Collisions (ICPEAC 2003), 23-29 July 2003 Stockholm, Sweden.
- 8^{th} ICATPP Conference on Astroparticle, Particle, Space Physics, Detectors and Medical Physics Application, Villa Erba, Como, Italy, 6-10 October 2003.
- IEEE 2003, Nuclear Science Symposium (NSS) and Medical Imaging Conference (MIC), 19-24 October 2003, Portland, Oregon, USA.

References

1. http://home.cern.ch/riegler
2. F.M. Newcomer et al., IEEE Trans. Nucl. Sci., **40**, No. 4, 630(1993).
3. Performance study of a MWPC prototype for the LHCb Muon System with the ASDQ chip, A. Kachtchouk et al., LHCb-MUON 2000-062.
4. S. Baccaro, A. Festinesi, B. Borgia, "Gamma and neutron irradiation facilities at ENEA-Casaccia Center (Rome)", Report **CERN-CMS/TN, 95-192** (RADH), 1995.
5. LHCb Collaboration, "LHCb: muon system technical design report", **CERN LHCC MUON 2001-010**, LHCb TDR 4, 28 May 2001.
6. LHCb Collaboration, "LHCb: Addendum to muon system technical design report", CERN LHCC MUON 2003-002, LHCb TDR 4 Addendum 1, 15 January 2003.
7. F. Sauli, Nucl. Instrum. Meth. **A386** (1997) 531.
8. G. Bencivenni et al., Nucl. Instrum. Meth. **A478** (2002) 245.
9. G. Bencivenni et al., Nucl. Instrum. Meth. **A488** (2002) 493.
10. G. Bencivenni et al., Nucl. Instrum. Meth. **A494** (2002) 156-162.
11. M. Alfonsi et al., High-rate particle triggering with triple-GEM detector, proceeding of 9^{th} Pisa meeting on advanced detectors, La Biodola, Isola d'Elba, Italy, May 25-31, 2003; accepted for publication on Nucl. Instrum. Meth. A.
12. S. Bachmann et al., Nucl. Instrum. Meth. **A438** (1999) 376.
13. A. Balla et al., Muon Off-Detector electronics: The IB system, LHCb note, LHCb 2003-023

NEMO

M. Cordelli, A. Martini, L. Trasatti (Resp.)

1 Activity

In the framework of an european effort toward the construction of a kilometer cube detector for neutrino astronomy, the NEMO project has studied in detail the best possible sites im the Mediterranean sea, and produced several instruments to study the marine depths. During the year 2003 the group has participated in the ANTARES effort and has been preparing for the Catania Test Site. A pilot project, NEMO Phase 1, is proceeding toward the construction of two towers at the Catania Test Site.

The experiment includes groups from: INFN Bari, Bologna, Catania, Genova, LNF, LNS, Messina, Roma1.

The LNF group has continued working on the prototype of NERONE, an instrument to measure with great accuracy the water transparency using measurements performed at several distances from the source. The mechanics, data acquisition and underwater movement using a small stepping motor is now working properly. We are currently improving the quality of the laser light source and plan several deployments during 2004.

OPERA

F. Bersani Greggio (Ass.), E. Blanco (Osp.), C. Di Troia (Dott.),
B. Dulach, G. Felici, A. Franceschi, F. Grianti (Ass.), A. Gambarara (Tecn.),
A. Mengucci (Tecn.), T. Napolitano, A. Paoloni (Ass. Ric.), M. Spinetti (Resp.),
L. Terminiello (Ass.), F. Terranova, M. Ventura (Tecn.), L. Votano

In collaboration with:

LNF-SEA: A. Balla, G. Corradi, U. Denni, A. Frani, G. Paoluzzi, G. Papalino
LNF-SPAS: A. Cecchetti, D. Orecchini
LNF-SSCR: G. Bisogni, G. Catitti, A. Ceccarelli, E. Iacuessa, A. Tiburzi
LNF Divisione acceleratori (Magnet and Power supply Group): M. Incurvati, C. Sanelli

1 The experiment

The aim of the OPERA experiment [1] is the observation of $\nu_\mu \to \nu_\tau$ oscillations in the parameter region indicated by Super-Kamiokande as the explanation of the zenith dependence of the atmospheric neutrino deficit. OPERA is a long baseline experiment to be located at the Gran Sasso Laboratory (LNGS) in the CNGS neutrino beam from the CERN SPS. The detector design is based on a massive lead/nuclear emulsion target. The target is made up of emulsion sheets interleaved with 1mm lead plates and packed into removable "bricks" (56 plates per brick). The bricks are located in a vertical support structure making up a "wall". Nuclear emulsions are used as high resolution tracking devices, for the direct observation of the decay of the τ leptons produced in ν_τ charged current interactions. Electronic detectors, positioned after each wall, locate the events in the emulsions. They are made up of extruded plastic scintillator strips read out by wavelength-shifting fibers coupled with photodetectors at both ends. Magnetised iron spectrometers measure charge and momentum of muons. Each spectrometer consists of a dipolar magnet made of two iron walls interleaved with pairs of precision trackers. The particle trajectories are measured by these trackers, consisting of vertical drift tube planes. Resistive Plate Chambers (RPC) with inclined strips, called XPC, are combined with the precision trackers to provide unambiguous track reconstruction in space. Moreover, planes of RPCs (Inner Tracker) are inserted between the magnet iron plates. They allow a coarse tracking inside the magnet to identify muons and ease track matching between the precision trackers. They also provide a measurement of the tail of the hadronic energy leaking from the target and of the range of muons which stop in the iron. A block of 31 walls+scintillator planes, followed by one magnetic spectrometer constitutes a "super-module". OPERA is made up of two supermodules located in the Hall C of LNGS (see Fig. 1). The total number of bricks amounts to 206,336 resulting in a target mass of 1766 tons.
The discovery potential of OPERA originates from the observation of a ν_τ signal with very low background level. The direct observation of $\nu_\mu \to \nu_\tau$ appearance will constitute a milestone in the study of neutrino oscillations. Moreover, OPERA has some sensitivity to the sub-dominant $\nu_\mu \leftrightarrow \nu_e$ oscillations in the region indicated by the atmospheric neutrino experiments. It has been shown [2] that the CNGS beam optimized for ν_τ appearance, will improve significantly (about a factor of five for ICARUS and OPERA combined, a factor of three for OPERA alone) the current limit of CHOOZ and explore most of the region $\sin^2 2\theta_{13} \simeq \mathcal{O}(10^{-2})$.
Opera is an international collaboration (Belgium, China, Croatia, France, Germany, Israel, Italy, Japan, Russia, Switzerland, and Turkey) and the INFN groups involved are Bari, Bologna, LNF (Frascati), LNGS (Gran Sasso), Naples, Padova, Rome and Salerno.

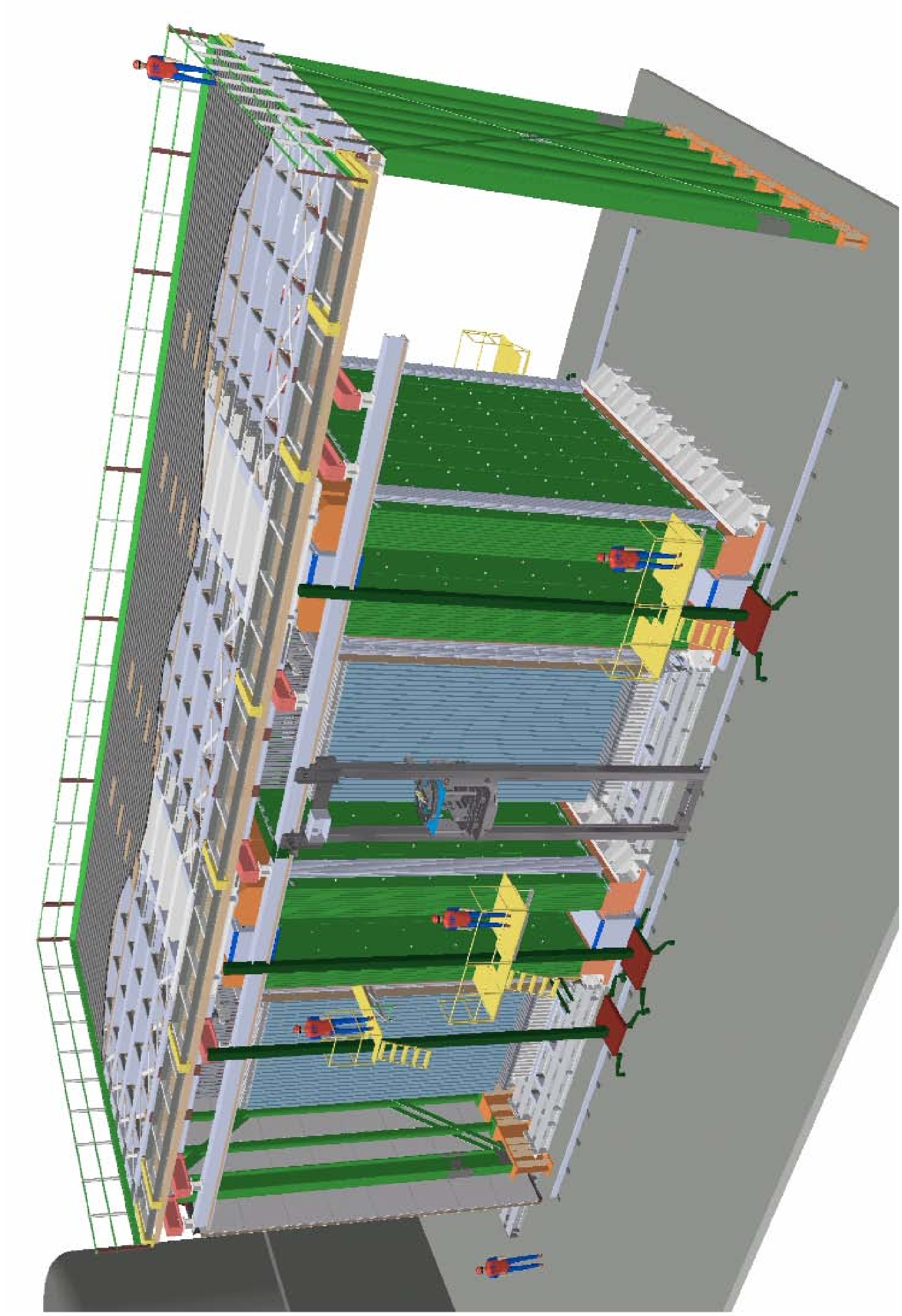

Figure 1: Side view of OPERA.

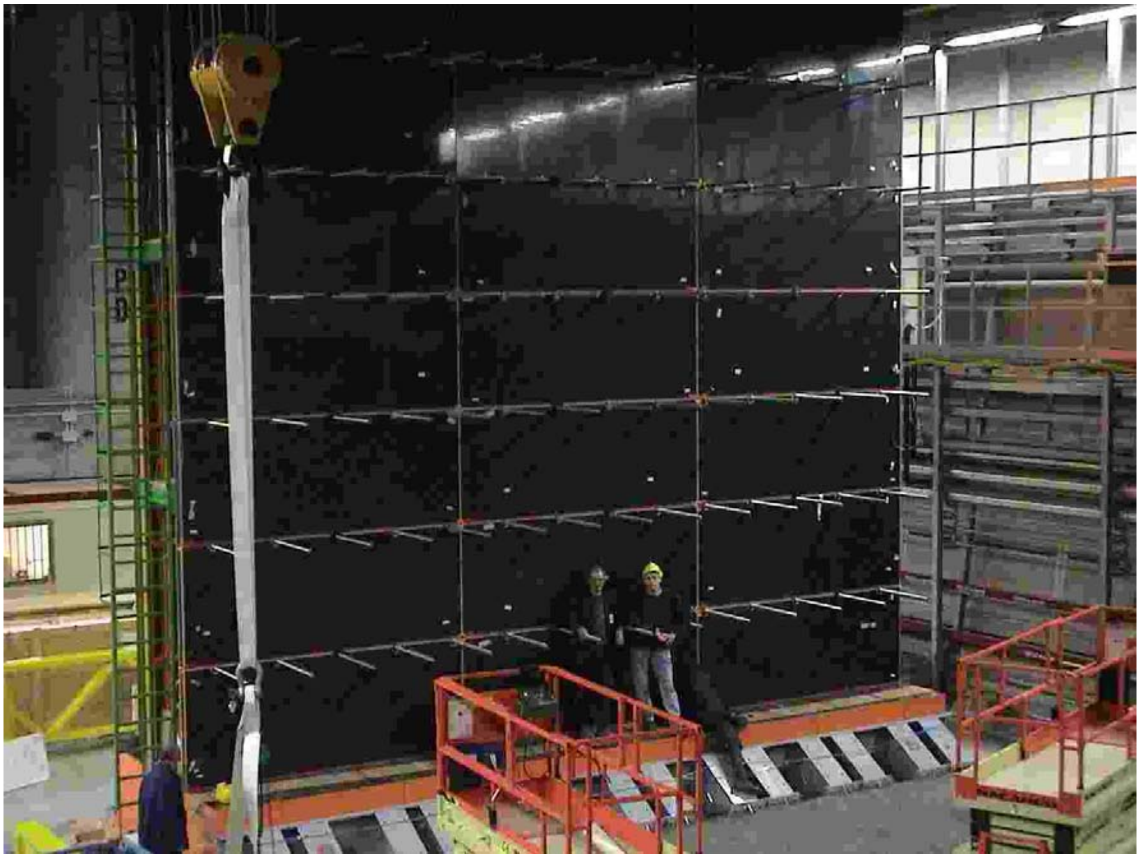

Figure 2: Installation of the first RPC plane at LNGS.

2 Overview of the OPERA activities in 2003

The prototyping phase of the electronic detectors has been completed in 2002 (spectrometers, drift tubes) and 2003 (target tracker). The installation of OPERA at LNGS started in February 2003. It was temporarily halted in May, after sealing of the experimental hall due to the investigations on the accidental Borexino pseudocumene discharge in summer 2002 and it has been restored in August. At the time of writing (January 2004), the lower return yokes of the two magnets have been installed together with the connecting support structure. Two vertical walls have been positioned and fully instrumented with Resistive Plate chambers (Fig. 2). The completion of the first spectrometer is foreseen in June 2004 while the installation of the target tracker will start in fall 2004. The mass production of nuclear emulsions started in April 2003 and will end in spring 2005. After production at Fuji Inc., the emulsion sheets are refreshed underground in Japan and sent to Gran Sasso. The emulsion storage area, located in an experimental hall of LNGS, was built in summer 2003. The development of the scanning system has improved significantly. A peak scanning power of 20 cm^2/h has been reached by the european laboratories while the current scanning speed at 90% efficiency is of the order of 10 cm^2/h.

3 Activities in Frascati

The Frascati group is responsible for the design and construction of the dipolar magnets and the general support structure for the subdetectors. It shares responsibility with INFN Padova and LNGS for the construction and installation of the bakelite RPC planes (Inner Tracker). Frascati and Naples also designed and prototyped the wall support structure housing the lead/emulsion bricks. Moreover, the group contributes to software development and to the analyses aimed at assessing the performance of the experiment after the completion of the CNGS programme. Finally, since 2002 LNF is involved in the construction of the Brick Assembly Machine (BAM).

3.1 OPERA General layout

The overall support structure for the OPERA subdetectors has been designed by LNF-SPAS in collaboration with external firms. It has been re-optimized in 2002 for the two-spectrometer design [3] and finalized at the beginning of 2003. The studies included risk analysis and full seismic response. Tendering and ordering for the support structure have been carried out in 2003. The installation of the upper support rails and the seismic dumping structure will start in summer 2004, after completion of the first spectrometer. LNF-SPAS follow closely the installation procedure at LNGS, validate the positioning of the slabs, coordinate material transportation and survey the installation tasks with the external firms operating in the underground hall.

3.2 Magnets

The mass production of the iron for both spectrometers has been carried out in 2003. During the production phase, chemical analyses were done by the steel producers on a heat by heat basis. Moreover, the magnetic properties of the steel produced for the iron walls and return yokes were checked in a direct manner: small toroidal samples were produced and, for each sample, hysteresis curves have been drawn at different H_{max} and the coercivity has been determined. A systematic difference between the properties of the steel used for the vertical slabs and the one used to construct the prototype of the spectrometer [4] has been observed. It was traced back to the Manganese fraction allowed to be compliant with the mechanical specifications. The monitoring system was validated in 2002 with a full-height prototype built in Frascati. It is based on a set of pick-up coil read during current ramp-up ("ballistic measurements"). Relative variations of the field can be monitored indirectly by the power supply current monitors. However, additional information will be provided by a set of Hall probes glued to the RPC, which measure the fringe field in the 2 cm air gap. These data will be used to validate the simulation and to monitor possible long term drifts of the field. Similarly, Hall probes will monitor the fringe field in air outside the RPC gaps, particularly in the region where the phototubes reading the scintillator bars are located. The Hall probe system has been designed in summer 2003 [5] and delivered to LNGS in January 2004. The magnetization coils will be connected to a power supply located at the top of the spectrometer [6]. It has to deliver a stable steady current up to 1700 A with a maximum output voltage of 20 V. The power supply specifications have been finalized in 2003 in collaboration with LNGS (A. Fulgenzi) and LNF Magnet and Power supply Group; the tender is in progress and the delivery at LNGS is foreseen at the end of 2004.

3.3 Wall support structure

The wall support structure is made of thin stainless steel vertical bands welded to light horizontal trays where the bricks are positioned with a precision of one millimeter. The structure is suspended through rods and joints from the general support structure and tensioned from the bottom through a spring system. The prototyping phase was completed in 2002. Three prototypes have been built. A full width and 1 m high prototype was used to test the Brick Manipulator system in Annecy; one full size prototype was completed before the start-up of the mass production and sent to Gran Sasso. Moreover, one prototype (full height and 1 m wide) was assembled at LNF in 2000 and tested in 2001. Long term elongations due to the weight of dummy bricks have been monitored also in the subsequent years. Tendering and ordering have been completed after final definition of the brick dimensions. First delivery at LNGS is expected in September 2004. In the meanwhile, the detailed installation procedure was finalized by LNF-SSCR and the installation tooling is under construction at Frascati. The desing of the springs connecting the wall to the support structure has been completed and mass production has started.

3.4 Inner trackers

The mass production of the detectors started in Jan 2003 and the RPC for the first spectrometer have already been produced. Several validation tests are in progress [15]: test of gas tightness at the production site, mechanical tests, electrical tests and efficiency measurements with cosmic muons. The mechanical tests have been fully automatized. Presently, after a leakage test, a mobile bridge housing a set of pistons is moved in the proximity of the spacers that connect the two bakelite electrodes and fix the depth of the gas volume. The pistons are lowered in order to exert pressure onto the upper RPC surface. An abnormal variation of pressure indicates the presence of unglued spacers. A further test determines the exact position of the defective buttons. The electrical tests [7] have been designed to measure the current-voltage characteristics in pure argon, the current-voltage characteristics in gas mixture (Argon 75.5%, TFE 20%, isobutane 4%, SF_6 0.5%) and the short term behaviour of the RPC at voltage. The facility developed in 2003 allows to test 48 RPCs simultaneously. The current-voltage characteristics in argon allows to check the cleanliness of the internal surface of the gap and to measure the average resisitivity of the two electrodes. The chambers are characterized by their current derivative dI/dV, their primer voltage at fixed currents (I=100 nA and 500 nA) and their current at nominal operating voltage. Finally, a short term test is performed (for minimum 24 hours up to few days). The RPC is kept at fixed voltage and the time stability of the current is monitored. The cosmic ray test [16] is carried out employing a test facility built at the beginning of 2003. Two large planes of glass RPC are used for triggering purpose. The RPCs under tests are placed inside boxes, (12 RPCs/box), in vertical position and their efficiency are computed selecting isolated cosmic muons. The overall fraction of accepted RPC is $\sim$83%. The main source of rejection is due to the poor gluing of the spacers: about 10% of the RPC fail the mechanical test. Failure at the electric test contribute to 0.5%; poor or strongly non-uniform efficiencies are observed in 6.5% of the RPC (failure of the cosmic ray test). The tasks concerning the design and construction of the RPC electronics [17] are shared among LNF-SEA (strip boards, current monitoring, fast signals for TDC), Padova (front-end boards) and Naples (controller boards interfaced to DAQ) and coordinated by G. Felici (LNF). The design of the strip board has been finalized in December 2002 and the production has been completed in 2003. The final prototype of the current monitoring system [8] has been built and tested at LNGS. The production will start in spring 2004. The prototyping of the front-end timing board to be connected to the strip board has been completed while the design of the remote part of the timing board is in progress [8]. The mass production of this system is expected to start in summer 2004.

3.5 Brick Assembly Machine

During 2003 an alternative solution for brick packaging has been considered by LNF-SSCR. Under this hypothesis, the tightness of the brick is guaranteed by adhesive tapes and pressure is exerted

Figure 3: Shear force tests of the lead/emulsion brick at LNF.

mechanically through springs. The main advantage of this option is that vacuum is not needed and the classical stringent requirements on leakage rate, which imply dedicated welding and packaging procedures for the lead/emulsion stack, can be sidestepped. The new procedure was tested in Frascati and several mechanical tests have been done (Fig. 3). Moreover, one brick has been exposed to a testbeam to evaluate the precision in the lead/emulsion positioning, the light tightness and the unpacking procedure. Preliminary results show performances comparable to the baseline (vacuum) option. A final decision will be taken early in 2004. LNF has also gained experience in the construction of the vacuum-based option and contributed to the preparation and completion of the tender for the construction of the BAM.

3.6 Software and analysis

In 2003 significant modifications of the OPERA offline chain has been made. The final geometry of the experimental setup was implemented in Geant3 through an AliROOT-based framework. The detector response ("digitization") has been finalized for all the electronic detectors. LNF contributed to the simulation of the magnetic spectrometers, the embedding of the magnetic field maps and the development of reconstruction algorithms for charged particles [9]. The sensitivity of the CNGS beam to the sub-dominant $\nu_\mu \leftrightarrow \nu_e$ oscillations has been updated including the effect of the CP violation phase and the lack of knowledge of the neutrino mass hierarchy (sign of Δm^2_{13}) [13]. Studies of the performance of an OPERA like detector at a future Neutrino Factory have also been carried out [14].

References

1. M. Guler *et al.*, OPERA proposal, CERN/SPSC 2000-028, SPSC/P318, LNGS P25/2000.
2. M. Komatsu, P. Migliozzi, F. Terranova, J. Phys. G29 (2003) 443.
3. See "LNF 2002 Annual Report", S.Dell'Agnello ed., LNF-03/010 (IR), p.59.
4. G. Di Iorio et al., *Measurements of the Magnetic Field in the Prototype of the OPERA Spectrometer*, OPERA note, LNF-01/028.
5. F. Terranova, *Specifications for the Hall-probe system of the OPERA iron spectrometer*, OPERA Note.
6. A. Fulgenzi et al., *Specifications of n.2 power supplies for the OPERA magnets*, OPERA note.
7. A. Paoloni, *Conditioning test*, Talk at the OPERA coll. meeting (LNGS, 19 -23 May, 2003).
8. G. Corradi, *RPC current monitor and tracking timing signal generation*, Talk at the OPERA coll. meeting (LNGS, 19 -23 May, 2003).
9. F. Terranova, *A full simulation of charge and momentum reconstruction in the OPERA spectrometers*, OPERA Note.

Conference talks by LNF authors

10. A. Paoloni, *Long term operation test of RPCs for the OPERA experiment*. Talk at the VII Workshop on Resistive Plate Chambers and Related Detectors (Clermont-Ferrand, France, 20-22 Oct. 2003), to appear in Nucl. Instrum. Meth.
11. F. Terranova, *The OPERA magnetic spectrometer*, Talk at IEEE Nuclear Science Symposium, (Portland, Oregon, 20-24 Oct. 2003).
12. F. Terranova, *On-peak and off-peak neutrino oscillation experiments*, Talk at 19th International Workshop on Weak Interactions and Neutrinos WIN03 (Lake Geneve, Wisconsin, 6-11 Oct. 2003).

Publications by LNF authors

13. P. Migliozzi and F. Terranova, Phys. Lett. B563 (2003) 73.
14. D. Autiero et al., *The synergy of the golden and silver channels at the neutrino factory*, hep-ph/0305185, to appear in Eur. Phys. J.
15. A. Garfagnini et al., *Quality control tests on RPCs for the OPERA experiment* , Proceedings of the VII Workshop on Resistive Plate Chambers and Related Detectors (Clermont-Ferrand, France, 20-22 Oct. 2003), to appear in Nucl. Instrum. Meth.
16. C. Gustavino et al., *The OPERA test facility at the Gran Sasso*, Proceedings of the VII Workshop on Resistive Plate Chambers and Related Detectors (Clermont-Ferrand, France, 20-22 Oct. 2003), to appear in Nucl. Instrum. Meth.
17. G. Sorrentino et al., *The OPERA muon spectrometer tracking electronics*, Proceedings of the VII Workshop on Resistive Plate Chambers and Related Detectors (Clermont-Ferrand, France, 20-22 Oct. 2003), to appear in Nucl. Instrum. Meth.

PVLAS

E. Zavattini[1], G. Zavattini[2], A. Zanetti[1], G. Ruoso[3], E. Polacco[4],
E. Milotti[5], S. Marigo[3], M. Karuza[1], U. Gastaldi[3], G. Di Domenico[2], F. Della Valle[1],
R. Cimino(Resp.loc)[6], S. Carusotto[4], G. Cantatore[1]

1) Dipartimento di Fisica and INFN, Trieste; 2)Dipartimento di Fisica and INFN, Ferrara;
3) INFN, Laboratori Nazionali di Legnaro; 4) Dipartimento di Fisica and INFN, Pisa;
5) Universita' di Udine and INFN Trieste; 6) INFN, Laboratori Nazionali di Frascati;

Vacuum magnetic birefringence is an effect predicted by Quantum Electro-Dynamics (QED), but not yet experimentally confirmed. According to this view, the quantum vacuum behaves as an optically active medium when perturbed by an external magnetic field. A linearly polarised laser light beam can be used as a probe of this effect: after propagating through a vacuum region in the presence of a transverse magnetic field its polarization state will change to elliptical, and the parameters of the polarization are directly related to the fine structure constant and the Compton wavelength of the electron. Contributions for a vacuum magnetic birefringence could also come from the existence of light scalar/pseudoscalar particles that couple to two photons. The PVLAS collaboration has developed an optical ellipsometer capable of detecting very small changes in the light polarization state induced by a time-varying magnetic field. The apparatus is based on a high finesse, high quality factor Fabry-Perot (FP) optical resonator and a superconducting dipole magnet housed in a rotating cryostat. The cryostat is placed over a turntable which can rotate at frequencies up to a few Hertz. Figure 1 shows the PVLAS site. During 2003 the experiment has continued both data taking and analysis. In addition, the vacuum part of the apparatus has been redesigned in order to improve the pneumatic vacuum base pressure and to be able to reduce the mechanical coupling between the rotating field and the permanent magnets of the vacuum ion pumps. This upgrade has been implemented and successfully tested. Furthermore, a structure in non-magnetic material, for accessing the cryostat and the upper optical bench, has been designed.

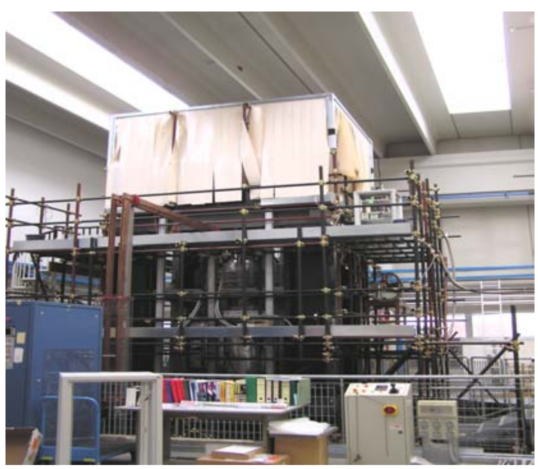

Figure 1: *View of the PVLAS granite tower holding the optics.*

RAP

S. Bertolucci, G.O. Delle Monache, G. Ceccarelli (Tecn.), R. Ceccarelli (Tecn.),
M. De Giorgi (Tecn.), D. Di Gioacchino, V. Fafone, C. Ligi (Art.23), R. Lenci (Tecn.),
A. Marini, G. Mazzitelli, G. Modestino, G. Pizzella (Ass.), S. Panella (Lau.),
L. Quintieri (Art.23), S.Roccella (Dott.), G. Raffone, F. Ronga (Resp.Naz.), P. Tripodi (Ass.)
and P. Valente (Art.23)

1 Aim of the experiment

The primary goal of the experiment RAP [1] is to measure the vibrations of a small cylindrical test mass when hit by electrons provided by the DAΦNE Beam Test Facility (BTF).
The experiment was motivated by the studies [2] of the signals due to the interactions of cosmic rays impinging the gravitational wave antenna NAUTILUS. In particular, in a run of the detector at thermodynamic temperature $T = 1.5K$ the results are in agreement with the thermo-acoustic model (TAM), while in a run at $T = 0.14K$ (below T_c, the transition temperature to the superconducting state) large signals have been detected at a rate higher than expected.
TAM accounts for the mechanical vibrations originated by the local thermal expansion due to the warming up of the material crossed by particles loosing their energy in the interaction. More precisely, the detectable vibrational energy E_n in the n$-th$ longitudinal vibration mode due to a specific energy loss, dW/dx, of a particle impinging a cylindrical bar is [3]:

$$E_n \propto \gamma^2 \left[\frac{dW}{dx}\right]^2 F_n^2$$

Here F_n is a function of geometrical parameters related to the particle track in the absorber and γ is the Grüneisen parameter of the material, proportional to the ratio of the coefficient of thermal expansion to the specific heat at constant volume.
The test mass of RAP can be operated either in the superconducting or in the normal state in order to: (a) verify if a higher efficiency mechanism (perhaps related to γ) for the particle energy loss conversion into mechanical energy takes place when the bar is in the superconducting state and (b) confirm the results on TAM obtained by previous experiments [4] at room temperature.

2 Setup

The experimental setup is composed by the beam and the detector.
The characteristics of the DAΦNE BTF e^+/e^- beam are described elsewhere in this report.
The test mass, the suspension system, the cryogenic and vacuum system, the mechanical structure needed to host the cryostat, the readout and the data acquisition system are parts of the detector.
The oscillating test mass is a cylindrical bar (2R=181.7 mm, L=500 mm) made of Al5056, the same aluminum alloy used in NAUTILUS. The resonance frequency of the first longitudinal mode of vibration is 5.096 kHz at T=296 K.
The suspension system is a cascade of seven attenuation stages, each consisting of a flexible joint connecting and supporting an inertial mass. It provides a -150 dB attenuation inside the frequency window of interest and the thermal link between the bar and the dilution refrigerator. Fig.1(left) shows the assembly of the test mass and the suspension system in the cryostat.
The cryogenic and vacuum system is composed by a commercial cryostat (height=3200 mm, external diameter=1016 mm) and a ^{3}He-^{4}He dilution refrigerator (base temperature=100 mK, cooling power at 120 mK=1mW). Fig.1(right) shows the layout of the thermal screens of the cryostat.

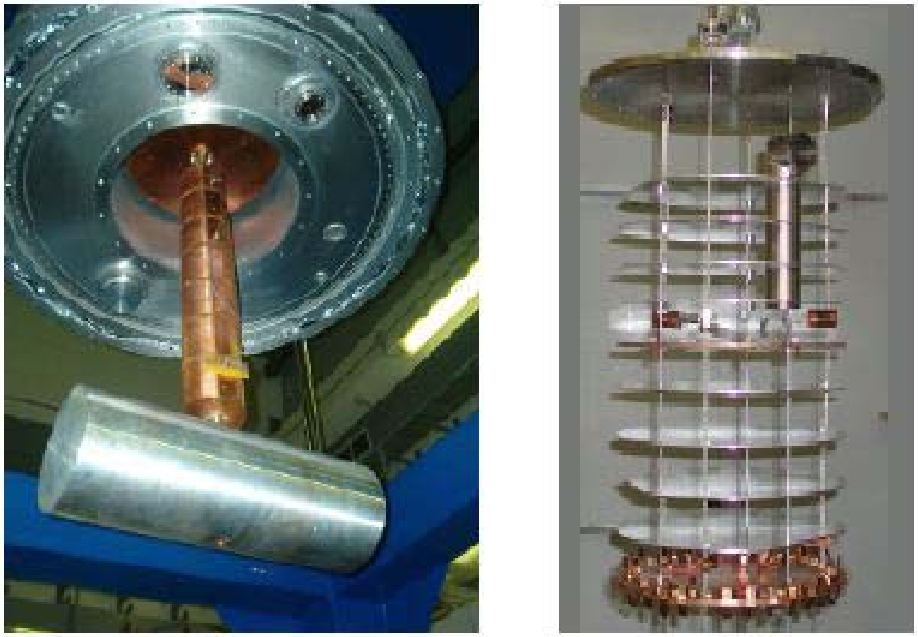

Figure 1: *Suspension system and test mass with the PZT insert (left); thermal shields (rigth). The* e^+e^- *beam is normal to the cylinder longitudinal axis and to the vertical suspension axis.*

The mechanical structure encloses the cryostat allowing an easy positioning of the detector on the beam line and the consequent removal at the end of the dedicated periods of data taking.
The readout is performed by two piezoelectric ceramics (PZT26), connected in parallel and inserted in the test mass at the position opposite to the suspension point (Fig.1 left). The signal is pre-amplified by a low-noise custom JFET circuit (V_{noise} ~1nV/$\sqrt{\text{Hz}}$) and amplified by a Stanford SR560 amplifier (V_{noise} ~4 nV/$\sqrt{\text{Hz}}$ at high gain (G=50000)). Procedures [5], based on the injection of a known waveform in the PZT's, are used to calibrate the readout system.
The data acquisition system , based on a 200 ksample/s 16 bit VME ADC (VMIC 3123) and a VME Pentium III CPU (VMIC 7740) running Linux, has been developed in the LabVIEW environment (with low-level C calls). Data originated from the PZT's, from the thermometry together with data related to the beam energy and timing are collected and logged to disk with a throughput of 0.3 MB/s. The system performs also the online monitoring of the measured amplitude, with interactive analysis capability based on Fast Fourier Transforms (FFT) (Fig.2).

3 Activities in the year 2003

In the third quarter the detector was assembled on the beam line and a first short technical run was performed at room temperature and low beam current. The run was aimed to test the whole detector when exposed to the beam and to possibly reproduce the results already obtained by the previous experiments. As a very preliminary result, we measured an amplitude of the first longitudinal mode of vibration equal to ∼ 70% of the value predicted by TAM.
In the last quarter, after the removal from the beam line, the bar was cooled down to liquid He temperature in order to characterize the performances of the cryostat setup.

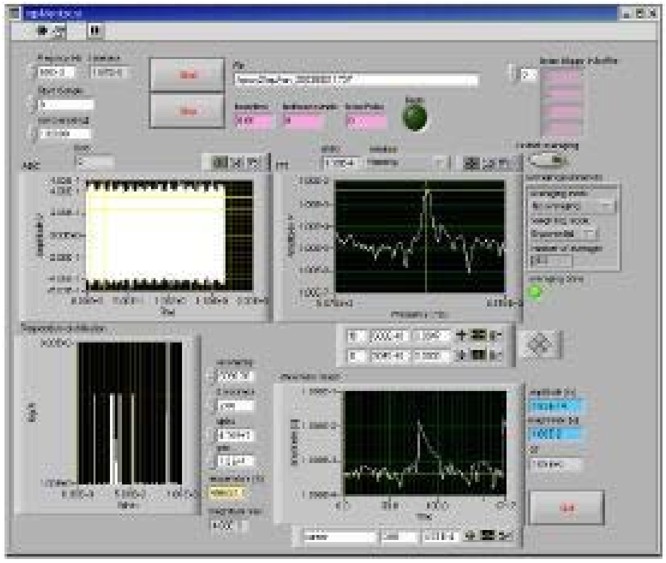

Figure 2: *Online display of the bar signal amplitude (top left), FFT of the signal at the resonance frequency (top right) and time chart of the amplitude at the resonance frequency (bottom right), following the beam hit.*

4 Planned activities in the year 2004

Physics runs with the bar at temperatures above and below T_c are planned.

5 List of Conference Talks by LNF Authors in Year 2003

1. G. Mazzitelli, RAP Collaboration: Thermoacoustic Detection at the DAΦNE Beam Test Facility, 5th E. Amaldi Conference on Gravitational Waves, Tirrenia, Italy.
2. P. Valente, RAP Collaboration: Acoustic detection of particles in ultracryogenic resonant antenna (RAP), 9th Pisa Meeting on Advanced Detectors, Pisa, Italy
3. C. Ligi, RAP Collaboration: Rivelazione acustica di particelle, LXXXIX Congresso Nazionale SIF, Parma, Italy.

References

1. S. Bertolucci *et al.*, Rivelazione Acustica di Particelle - RAP Proposal, LNF-01/027(IR)(2001).
2. P. Astone *et al.*, Phys. Rev. Lett.,**84**,14 (2000); P. Astone *et al.*, Phys.Lett.B,**499**,16 (2001); P. Astone *et al.*, Phys.Lett.B,**540**,179 (2002).
3. See for instance: G. Liu and B. Barish, Phys. Rev. Lett., **61**, 271 (1988) and references therein.
4. M.A. Grassi-Strini *et al.*, J.Appl.Phys., **51**, 948 (1980); G.D. van Albada *et al.*, Rev Sci Instrum.,**71**,1345 (2000).
5. G.V. Pallottino and G. Pizzella, Nuovo Cim.B,**45**, 275 (1978).

ROG

D. Babusci, F. Campolungo (Tecn.), V. Fafone, G. Giordano,
M. Iannarelli (Tecn.), R. Lenci(Tecn.), A. Marini, G. Modestino, G. Pizzella (Resp. Ass.),
L. Quintieri, F. Ronga (Resp.), E. Turri(Tecn.),
Collaboration with Roma 1 La Sapienza, Roma 2 Tor Vergata, Leiden University

1 Introduction

The ROG group is currently operating two cryogenic gravitational wave (GW) bar detectors: EXPLORER (at CERN) and NAUTILUS (at LNF). The main goal of this search is the direct detection of the gravitational waves that could be emitted by astrophysical sources (Supernovae, Coalescing Binaries, etc.). Such detection could be of enormous interest for general relativity and for astrophysics.

The experimental search for GWs was started by Joseph Weber in the early 60's, at a time when very little was known about their possible sources. He developed the first resonant-mass detector, made of a massive bar with a fundamental longitudinal frequency of about 1.6 kHz and a motion sensor converting the vibrations of the bar into an electric signal. His efforts stimulated the birth of new generations of resonant detectors, involving the use of cryogenic and superconducting techniques for noise reduction and development of new detectors based on laser interferometry between widely spaced bodies.

The principle of operation of resonant-mass detectors is based on the assumption that any vibrational mode of a resonant body that has a mass quadrupole moment, such as the fundamental longitudinal mode of a cylindrical bar, can be excited by a GW with nonzero energy spectral density at the mode eigenfrequency.

The mechanical oscillation induced in the antenna (made of a high Q material, at least of the order of 10^6) by the interaction with the GW, is transformed into an electrical signal by a motion or strain transducer and then amplified by an electrical amplifier. The sensitivity of the detector is limited by three sources of noise which, referred to the output are: (1) the narrowband thermal noise, as the input wideband stochastic dissipative force, due to the internal friction in the resonant mass, appears at the output after passing through the mechanical transfer function of the system; (2) the wideband amplifier noise, which appears directly at the output; (3) the narrowband back-action noise, originated from the back-energy flow from the amplifier, which excites the resonant mass. The useful bandwidth of such detectors is by no means limited to the very narrow width of the high Q mechanical resonance. Rather, it is the amplifier noise that limits the bandwidth. The lowest spectral noise is found in the frequency region where the narrowband (thermal plus back-action) noises dominate the amplifier noise, and there the noise level is the sum of the two. As a consequence, any reduction in the amplifier noise and/or increase in coupling, increases the antenna bandwidth.

During these years, experimentalists devoted a continuous effort to improve the antenna sensitivity. All the upgrades are mainly devoted to:

- increase the duty cycle and lower the background noise, by upgrading the cryogenics to minimize maintenance stops and to ensure more stable operating temperature, and by acting on the vibration attenuation system, including the thermal links between refrigerating stages and the electromechanical sensitive components.
- improve the sensitivity and the useful bandwidth, by acting on the readout components. These efforts promise to be successful, as recently shown by EXPLORER and NAUTILUS where upgraded transducers, more strongly coupled to the bar and less noisy single stage

SQUID amplifiers have been used. Even better results are expected very soon with the development of double stage SQUID amplifiers with energy resolution of less than 100 quanta and of a high-Q superconducting LC coupling circuit resonating at the bar frequency. This activity is currently in progress in the laboratories in collaboration with the IFN-CNR (Istituto di Fotonica e Nanotecnologie) in Rome.

2 NAUTILUS and EXPLORER

The ultra-cryogenic detector NAUTILUS [1)] is operating at the Frascati INFN National Laboratory since December 1995. It consists of an Al5056 cylindrical bar, 2300 kg in weight and 3 meters in length, cooled to a temperature of 0.1 K by means of a dilution refrigerator, and equipped with a resonant capacitive transducer and a dc SQUID amplifier. The two characteristic resonance frequencies, due to the coupling of the antenna and the transducer are about 926 and 941 Hz. NAUTILUS is equipped with a cosmic ray detector.

NAUTILUS has taken data until February 2002, when it was warmed up for improvements. The bar was replaced by a new bar tuned at 935 Hz, the frequency where a pulsar, remnant of the SN1987A, is supposed to emit gravitational waves [2)]. A new readout chain (the same used for EXPLORER), plus a new suspension cable, to provide a more stable position setting, were mounted [3)]. The new run started in May 2003. For the time being, the temperature of the bar is 3.5 K. The resulting strain noise (the minimum detectable spectral density) is $\tilde{h} \simeq 2 \cdot 10^{-21} / \sqrt{Hz}$ around 935 Hz, and $\tilde{h} \leq 10^{-20} / \sqrt{Hz}$ over about 30 Hz (see upper part of Figure 1). The noise temperature is 1 mK, corresponding to an adimensional amplitude of GW bursts $h = 2.5 \cdot 10^{-19}$. The duty cycle is now very high (about 90%), mainly limited by the cryogenic maintenance operations. The high duty cycle and the stationary behaviour are very important to collect the data needed to further investigate the coincidence excess between EXPLORER and NAUTILUS [4, 5)] found in the 2001 data[1]. Better results in terms of sensitivity are expected when the system will be cooled down to 0.1 K (see lower part of Figure 1).

The EXPLORER antenna is located in CERN and is very similar to NAUTILUS, but is cooled to 2.6 Kelvin [6)]. EXPLORER has taken data until August 2002. In August 2002 the superconducting circuit connected to the SQUID was damaged. To repair the damage it was necessary to warm and to open the antenna. The new run started in December 2002 and was stopped in December 2003 for the shut down during Christmas holidays at CERN. The duty cycle was very high (of the order of 90%) and the noise temperature of the order of 2 mK [3)].

In 2003 the cosmic ray detector installed during the previous year (see Figure 2), started to take data. Thanks to the larger bandwidth obtained with the new readout installed in 2001 [7)], a good time resolution (less than 10 ms) in the determination of the events due to the passage of cosmic rays was reached. Figure 3 shows the improvement in time resolution of EXPLORER due to the bandwidth broadening.

---

[1]In 2001 EXPLORER and NAUTILUS were the only two detectors running. Their sensitivity was the best ever reached by GW detectors. The coincidence excess was found from sidereal hour 3 to sidereal hour 5. We obtained 7 coincidences in this two-hour interval with a background of 1.7. The excess appears to have some statistical significance, as the two largest excesses occur in two neighboring hours (the events in each hour are totally independent from those in a different hour). On the contrary, no significant coincidence excess appears at any solar hour. The event energies of NAUTILUS appeared strongly energy correlated with those of EXPLORER, for the seven coincidences in these two sidereal hours, when the antenna is optimally oriented with respect to the Galactic Disk.

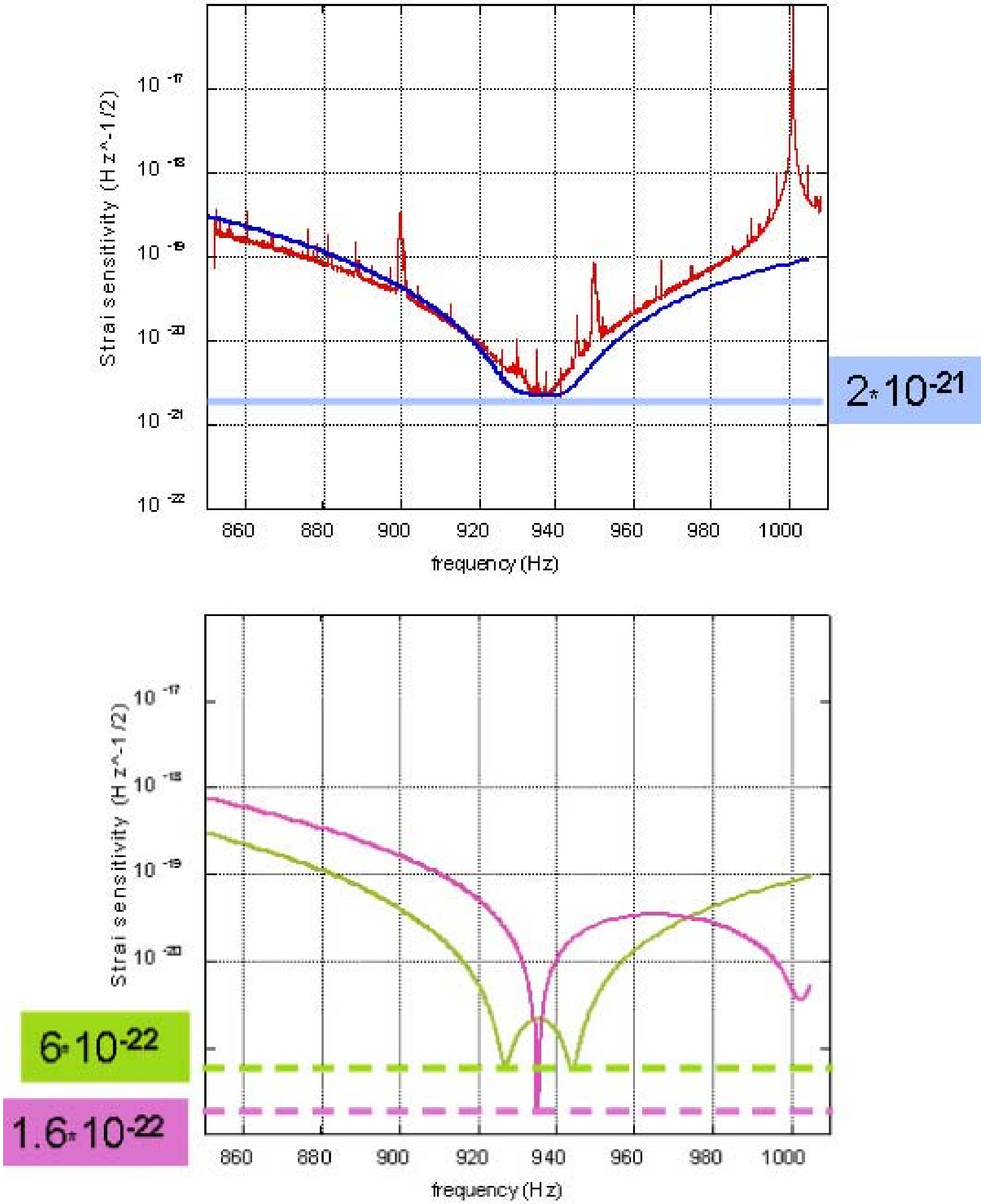

Figure 1: Top: experimental strain sensitivity of NAUTILUS in 2003, with the bar cooled at 3.5 K (red line) compared to the expected curve at this temperature (blue line). Bottom: expected strain sensitivity with the bar cooled to 0.15 K. The two curves refer to different polarization fields in the capacitive transducer. The green curve is optimized for burst detection and the purple curve for the search for the signal emitted at 935 Hz by the pulsar remnant of SN1987A.

Figure 2: The EXPLORER detector at CERN with the new cosmic ray detector installed in 2002.

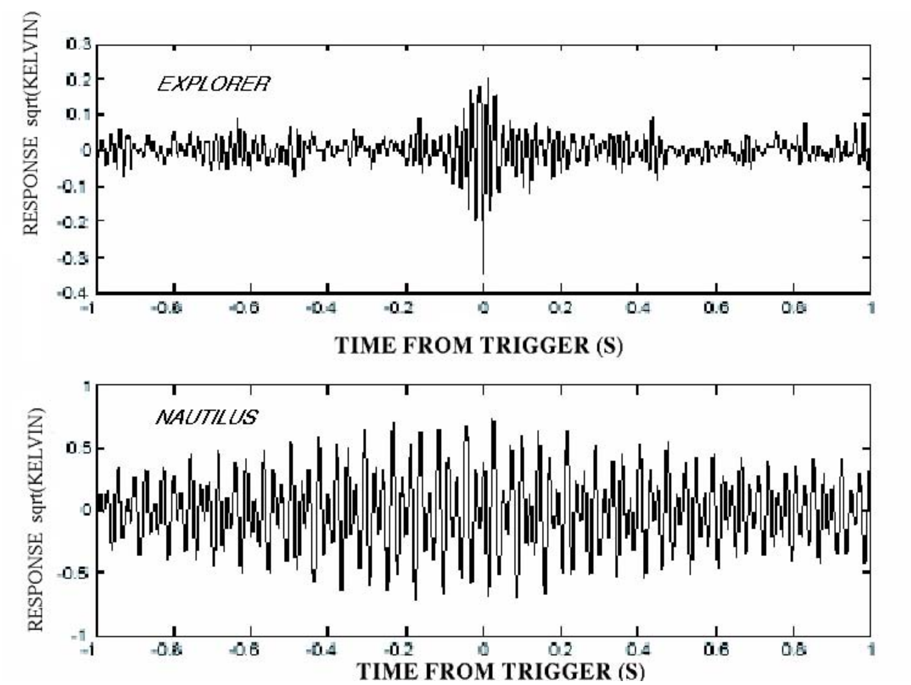

Figure 3: Two events triggered by cosmic ray showers. The upper part shows an event detected by EXPLORER with the new readout. The lower part shows a similar event detected by NAUTILUS in 2001, with the old readout. The improvement in the arrival time resolution can be clearly seen. The time resolution of NAUTILUS in 2003 is the same as that of EXPLORER (less than 10 ms).

The LNF group has major responsibilities in the maintenance and running of NAUTILUS (including the production of liquid helium), in the maintenance, building and running of the cosmic ray detectors, in the development of a new nearly quantum limited signal readout, in the data acquisition and in many items of data analysis.

3 Advanced detectors

The LNF group is involved in the development of resonant-mass detectors of spherical shape. A single sphere is capable of detecting gravitational waves from all directions and polarizations and is capable of determining the direction information and tensorial character of the incident wave. A sphere will have a larger mass than the present bars (with the same resonance frequency), turning into an increased cross section and improved sensitivity. Omnidirectionality and source direction finding capability make a spherical detector a unique instrument for gravitational wave astronomy with respect to all present detectors. At present, two small spheres (about 1 ton) are being developed: one in Brasil and one (MiniGRAIL) in Holland. The ROG group is collaborating with the Leiden University group for the development of MiniGRAIL, mainly on new readout chains, the data acquisition and the effect of cosmic rays. In 2003 the sphere was cooled down to 79 mK, a record temperature for masses of the order of 1 ton [8] and it is now ready for the first run with two readout lines, partially developed by the ROG group.

4 Main data analysis results obtained in 2003

The main analyses using the NAUTILUS and EXPLORER data, just published or in progress, are the following:

- All five resonant-mass detector groups[2] formed the International Gravitational Event Collaboration (IGEC), during the Second Amaldi Conference in 1997 at CERN, and agreed in a data exchange protocol to search for short GW bursts. All the data collected by the IGEC members in the years 1997-2000 were analyzed and new upper limits[3] for amplitude and rate of GW bursts have been set [9].
- Search for monochromatic signals. The present sensitivity of NAUTILUS allows the detection at $S/B = 1$ of a continuous GW signal around 1 kHz of amplitude $h \simeq 5 \cdot 10^{-26}$ with an observation time of 100 days [10].
- Search for coincidences with gamma ray bursts [11].
- A search for GW bursts with the data collected in 2003 by EXPLORER and NAUTILUS is in progress.
- A further study of the excitation of NAUTILUS and EXPLORER due to the passage of cosmic rays is in progress.

---

[2]ALLEGRO at the Louisiana State University, AURIGA at the INFN Legnaro Laboratories, NIOBE in Perth (Western Australia), EXPLORER and NAUTILUS.

[3]These upper limits do not contradict the coincidence excess found in 2001 by EXPLORER and NAUTILUS, because of the lower sensitivity of the IGEC detectors with respect to the sensitivity that the ROG detectors achieved in 2001.

5 List of Conference Talks by LNF Authors in Year 2003

1. G. Pizzella, Search of coincidences with the gravitational wave detectors EXPLORER and NAUTILUS, X Marcel Grossmann Meeting on General Relativity, Rio de Janeiro, Brasil
2. V. Fafone, Present status of MiniGRAIL, X Marcel Grossmann Meeting on General Relativity, Rio de Janeiro, Brasil
3. G. Modestino, Gravitational wave resonant detectors data analysis for searching counterpart of gamma ray bursts, LXXXIX Congresso Nazionale SIF, Padova

References

1. P. Astone *et al.* (ROG Collaboration), "The gravitational wave detector NAUTILUS operating at T = 0.1 K", Astropart. Phys. **7**, 231 (1997).
2. J. Middleditch *et al.*, New Astronomy **5**, 243 (2000).
3. P. Astone *et al.* (ROG Collaboration), "The next science run of EXPLORER and NAUTILUS", Proceedings of the 5th E. Amaldi Conference on Gravitational Waves, Class. Quantum Grav. **21**, (2003).
4. P. Astone *et al.* (ROG Collaboration), "Study of the coincidences between the gravitational wave detectors EXPLORER and NAUTILUS in 2001", Class. Quantum Grav. **19**, 5449 (2002).
5. P. Astone *et al.* (ROG Collaboration), "Comments on the 2001 run of the EXPLORER/NAUTILUS gravitational wave experiment", Class. Quantum Grav. **20**, S785 (2003).
6. P. Astone *et al.* (ROG collaboration), "The EXPLORER gravitational wave antenna: recent improvements and performances", Class. Quantum Grav. **19**, 1905 (2002).
7. P. Astone *et al.* (ROG collaboration), "Increasing the bandwidth of resonant gravitational antennas: the case of Explorer", Phys. Rev. Lett. **91**, 111101(4) (2003).
8. A. de Waard *et al.*, "Cooling down MiniGRAIL to milli-Kelvin temperatures", Proceedings of the 5th E. Amaldi Conference on Gravitational Waves, Class. Quantum Grav. **21**, S465 (2003).
9. P. Astone *et al.* (IGEC Collaboration) "Methods and results of the IGEC search for burst gravitational waves in the years 1997-2000" Phys. Rev. D **68**, 022001 (2003).
10. P. Astone *et al.* (ROG collaboration), "All sky upper limit for gravitational radiation from spinning neutron stars" Class. Quantum Grav. **20**, S665 (2003).
11. P. Astone *et al.* (ROG collaboration), "Searching for counterpart of gamma-ray bursts with resonant gravitational wave detectors", Proceedings of the 5th E. Amaldi Conference on Gravitational Waves, Class. Quantum Grav. **21**, S759 (2003).

VIRGO

D. Babusci, G. Giordano (Resp.), M. Iannarelli (Tecn.), E. Turri (Tecn.)

1 Introduction

Virgo is a collaboration between Italy (INFN) and France (CNRS) for the construction of an interferometric detector of gravitational waves (GW). The participating laboratories are: LAPP-Annecy, IPN-Lyon, OCA-Nice, LAL-Orsay and ESPCI-Paris for CNRS and Firenze/Urbino, Frascati, Napoli, Perugia, Pisa, Roma for INFN.

The aimed sensitivity should allow to detect, in the frequency range between a few Hz and a few kHz, GW emitted by coalescing binary compact stars, gravitational collapses, spinning neutron stars or the stochastic GW background.

Virgo will be a recycled (power enhancement factor $\simeq 50$) Michelson interferometer, having in each arm a 3 km Fabry-Perot (FP) cavity with finesse of 50. The interferometer (ITF) will be illuminated by a 25 W Nd:YAG laser ($\lambda = 1.064\ \mu m$), stabilized through a monolithic reference cavity and filtered by a high-finesse triangular mode cleaner of 144 m length.

The first phase of Virgo construction, the realization of the central interferometer (CITF), was completed by end 2000, and the commissioning activity with the CITF ended in July 2002.

The construction of the full ITF (two 3 km arms) was completed in June 2003. The optical path is completely under vacuum and all the optical components are suspended in vacuum by anti-seismic Super Attenuators capable of reducing the seismic noise by more than a factor 10^{12} above a few Hz.

2 Responsibility of the Frascati Group

The Frascati group has the responsibility of the "linear alignment", that is the system providing the information about the misalignment of the ITF mirrors during the standard operation of Virgo. It will employ 8 quadrant photodiodes (QPHD) placed on the beams emerging from the ITF; demodulating the up-down and left-right differencies, the misalignments status will be derived.

3 Activity in 2003

Almost all the electronic components of our system (quadrant photodiode front-end electronics, demodulation modules, reference signal shifters and splitters) have been modified due to the difference in the laser modulation frequency between the CITF and the full Virgo cases. We also upgraded the DC part of the quadrant photodiodes front-end electronics, introducing an adjustment of the offsets and increasing the DC gain.

We performed the simulations of the alignment signals to be expected in the single arm operation, in recombined mode and in the full ITF configuration.

The benches on the north and west terminal towers have been installed, together with the telescopes in front of the quadrant photodiodes, including the large lenses that receive the beam transmitted by the FPs end mirrors. We have also installed all the electronics required for these photodiodes. Remotely controlled laser shutters, to be placed in front of each of our quadrant photodiodes, have been built and will be soon installed, together with their driving electronics, currently being assembled.

The commissioning of the full Virgo ITF will follow three steps:

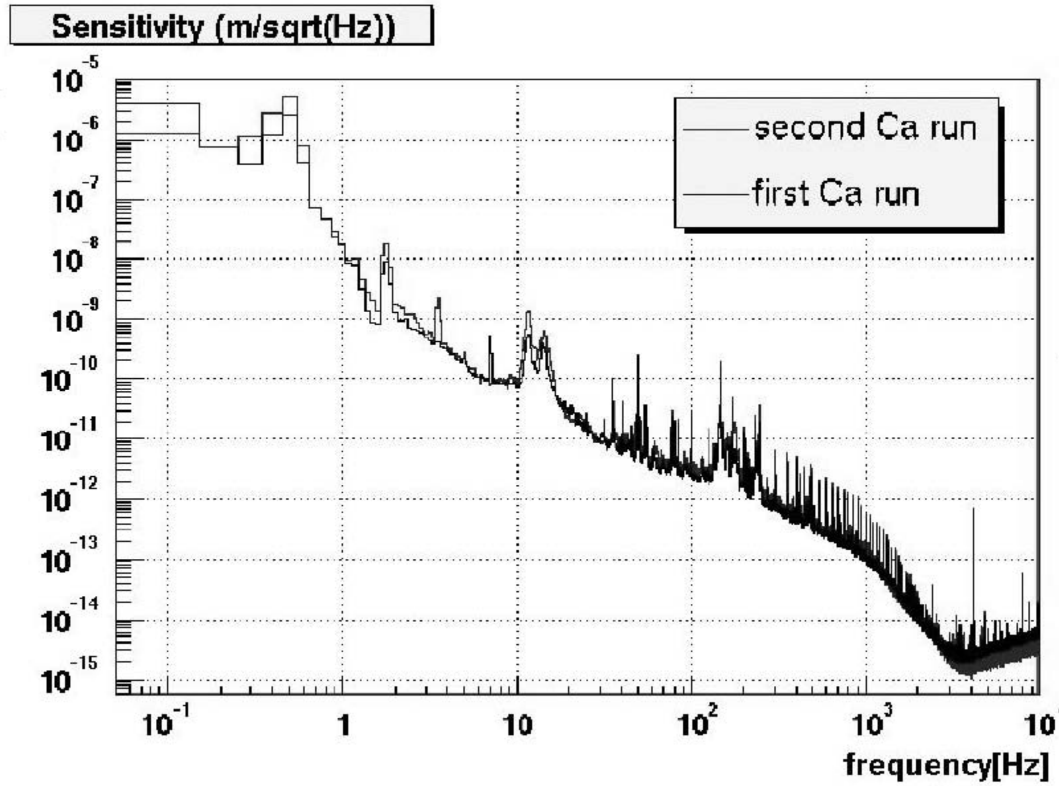

Figure 1: *Sensitivity (meters/$\sqrt{Hz}$) of the North-arm Fabry-Perot to variations of its length in different commissioning runs.*

- commissioning of a single FP;
- recombination of the two FPs (non-recycled Michelson);
- recycled Michelson (final configuration).

The first phase, began in July 2003 on the North-arm FP and is now close to completion. The sensitivity of the cavity to variations of its length has been extensively studied (see fig.1) and continuously improved. The linear alignment is currently being implemented.

4 Activity in 2004

The goal of the commissiong work is to have the full Virgo ITF locked in a stable way by the end of the year.

5 Publications

1. F. Acernese *et al.*, Data analysis methods for non-Gaussian, nonstationary and nonlinear features and their application to VIRGO. Class. Quantum Grav. **20**, S915 (7 Sep. 2003).
2. F. Acernese *et al.*, Status of VIRGO. Published in Class. Quantum Grav. **20**, S609 (2003).

WIZARD

S.Bartalucci, G.Basini, F.Bongiorno (Ass.), L.Bongiorno (Ass.Ric.),
G.Mazzenga (Tecn.), M.Ricci (Resp.)

Participant Institutions:

ITALY: INFN Bari, LNF, Firenze, Napoli, Roma2, Trieste;
CNR Ist. Fisica Applicata "Nello Carrara" Firenze;
ASI (Italian Space agency);
Electronic Engineering Department, University of Roma 2 "Tor Vergata";
RUSSIA: MePhi Moscow;
FIAN Lebedev Moscow;
IOFFE St Petersburg;
TsSKB-Progress Samara;
SWEDEN: KTH Stockholm;
GERMANY: Siegen University;
USA: NASA Goddard Space Flight Center;
New Mexico State University.

1 Experimental Program and Scientific Objectives

The WIZARD experimental program is devoted to the extensive study of cosmic ray spectra (particles, antiparticles, isotopes, abundances and search for antimatter) in several energy ranges achievable through different apparata on board stratosferic balloons and long duration satellite missions. WIZARD is an International Collaboration between several Universities and Research Institutions from Russia, Sweden, Germany, USA together with the Space Agencies NASA, RSA (Russia), SNSB (Sweden), DLR (Germany) and ASI. The experimental activities are carried out through three main programs:
Balloon flights;
Satellite missions NINA-1 and NINA-2;
Satellite mission PAMELA.
We refer to previous editions of this report for the description of the activities related to the balloon flights and to the two NINA missions.

1.1 The satellite mission PAMELA

PAMELA is a cosmic ray space experiment that will be installed on board a Russian satellite (Resurs-DK1) whose launch is foreseen in 2004 from the cosmodrome of Baikonur, Kazakhistan, by a Soyuz TM2 rocket. The satellite will fly for at least 3 years in a low altitude, elliptic orbit (300-600 km) with an inclination of 70.4 degrees. The PAMELA telescope consists of a magnetic spectrometer including a permanent magnet coupled to a silicon tracker, a Transition Radiation Detector, an imaging silicon-tungsten calorimeter, a time-of-flight system, an anticoincidence detector, a shower tail catcher scintillator and a neutron detector [1, 2]. A sketch of the PAMELA instrument is shown in fig.1.

The total height of PAMELA is 120 cm, the mass is 440 kg, the power consumption is 385 W and the geometrical factor is 20.5 cm^2 sr.

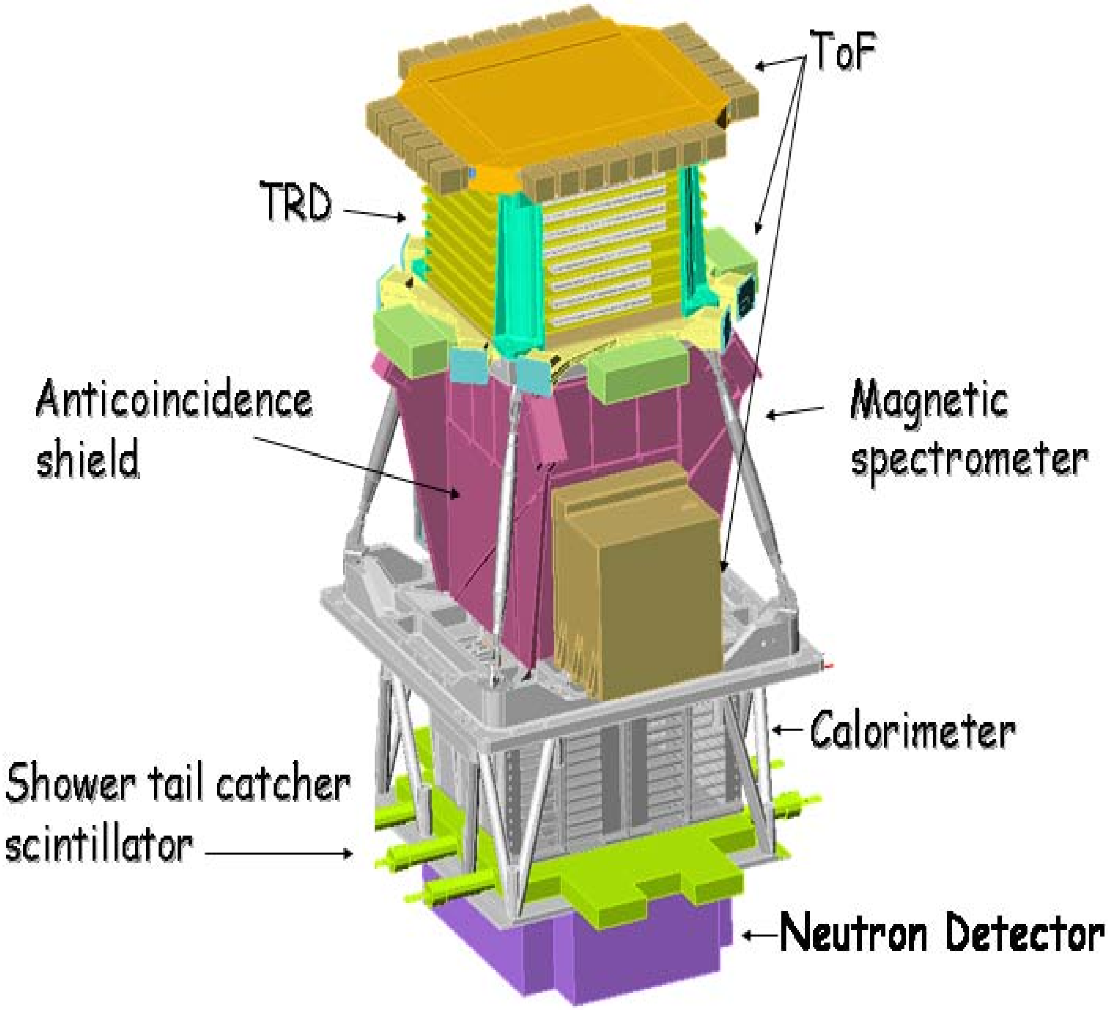

Figure 1: The PAMELA telescope and its main detectors.

The observational objectives of the PAMELA experiment are to measure the spectra of antiprotons, positrons and nuclei in a wide range of energies, to search for antimatter and for indirect signatures of dark matter and to study the cosmic ray fluxes over a portion of the solar cycle.

The main scientific goals can be schematically listed as the following:

a) measurement of the antiproton spectrum in the energy range 80 MeV - 190 GeV;
b) measurement of the positron spectrum in the energy range 50 MeV - 270 GeV;
c) search for antinuclei with a sensitivity of $\sim 3 \times 10^{-8}$ in the $\overline{He}/He$ ratio;
d) measurement of nuclei spectra (He, Be, C) at energies up to 700 GeV/n;
e) measurement of the electron spectrum in the energy range 50 MeV - 2 TeV.

In addition, the PAMELA experiment will be able to measure the light nuclear component of cosmic rays and investigate phenomena connected with Solar and Earth physics.

Activity in the year 2003 has covered the following items:

- Integration and tests (vibration, thermal, vacuum) of Mass Dimensional and Thermal Model (MDTM) at TsSKB Progress plant (Samara, Russia).
- Compatibility and acceptance tests of MDTM with Satellite Pressurized Container.
- Integration of PAMELA Engineering Model in Roma 2 clean rooms.
- Test at CERN SPS-H2 beam of Flight Spectrometer, Flight Calorimeter and Flight Anticounters (protons and electrons up to 300 GeV/c).
- Completion of TRD Gas System and PAMELA general cooling system.
- Integration in the PAMELA FM of magnet, tracker, S2 and S3 TOF counters, Anticoincidence detector, Calorimeter, Shower tail catcher scintillator and Neutron detector .
- Tests of flight CPU.
- Specifications of the PAMELA downlink system.
- Development of control and command software and of general instrument Montecarlo simulation (GPAMELA).

2 Activity of the LNF group during year 2003

The LNF WIZARD group has been fully involved in all the balloon and satellite programs.
During the year 2003 the activity for the PAMELA experiment has been carried on as follows:

- Responsibility of the Mechanical Ground Support Equipment (MGSE) for the assembly and integration of the whole apparatus.
- Organization and coordination of beam test set-up at CERN SPS.
- Responsibility of the counting detectors and trigger for beam tests.
- Preparation and tests of the Mass Dimensional and Thermal Model at TsSKBProgress plant (Samara, Russia).
- Preparation and assembly of the Technological (Engineering) Model.
- Preparation and assembly of the Flight Model.

3 Programmed activity of the LNF group during year 2004

- Completion of PAMELA Technological Model (TM).
- Final acceptance tests of PAMELA TM at TsSKB Progress plant.
- Completion of PAMELA Flight Model, integration and ground tests.
- Delivery of Flight Model to Russia.
- Flight readiness tests and integration with spacecraft Resurs DK1.
- Launch from the Baikonur space center.
- Data taking: first phase and establishment of downlink procedures.

4 List of Publications in 2003

1) "Status of the PAMELA experiment"; M.Simon for the Pamela Collaboration, Proc. 28th International Cosmic Ray Conference (Tsukuba, Japan, 2003) OG 1.5 p.2117

2) "Solar Particle Events observation capabilities of PAMELA experiment"; M.Casolino for the Pamela Collaboration, Proc. 28th International Cosmic Ray Conference (Tsukuba, Japan, 2003) SH 1.5 p.3477

3) "The Space Mission PAMELA"; M.Circella for the Pamela Collaboration, 9th Pisa Meeting on Advanced Detectors "Frontier Detectors for Frontier Physics", La Biodola (Isola d'Elba), 25-31 May 2003

4) "Energy spectra of atmospheric muons measured with the CAPRICE98 balloon experiment"; M.Boezio et al.,Phys.Rev. D67 (2003)072003

5) "The Cosmic Ray Proton and Helium Spectra measured with the CAPRICE98 balloon experiment"; M.Boezio et al., Astropart.Phys. 19 (2003)583

6) "Measurement of the Deuterium Flux in the Kinetic Energy Range 12-22 GeV/n with the CAPRICE98 Experiment"; Proc. 28th International Cosmic Ray Conference (Tsukuba, Japan, 2003) OG 1.1 p. 1801

7) "Measurement of High Energy ^3He in Cosmic Rays by the CAPRICE98 Balloon Experiment"; Proc. 28th International Cosmic Ray Conference (Tsukuba, Japan, 2003) OG 1.1 p.1809

8) "Composition of Cosmic Ray Particles in the Atmosphere as Measured by the CAPRICE98 Balloon Borne Apparatus"; Proc. 28th International Cosmic Ray Conference (Tsukuba, Japan, 2003) HE 3.1 p.1627

9) "Isotope composition of secondary hydrogen and helium above the atmosphere"; V.Bidoli et al., Jour. Geoph. Res. Lett. 108, A5 (2003)1211

10) "The small satellite NINA-MITA to study Galactic and Solar Cosmic Rays in low altitude polar orbit"; G.Furano et al., Adv.Space res. vol.31, n.2 (2003) 351

References

1. M.Simon for the PAMELA collaboration: "Status of the PAMELA experiment ", Proc. 28th International Cosmic Ray Conference (Tsukuba, Japan, 2003) OG 1.5 p.2117
2. O. Adriani et al. "The PAMELA experiment on satellite and its capability in cosmic ray measurements", NIM A478 (2002)114

AIACE

E. De Sanctis (Dir.), M. Mirazita (Ass.),
A. Orlandi (Tech.), W. Pesci (Tech.), E. Polli, F. Ronchetti (Dott.),
P. Rossi (Resp.), A. Viticchié (Tech.)

1 Introduction

AIACE stands for Attività Italiana A CEbaf. It is the collaboration of the INFN groups of Frascati and Genova which participate into the physics program carried out in the Hall B at the 6 GeV Continuous Electron Beam Accelerator Facility (CEBAF) at the Jefferson Laboratory (JLab), located in Newport News, Virginia (USA). At present, the Hall B collaboration counts about 140 physicists from 35 Institutions from seven Countries.

Hall B is devoted to experiments that require the detection of several loosely correlated particles in the final state, and the CLAS detector [1], a large acceptance spectrometer, is unique in design to accomodate these requirements and to perform a very broad spectrum of physics measurements.

The themes of the Hall B scientific program are the precision study of the structure of the nucleon and the nature of the strong interaction. Experiments aim to clarify the interplay between hadronic and partonic degrees of freedom and the effectiveness of the traditional nucleon-nucleon theories or QCD inspired models.

This scientific program can be summarized in the following main topics:

- *Search for exotic mesons and baryons*
- *Baryon Resonances*
- *Spin Structure Functions in the Resonance Region*
- *Nucleon Tomography*
- *Dynamics of the Strong Interactions*

In the period covered by this report the Frascati group has carried out:

- the completion of the data analysis for the determination of the angular distributions of the deuteron photodisintegration cross section between 0.5 and 3.0 GeV. This include the write-up of two papers (to be submitted to Physical Review Letters and Physical Review C).
- The write-up of the paper on the calculation of polarization observables in high-energy deuteron photodisintegration within the Quark-Gluon String model (QGS).
- The start-up of data analysis for the search of the pentaquark baryon state Θ^+ in the reaction channel $\gamma d \to \Theta^+\Lambda(1115)$.
- The start-up of the project for the construction of a new start counter for CLAS.
- The installation of a new system to monitor the Large Angle Calorimeter High Voltage, using Java application and a graphical user interface.

In addition, the Frascati group has participated to the various CLAS production runs, to data taking and to the relative discussions of the analysis work.

2 Deuteron photodisintegration between 0.5 and 3.0 GeV (Experiment E-93-017)

The interplay between the nucleonic and partonic pictures of the strong interaction represents one of the major issues in contemporary nuclear physics. In fact, Quantum Chromodynamics (QCD) has been successfully applied in describing the structure and production of hadrons at high energies (where perturbation theory can be used), but nuclear reactions have been conventionally described in terms of baryons and mesons rather than quarks and gluons. So, one expects that the classical nucleonic description must break down once the probing distances become comparable to those separating the quarks. The challenge is to study this transition region by looking for the onset of some experimentally accessible phenomenon naturally predicted by perturbative QCD (pQCD).

The simplest is the constituent counting rule (CCR) for high energy exclusive reactions [2, 3], in which $d\sigma/dt \propto s^{-n+2}$, with n the total number of pointlike particles in the initial plus final states. Here s and t are the usual relativistic invariant Mandelstam variables for the total energy squared and the four-momentum transfer squared, respectively.

Deuteron photodisintegration is especially suited for this study, since the known electromagnetic reaction mechanism can be separated from the nuclear structure. To this aim a broad deuteron photodisintegration program has been carried out at SLAC [4, 5, 6] and at Jefferson Lab in all three experimental Halls [7, 8, 9, 10, 11] using different experimental methods.

The data obtained so far show that a transition to QCD scaling seems to exist, but its borders are not well-defined. Scaling seems to be confirmed for center-of-mass proton angles $\vartheta_p^{\rm CM} = 69°$ and 89° [7] at already $E_\gamma = 1$ GeV photon energies, while at the forward angles $\vartheta_p^{\rm CM} = 52°$ and 36°, the cross section falls off more slowly than s^{-11} until about 3 and 4 GeV beam energy, respectively [8]. By contrast, polarization observables for $\gamma d \to pn$ measured at 90° and for photon energies up to 2 GeV can not be consistently interpreted in a perturbative picture [9].

In this context, several models attempt to account for the experimental results using different strategies. Some include QCD degrees of freedom in a low-energy description like the Reduced Nuclear Amplitude model (RNA) [12], the Hard Quark Rescattering Mechanism model (HRM) [13, 14, 15, 16], and the Quark Gluon String model (QGS) [17, 18, 19]. Others extrapolate the conventional N-π interaction mechanisms to higher energy, such as the Asymptotic Meson Exchange Current model (AMEC) [20].

So, a better insight into the competing models can be obtained by angular distributions of the differential cross section over a broad angular and energy range.

To this end, the CLAS experiment E93-017 performed an extensive measurement of the deuteron photodisintegration cross section between 0.5 and 3.0 GeV and over an almost complete proton angular range ($\vartheta_p^{\rm CM} = 10°$–$160°$). The CLAS data agree with those measured by other experiments where available and extend to the very forward and backward angular regions. They show a persistent forward-backward angle asymmetry over the explored energy range as can be seen in Fig. 1, where a sample of the measured differential cross sections are shown.

Moreover, the extensive cross section data obtained by CLAS allows one for the first time to make a detailed study of the energy dependence of the $d(\gamma, p)n$ differential cross section at fixed angles to look for the onset of cross section scaling at some incident photon energy. The result is under the review of the CLAS collaboration and will be published soon.

3 Polarization observables in high-energy deuteron photodisintegration within the Quark-Gluon Strings model

As stated above, the Quark Gluon String model is a non-perturbative approach, which has been extensively used for the description of hadronic reactions at high energies [22]. This model has been applied for the description of the deuteron photodisintegration reaction, using QCD motivated non-linear nucleon Regge trajectories [23], with full inclusion of spin variables and assuming the dominance of the amplitudes that conserve s-channel helicity. The interference between the isoscalar and isovectorial components of the photon has been also taken into account, leading to forward-backward asymmetry in the cross section.

Nevertheless, the dependence of the photodisintegration cross-section has been shown to be a potentially misleading indicator for the success of pQCD. Thus, further theoretical developments and experimental tests of nonperturbative quark models will be necessary. To this aim, polarization observables are very important to further constrain the different approaches.

In this context, the QGS model predictions for the asymmetry, Σ, and the polarization transfer to the proton, C_z, for photon energies E_γ=(1.2-6) GeV have been calculated in Ref. [19] (for the definitions of these observables in terms of helicity amplitudes see Ref. [24]). In the left panel of Fig. 2 the QGS model results for the asymmetry Σ (dashed line), calculated for linearly polarized photons, are shown as a function of the photon energy, E_γ, for different angles $\vartheta_p^{\rm CM}$. The QGS model predicts a slow decrease of $\Sigma(90°)$ with the photon energy from 0.6 (at 1.5 GeV) to 0.2 (at 5-6 GeV). Also at the other angles, the asymmetry Σ is a decreasing function of E_γ , although smaller in absolute magnitude. At 6 GeV it can even become negative at 70° and 110°. Also shown in Fig. 2 are the experimental data from Ref. [25] which are available only at $\vartheta_p^{\rm CM} = 90°$. The data are compatible with the QGS model prediction at 1.5 GeV. Unfortunately, at lower energies, where resonance amplitudes are important, the QGS model cannot be applied.

In the right panel of Fig. 2 the QGS model predictions of the polarization transfer C_z for circularly polarized photons are shown as a function of E_γ at different $\vartheta_p^{\rm CM}$ angles. Also in this case, experimental data are available only at $\vartheta_p^{\rm CM} = 90°$. As it can be seen, for photon energies $E_\gamma \geq 1.5$ GeV the data [9] are in reasonable agreement with the QGS model results.

4 Search of the pentaquark baryon state Θ^+ in the reaction channel $\gamma d \to \Theta^+\Lambda(1115)$

The constituent quark model describes light mesons as bound states of a quark and an antiquark ($q\bar{q}$), and baryons as bound states of three quarks (qqq). Pratically all well-established particles can be categorized using this naive model. At the same time quantum chromodynamics (QCD) predicts the existence of the so-called exotic mesons and baryons with more complicated internal structure.

The possibility of observable exotic multiquark states has been the subject of speculation for over three decades and has generated a large literature, but searches for exotic multiquark resonances have been largely unsuccessful in spite of efforts over three decades.

The recent discovery of the Θ^+ baryon [26, 27, 28, 29, 30, 31, 32, 33] with strangeness S=+1 has opened a new era in the baryon spectroscopy. Jefferson Lab has been at the forefront of these exciting developments. In addition to the observation of the Θ^+ on the deuteron [28], the CLAS collaboration was the first to observe Θ^+ production on proton targets [29, 30]. Both these results are shown in Fig. 3.

A broad search for Θ^+ signal is in progress in Hall B in several reaction channels in the available data on deuteron and proton. Moreover, new proposals have been approved, with high priority, by the Panel Advisory Committee to confirm the present Θ^+ signal with higher statistics and to perform precise measurements of its mass and width and of its quantum numbers. The new data will be taken in the first part of the year 2004.

The Aiace group is involved in this program: two new approved proposals are signed by the members of the group which also partecipate to the construction of the new Start Counter of the CLAS detector, necessary to run the new experiments at higher rates. Moreover, they are looking at the Θ^+ signal in the reaction channel $\gamma d \to \Theta^+\Lambda(1115)$ in the available data on deuteron.

5 List of Publications

1. Photoproduction of the ω mesons on the proton at large momentum transfers.
   M. Battaglieri *et al.* and CLAS Collaboration, Phys. Rev. Lett. 90 (2003) 022002.

2. A complete measurement of the F_2 proton structure function in the resonance region and the evaluation of the moments.
   M. Osipenko *et al.* and CLAS Collaboration, Phys. Rev. D 67 (2003) 092001.

3. Polarization observables in high-energy deuteron photodisintegration within the Quark-Gluon String model.
   V.Yu Grishina *et al.*, Eur. Phys. J A 18 (2003) 207

4. Deuteron photodisintegration in the quark-hadron picture.
   P.Rossi, Eur. Phys. J. A 17 (2003) 433.

5. First measurement of transferred polarization in the exclusive $\vec{e}p \to e'K^+\vec{\Lambda}$ reaction.
   D. Carman *et al.* and CLAS Collaboration, Phys. Rev. Lett. 90 (2003) 131804.

6. The Cebaf Large Acceptance Spectrometer.
   B. Mecking *et al.* and CLAS Collaboration, Nucl. Instr. and Meth. A 503/3, (2003) 513.

7. Measurement of inclusive spin structure functions of the deuteron with CLAS.
   J. Yun *et al.* and CLAS Collaboration, Phys. Rev. C 67 (2003) 055204.

8. Measurement of $ep \to e'p\pi^+\pi^-$ and baryon resonance analysis.
   M. Ripani *et al.* and CLAS Collaboration, Phys. Rev. Lett. 91 (2003) 022002.

9. Observation of nuclear scaling in the A(e,e') reaction at $x_{Bjorken} \geq 1$.
   K. Sh. Egiyan *et al.* and CLAS Collaboration, Phys. Rev. C 68 (2003) 014313.

10. Study of the $\Delta(1232)$ using single and double polarization asymmetries.
    A. Biselli *et al.* and CLAS Collaboration, Phys. Rev. C 68 (2003) 035202.

11. Measurement of polarized structure function $\sigma_{LT'}$ for $p(\vec{e}, e'p)\pi^0$ in the $\Delta(1232)$ resonance region.
    K. Joo Phys. Rev. C Rapid Comm. 68 (2003) 032201.

12. Measurement of beam-spin asymmetries for deep inelastic π^+ electroproduction.
    H. Avakian *et al.* and CLAS Collaboration, submitted to Phys. Rev. Lett.; hep-ex/0301005.

13. Hyperon photoproduction in the nucleon resonance region.
    J. W. C. McNabb *et al.* and CLAS Collaboration, submitted to Phys. Rev. Lett.; nucl-ex/0305028.

14. Measurement of the spin structure functions of the resonance region for Q^2 from 0.15 to 1.6 GeV^2.
    R. Fatemi *et al.* and CLAS Collaboration, Phys. Rev. Lett. 91 (2003) 222002.

15. Observation of an exotic S=+1 baryon in exclusive photoproduction from the deuteron.
    S. Stepanyan *et al.* and CLAS Collaboration, Phys. Rev. Lett. 91 (2003).

16. Two-nucleon momentum distributions measured in $^3He(e, e'pp)n$.
R. Niyazov *et al.* and CLAS Collaboration, accepted by Phys. Rev. Lett.; nucl-ex/0308013.

17. Tensor polarization of the ϕ meson photoproduced at high t.
K. McCormick *et al.* and CLAS Collaboration, submitted to Phys. Rev. C Rapid Comm. hep-ex/0311024.

18. Observation of an exotic baryon with S=+1 in photoproduction from the proton.
V. Kubarovsky *et al.* and CLAS Collaboration, accepted by Phys. Rev. Lett.; hep-ex/0311046.

6 Presentation at Conferences

1. *Physics of the CLAS Collaboration: Recent Results and Perspectives.*
Patrizia Rossi
Invited talk at the "XLI INTERNATIONAL WINTER MEETING ON NUCLEAR PHYSICS"
Bormio (Italy), January 26-February 2, 2003.

2. *Experimental Studies of Hard Disintegration of the Deuteron.*
Marco Mirazita
Invited talk at the " FIU/JLAB WORKSHOP ON THE DEUTERON"
Miami, FL (USA), March 27-29, 2003.

3. *Angular Distributions for the $\gamma d \rightarrow pn$ Reaction in the Few GeV Region.*
Federico Ronchetti
Contributed talk at the "17th INTERNATIONAL IUPAP CONFERENCE ON FEW-BODY PROBLEMS IN PHYSICS"
Durham, NC (USA), June 9-14, 2003.

4. *Misura della Beam Single Spin Asymmetry in $\vec{e}p \rightarrow e'\pi^+X$ nella Regione Profondamente Anelastica.*
Marco Mirazita
Contributed talk at the "LXXXIX CONGRESSO SIF"
Parma (Italy), September 17-22, 2003.

5. *Deuteron Photodisintegration at CLAS.*
Patrizia Rossi
Invited talk at the "6th WORKSHOP ON ELECTROMAGNETICALLY INDUCED TWO-HADRON EMISSION"
Pavia (Italy), September 24-27, 2003.

6. *Deuteron Two-Body Photodisintegration in the Quark-Hadron Picture.*
Patrizia Rossi
Invited talk at the "INTERNATIONAL WORKSHOP ON PROBING NUCLEONS AND NUCLEI VIA THE (E,E'P) REACTION"
Grenoble (France), October 14-17, 2003.

References

1. B. Mecking *et al.*, Nucl. Instr. and Meth. A**503/3**, (2003) 513.

2. S. L. Brodsky, G. L. Farrar - Phys. Rev. Lett. **31**, (1973) 1153.

3. V. Matveev *et al.*, Lett. Nuovo Cimento **7**, (1973) 719.
4. J. Napolitano *et al.*, Phys. Rev. Lett. **61**, (1988) 2530.
5. S. J. Freedman *et al.*, Phys. Rev. C **48**, (1993) 1864.
6. J. E. Belz *et al.*, Phys. Rev. Lett. **74**, (1995) 646.
7. C. Bochna *et al.*, Phys. Rev. Lett. **81**, (1998) 4576.
8. E. C. Schulte *et al.*, Phys. Rev. Lett. **87**, (2001) 102302-1.
9. K. Wijesooriya *et al.*, Phys. Rev. Lett. **86**, (2001) 2975.
10. E. C. Schulte *et al.*, Phys. Rev. C **66**, (2002) 042201R.
11. P. Rossi, Eur. Phy. J. **A 17**, (2003) 433.
12. S. L. Brodsky, J. R. Hillier, Phys. Rev. C **28**, (1983) 475.
13. L. L. Frankfurt *et al.*, Phys. Rev. Lett. **84**, (2000) 3045.
14. M. M. Sargisan, **nucl-th/0208027** (2003).
15. M. M. Sargisan, **nucl-th/0309054** (2003).
16. B. Julia-Diaz and T. S. H. Lee, Mod. Phys. Lett. **A18**, (2003) 200.
17. L.A. Kondratyuk,*et al.*, Phys. Rev. C **48**, (1993) 2491.
18. V.Yu. Grishina, *et al.*, Eur. Phys. J. A **10**, (2001) 355.
19. V.Yu. Grishina, *et al.*, Eur. Phys. J. A. **18**, (2003) 207
20. A. E. L. Dieperink, S. I. Nagorny - Phys. Lett. B **9**, (1999) 456.
21. R. Crawford *et al.*, Nucl. Phys. A **603**, (1996) 303.
22. A. B. Kaidalov, Z. Phys. C **12**, (1982) 63.
23. M. M. Brisudova *et al.*, Phys. Rev. D **61**, (2000) 054013.
24. V.P. Barannik *et al.*, Nucl. Phys. A **451**, (1986) 751.
25. F. Adamian *et al.*, Eur. Phys. J. A **8**, (2000) 423.
26. T. Nakano *et al.*, Phys. Rev. Lett. **91**, (2003) 012002; hep-ex/0301020.
27. V. Barmin *et al.*, Phys. At. Nucl., **66**, (2003) 1715; hep-ex/0304040.
28. S. Stepanyan *et al.*, Phys. Rev. Lett. **91**, (2003) 252001; hep-ex/0307018.
29. V. Kubarovsky, hep-ex/0307088.
30. V. Kubarovsky *et al.*, accepted by Phys. Rev. Lett.; hep-ex/0311046.
31. J. Barth *et al.*, hep-ex/0307083.
32. A. E. Asratyan *et al.*, hep-ex/0309042.
33. A. Airapetian *et al.*, hep-ex/0312044.

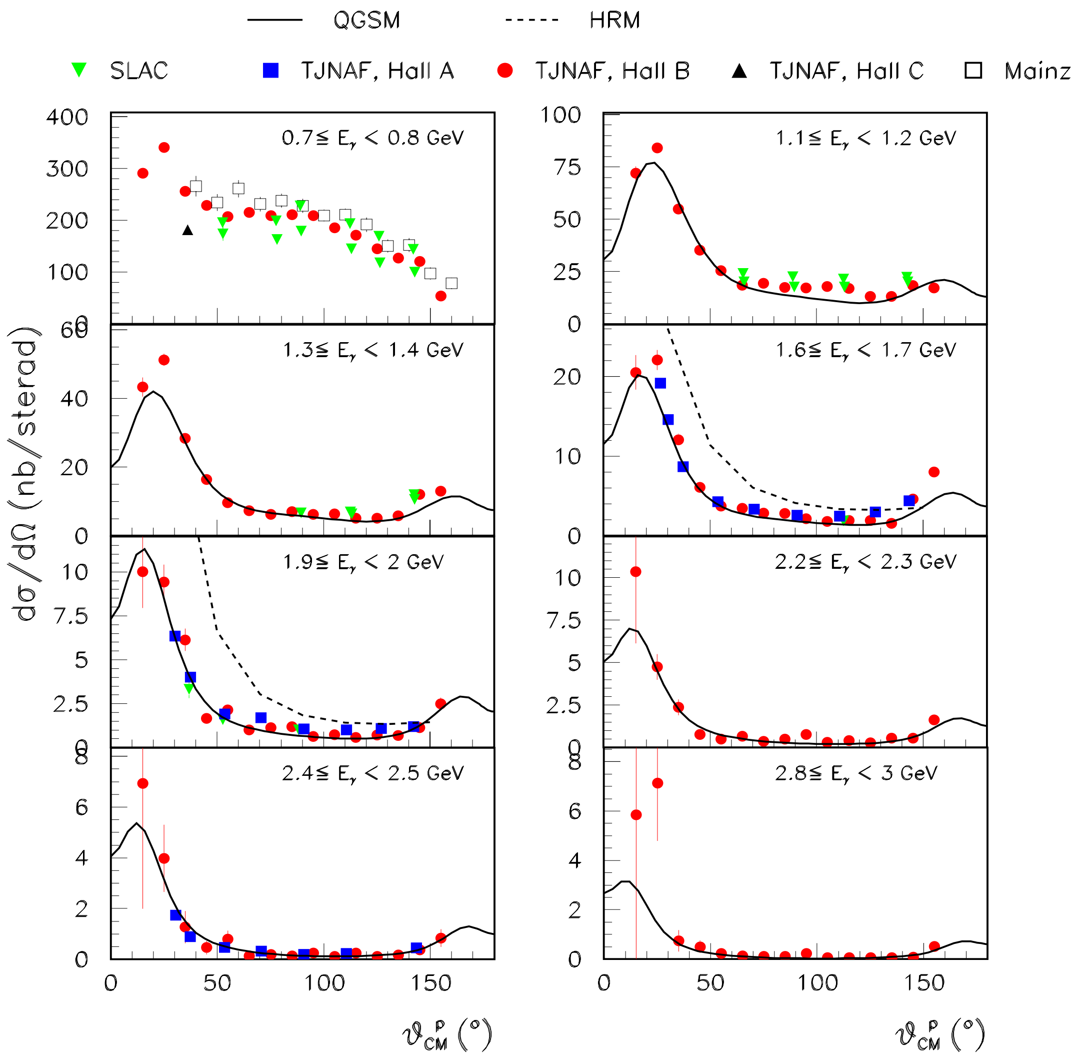

Figure 1: Angular distributions of the deuteron photodisintegration cross section measured by the CLAS (full red circles) in the incident photon energy range $0.5 - 3.0$ GeV. Results from Mainz [21] (open squares), SLAC [4, 5, 6] (full green triangles), JLab Hall A [10] (full blue squares) and Hall C [7, 8] (full black triangles) are included. For incident photon energies higher than 1 GeV, the solid line represents the non perturbative calculation of the QGS model [18] which well reproduces the data, while the dashed line represents the predictions of the HRM [13] model.

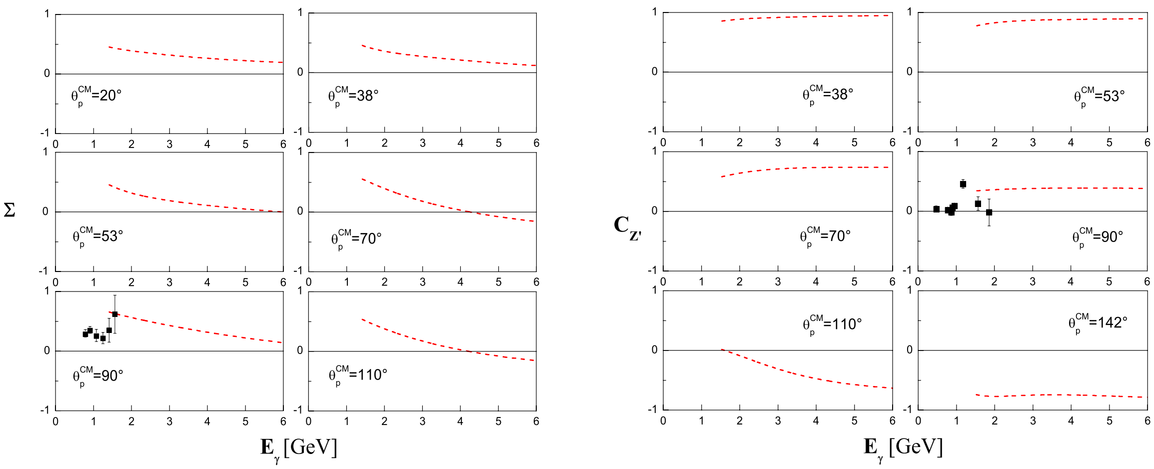

Figure 2: Polarization observables as predicted by the QGS model. Left panel: the asymmetry Σ for linearly polarized photons as a function of the photon energy. Also shown are the experimental data from Ref. [25]. Right panel: polarization transfer C_z for circularly polarized photons compared to the experimental data from Ref. [9].

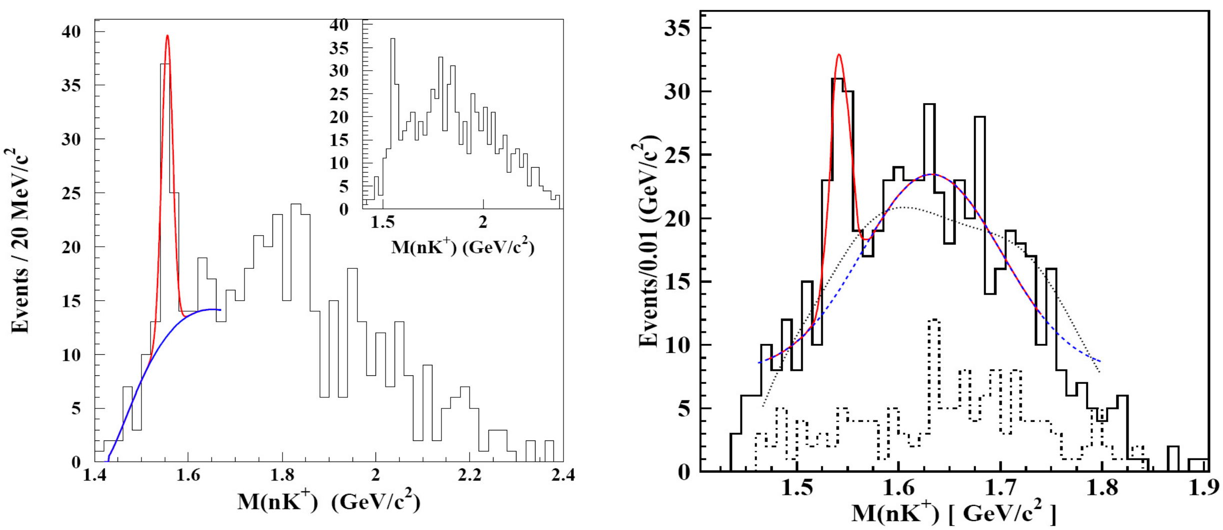

Figure 3: Mass peaks of the pentaquark candidate baryon, Θ^+, decaying to nK^+. The neutron (n) is reconstructed indirectly from the missing 4-momentum of the event. The left panel shows the nK^+ invariant mass spectrum in the reaction $\gamma p \to \pi^+ K^- K^+ (n)$ [29, 30]. The background function used in the fit is obtained from the simulation. The plot in the inset shows the same variable with a looser set of polar angule cuts. The right panel shows the nK^+ invariant mass spectrum in the reaction $\gamma d \to p K^- K^+ (n)$ [28]. The solid line is the fit to the peak plus the background, while the dashed one is the fit to the background alone. The dotted curve is the shape of the simulated background. The dash-dotted histogram shows the spectrum of events associated with $\Lambda(1520)$ production (i.e. $\gamma d \to \Lambda(1520) K^+ (n)$ with $\Lambda(1520) \to p K^-$).

DEAR / SIDDHARTA

M. Bragadireanu (Bors. UE), M. Catitti (Bors.), C. Guaraldo (Resp. Naz.), M. Iliescu, V. Lucherini, F. Lucibello (Tech.), C. Petrascu, D. Sirghi (Bors. PD), F. Sirghi (Bors. UE)

1 Introduction to the 2003 activities

1.1 The DEAR scientific program

The objective of DEAR (DAΦNE Exotic Atom Research) is the precise determination of the isospin dependent antikaon-nucleon scattering lengths, through a percent level measurement of the K_α line shift and width in kaonic hydrogen, and a similar (the first one) measurement of kaonic deuterium. The shift, with respect to the purely QED calculated value, and the broadening of the line (width) are due to the effect of the strong interaction between antikaon and nucleon, when the overlap between the two wavefunctions is verified; this effect is present and measurable for the 1s level.

The shift ϵ and the width Γ of the 1s state of kaonic hydrogen are related in a fairly model-independent way (Deser-Trueman formula) to the real and imaginary part of the complex s-wave scattering length, a_{K^-p}:

$$\epsilon + i\Gamma/2 = 412 \cdot a_{K^-p}\ eV\ fm^{-1} \tag{1}$$

A similar relation applies to the case of kaonic deuterium and to its corresponding scattering length, a_{K^-d}:

$$\epsilon + i\Gamma/2 = 601 \cdot a_{K^-d}\ eV\ fm^{-1} \tag{2}$$

The measured scattering lenghts are then related to the isospin-dependent scattering lengths, a_0 and a_1:

$$a_{K^-p} = (a_0 + a_1)/2, \quad a_{K^-n} = a_1 \tag{3}$$

The extraction of a_{K^-n} from a_{K^-d} requires a more complicated analysis than the simple impulse approximation (K^- scattering from each - free - nucleon): higher order contributions associated with the K^-d three-body interaction have to be taken into account. This means solving the three-body Faddeev equations by the use of potentials, taking into account the coupling among multichanneled interactions.

An accurate determination of the K^-N isospin dependent scattering lengths will place strong constraints on the low-energy K^-N dynamics, which in turn constraints the SU(3) description of chiral symmetry breaking. Crucial information about the nature of chiral symmetry breaking, and to what extent the chiral symmetry must be broken, is provided by the calculation of the so-called meson-nucleon sigma terms. The sigma term is then a quantity which directly gives the degree of chiral symmetry breaking. Consequently, its relation to the scattering amplitude represents the corresponding low-energy theorem in the soft meson limit.

A phenomenological procedure, which implies dispersion relations and suitable extrapolations should allow to extract the sigma terms from the measured amplitudes. Presently only estimates, with 70% uncertainties, exist; a measurement of the K^-N scattering lengths at few percent level should allow the determination of these quantities with a precision better than 20%.

The sigma terms are also important inputs for the determination of the strangeness content of the proton. The strangeness fraction depends both on kaon-nucleon and on pion-nucleon sigma terms, being more sensitive to the first ones.

1.2 Summary of the 2003 activities

During the year 2003 the DEAR activities were focussed on:

i) finalize the kaonic nitrogen analysis;

ii) refine and finalize the analysis of the kaonic hydrogen data (collected in the period 31 October - 23 December 2002);

iii) identify a new triggerable detector (Silicon Drift Detector, SDD) which should allow a future eV-level precision measurement of kaonic hydrogen and of kaonic deuterium (such an evolution of DEAR will be named SIDDHARTA);

iv) on-beam test of a prototype array of SDD detectors;

v) design and Monte Carlo simulations of the new setup

All these activities are described in the rest of this Report.

2 DEAR kaonic nitrogen results

The kaonic nitrogen analysis was the first measurement ever of transition yields of this kind of exotic atom (data collected in October 2002). The results are included in the paper "Kaonic nitrogen X ray transition yields in a gaseous target", submitted for publication to Phys. Lett. B.

3 DEAR kaonic hydrogen results

At the end of 2002 in a dedicated run, DEAR performed the kaonic hydrogen measurement, with a target filled with hydrogen in cryogenic and pressurized conditions: 23 K and 1.82 bar. The kaonic hydrogen measurement lasted from 30 October to 22 December 2002. It was divided into two periods:

- from 30 October to 16 December - continuous run with the kaonic hydrogen; the total integrated luminosity, measured by the DEAR kaon monitor, was about 58 pb^{-1};
- from 16 December to 22 December - background run - with no collisions in the DEAR Interaction Region - with a statistics equivalent to about half of the kaonic hydrogen one - in order to have the pure-background measurement.

In the first part of 2003 a procedure of Charge Transfer Corrections, raw-by-raw for each one of the 16 CCDs present in the DEAR setup, was first optimized (starting with the calibration data performed during data taking) and then applied to the whole volume of data. This procedure allowed an improvement of the energy resolution by about 14%, and an increase of statistics by about 10%.

After having obtained this good-quality data set, two independent analyses were performed, in order to extract the kaonic hydrogen signal:

- a simultaneous fit of the kaonic hydrogen spectrum and of the no-collision background data taken in December 2002;
- a constrained fit of the kaonic hydrogen data and of the whole bulk of 2002 data (kaonic nitrogen of April 2002, kaonic nitrogen of October 2002 and low-occupancy CCD no-collision data of December 2002).

In these fits, in order to avoid systematic errors due the the unknown relative yields of kaonic hydrogen, a cut has been performed in the energy region fitted, such as to avoid the region where the knowledge of relative yields would be mandatory (7.7 to 8.8 keV). It was checked with Monte Carlo simulation that the systematic errors introduced by that cut were negligible (at the level of eV).

The kaonic hydrogen significance is about 6σ (sum of the individual lines).

The results obtained from the two analyses are in very good agreement, and a mean value of these results is given below:

$$\epsilon = -(200 \pm 45)\ eV \tag{4}$$

$$\Gamma = (258 \pm 137)\ eV \tag{5}$$

In (4) and (5) only statistical errors are reported; the systematic ones are under study.

In Figure 1 the kaonic hydrogen spectrum with the fitting function is shown, while in Figure 2 the continuous background subtracted spectrum is shown.

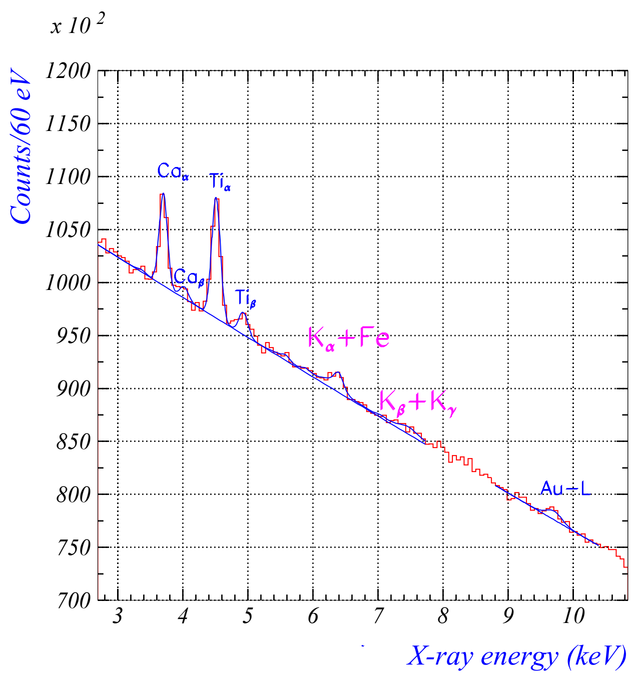

Figure 1: *The kaonic hydrogen spectrum with the fitting function.*

The DEAR measurement represents the most precise measurement of kaonic hydrogen performed to date. It gives new energy to the community of those working in the low-energy kaon-nucleon interactions, related to non-perturbative tests (see Section 1.1).

Starting from the success of this measurement, a continuation of the scientific program on exotic atoms is foreseen based on the happy marriage between the good-quality "kaon beam" delivered by DAΦNE and a setup with a cryogenic target maximizing the number of kaons stopped inside, equipped with good quality X-ray detectors: the new experiment SIDHARTA (Silicon Drift Detector for Hadronic Atom Research by Timing Application), which represents a new step in the study of kaonic atoms at DAΦNE.

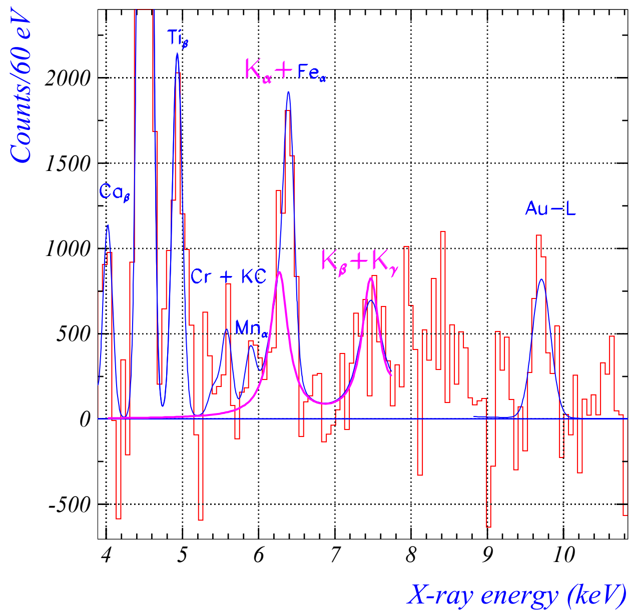

Figure 2: *The background subtracted kaonic hydrogen spectrum with the fitting function.*

4 From DEAR to SIDDHARTA

4.1 Motivations

As stated in the previous Section, DEAR has performed the most precise kaonic hydrogen measurement to present. This was possible due to the continuous work, performed in collaboration with the DAΦNE staff, of background reduction: by using appropriate machine optics and shielding solutions. During the DEAR history a dramatic background reduction, a factor about 100, was achieved.

However, as seen in Figure 1, the ratio S/B is still not sufficient (about 1/80) to allow to perform an eV precision measurement, and there is no room left for additional shielding which should allow important additional background reduction.

In these conditions only a careful re-consideration of the whole setup, and especially of the detector part, can allow important step forwards. DEAR used the CCDs (Charge Coupled Device) for X-ray detection. These were excellent X-ray detectors, with very good energy resolution (about 140 eV FWHM at 6 keV), but with the drawback of being non-triggerable devices (since the readout time per device is at the level of 10 s). A new detector has been identified, which preserves all good features of CCDs (energy resolution, stability and linearity) and is triggerable - i.e. fast (at the level of 1μs): the Silicon Drift Detector (SDD), specifically designed for spectroscopical use.

A first test of an array of SDD devices was performed in July 2003 at the Beam Test Facility (BTF) of Frascati, in realistic (i.e. DEAR-like) conditions. The results of these tests are briefly reported below.

4.2 SDD tests at BTF

In the period 21-31 July 2003 a test of a prototype array of 7 SDDs, 5 mm^2 each, was performed at the BTF).

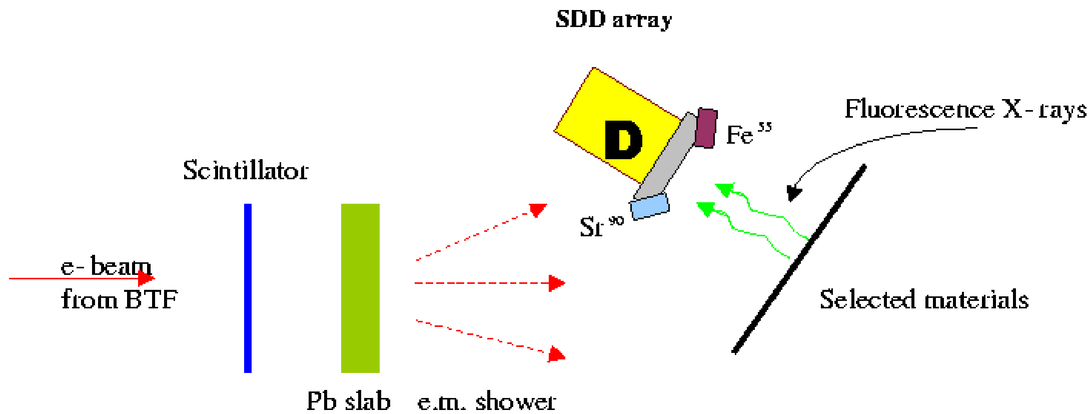

Figure 3: *The test experimental setup mounted in the BTF area*

Fig. 3 shows a scheme of the setup configuration. The beam coming from the BTF (510 MeV electrons, 50 Hz) hits a thin scintillator to provide a fast trigger signal, then is degraded in a 2 cm thick lead layer. The emerging secondaries from the e.m. cascade generated in lead, hit a set of selected materials (Cu, Zr) disposed at about 45 degrees with respect to the primary beam line. Fluorescence X-ray transitions are then excited and reach the SDD. The detector can see the "signal" represented by the Cu and Zr fluorescence lines, superimposed to a continuous background represented by the secondaries (electrons, positrons, photons) generated in the e.m. cascade. Being the "signal" created by the latter, this background is "synchronous" to the "signal". To generate an "asynchronous" background, i.e. not time-correlated with the "signal", two radioactive sources were employed (see Fig 3). One, a Sr source, due to its beta spectrum of maximum energy 2.24 MeV, produced a continuous background of soft electrons and photons. The other, a Fe source, produced a structured asynchronous background represented by the K_α and K_β Manganese lines.

After having performed tests on stability and linearity, the main goal was pursued: namely a test of the trigger capability, in conditions of background rate similar to those found in DEAR when kaonic hydrogen was measured.

The results of this tests are very encouraging: a trigger rejection factor of $5 \cdot 10^{-5}$ was measured. Extrapolated to SIDDHARTA conditions, this number translates into a S/B ratio in the region of interest about 20/1. By triggering the SDDs, the asynchronous e.m. backgroung (mainly due to Touschek effect) can therefore be completely eliminated. In Figure 4 the results of the trigger capability test are reported.

The remaining synchronous background (the one intimately related to the processes started by the primary kaon) was studied by Monte Carlo simulations and the result is a S/B ratio of the order 8/1.

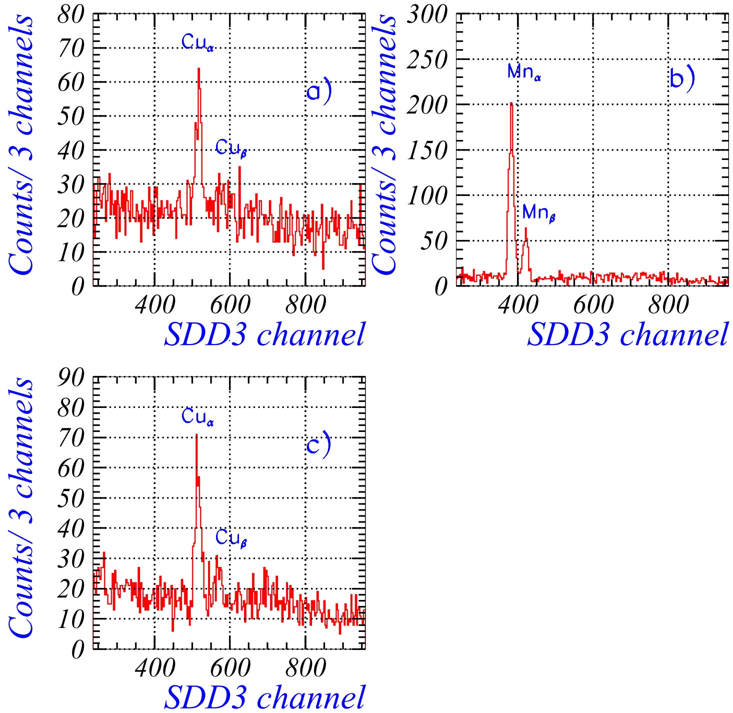

Figure 4: *a) Trigger OFF (16 hours); Cu signal visible; no asynchronous background (Fe and Sr sources out); continuous background: synchronous from primary beam; rate = 5 Hz. b) Trigger OFF (20 minutes); Cu signal embedded in background; structured asynchronous background (Mn K_α and Mn $K_{|beta}$ from Fe); continuous background: synchronous from primary beam and asynchronous from Sr source; rate = 60 Hz (DEAR - like); c) Trigger ON (16 hours); Cu signal visible; structured asynchronous background completely cut; continuous background: synchronous from primary beam; rate about 5 Hz - as a).*

5 Activity in 2004

Based on the very encuraging results obtained in the BTF testing of the SDDs, the activity in 2004 is focussed in the following directions:

- long-duration SDD testing in the laboratory (stability, linearity, etc.);
- definition and start of the SDD production process (at PN Sensors and MPE, Munchen);
- SIDDHARTA setup design: mechanics, cryogenics, electronics - in close collaboration with the DAΦNE staff, based on Monte Carlo simulation for optimization of the signal. A preliminary drawing already exists, Figure 5; Monte Carlo simulation shows that the signal increases by a factor about 30 in the new geometry, with respect to DEAR, with a beam-pipe diameter of 4-5 cm;
- design of acquisition electronics and tests.

Apart from an eV precision measurement of kaonic hydrogen and the first measurement of kaonic deuterium, due to the trigger capabilities of SDDs and to efficiency of the SDDs extended up to tens of keV, SIDDHARTA is performing studies of feasibility for the following measurements:

- kaonic helium;
- other light kaonic atoms;
- measurement of other types of hadronic exotic atoms (sigmonic hydrogen for example).

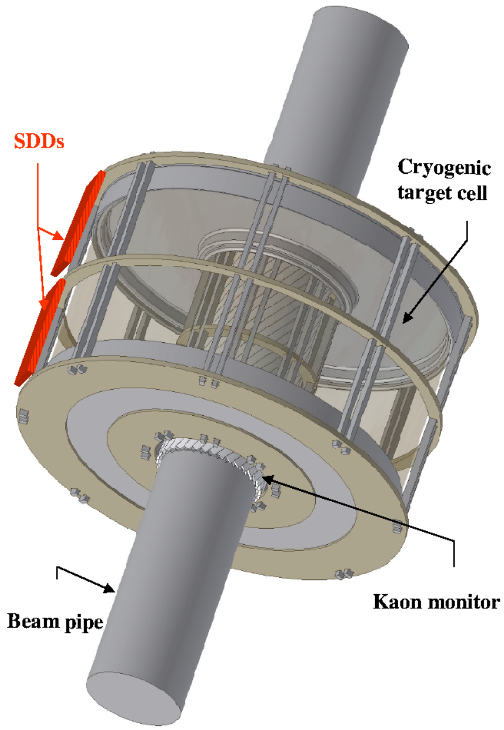

Figure 5: *Preliminary SIDDHARTA setup.*

6 Publications 2003

6.1 List of Conference Talks given by LNF Authors in Year 2003

1. C. Curceanu (Petrascu), **Kaonic nitrogen and hydrogen from DEAR**, "XLI International Winter Meeting on Nuclear Physics" Bormio, Italy, January 26-February 2, 2003.

2. M. Iliescu, **The DEAR experiment at DAΦNE**, "LNF Spring School", Frascati, Italy, May 19-23, 2003.

3. C. Guaraldo, **First results on kaonic hydrogen from DEAR at DAΦNE**, "4th International Conference on Perspectives in Hadronic Physics", Miramare-Trieste, Italy, May 12-16, 2003.

4. C. Curceanu (Petrascu), **Last results from the DEAR experiment at DAΦNE**, "HADRON SPECTROSCOPY", Tenth International Conference on Hadron Spectroscopy, Aschaffenburg, Germany, August 31 - September 6, 2003.

5. C. Curceanu (Petrascu), **Future precision measurements on kaonic hydrogen and kaonic deuterium with SIDDHARTA**, "HadAtom03", Workshop on Hadronic Atoms, European Centre for Theoretical Nuclear Physics and Related Areas (ECT*), 13-17 October 2003, Trento, Italy.

6. C. Curceanu (Petrascu), **Primi risultati sull'idrogeno kaonico dell'esperimento DEAR**, Invited talk at the "LXXXIX Congresso Nazionale Societa' Italiana di Fisica", 17-22.09.2003, Parma, Italy

6.2 Papers

1. J. Zmeskal *et. al.* (DEAR Collaboration), **The DEAR experiment**, Proceedings of the "EXA 2002 - International Workshop on Exotic Atoms - Future Perspectives", Vienna, Austria, 28-30 November, 2002, Austrian Academy of Sciences Press (2003), 113.
2. C. Curceanu (Petrascu) *et. al.* (DEAR Collaboration), **Kaonic nitrogen and hydrogen from DEAR**, Proceedings of the "XLI International Winter Meeting on Nuclear Physics" Bormio, Italy, January 26-February 2, (2003) 21.
3. C. Guaraldo *et. al.* (DEAR Collaboration), **First results on kaonic hydrogen from DEAR at DAΦNE**, Proceedings of the "4th International Conference on Perspectives in Hadronic Physics", Miramare-Trieste, Italy, May 12-16, 2003.
4. C. Curceanu (Petrascu) *et. al.* (DEAR Collaboration), **Last results from the DEAR experiment at DAΦNE**, Proceedings of "HADRON SPECTROSCOPY", Tenth International Conference on Hadron Spectroscopy, Aschaffenburg, Germany, August 31 - September 6, 2003.
5. M. Cargnelli *et. al.* (DEAR Collaboration), **DEAR - Kaonic Hydrogen: First Results**, Proceedings of 4th International Workshop on CHIRAL DYNAMICS 2003 Theory and Experiment, Bonn, Germany, September 8-13, 2003.
6. M. Cargnelli *et. al.* (DEAR Collaboration), **Kaonic Hydrogen - Status of the DEAR Experiment**, Progress of Theoretical Physics Supplement No. 149, pp.240-246, 2003.
7. C. Curceanu (Petrascu) *et. al.* (DEAR Collaboration), **Future precision measurements on kaonic hydrogen and kaonic deuterium with SIDDHARTA** Proceedings of "HadAtom03", Workshop on Hadronic Atoms, European Centre for Theoretical Nuclear Physics and Related Areas (ECT*), 13-17 OCTOBER 2003, TRENTO, ITALY.
8. M. Cargnelli *et. al.* (DEAR Collaboration), **DEAR - Kaonic Hydrogen: First Results**, Proceedings of "HadAtom03", Workshop on Hadronic Atoms, European Centre for Theoretical Nuclear Physics and Related Areas (ECT*), 13-17 OCTOBER 2003, TRENTO, ITALY.
9. G. Beer *et. al.* (DEAR Collaboration), **Kaonic nitrogen X ray transition yields in a gaseous target** Phys. Lett. **B**, to appear (2003).

6.3 Technical Notes

1. SIDDHARTA Collaboration, **Tests of prototype Silicon Drift Detectors to be used in SIDDHARTA (Silicon Drift Detector for Hadronic Atom Research by Timing Application) performed at the Beam Test Facility (BTF) of LNF in the period 21 - 31 July 2003,**, SIDDHARTA Note-IR-1, Aufust 25, 2003.
2. C. Curceanu (Petrascu), **The Preliminary SIDDHARTA experimental setup**, SIDDHARTA Note-IR-3, August 25, 2003.
3. C. Curceanu (Petrascu), **Preliminary Monte Carlo simulation of the SIDDHARTA toroidal setup**, SIDDHARTA Note-IR-4, November 24, 2003.

DIRAC

P. Gianotti (Resp.), M. Giardoni, C. Guaraldo, M. Iliescu, A. Lanaro, P. Levisandri, V. Lucherini, C. Petrascu

1 Introduction

The goal of the DIRAC (Dimeson Relativistic Atomic Complex) experiment at CERN was to measure (with 10 % accuracy) the lifetime of Pionic Atoms ($A_{2\pi}$), a weakly bound $\pi^+\pi^-$ system, produced by proton-nucleus interactions at 24 GeV/c. This allows to determine, in a model independent way, the difference between the isoscalar (a_0) and isotensor (a_2) S-wave pion-pion scattering lengths with 5 % accuracy.

The above mentioned scattering lengths a_0, a_2 have been calculated in the framework of Chiral Perturbation Theory [1)] by means of an effective Lagrangian with a precision better than 2.5 % [2)]. The present theoretical estimate of the lifetime of the ground state of the pionic atom is $(2.9 \pm 0.1) \cdot 10^{-15} s$ [3)]. These results are based on the assumption that the spontaneous chiral symmetry breaking is due to a strong quark condensate, as confirmed recently [4, 5)]. An alternative scenario, with an arbitrary value of the quark condensate [6)], foresees larger values of a_0, a_2. Therefore a measurement of scattering lengths allows to improve the current understanding of chiral symmetry breaking in QCD and to verify the magnitude of the quark condensate.

The DIRAC experimental apparatus, located at the CERN PS East Hall, is a double arm magnetic spectrometer (see fig. 1). It consists of high resolution tracking and particle identification detectors to measure, with high efficiency, charged pion pairs with small relative momentum ($Q < 3$ MeV/c), and small opening angle ($\simeq$ 0.35 mrad). The experiment was approved in 1996, the commissioning was done at the end of 1998 and the data taking started in the spring of 1999.

The DIRAC Collaboration includes 96 participants from 18 international Institutes. 10 % of the participants are from Italian Institutes (INFN-LNF and Trieste University/INFN). About 25 % of leadership roles within the collaboration is granted to INFN members. The yearly budget contribution from INFN to the Experiment amounts to $\sim$ 20 % of the total budget.

The LNF group has contributed to the experiment by providing 2 large threshold Cherenkov counters for e^+e^- identification. The counters use gaseous nitrogen as radiator. Each counter is equipped with 20 mirrors and 10 photomultipliers. The Cherenkov detectors ensure e^+e^- rejection at the trigger level with 99.5 % efficiency, and 15 photoelectrons are on average detected in each counter.

2 Activity in 2003

During 2003 the main activities of the DIRAC collaboration were the data taking completion, and the data analysis. The LNF-DIRAC group contributed to both. The DIRAC data collection took place from May to October 2003 and during that period the LNF group kept the responsibility of maintaining and monitoring the performance of the Cherenkov detectors. Furthermore, the group participated to the offline data quality checks.

The main goal of the 2003 data analysis was to determine $A_{2\pi}$ lifetime for the data sample taken at 24 GeV using the 94μm and the 98μm thick Nickel targets. Two independent tracking procedures, and two complementary background reconstruction strategies have been used to check the results and to evaluate the systematic errors. A final sample of 9275 atomic pairs has been detected. Together with the event selection procedure, a detailed study of the systematic errors has

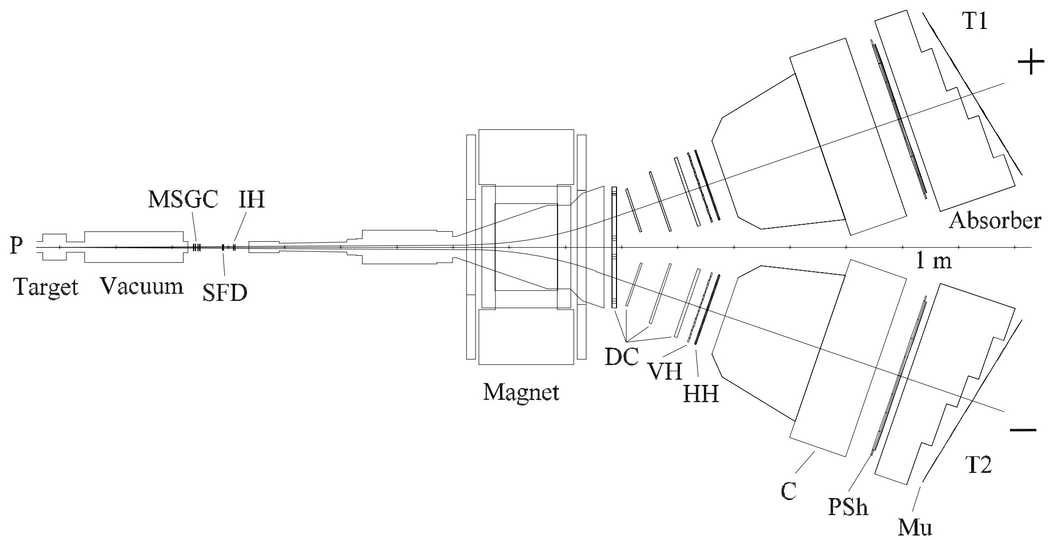

Figure 1: *Schematic top view of the DIRAC spectrometer. Upstream of the magnet: microstrip gas chambers (MSGC), scintillating fiber detectors (SFD), ionization hodoscopes (IH). Downstream of the magnet: drift chambers (DC), vertical and horizontal scintillator hodoscopes (VH,HH), Cherenkov counter (C), preshower detector (PSh) and muon detector (Mu).*

been carried out. The major sources of these uncertainties have been identified in the knowledge of the pion multiple scattering in the target and detector materials, and in the scintillating fiber detector response to two close tracks. The information on multiple Coulomb scattering, available in literature, is not accurate enough to allow a reduction of the systematic error. Therefore, some dedicated measurements were performed, and the data analysis is on the way. Concerning the scintillating fiber detector response, alternative selection criteria have been implemented excluding the information coming from this detector. The atomic pair sample selected with this method is consistent with that obtained using the full reconstruction even if in this case the level of background is higher.

In order to determine the uncertainty due to the background evaluation some data taking using a multi-layer Ni target were performed. Single and multi-layer target event distributions are identical in all respects but one: the multi-layer target yields a lower number of dissociated pairs due to the annihilations in the gaps among the different foils. This allows to obtain the atomic pair signal as the difference between the single and the multilayer target distributions.

A big effort has also been made to improve the MonteCarlo description of the DIRAC detector. A MonteCarlo event generator for atoms, non-Coulomb and Coulomb pairs was implemented to check the consistency of the background fraction obtained through the measurement of the accidental pairs. By means of this new tool, we proved that the background reconstruction is correct at the per-mille level. The quality of the MonteCarlo description of the data can be checked in fig. 2 where the atomic pair spectrum for both the real and the MonteCarlo data is shown.

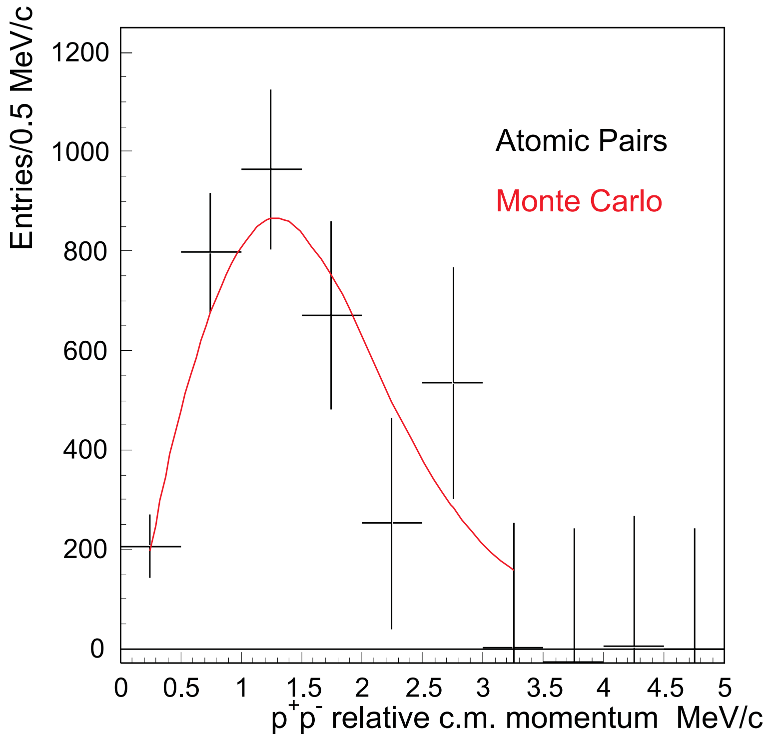

Figure 2: *Nickel target data 2001: atomic pairs spectrum; the red curve is the MonteCarlo simulation result.*

Therefore, we calculate a first preliminary value for the $A_{2\pi}$ lifetime:

$$\tau = (3.12^{+0.92}_{-0.72}(stat) \pm 0.8(SST)) \cdot 10^{-15}s \tag{1}$$

3 Planned activity in 2004

In the physics runs from 1999 up to the end of 2003 many thousands of "atomic pairs" have been accumulated with different nuclear targets: Pt, Ti, Ni. Table 1 summarizes the number of atomic pairs detected using Ni targets. DIRAC data taking is completed. Therefore the main activity of the DIRAC collaboration during 2004 will be the data analysis. With the analysis done up to now we were able to bring down the systematic uncertainty to the same level of the statistical error. By analysing the full data sample, we will be able to reduce further the statistical and the systematic errors in order to fulfill the initial requirements. These will be the main activities of the 2004 data analysis.

Table 1: *Atomic pairs detected in the different run periods.*

	Ni2000 (24 GeV)	Ni2001 (24 GeV)	Ni2002 (20 GeV)	Ni2002 (24 GeV S)	Ni2002 (24 GeV M)	Ni2003 (20 GeV S)	Ni2003 (20 GeV M)
$Q_L < 1$ $Q_T < 3$	1468 ± 257	5193 ± 392	1796 ± 266	2560 ± 370	539 ± 237	1146 ± 178	348 ± 172

4 List of 2003 publications

1. B. Adeva *et al.*, "DIRAC: A high resolution spectrometer for pionium detection", Nucl. Instr. Meth. A515 (2003) 49.

2. C. Santamarina *et al.*,"A Monte Carlo calculation of the pionium break-up probability with different sets of pionium target cross sections", J. Phys. B: At. Mol. Opt. Phys. 36 (2003) 4273.

References

1. S. Weinberg, Physica **A96** (1979), 327; J. Gasser and H. Leutwyler, Phys. Lett **B125** (1983) 325; ibid Nucl. Phys.**B250** 465, 517, 539.

2. G. Colangelo, J. Gasser and H. Leutwyler, Nucl. Phys. **B603** (2001) 125 .

3. A. Gall, J. Gasser, V. Lyubovitskij, A. Rusetsky, Phys. Rev. D **64** (2001) 016008.

4. G. Colangelo, J. Gasser and H. Leutwyler, Phys. Rev. Lett. **86** (2001) 5008.

5. S. Pislak *et al.*, Phys. Rev. Lett. **87** (2001) 221801.

6. M.Knecht *et al.*, Nucl. Phys. **B457** (1995) 513.

FINUDA

L. Benussi(Ass. Ric.), M. Bertani, S. Bianco, M.A. Caponero (Ass.), F.L. Fabbri(Resp.), P. Gianotti, M. Giardoni, V. Lucherini (Resp.), E. Pace, M. Pallotta, L. Passamonti(Tecn.), D. Pierluigi(Tecn. Art.15), F. Pompili(Art.23.), A. Russo(Tecn. Art.15), S. Tomassini(Art.23)

1 Introduction

FINUDA (meaning FIsica NUcleare a DAΦNE) is an experiment whose aim is to study hypernuclei formation and decay within the same apparatus. Hypernuclei are nuclei in which an ordinary bound nucleon is replaced by a hyperon, a baryon containing s (strange) quarks. The added flavour enlarges the basic nucleon-nucleon interactions giving information on the modification of the properties of baryon-baryon interaction in the presence of strangeness.

The DAΦNE e^+e^- collider is optimized in *Luminosity* at the *c.m.* energy corresponding to the $\phi(1020)$ meson. The huge number of ϕs, produced (almost) at rest, decay with a $B.R.$ of 0.49 into back-to-back pairs of slow (127 MeV/c) charged kaons. The K^-s, stopped in a target, can produce hypernuclei, through the reaction:

$$K^- + n \rightarrow \pi^- + \Lambda \tag{1}$$

The levels of the produced hypernuclei can be obtained by measuring the momentum of the emitted (*prompt*) π^-. Since the kaons from DAΦNE have a very low (127 MeV/C) and sharp momentum, they can be stopped in very thin targets, allowing unprecedent resolution (0.3%) to be reached in hypernuclear spectroscopy. Moreover, the subsequent decay of the hypernucleus, both *mesonic* ($p\pi^-$) and $non-mesonic$ (np or nn) can be detected by FINUDA, that can hence study simultaneously the formation and decay of hypernuclei within the same apparatus, a feature never reached in any other experiment.

FINUDA is a large acceptance magnetic spectrometer based on a medium sized superconducting solenoid (2.7 m long and 2.4 m diameter), operating at a maximum field of 1.1 T. The solenoid is equipped with tracking detectors, time-of-flight scintillator barrels and vertex detectors, also embedding a system of multiple targets. A He-bag is used to fill the volumes between the tracking detectors with He gas in order to reduce the deterioration of momentum resolution due to multiple scattering.

The FINUDA Collaboration is formed by almost 40 physicists from LNF, several INFN sections and Universities (Torino, Bari, Trieste, Pavia, Bologna, Brescia) and with the participation of researchers from the TRIUMF Laboratory of Vancouver, Canada. In 2003 groups of physicists coming from Japan (KEK) and South Korea (Seoul National University) joined the Collaboration.

An extensive and updated description of the FINUDA experiment can be found in [1] and [2].

2 FINUDA activity in 2003

The year 2003 has been crucial for FINUDA. The new IP2 interaction region, which includes a beryllium pipe, was inserted inside FINUDA, followed by the installation of the vertex detectors around beam pipe and by the roll-in of the spectrometer (January-April). After that, two periods of data taking with magnetic field OFF and ON (3-4 weeks each) were done to calibrate and align the detectors (May-July). Finally, after DAΦNE startup (September), the period of on-beam activity began. Such period was divided in two parts: first period for tuning and debugging the detectors with beams circulating inside DAΦNE (this task could never be done before). At the

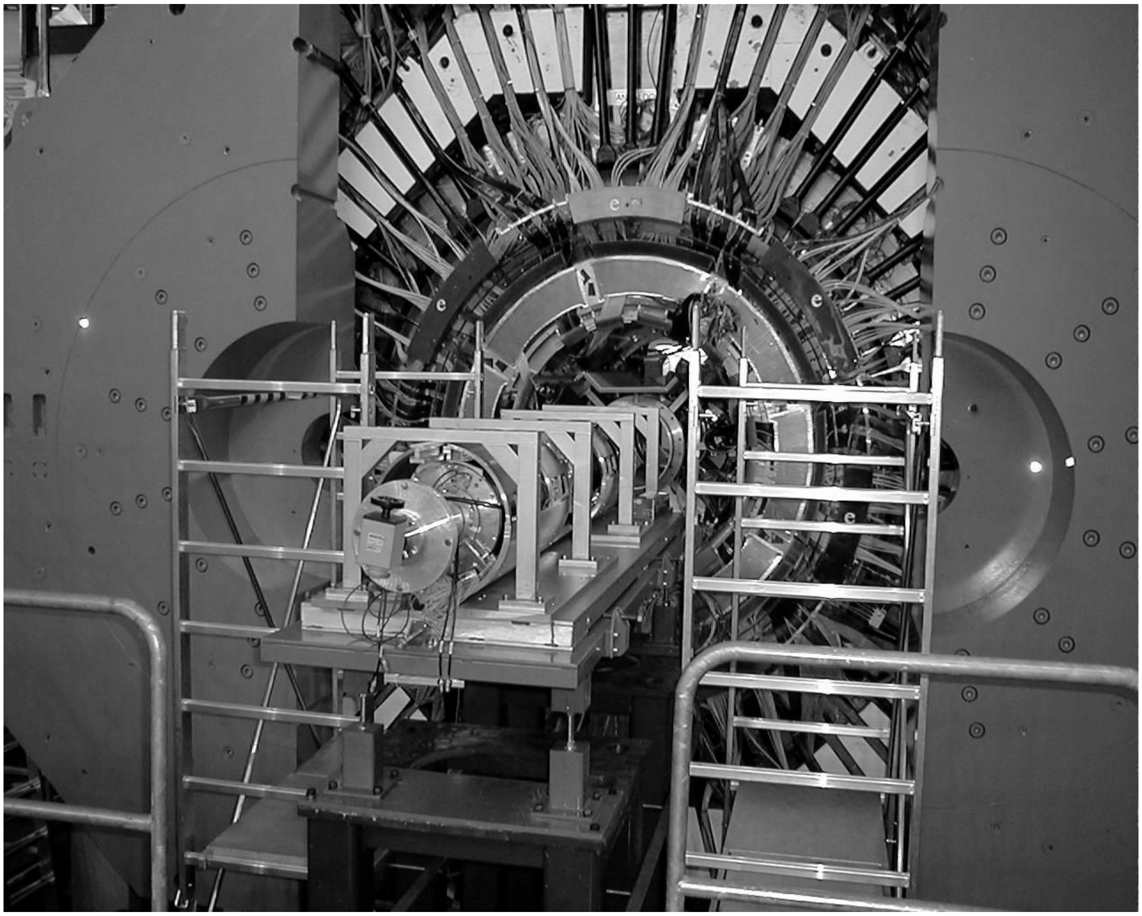

Figure 1: *Insertion of IP2 beam pipe inside FINUDA.*

same time DAΦNE commissioned its new optics configuration. These two phases lasted up to November. Then from December 1st, the period of physics data taking followed and continued until March 21, 2004, when the integrated luminosity delivered to FINUDA reached the milestone of 250 pb^{-1}.

2.1 Activity from January to April 2003

In the first months of 2003 there was a long shut-down period of DAΦNE in order to:

- remove the already installed and operating inner layer of Drift Chambers (8 Elements) in order to allow the insertion of beam-pipe and vertex detectors.
- insert the new IP2 beam pipe inside FINUDA;
- install the FINUDA vertex detectors around the new beam pipe;
- re-insert and connect the inner Drift Chambers layer;
- roll-In FINUDA;
- perform the final connections and He-bag closure;
- install and modify several of DAΦNE elements to improve the collider and to adapt the machine operation to the new optics deriving from the insertion of the FINUDA solenoid.

The detectors of the FINUDA spectrometer were already installed and tested during the shut-down periods of 2002 except for the vertex ones. The reason was that the detectors of the vertex region had to be installed after the mounting of the beam pipe (provided with a 500 μm thick beryllium window in corrispondence of the IP2 interaction region). Such beam pipe was ready at the beginning of 2003. In January-February 2003 the beam pipe for IP2 underwent final tests of its permanent magnet elements and was finally inserted and aligned inside FINUDA (fig.1).

The vertex detectors, in which the targets are embedded, were then installed. The insertion of the inner vertex detector, the scintillator barrel called tofino, is shown in fig.2.

Figure 2: *Tofino scintillator barrel mounted around the beam pipe.*

After mounting tofino, the next step was to mount the delicate detectors made of two layers of Si microstrips, which provide high spatial resolution for the crossing particles in both azimuthal and radial coordinates. They also provide the information of energy loss inside the detector. Between the inner layer (ISIM) and the outer layer (OSIM) lays the multitarget system of FINUDA. For the first phase of FINUDA runs, the following targets have been selected: ^{12}C (three targets), ^{6}Li (two targets), and ^{7}Li, ^{27}Al, ^{51}V (one target each). To mount and align this fragile and complex system a special custom-built and remotely-controlled robot was used.

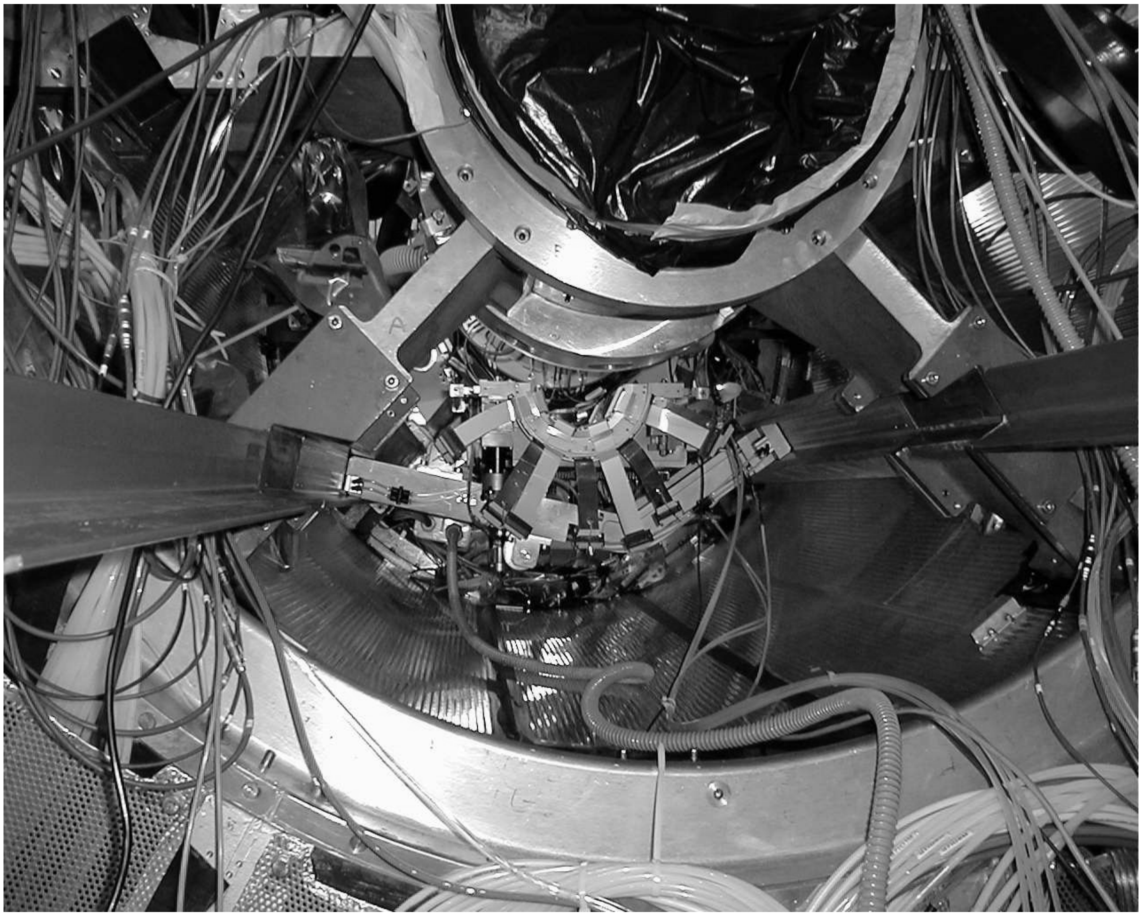

Figure 3: *Installation of Si microstrips using the special robot.*

Fig.3 shows one of the phases of this critical and important installation.

After completing the installation of the vertex detectors and their alignment, the inner layer of Drift Chambers that had been previously removed was re-installed. The roll-in of the FINUDA spectrometer on DAΦNE was accomplished at the end of April 2003 (fig.4).

2.2 Activity from May to July 2003

The Roll-In was followed by the the connection and the closing of the He-bag windows. In mid May FINUDA was ready for data taking with all its detectors operational. Data taking started on May 12, 2003, with the solenoid magnetic field OFF, in order to collect data with straight cosmic rays for a fist overall detector alignment (three weeks, 2.5 millions of events).

In the mean time, the FINUDA solenoid was undergoing the cooling phase. At the end of June 2003 the cooled solenoid was switched ON at its nominal 1.1 T magnetic field, and a four week period of data taking with cosmic rays was performed (about 3 millions of events). This further debugging and alignment was needed for the Drift Chambers which are not fully efficient with magnetic field OFF (their voltage dividers are displaced to take into account the effect of the Lorentz angle).

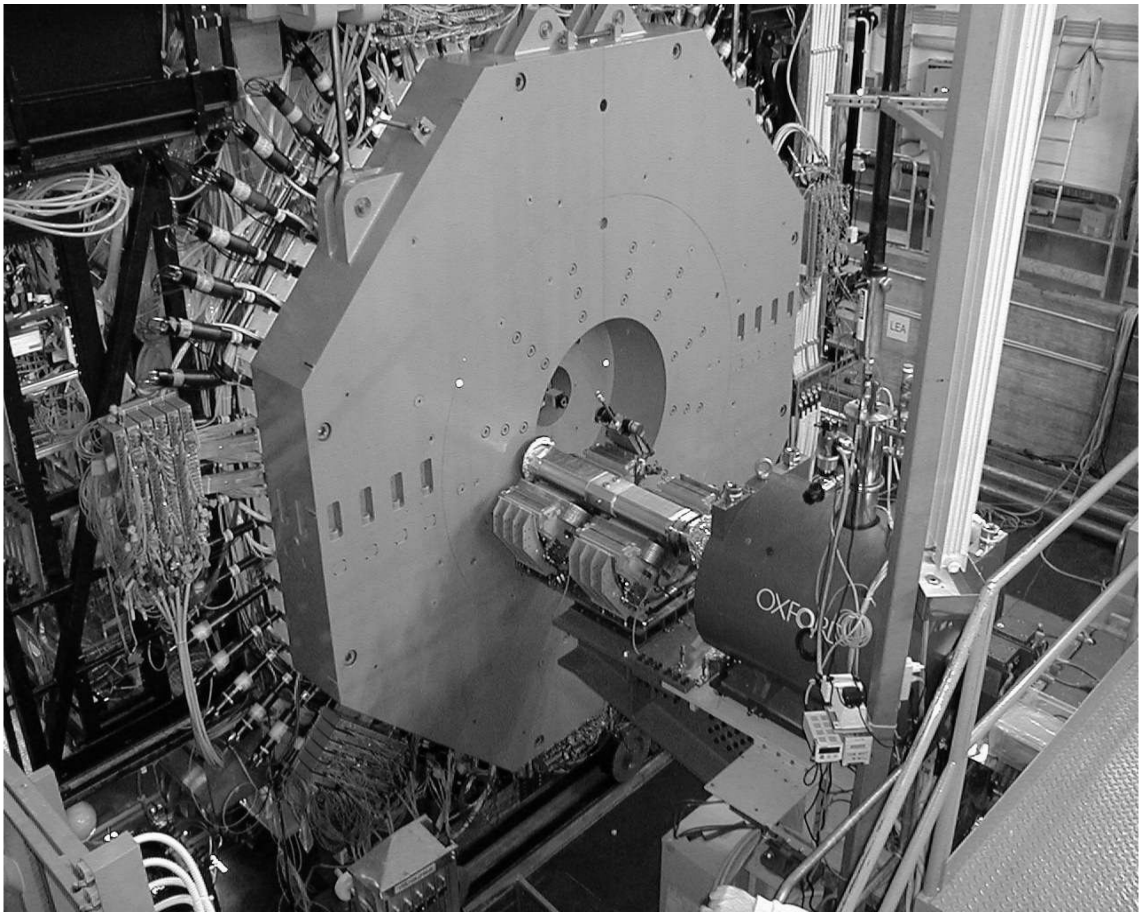

Figure 4: *The Roll-In of FINUDA.*

2.3 Activity from August to November 2003

THe DAΦNE startup initially scheduled for July 2003, was delayed due to a general shortage of water supply at LNF, that prevented an adequate cooling during the very hot summer. FINUDA took advantage of the August period to improve and optimize the DAQ and storage systems and to recover some faulty straw channels.

The following weeks were used to find the correct operating conditions of the collider in the completely new optics. Upon request of the accelerator team, the magnetic field of FINUDA was lowered to 1.0 T. FINUDA used this period to monitor for the first time the performance of the detectors, in particular the vertex ones, with circulating beams. Thanks to the full collaboration with the DAΦNE team proper beam conditions were achieved at beginning of October, when the FINUDA detectors were left continuosly switched on and started to take data. The period from October to November was used to improve DAΦNE operation (vacuum, beam life-time, luminosity, background reduction).

2.4 Activity in December 2003

From December 1st 2003 the physics data taking of FINUDA begun. Since the beginning, FINUDA overall behavior turned out in accordance with the expectations and data quality of events was good from the first days, with a tolerable rate of background. As early as October 2003, not only typical Bhabha events could be immeadiately identified, but also those deriving from K_S decay into $\pi^+\pi^-$ (fig.5).

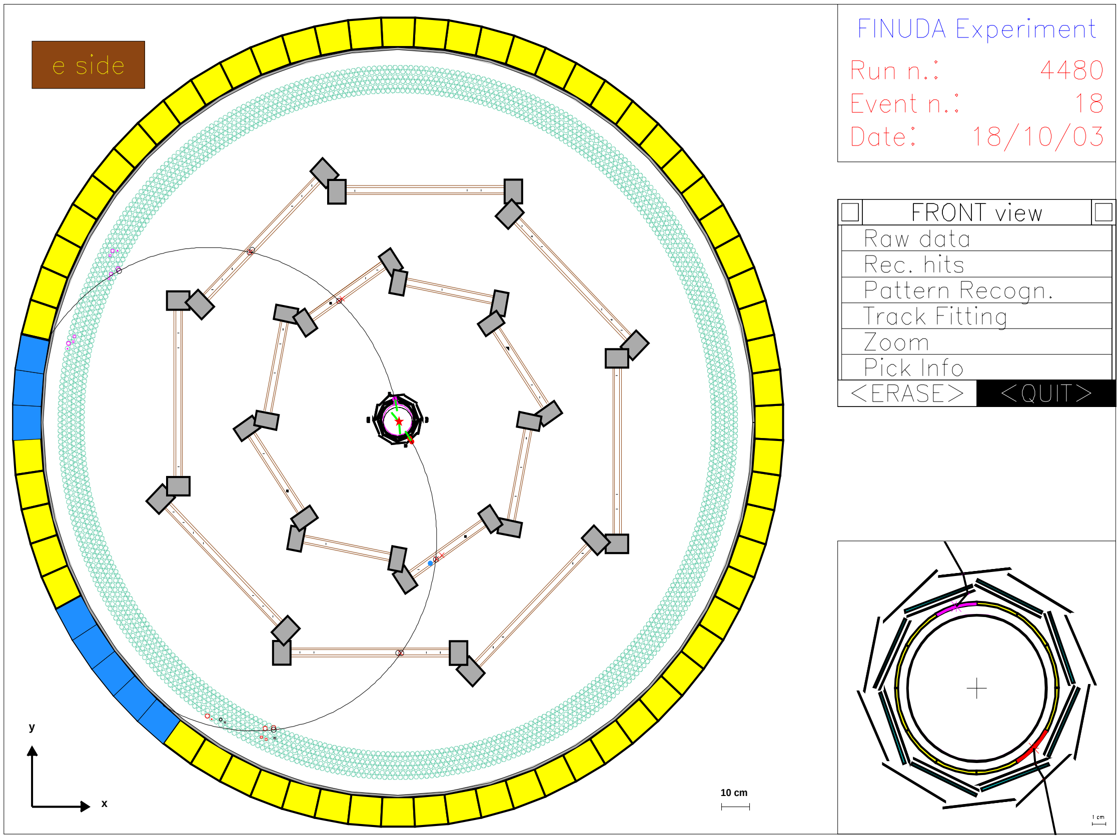

Figure 5: *An event from $e^+e^- \rightarrow \phi$ with $\phi \rightarrow K_S K_L$ and $K_S \rightarrow \pi^+\pi^-$. The inset shows an enlarged view of the vertex region. The magnetic field enters the plane of the figure.*

Even ρ^0's decays could easly be identified. This information was conveniently used to measure and monitor the machine luminosity and $\sqrt(s)$ (see fig.6 as an example of measured spectra for the invariant mass of $\pi^+\pi^-$ system) [3].

Already in the first days of operation, FINUDA could identify events generated from charged kaons interaction in the targets. The decays of K^+ stopped in the targets into both the channells $\mu^+\nu_\mu$ and $\pi^+\pi^0$ could be in fact easly recognized: fig.7 shows the momentum distribution of positive charges coming from K^+ stopping in the FINUDA targets.

Most importat was the early identification of hypernuclei formation events, with the characteristic emission of prompt π^- with momenta in the range $260 - 270$ MeV/c, accompained by the 236 MeV/c μ^+. These pions and muons come, respectively, from a K^- interaction in one of the targets and from a K^+ stopped and decaying in the opposite target (fig.8).

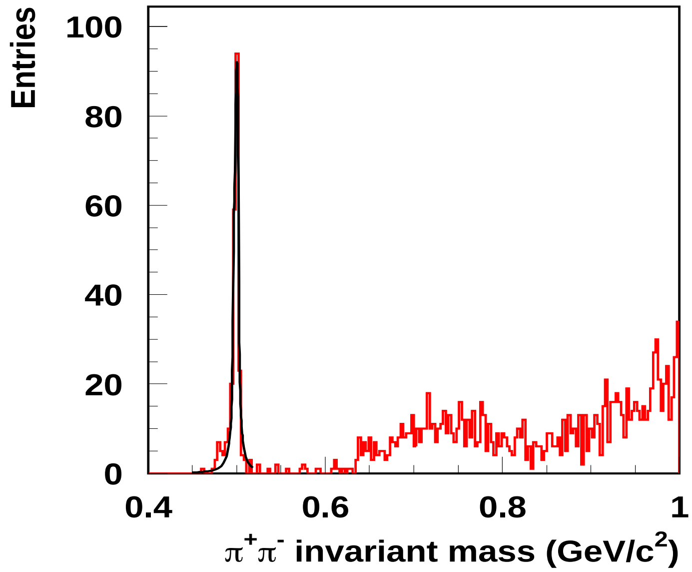

Figure 6: *The invariant mass of the $\pi^+\pi^-$ system. The narrow peak and the broad bump correspond to the K_S and ρ^0 decay, respectively.*

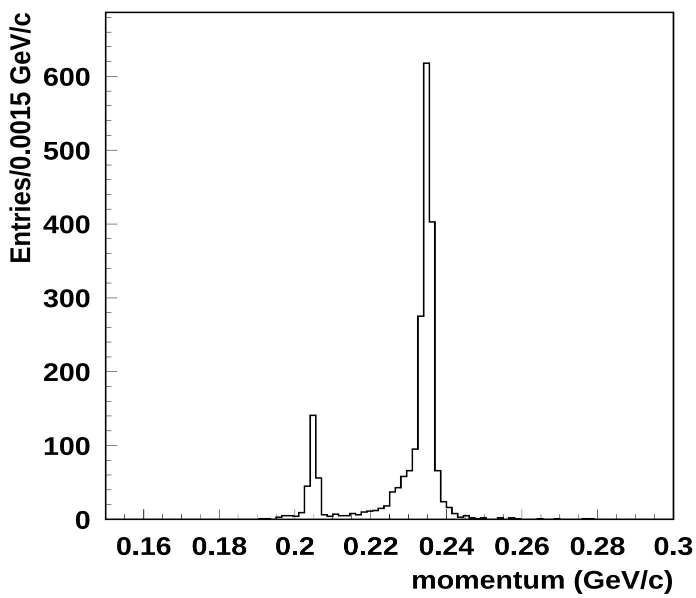

Figure 7: *Momentum ditribution of positive tracks coming from K^+ stopped in the FINUDA targets. The peaks at 236 MeV/c and 205 MeV/c, correspond to the two body decay $K^+ \rightarrow \mu^+\nu_\mu$ and $K^+ \rightarrow \pi^+\pi^0$, respectively.*

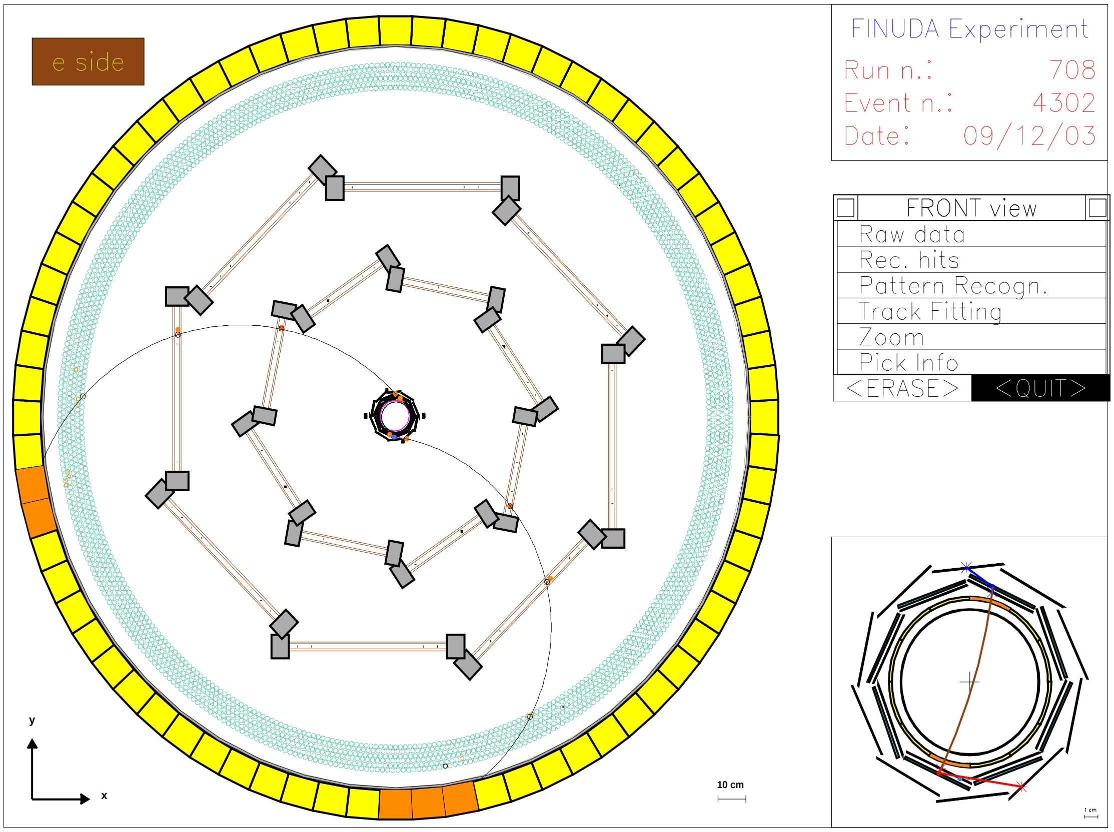

Figure 8: *Candidate event for hypernucleus formation. A* 260 MeV/c *negative track* (π^-) *exits from an upper FINUDA target, with a positive* 236 MeV/c *one* (μ^+) *coming out from an opposite target. The inset show an enlarged wiew of the vertex region. The magnetic field enters the page.*

Events in which hypernucleus formation was followed by hypernucleus decay into non-mesonic np channels could also be seen. All these events turned out with a counting rate in accordance with the calculated ones, taking into account the spectrometer acceptance and detector efficiencies, the machine luminosity and expected or known branching ratios. A very preliminary π^- spectrum corresponding to hypernuclei candidate events from a partial sample of the December 2003 data (sum of all the three ^{12}C targets) is shown as an example in fig.9, [4]. Two hypernuclear peaks (at least) can be clearly identified: the one corresponging to the ground state at 275 MeV/c and the excited state at 261 MeV/c of $^{12}C_\Lambda$.

3 Conclusions

In 2003 FINUDA has achieved remarkable results. The vertex detectors have been installed as soon as the beem pipe was inserted and aligned inside the spectrometer. Less than two weeks after the roll-in, data taking started with cosmic rays and magnetic field off in order to align the tracking detectors. When the superconducting magnet was cooled, cosmic rays events were collected again with magnetic field on at 1.1 T and used to align the Drift Chambers in standard operational mode. Soon after the beam conditions were safe for the operation of all detectors FINUDA started

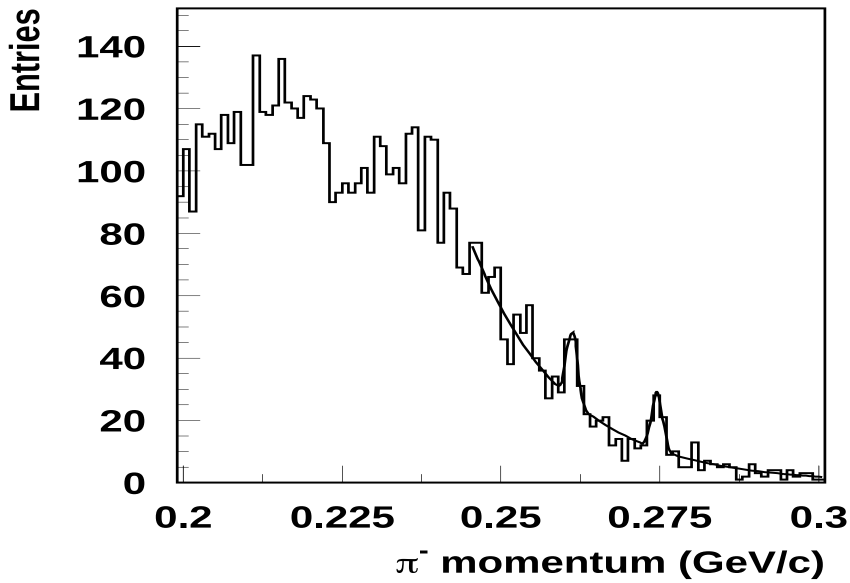

Figure 9: *Momentum distribution of π^- from K^- interactions into the ^{12}C targets (the line is only inteded to guide the eye). The two peaks at* 275 *MeV/c and at* 261 *MeV/c correspond to the ground state and the excited state of $^{12}C_\Lambda$ respectively.*

to debug the spectrometer in the collider enviroment, while DAΦNE continued to optimize its performance. As soon as the physics data taking started, FINUDA identified the physical events for which it has been built, and in the first month of regular operation (December 2003) significant hypernuclear spectra were measured.

These achievements sound as a firm confirmation of both the quality of the FINUDA spectrometer and the unique opportunity that DAΦNE offers to study hypernuclear physics.

References

1. P. Gianotti on behalf of the FINUDA Collaboration, Nucl. Phys. **A691**, 483c (2001).
2. A.Zenoni and P. Gianotti Europhysics News **33/5**, 157 (2002).
3. M. Agnello *et al.* First results from the FINUDA experiment at DAΦNE, in: Proc. HYP2003 VIII International Conf. on Hypernuclear and Strange Particle Physics (TJNAF, Oct. 2003).
4. L. Benussi *et al.*, FINUDA-LNF MEMO, 14.01.2004.

GRAAL

O. Bartalini (Dott.) P. Levi Sandri (Resp.)

1 Introduction

The Graal experiment aims at a more detailed knowledge of the baryon spectrum via the precise measurement of polarisation observables in photo-induced reactions on the nucleon.

The use of the electromagnetic probe and of its polarisation, coupled to large acceptance detectors with cylindrical symmetry and high efficiency in the detection of all final state particles, is the technique chosen in many laboratories to perform the ambitious program of a full determination of the scattering amplitude of a given photonuclear reaction. Such determination requires the measurement of the cross section, of the three single polarisation observables and of four appropriately chosen double polarisation observables.

The Graal esperiment is performed in collaboration between 6 INFN Sections (Roma2, LNF, Catania-LNS, Roma1, Genova and Torino), IPN-Orsay, ISN-Grenogle and INR-Moscow. The Frascati group is responsible of running and maintaining the ΔE/Δx scintillator barrel detector, the Montecarlo simulation program LAGGEN, the off-line reconstruction of events in the BGO calorimeter and the data analysis for coherent η photoproduction off the deuteron.

2 The Graal Beam and the Lagrange apparatus

The Graal facility provides a polarised and tagged photon beam by the backward Compton scattering of laser light on the high energy electrons circulating in the ESRF storage ring [1]. Using the UV line (350 nm) of an Ar-Ion laser we have produced a gamma-ray beam with an energy from 550 to 1470 MeV. Its polarisation is 0.98 at the maximum photon energy and the energy resolution has been measured to be 16 MeV (FWHM).

The Lagrange detector is formed by a central part surrounding the target and a forward part. Particles leaving the target at angles from 25^o to 155^o are detected by two cylindrical wire chambers with cathode readout, a barrel made of 32 strips of plastic scintillator parallel to the beam axis, used to determine the ΔE/Δx of charged particles, and the BGO rugby-ball made of 480 crystals of BGO scintillator.

The BGO ball is made of crystals of pyramidal shape with trapezoidal basis which are 21 radiation lengths long (24 cm). This calorimeter has an excellent energy resolution for photons [2], a good response to protons [3] and is very stable in time due to a continuous monitoring and calibration slow control system [4].

Particles moving at angles smaller than 25^o encounter two plane wire chambers, (xy and uv) two walls of plastic scintillator bars 3 cm thin located at 3 m from the target point, that provide a measurement of the time-of-flight for charged particles (700 ps FWHM resolution) followed by a shower wall made by a sandwich of four layers of Lead and plastic scintillators 4 cm thick that provides a full coverage of the solid angle for photon detection (with 95 % efficiency) and a 20 % efficiency for neutron detection.

Finally, two disks of plastic scintillator separated by a disk of Lead complete the solid angle coverage in the backward direction.

The beam intensity is continuously monitored by a flux monitor, composed by three thin plastic scintillators and by a lead/scintillating fibre detector that measures energy and flux [5].

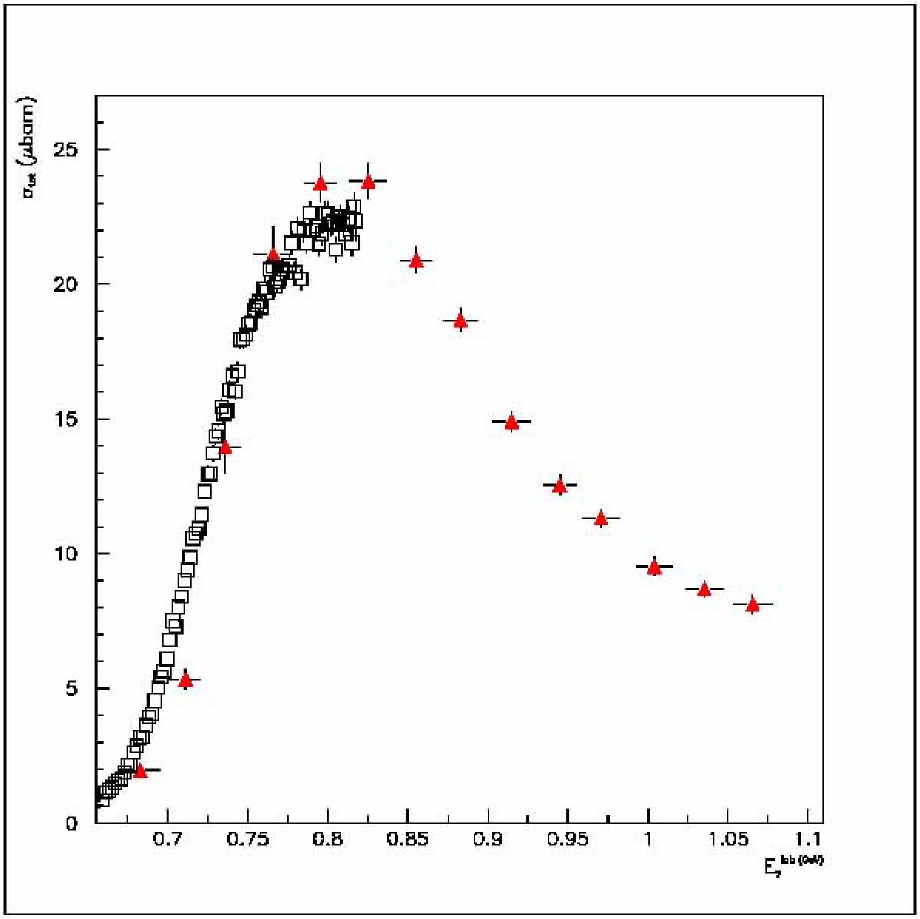

Figure 1: *Total cross section for η photoproduction off the Deuteron. Graal points are shown as triangles.*

3 2003 activity

During the year 2003 the Graal experiment has almost completed the data acquisition for a proton an deuteron targets. The procedure to install a new polarised target made of HD molecules in solid state has started. The target built and polarised in the Orsay laboratory must be transported to Grenoble and installed in the beam line without loosing it's polarisation. A test transportation with an unpolarised sample was successfully performed.

Data analysis for high energy η and π^0 photoproduction is being performed while for the reaction with π^+ photoproduction the final data were produced. Also the cross section and beam asymmetry data for the photoproduction of two π^0 and ω were obtained and the corresponding paper have been published or are being submitted. A special effort was performed in the analysis of η photoproduction off the deuteron and in the search for pentaquark states. The Frascati group has produced the data for the total cross section of the reaction $\gamma + d \rightarrow \eta + X$. Preliminary results of this analysis are shown in Figure 1.

4 Activity in 2004 and conclusions

The Graal experiment started data taking in 1997. It was run both with the green laser line giving rise to a photon beam of maximum energy of 1100 MeV and with UV multi-line with the corresponding gamma-ray beam of 1470 Mev maximum energy. The typical intensity was $2 \cdot 10^6 s^{-1}$ in both cases, very close to the design intensity. The detector was found very stable during the seven years of operation, with only minor maintenance problems.

Proton and deuteron targets of different lenghts were used and asymmetry data and cross sections have been produced for η, π^0, π^+, $2\pi^0$ and and ω photoproduction channels providing, for these reactions, the most extended and coherent data base available until now. The analysis of the Compton process on the proton, and of all the mentioned photoreactions on the quasi-free neutron of the deuteron target are underway.

During the year 2004 the new polarised target, made of HD molecules in frozen state will be installed replacing the present cryogenic target. Data taking will restart soon after the installation with the aim of measuring for the first time double polarisation observables in π^0 an η photoproduction, and the contribution from 500 to 1500 Mev to the GDH integral for both protons and neutrons.

5 Main recent publications

Phys. Lett. B 544 (2002) 113
Nucl. Phys. A 699 (2002) 218c
Phys. Lett. B 528 (2002) 215
Phys. Rev. Lett. 90, 222001 (2003)

References

1. Graal Collaboration, Nucl. Phys. A622, (1997) 110c.
2. P. Levi Sandri *et al.* Nucl. Inst. and Meth. in Phys. Research A370, (1996), 396.
3. A. Zucchiatti *et al.*, Nucl. Inst. and Meth. in Phys. Research A321, (1992), 219.
4. F. Ghio *et al.*, Nucl. Inst. and Meth. in Phys. Research A404, (1998), 71.
5. V. Bellini *et al.*, Nucl. Inst. and Meth. in Phys. Research A386, (1997), 254.

HERMES

M. Albicocco, E. Avetissyan (Ass.), N. Bianchi (Resp. Naz.), A. Borysenko (Ass.),
G.P. Capitani (Resp. Loc.), E. De Sanctis, P. Di Nezza, A. Fantoni, A. Funel (Dott.),
C. Hadjidakis (Ass.), D. Hasch (Ass.), V. Muccifora, K.A. Oganessyan (Ass.),
A. Orlandi (Tecn.), W. Pesci (Tecn.), E. Polli, A.R. Reolon, C. Schill (Ass.), A. Viticchié (Tecn.)

1 Introduction

HERMES (HERa MEasurement of Spin) is an experiment at DESY mainly dedicated to study the spin structure of the nucleon. Nucleons (protons and neutrons) are the basic ingredients of the matter of the known universe and their most important quantum number is the spin 1/2. The nucleon is a composite object which can be described in terms of moving quarks of different flavors (up, down and strange) in different configurations (valence and sea) and gluons. Up to year 2000, HERMES collected data with a longitudinally polarized positron beam of 27.5 GeV on longitudinally polarized H, D and ^{3}He internal gas targets. From these runs HERMES provided the most accurate and complete data set for the polarized structure function g_1 and allowed a direct flavor decomposition of the nucleon spin [1]. Runs on several unpolarized nuclear gas targets have been also collected.
In 2002-2003 first data with a transversely polarized hydrogen target have been collected. The preliminary analysis on a reduced data sample has shown a small but clearly non-zero azimuthal asymmetry for both positive and negative pions (see Fig. 1 left). These data provide the first evidence for the so called Collins effect, which is related to the convolution of the chiral-odd transversity distribution $h_1(x)$ with a time-odd spin-dependent fragmentation function, and of the so called Sievers effect, which is related to chiral-even and time-odd distribution and spin independent fragmentation function. Much more data are present in the current data taking and analysis.
In 2003 an evidence was found for a narrow baryon state in quasi-real photoproduction on a deuterium target through the decay channel $pK^0_S \to p\pi^+\pi^-$ [2] (see Fig. 1 right). This state may be interpreted as the predicted S=+1 exotic $\Theta^+(uudd\overline{s})$ pentaquark baryon. No signal for an hypothetical Θ^{++} baryon was observed on the pK^+ invariant mass distribution. The absence of such a signal indicates that an isotensor Θ is excluded and an isovector Θ is unlikely.

2 The LNF HERMES group

HERMES is a Collaboration of about 180 physicists from 31 Institutions from 12 Countries. Italy participates with 4 groups and more than 30 physicists from Bari, Ferrara, Frascati and Rome. A Frascati physicist (P. Di Nezza) is the deputy spokesman and run-coordinator of the experiment.
The Frascati group is responsible for the electromagnetic calorimeter and has participated in the project and in the construction of two RICH detectors. It is currently involved in the project of a new recoil detector to be installed in 2004-2005. A Frascati physicist (D. Hasch) has the responsibility of the analysis working groups of azimuthal asymmetries in semi-inclusive processes and of the pseusoscalar meson exclusive production. Frascati physicists are involved in the analysis of many other physics processes. In addition they are playing a major role in the physics paper draftings and in the editorial process being the leading authors of about one third of the HERMES Collaboration physics publications.

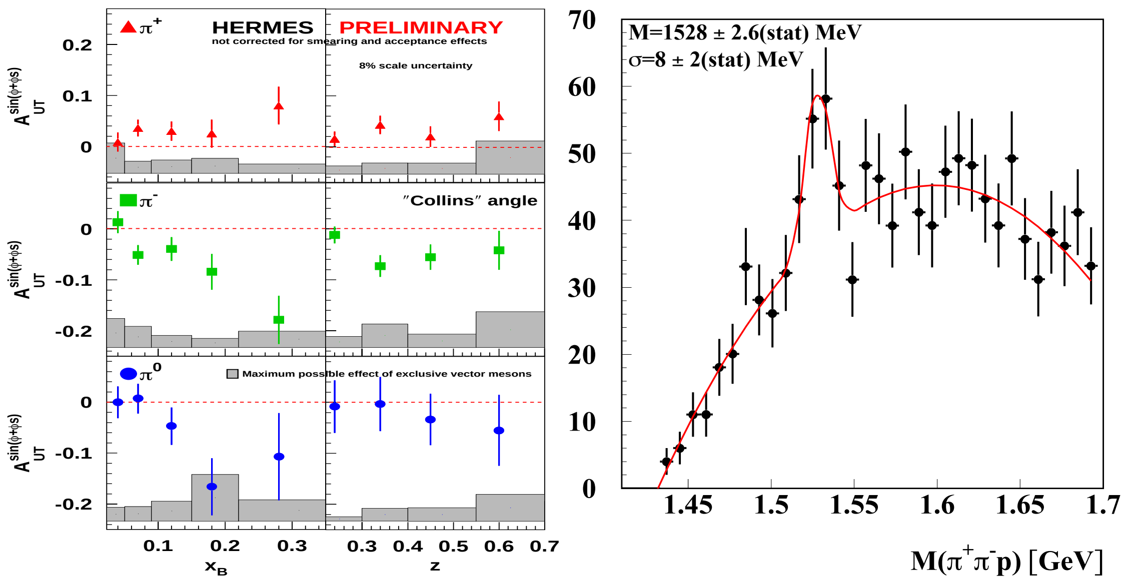

Figure 1: *Left : Collins type azimuthal asymmetries for pions produced by an Unpolarized positron beam on a Transversely polarized hydrogen target, as a function of the scaling variables for distribution (x_B) and fragmentation (z) functions. Right : evidence for photoproduction of an S=+1 exotic baryon, Θ^+, in the pK^0_S invariant mass (the systematic errors on M and σ are 2.1 MeV and <1 MeV, respectively.*

3 Experimental activity of the LNF group in 2003

3.1 Calorimeter

The HERMES calorimeter consists of a wall of 840 Lead-Glass blocks [3]. The calorimeter is the basic detector for the main trigger and for the positron-hadron separation. It is used to reconstruct energy and angle of photons, π^0 and η. The responsibility of the calorimeter required the on-line monitoring and check of the status of detector for the whole period of data taking. During 2003 several reproductions of existing data with the re-calibration of all detectors, including the calorimeter were performed, in particular the offline calibration of HERMES calorimeter for 96d, 97d, 99c, 2002b productions. In addition, new codes for a more precise position reconstruction of the shower, for a better comparison of the energy reconstruction with the momentum (see Fig. 2), for accounting for the photon showering in the preshower detector and for correcting for the impact angle and longitudinal shower differences as a function of energy, were implemented into the production program. These improvements were needed by the urgent and hard requirement to detect and reconstruct with the highest accuracy and efficiency the single photons from the deeply virtual Compton scattering processes. During data taking before 2003, there were some cases of calorimeter malfunction, mostly due to shortcuts in the photomultiplier voltage dividers. All the 840 PMTs were recovered with the deposition of an insulator film on the socket and no additional shortcuts have occurred in the most recent running period.

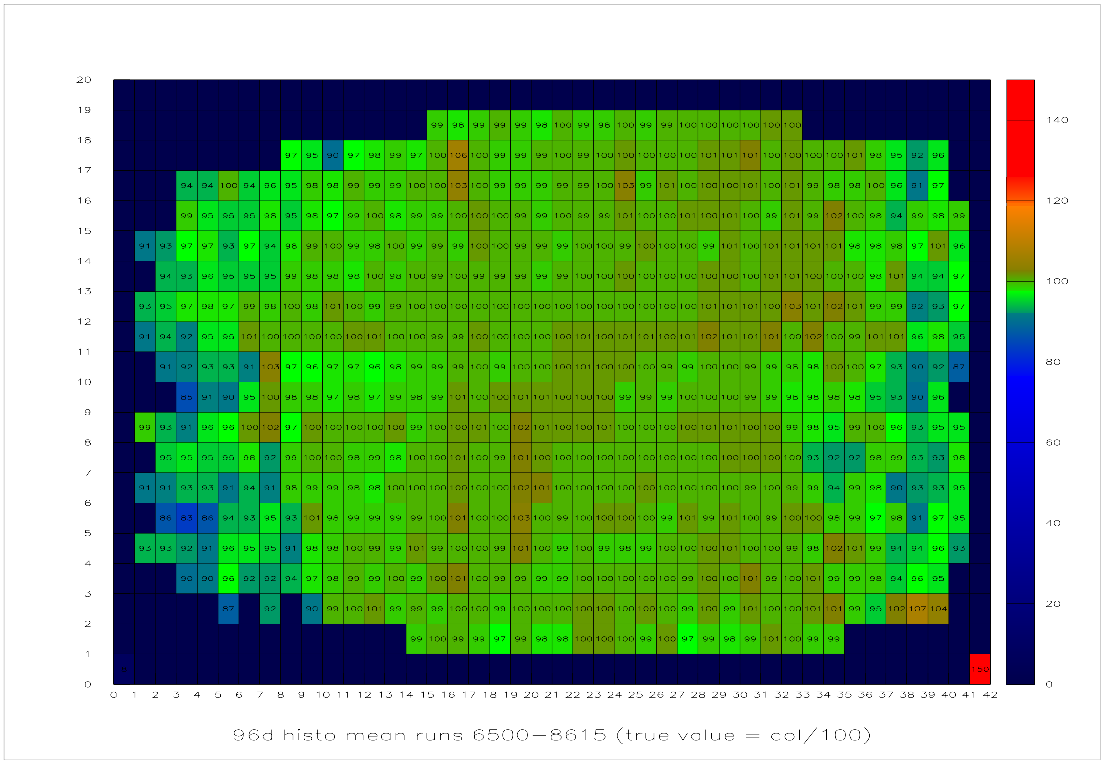

Figure 2: *Ratio (x100) of the positron energy (as measured by the calorimeter) and the momentum (as measured by the tracking system) for each lead glass block of the calorimeter wall and for a sample of runs. For the outer blocks the statistics for this reduced number of runs is not sufficient for an accurate evaluation of this ratio.*

3.2 Recoil detector

The recent proof of factorization for exclusive processes and their interpretation in terms of Generalized Parton Distributions to describe the nucleon structure, suggested the detailed investigation of these processes in which a fast meson or a photon is emitted in the forward direction while the slow nucleon is recoiling intact at large angle. Several exclusive processes have been already investigated by HERMES with the missing mass technique [4)]. To better identify these processes, a compact Recoil Detector (see Fig. 3) is under construction to be installed around the target. Basically, it will consist of silicon detectors located under vacuum inside the beam pipe, a SciFi tracking system and a Lead-Scintillator barrel. The Frascati group is involved in the latter detector which will be used to detect photons from the π^0 decay. Simulations and cosmic ray tests have been performed to optimize the efficiency for the photon detector and for the π^0 reconstruction and to define the final design of the barrel. It will consist of three layers of scintillating strips with a WLS fiber system readout. Multi-anode photomultipliers will be used with specially designed fan-in/preamplifiers to ensure capable transmittance of the signal. A photon detector prototype was first tested in GSI (Darmstadt) with proton and pion beams of 600 MeV/c. Results of these tests confirmed the capability of the photon detector to identify events with 20-25 MeV maximum energy deposition for π^0 decay into 2 photons. In addition the separation of π^+ and protons by

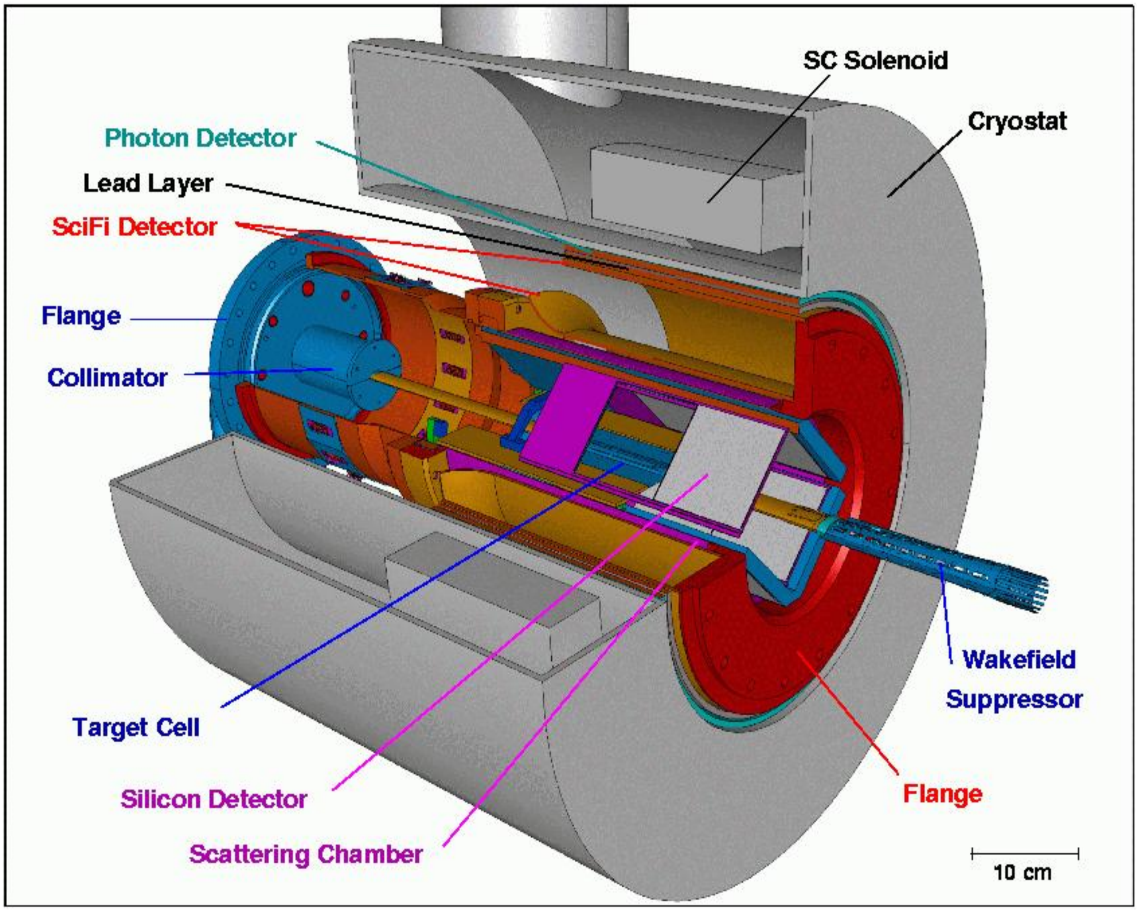

Figure 3: *3-D view of the Recoil Detector project.*

energy loss was demonstrated. In Frascati the final readout electronics and the scintillator light collection scheme was successfully tested resulting in a signal of about 30 photoelectrons per minimum ionizing particle. The detector has been assembled in Frascati (see Fig. 4) and the transport and installation in DESY is foreseen for the current year.

3.3 Technical software

The Particle Identification (PID) is crucial for any analysis of HERMES data. To separate hadrons and leptons a Bayesian algorithm has been applied. The necessary probability distributions are extracted from the responses of four particle identification detectors: the lead glass calorimeter, a preshower detector, a transition radiation detector and a threshold Cerenkov detector. The latter was replaced by a ring imaging Cerenkov detector (RICH) in 1998. LNF members were main responsible for PID. In particular they worked on the maintenance and code development of the PID library function, on the PID calibration, on the new 98,97,96 data productions, on the flux corrections to PID for different physics analyzes, on the influence of dead calorimeter blocks in semi-inclusive analysis. The contribution of the individual detectors to the main experimental trigger as a function of the event kinematics has been also extensively studied.

Figure 4: *The photon detector for the Recoil Detector under construction: details of the WLS fiber system (left) and of the electronic readout developed in Frascati (right).*

At low momenta, the PID was obtained with the Time of Flight technique by using scintillator hodoscopes.
In 2003 the LNF group acted also as Linux administrator and represented HERMES on DESY Linux user meeting, where user requirements and future strategy for Linux support were discussed.

4 Data analysis and physics results of the LNF group in 2003

4.1 Quark-hadron duality in spin structure function

The quark-hadron duality concept was introduced by Bloom and Gilman to describe the relationship between phenomena in the nucleon resonance region and the deep-inelastic region. The duality was observed from long time in the case of unpolarized structure functions [5]. In HERMES the validity of duality, i.e. the successful description of the nucleon resonance region in terms of the partonic variable x and of quark degrees of freedom instead of the usual nucleonic excitation variable W, has been shown for the first time in the case of spin structure functions. The study of the integral of the spin dependent photon-nucleon cross section, that enters in the generalized Gerasimov-Drell-Hearn sum rule [6], has been extended to the polarized deuteron target in addition to the already analyzed and published ones on the Helium-3 and hydrogen targets by the LNF group [7]. Two papers on duality and GDH have been published in 2003 (Pub. 2 and 3).

4.2 Single-spin azimuthal asymmetries

Single-spin azimuthal asymmetries have been recently recognized as a powerful source of information on the structure of the nucleon complementary to the inclusive deep-inelastic scattering. In particular, it has been suggested that target-spin asymmetries may provide information on the still unmeasured transversity distribution, which describes the probability to find a quark with its spin parallel or anti-parallel to the spin of the nucleon. The transversity function $h_1(x)$ enters at

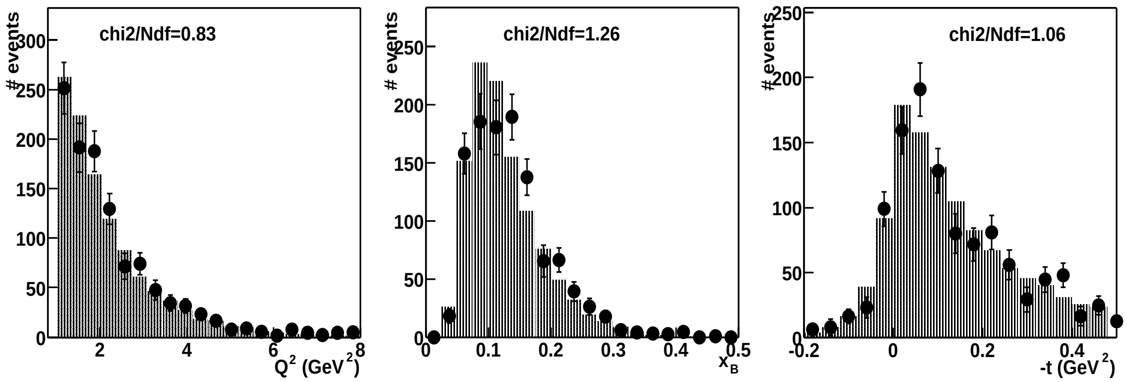

Figure 5: *Event distributions for exclusive π^+ electroproduction, compared with a MonteCarlo based on a Generalized Parton Distribution generator which includes the pion-pole term.*

the same leading order level of the well known $f_1(x)$ and $g_1(x)$ functions in the description of the nucleon structure, but its chiral-odd nature does not allow to be measured in inclusive DIS [8]. First measurements on a longitudinally polarized hydrogen target have been proposed, analyzed and published in the recent years by the LNF group [9]. In 2003 a similar analysis has been published on a longitudinally polarized deuterium target (Pub. 5). A new analysis has been performed by investigating beam-spin asymmetries, i.e with polarized beam and unpolarized hydrogen and deuterium targets, for charged (see Fig. 6 left) and neutral pions. These asymmetries represent as a possible tool to investigate the unknown twist-3 unpolarized distribution $e(x)$ [10]. With this respect beam-spin asymmetry for several data taking years were extracted and analyzed for checking the statistical and systematic compatibility. Studies of the possible ρ^0 contribution in the single pion asymmetry were performed.

4.3 Exclusive production of pions

The exclusive production of mesons and photons (DVCS) on the nucleon gives access to the new Generalized Parton Distribution (GPD). GPDs are able to provide a 3-D view of the nucleon with the determination of the full correlation of the partonic variables (position and momentum) and to investigate the orbital motion of partons [11]. In addition, the measurement of exclusive π^+ cross section is related to the largely unknown space-like pion form factor. With the HERMES experiment, results on the single spin asymmetry (SSA) on a longitudinally polarized target has already been analyzed and published by the LNF group. Currently the SSA on a transversely polarized target and the total cross section are under study. For the latter, in order to determine the acceptance of the detector, two different Monte Carlo based on the GPDs generators have been developed to correct the data for the detector acceptance (see Fig. 5).

4.4 Medium modification of parton fragmentation function

It is well known that the parton *distribution* functions are modified by the nuclear medium. HERMES has measured the medium modification of the parton *fragmentation* function on a ^{14}N target [12]. The analysis of new data taken on a Krypton target have revealed for the first time, different effects for parton fragmentation into different hadrons. In contrast to the similarity between π^+, π^- and π^0, a significant difference was found between K^+ and K^- and between p and

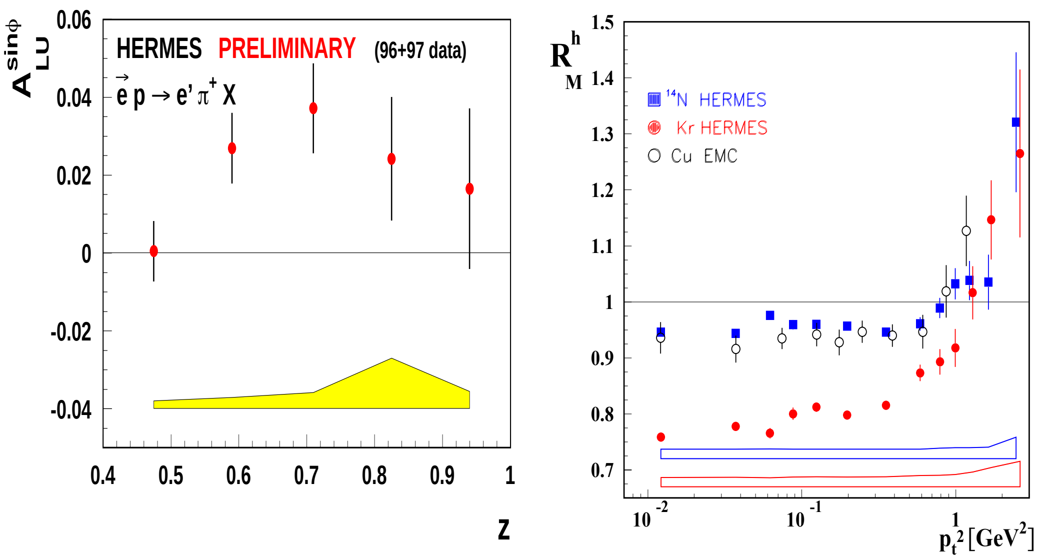

Figure 6: *Left : Azimuthal moment distribution of semi-inclusive production of* π^+ *(around the leptonic scattering plane) by a Longitudinally polarized positron beam on an Unpolarized hydrogen target. Right : Ratio of Multiplicities for hadrons produced with nuclear targets with respect to the Deuterium ones, as a function of the transverse momentum. The systematic uncertainties of the data are given as bands in the bottom part of the figures.*

$\overline{p}$. In addition, the so called Cronin effect has been observed in the p_T-broadening of the hadron distribution in nuclei (see Fig. 6 right). These results provide information on the partonic energy loss and scattering probability and on the hadron formation time, which are necessary ingredients to understand the heavy-ion interactions at high energy which are performed to study the Quark Gluon Plasma [13]. A paper on this topic has been published in 2003 (Pub. 7).

5 Phenomenology on HERMES physics of the LNF group in 2003

5.1 Quark-hadron duality

The quark-hadron duality has been investigated by comparing resonance region data for both unpolarized structure function (from JLab) and polarized structure function (from HERMES) with different parameterizations of world data in the DIS region. Both perturbative and non-perturbative QCD predictions have been used. After the subtraction of target mass corrections and large x re-summation effects, a sizable suppression of $1/Q^2$ terms have been found in both polarized and unpolarized data, except for the low Q^2 polarized data (see Fig. 7). A paper on this subject has been written in 2003 (Pub. 13).

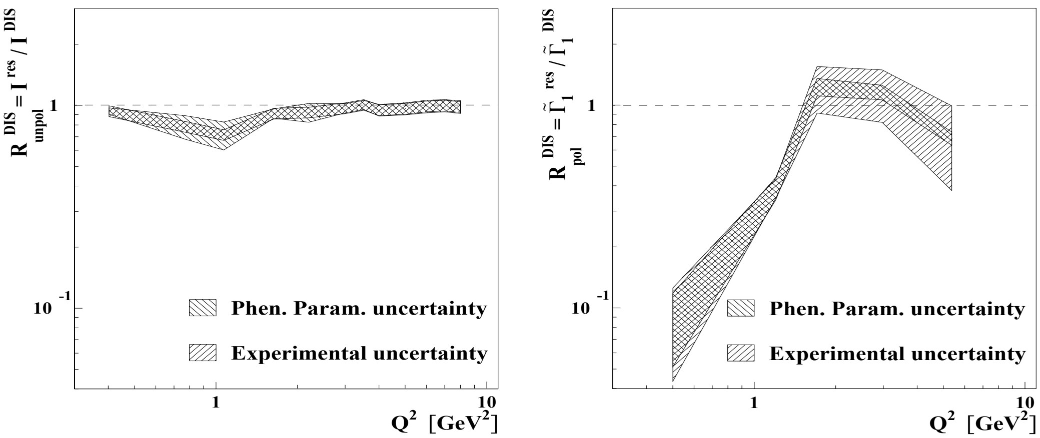

Figure 7: *Investigation of the quark-hadron duality for unpolarized (left) and polarized (right) structure functions.*

5.2 New distribution functions

Different leading and sub-leading distribution functions are accessible by measuring unpolarized, single-polarized and double-polarized azimuthal distribution of hadrons in semi-inclusive DIS [14]. The observation of these new distribution functions often requires the existence of new time-odd fragmentation functions. Mechanisms have been studied to generate time-odd spin-dependent leading and sub-leading fragmentation functions, favored candidates for filtering the transversity properties of the nucleon. They complement and are consistent with the approach that was employed to generate the time-odd distribution functions, representing the number density of unpolarized (transversely polarized) quarks in the transversely polarized (unpolarized) nucleon, that fuel the single-spin and spin-independent azimuthal asymmetries in hard scattering processes. Several papers on this subject have been published in 2003 (Pub. 19-21 and 24).

5.3 Nuclear medium effects in fragmentation

Predictions for semi-inclusive deep inelastic lepton-nucleus scattering have been calculated by taking into account the rescaling of fragmentation functions in the nuclear medium, in analogy of what was introduced for nuclear structure functions [15] . Both the effects of gluon radiation by the struck quark and the absorption of the produced hadron were considered. In this framework, the gluon radiation covers a larger window in virtuality Q^2 because of the increased deconfinement of quarks inside nuclei. It has been found that most of the medium effects are due to modifications of the fragmentation process into the final hadron which formation appears to occur at distance typically larger than the nuclear size. A paper on this subject has been published in 2003 (Pub. 1) and a second one in is the final drafting stage.

6 Outlook

In 2004, the data taking with a transversely polarized hydrogen target will continue. The photon detector of the Recoil Detector will be completed and installed. The ongoing physics analysis and the phenomenological investigations will be completed. New analysis will be performed on data with the polarized transverse target for which a large azimuthal asymmetry for the exclusive pion production is expected to arise from the interference of pseudoscalar and pseudovector amplitudes of GDPs. The relationship between the nuclear effects in the hadron leptoproduction and the interpretation of the neutrino oscillation experiments will be exploited.

7 Conferences by LNF Authors in Year 2003

7.1 Conference Talks

1. E. Avetissyan, Single-spin asymmetries, Int. Eur. Conf. on HEP, Aachen (Germany)
2. N. Bianchi, The spin of the nucleon, Winter meet. on nucl. phys., Bormio (Italy)
3. N. Bianchi, DIS studies of the Deuteron, Work. on the Deuteron, Miami (USA)
4. N. Bianchi, Modifica della frammentazione nel mezzo nucleare, LXXXIX SIF, Parma (Italy)
5. N. Bianchi, Summary talk of the transversity workshop, Hadron Structure, Santorini (Greece)
6. A. Borysenko, The Hermes Recoil Detector, LXXXIX SIF, Parma (Italy)
7. P. Di Nezza, Nuclear Effects in DIS Hadronization, Hadron Structure, Santorini (Greece)
8. A. Fantoni, Generalised GDH integral, Workshop on Compton scattering, Trento (Italy)
9. A. Fantoni, Quark-Hadron Duality in Structure Funct., DIS2003, St. Petersburg (Russia)
10. A. Fantoni, Quark-Hadron Duality in Structure Functions, LXXXIX SIF, Parma (Italy)
11. C. Hadjidakis, Excl. SSA, Workshop on Transversity, Athens (Greece)
12. C. Hadjidakis, Exclusive π^+ production, LNF Spring School, Frascati (Italy)
13. D. Hasch, Transversity measurements, Photon 2003, Frascati (Italy)
14. D. Hasch, SSA in excl. meson electroproduction, CIPANP 2003, New York (USA)
15. D. Hasch, SSA with long. pol. targ. and beams, Workshop on Transversity, Athens (Greece)
16. V. Muccifora, Nucl. eff. in the hadr. in DIS, Winter meet. on nucl. phys., Bormio (Italy)
17. V. Muccifora, Hadr. in DIS, Conf. on Strangeness in quark matter, Atlantic B. (USA)
18. V. Muccifora, Nucl. eff. on the hadron formation, E.m. int. of nuclei, Moscow (Russia)
19. V. Muccifora, Hadronization process in DIS, NAPP03, Dubrovnik (Croatia)
20. K.A. Oganessyan, Novel Transversity Properties in SIDIS, CIPANP 2003, New York (USA)
21. K.A. Oganessyan, Transversity in ep Scattering, DIS2003, St. Petersburg (Russia)
22. K.A. Oganessyan, Azim. Asymm. in Hard QCD, Work. on QCD, Villefranche (France)
23. C. Schill, Longitudinal SSA for pions and kaons, DIS2003, St. Petersburg (Russia)
24. C. Schill, Longitudinal SSA, CIPANP 2003, New York (USA)

7.2 Conference organization and advisoring, Seminars

1. N. Bianchi, (Convener) Transversity workshop, Athens (Greece).
2. E. De Sanctis, (Chair) Hadron Structure, Santorini (Greece).
3. E. De Sanctis, (Organizer) LNF Spring School, Frascati (Italy).
4. A. Fantoni, (Seminar) University of Virginia, Charlottesville (USA).
5. D. Hasch, (Seminar) Frascati, Italy.
6. K.A. Oganessyan, (Seminar) Wayne State University, Detroit, USA.
7. K.A. Oganessyan, (Seminar) University of Notre Dame, USA.
8. K.A. Oganessyan, (Seminar) Jefferson Lab, USA.

8 Publications of LNF Authors in Year 2003

1. A. Accardi, V. Muccifora, H.J. Pirner, Hadron production in deep inelastic lepton-nucleus scattering, Nucl. Phys. A 720 (2003) 131
2. A. Airapetian et al., The Q^2 Dependence of the Generalized Gerasimov-Drell-Hearn Sum Rule for the Deuteron, Proton and Neutron, Eur. Phys. Jour. C 26 (2003) 527
3. A. Airapetian et al., Evidence for Quark-Hadron Duality in the Proton Spin Asymmetry A_1, Phys. Rev. Lett. 90 (2003) 092002
4. A. Airapetian et al., Q^2 Dependence of Nuclear Transparency for (In)coherent ρ^0 production, Phys. Rev. Lett. 90 (2003) 052501
5. A. Airapetian et al., Measurement of single-spin azimuthal asymmetries in semi-inclusive electroproduction of pions and kaons on a longitudinally polarized deuterium target, Phys. Lett. B 562 (2003) 182
6. A. Airapetian et al., Double spin asymmetries in the cross section of diffractive ρ^0 and ϕ production at intermediate energies, Eur. Phys. Jour. C 29 (2003) 171
7. A. Airapetian et al.,Quark Fragmentations to $\pi^{\pm}$, π^0, $k^{\pm}$, p, $\bar{p}$ in the Nuclear Environment, Phys. Lett. B 577 (2003) 37
8. A. Airapetian et al, Nuclear Effects on $R = \sigma_L/\sigma_T$ in Deep Inelastic Scattering, Phys. Lett. B 567 (2003) 339
9. A. Airapetian et al., Flavor Decomposition of the Sea Quark Helicity Distributions in the Nucleon from Semi-inclusive Deep-inelastic Scattering, Phys. Rev. Lett. in press, hep-ex/0307064
10. A. Airapetian et al, Evidence for a Narrow $|S|$=1 Baryon State at a Mass of 1528 MeV in quasi-real Photoproduction, Phys. Lett. B in press, hep-ex/0312044
11. A. Airapetian et al, Nuclear Polarization of Molecular Hydrogen Recombined on a non-metallic Surface, Eur. Phys. Jour. D in press, DESY-03-168
12. A. Airapetian et al., The time-of-flight technique for the HERMES experiment, Nucl. Instr. and Meth., in press, hep-ex/0301010
13. N. Bianchi, A. Fantoni, and S. Liuti, Parton-hadron duality in unpolarized and polarized structure functions, Phys. Rev. D in press, hep-ph/0308057
14. N. Bianchi, Exclusive Meson and Photon Production at HERMES, Int. Journ. of Modern Phys. A 18 (2003) 1311
15. N. Bianchi, Nuclear Effects in Hadron Leptoproduction, Few-Body Systems 15 (2003) 99
16. N. Bianchi, Nuclear Attenuation in SIDIS, NATO Science Series II vol 111 (2003) 109
17. A. Borysenko, The HERMES recoil detector, Nucl. Phys. B 125 (2003) 189
18. A. Fantoni, Quark-hadron duality and Q2 evolution of the GDH integral in the HERMES experiment, Eur. Phys. J. A 17 (2003) 385
19. L.P. Gamberg, D.S. Hwang, K.A. Oganessyan, Chiral-Odd Fragmentation Functions in Single Pion Inclusive Electroproduction, hep-ph/0311221, Phys. Lett. B, in press
20. L. Gamberg, G.R. Goldstein, K.A. Oganessyan, A mechanism for the T-odd pion fragmentation function, Phys. Rev. D 68 (2003) 051501
21. L. Gamberg, G.R. Goldstein, K.A. Oganessyan, Novel Transversity Properties in Semi-Inclusive Deep Inelastic Scattering, Phys. Rev. D 67 (2003) 071504
22. D. Hasch, Transversity measurements at Hermes, Nucl. Phys. B 126 (2003)
23. V. Muccifora, Hadronization in Deep Inelastic Scattering at HERMES, Journ. of Phys. G 30 (2003) S103
24. K.A. Oganessyan, L.S. Asilyan, M. Anselmino, E. De Sanctis, Spin-independent and double-$cos\phi$ asymmetries in semi-inclusive pion electroproduction, Phys. Lett. B564 (2003) 60

References

1. HERMES Coll.: Phys. Lett. **B 404**, 383 (1997); Phys. Lett. **B 442**, 484 (1998); Phys. Rev. Lett. **81**, 5519 (1998); Phys. Lett. **B 464**, 123 (1999); Phys. Rev. Lett. **84**, 2584 (2000); Phys. Lett **494**, 1 (2000); Phys. Rev. Lett. **92**, 012005 (2004).
2. A. Airapetian at al., HERMES Coll.: Phys. Lett. **B 585**, 21 (2004).
3. H. Avakian et al., Nucl. Instrum. Meth. **A 417**, 69 (1998).
4. HERMES Coll.: Phys. Rev. Lett. **87**, 182001 (2001); Eur. Phys. J. **C 17**, 389 (2000) and Phys. Lett. **B535**, 85 (2002).
5. F.E. Close and N. Isgur, Phys. Lett. **B 509**, 81 (2001) and refs therein.
6. N. Bianchi and E. Thomas, Phys. Lett. **B450**,439 (1999).
7. HERMES Coll.: Phys. Rev. Lett. **82**, 3025 (1999) and Phys. Lett. **B 494**, 1 (2000).
8. V. Barone, A. Drago and P.G. Ratcliffe, Phys. Rept. **359**, 1 (2002) and refs therein.
9. HERMES Coll.: Phys. Rev. Lett. **84**, 4047 (2000); Phys. Rev. **D64** 097101 (2001).
10. R.L.Jaffe and X. Ji, Nucl. Phys. **B 375**, 527 (1992).
11. X. Ji, Phys. Rev. **D 62**, 7114 (1997) and M. Burkardt, Phys. Rev. **D 62**, 071503 (2000).
12. HERMES Coll.: Eur. Phys. J. **C 20**, 479 (2001).
13. E. Wang and X.-N. Wang , Phys. Rev. Lett. **89**, 162301 (2002).
14. K.A. Oganessyan, H.R. Avakian, N. Bianchi and P. Di Nezza, Eur. Phys. J. **C5**, 681 (1998); K.A. Oganessyan, N. Bianchi, E. De Sanctis and W.-D. Nowak, Nucl. Phys. **A 689**, 784 (2001).
15. R.L. Jaffe, F.E. Close, R.G. Roberts and G.G. Ross, Phys. Lett. **B 134**, 449 (1984).

FA-51: Astroparticle Physics

E. Nardi (Resp.)

1 Summary of the project

Our main goal is to study the effects of neutrino masses on the neutrino signal from a future Galactic core-collapse supernova. As complementary researches, we have been investigating some general neutrino properties, like their electromagnetic interactions, and we have also been working on models that try to explain the origin of the hierarchy of the fermion masses within Gran Unified Theories (GUTs).

2 Summary of the 2002 activity

During the year 2002 we have been carrying out researches on the following two topics:
1) Study of the electromagnetic properties of the neutrinos.
2) Elaboration of a new method to derive information on the neutrino masses from the measurement of the neutrino signal from a future Galactic core-collapse supernova;
The research related to the first topic was concluded in 2002. The results have been presented in one international conference [1], published in Phys. Rev. D. [2] (see also the LNF 2002 activity report). The second topic has been developed further during the year 2003, and it is still the object of active research.

3 Description of the 2003 activity

During the year 2003, besides developing further the new approach for studying neutrino mass effects in a supernova signal, we have also been working on the long standing problem of explaining the numerical values of the fermion masses and their hierarchy.

3.1 Explaining the fermion mass hierarchy with horizontal symmetries within SUSY $SU(5)$

Given the well known evidences for unification of the three gauge couplings, we started by assuming SUSY $SU(5)$ as a more fundamental theory underlying the Standard Model (SM). We have been exploring the possibility of extending the symmetries of the model by introducing an Abelian $U(1)$ horizontal symmetry to account for the suppression of the fermion mass from the electroweak scale down to the experimentally observed values. This framework was extensively studied in the past within the SM, where it proved to be reasonably successful. However, when applied to a GUT, two main problems are encountered: *i)* due to the fact that different fermions sit in the same group representation, the number of Abelian charges is highly reduced. This over-constrains the freedom of the models and implies that some mass values turn out to be in conflict with observations. *ii)* Certain mass ratios, as for example $m_\mu/m_s \sim 3$ and $m_e/m_d \sim 1/3$ remain unexplained. These mass ratios have always represented a challenge for GUT models, since even in minimal $SU(5)$ the leptons and down-type quarks sit in the same group representation, and therefore are forced to have the same Yukawa coupling, implying equal mass values at the GUT scale, as it is approximately true for m_b and m_τ.

Differently from usual models in which the horizontal symmetry is broken by a gauge singlet field, we adopt a scheme where the same **24** adjoint representation responsible for $SU(5)$ breaking, carries a horizontal charge and therefore breaks the horizontal $U(1)$ as well. Breaking the horizontal symmetry by means of an adjoint has interesting consequences, since now non trivial Clebsh-Gordan coefficients modify the effective operators for the fermion masses, yielding different contributions for the leptons and for the down-type quarks. As a first result [4] we showed that in this scheme b-τ Yukawa unification can only occur to some degree of approximation, but in general is not exact. This is not in contradiction with the most recent results that, within minimal SUSY $SU(5)$, seem to indicate only a partial success for b-τ Yukawa unification, with deviation at the level of 10%-20%. We are still developing our approach in the attempt of explaining all the problematic mass ratios, and of constructing a complete model for all the fermion masses, including the neutrinos.

3.2 Study of the neutrino signal from a future Galactic core-collapse supernova

We have elaborated a new method to study the effects of neutrino masses on a supernova neutrino signal. Differently from most of the methods proposed in the past, our method relies exclusively on the analysis of the full statistics of neutrino events, it is independent of astrophysical assumptions, and does not require the observation of any additional phenomenon to trace possible delays in the neutrino arrival times. The sensitivity of the method to the sub-eV neutrino mass range, defined as the capability of disentangling at 95% c.l. the case $m_\nu = 1\,\mathrm{eV}$ from $m_\nu = 0$, was tested by analyzing a set of synthetic neutrino samples modeled according to the signal that could be detected at SuperKamiokande (SK). Our first results indicate that for a supernova at the Galactic center success is achieved in more than 50% of the cases. In vew of the fact that the sensitivity of previous analysis was in general around 2-3 eV, we believe that our proposal is interesting, and it is worth trying to develop it further. We are presently studying the improvement that could be achieved by applying the method simultaneously to SK and KamLAND data, and what sensitivity could be achieved at future megaton neutrino detectors like HyperKamiokande.

4 List of conference talks in year 2003

1. *"Measuring neutrino masses with supernova neutrinos"*. E. Nardi. Talk given at the Tenth Marcel Grossmann Meeting, Rio de Janeiro, 20-26 July 2003.

References

1. *On the neutrino vector and axial vector charge radius.*
   E. Nardi. Talk given at the 10th Mexican School of Particles and Fields, Playa del Carmen, Mexico, 30 Oct - 6 Nov 2002. AIP Conf. Proc. **670**, 118 (2003); [arXiv:hep-ph/0212266].
2. *Bounds on the τ and μ neutrino vector and axial vector charge radius.*
   M. Hirsch, E. Nardi and D. Restrepo. Phys. Rev. **D 67:033005**, 2003.
3. *"Exploring the sub-eV neutrino mass range with supernova neutrinos,"*
   E. Nardi and J. I. Zuluaga. Submitted to Phys. Rev. **D** [arXiv:astro-ph/0306384].
4. *"b-τ Yukawa non-unification in supersymmetric SU(5) with an Abelian flavor symmetry"*.
   D. Aristizabal and E. Nardi, Phys. Lett. **B 578**, 176 (2004) [arXiv:hep-ph/0306206].
5. *"Measuring neutrino masses with supernova neutrinos"*.
   E. Nardi. Talk given at the Tenth Marcel Grossmann Meeting, Rio de Janeiro, 20-26 July 2003. [arXiv:astro-ph/0401624].

LF-11: SYNCHROTRON RADIATION SPECTROSCOPIES AND THE PHYSICS OF STRONGLY CORRELATED ELECTRON SYSTEMS

S. Bellucci, M. Benfatto, S. Di Matteo (Ass.), R. Gunnella (Ass.), K. Hatada (Ass)
C.R. Natoli (Resp.), P. Onorato (Ass), N. Perkins (Ass.), A. Tenore, Wu Ziyu (Visit.),

1 The Project

The aim of this project is the theoretical analysis of strongly correlated electron systems, like the manganites, the cuprates and the transition metal oxides. When appropriate, methods borrowed from field theory and statistical mechanics are used to bear on the description of the essential physics of such systems. At the same time in-depth theoretical studies of significant synchrotron radiation spectroscopies (absorption, dichroism, elastic and inelastic resonant x-ray scattering, etc.) that can shed light on charge and magnetic correlations in strongly interacting electronic systems are carried out. Finally, the theory underlying the multiple scattering programs used to analyse such spectroscopies is improved and applications are made to obtain structural and electronic information in condensed matter systems, with an eye to systems of biological relevance.

For completeness we report also on the part of this project concerning low-dimensional systems, like Nanotubes and Nanostructures, although this subject now constitutes a new initiative (LF61). S. Bellucci (100%), P. Onorato (100%), R. Gunnella (100%) and Wu Ziyu (50%) will migrate to it.

2 Physics of strongly correlated electron systems.

The research in this field has developed along three main directions:

- Analysis of synchrotron radiation experiments (resonant x-ray scattering, absorption and dichroism) in strongly correlated electron systems like V_2O_3 and $LaSr_2Mn_2O_7$.
- Analysis of the polar (magnetic) and axial (non-magnetic) toroidal multipoles of a system by means of x-ray dichroism and resonant scattering.
- Investigation of the physics of the complex magnetic oxides (LiV_2O_4, $MgTi_2O_4$, V_2O_3, Sr_2FeWO_6 and $Nd_{1-x}Sr_xMn_{1-x}Ru_xO_3$).

2.1 Analysis of synchrotron radiation experiments

We have extended the tensor analysis derived for circular and linear dichroism in photoemission and photoabsorption to Bragg-forbidden reflections in anomalous diffraction.

In the case of non magnetic material we have shown that it is possible to observe inversion-odd quantities in globally centro-symmetric materials (i.e. the same operator observed by natural circular dichroism in non centro-symmetric crystal) via an interference between the dipole-quadrupole and the quadrupole-quadrupole channels. Using a numerical *ab-initio* simulation based on the independent particle approach in the framework of multiple scattering theory, we have confirmed this finding via a quantitative analysis of the 'Finkelstein' (003) reflection in systems belonging to the corundum crystal class, like V_2O_3 and α-Fe_2O_3, having a global centre of inversion. The observed threefold modulation superimposed to the sixfold periodicity in the azimuthal scan of the 'Finkelstein' peak is in fact due to the interference between the two channels. [1)]

In order to treat magnetic effects, we have developed a relativistic extension of the Schrödinger Equation, obtained by eliminating the small component of the wave-function in the Dirac Equation,

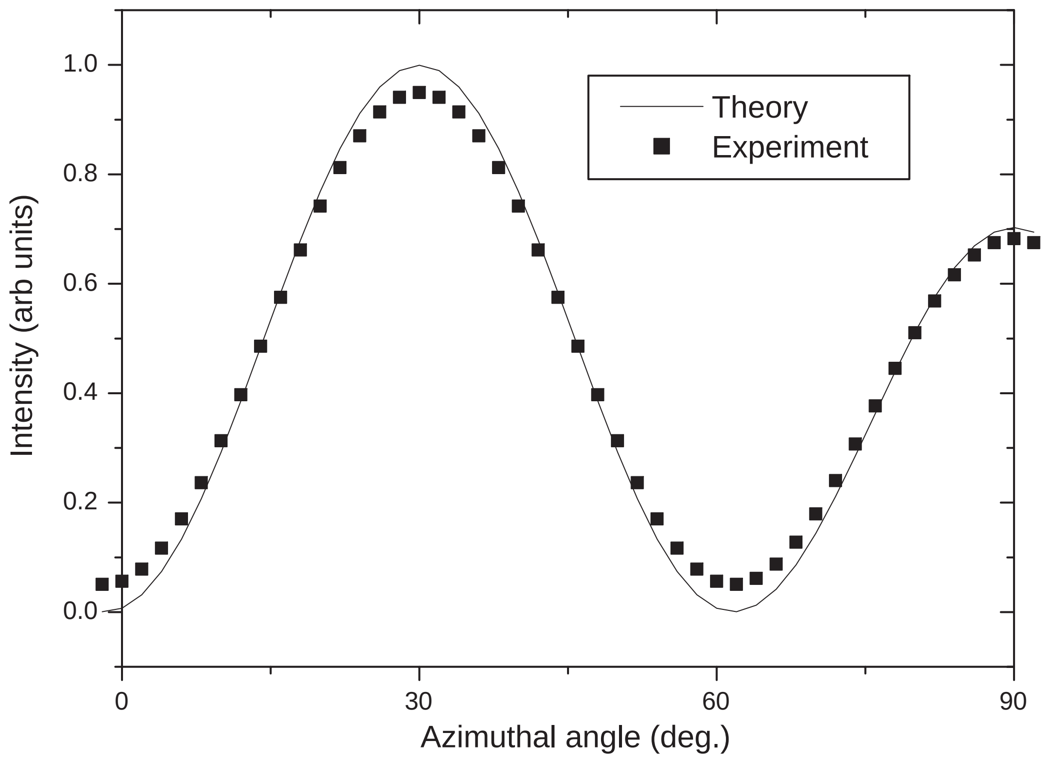

Figure 1: *Theoretical azimuthal scan for α-haematite (E=7109 keV) and comparison with the experimental data from Finkelstein et al., Phys. Rev. Lett., 69, 1612 (1992)*

thereby working with the usual non relativistic set of quantum numbers (l,m,σ) for the angular and spin momenta. Spin polarized atomic potentials were obtained following the prescription by von Barth and Hedin starting from non self-consistent but realistic spin dependent charge densities. Electric dipole-dipole (E1-E1), dipole-quadrupole (E1-E2) and quadrupole-quadrupole (E2-E2) transition were considered altogether. We have therefore interpreted recent x-ray resonant scattering experiments carried out in the monoclinic phase of V_2O_3 at the vanadium K-edge by Paolasini (L. Paolasini et al, Phys. Rev. Lett. 82, 4719 (1999)) We have obtained satisfactory agreement with experiments, both in energy and azimuthal scans (see fig. 1)

As a result we are able to show that all the main features of the Bragg-forbidden reflections with $h+k+l$ =odd and h odd or even can be interpreted in terms of the antiferromagnetic ordering only, i.e. they are of magnetic origin. No reduction of symmetry from the magnetic space group suggested by neutron scattering experiments, either due to orbital ordering or some other still unknown effect, is necessary to explain the observed patterns. In particular the energy scan of the (1,1,1) monoclinic reflection excludes the possibility of any kind of orbital ordering, contrary to what previously suggested by other authors. This work was presented at the JAERI International Workshop on X-Ray Scattering and Electronic Structure, December 11-12 (2003), Spring-8 Japan.

Another argument again involving V_2O_3 concerns the nature of the magnetic space group in its monoclinic phase. All experiments performed before 2000 had shown that the system admitted a different magnetic space group than suggested by a recent dichroic experiment at vanadium K edge (Goulon *et al.* Phys. Rev. Lett. 85, 4385 (2000)). In this latter work it was found that the systems allows non-reciprocal effects, implying that time-reversal and inversion symmetries are broken and only their product conserved, contrary to previous findings. This situation led to a further experiment to remove the stalemate (S. Di Matteo, A.G.M. Jansen, Phys. Rev. B 66, R100402 (2002)), so as to choose between two possible magnetic space groups: however no magnetic-electric effect was found in the system and this fact is not compatible with the presence of a non-reciprocal gyrotropic linear dichroism. This result solved a problem but raised another question: the correct interpretation of the dichroic experiment at the vanadium K edge. For this reason we have analysed this experiment in more detail, in order to give a coherent interpretation of all the recent x-ray resonant scattering in dichroic experiments in V_2O_3 [3]. Here we have performed numerical simulations based on the multiple scattering theory for both dichroic and resonant scattering spectra, analysing the experimental implications related to the different magnetic space symmetries. We have shown in this way the paradoxical consequences of the interpretation proposed by Goulon *et al* quoted above on the physics of this system and suggested how to perform correctly the dichroic experiment in order to dissipate any doubt on the behaviour of the system.

Finally, the last argument involving V_2O_3 has concerned the study of the monoclinic "nucleation" in the corundum phase of the Cr-doped samples when cooled from the paramagnetic insulating to the antiferromagnetic insulating phase. Such a study has not yet been fully developed and will be better analysed in the next future, but has constituted nonetheless the subject of a publication [4].

The role of the orbital degrees of freedom and their coupling to the Jahn-Teller distortion has been investigated through resonant x-ray scattering (RXS) in the bilayered manganite $LaSr_2Mn_2O_7$ at the Mn K edge [5]. The aim of such a work consisted in clarifying the origin of the so-called Bragg-forbidden orbital reflections for which two alternative mechanisms had been proposed. Its conclusions are that their origin lies in the Jahn-Teller distortion.

Last for item 1), the interpretation of iron K edge absorption spectra in naturally layered silicates has led to the description of their magnetic transition as an order/disorder one [6].

2.2 Analysis of the magnetic and non-magnetic anomalous scattering

The second direction of research is concerned with the analysis of the polar (magnetic) and axial (non-magnetic) toroidal multipoles of a system by means of x-ray dichroism and resonant scattering. In this direction we have completed the article, begun in 2002, about the possibility to have magnetoelectric ground states in the high-temperature superconducting cuprates and how to reveal them by means of resonant scattering and dichroic techniques [7]. At the same time a more general inspection of (magnetic and non-magnetic) toroidal multipolar expansion in condensed matter has been put forward. The main results of such a work regard the possibility to detect the toroidal moment in centro-symmetric magnetic systems by means of RXS and to separate in a similar way all the parity and time-reversal odd multipolar components. We have found that the system Li_2VOSiO_4 is well suited for such an analysis, [8] and have performed a detailed simulation by means of a relativistic extension of the FDMNES program, that illustrates under which conditions the magnetic toroidal moment can be detected. [9]

2.3 Investigation of the physics of the complex magnetic oxides

The third direction of research concerns the investigation of the physics of complex magnetic oxides such as LiV_2O_4, $MgTi_2O_4$, V_2O_3, Sr_2FeWO_6, $Nd_{1-x}Sr_xMn_{1-x}Ru_xO_3$ and the manganites which exhibit a whole variety of interrelated phenomena such as metal-insulator transitions, orbital and magnetic ordering, double exchange, geometrical frustration, heavy fermion behaviour and colossal magnetoresistance.

The interest to frustrated systems lies in the fact that their ground state is highly degenerate and can evolve in a variety of ways: they can freeze on cooling forming ice, remain liquid down to the lowest temperature due to quantum effects or, finally, lift their geometrical degeneracy through a phase transition that lowers the local symmetry. One of them is the intriguing paramagnetic transition-metal oxide LiV_2O_4. This compound has a spinel structure and its lattice consists of corner-shared tetrahedrons of $V^{+3.5}$ ions (pyrochlore lattice) located in slightly distorted oxygen octahedron. It is the first metal showing heavy fermion behavior without any f orbital, moreover LiV_2O_4 has some peculiar magnetic properties. The magnetic susceptibility and inelastic neutron scattering measurements indicate a spin liquid behavior over a large range of intermediate temperatures (for example, S.-H. Lee *et al.*, Phys. Rev. Lett. **86**, 5554 (2001)). On the other hand, analysis of recent neutron scattering experiments (A.P. Murani *et al.*, J. Phys.:*Condens. Matter* (2004)) revealed that in addition to antiferromagnetic correlations, ferromagnetic-like correlations on V sites appeared over some temperature range. The minimal model, that we have considered by means of an exact diagonalization study, includes both purely Heisenberg-like contribution from the super-exchange interaction among localized spins and an effective ferromagnetic double-exchange contribution driven by the itinerant electronic excitations. We have calculated the total spin correlation functions and, consistently with experimental observations, their temperature dependence shows a crossover from antiferromagnetic to ferromagnetic behavior when the temperature is increased. The increasing population of the magnetic states with temperature results in the formation of a non-zero residual magnetic moment which is also observed in the experiments [10)].

$MgTi_2O_4$ is another spinel, which recently has attracted much attention (M.Schmidt, cond-mat/0308101). It undergoes a metal-insulator transition on cooling below $T = 260$K, which is accompanied by strong lattice distortion leading to the formation of helical chains of short and long bonds running along the tetragonal c axis, a unique example of chiral ordering of the spinel structure. In order to study the low temperature phase of $MgTi_2O_4$, we have derived an effective spin-1/2, pseudospin-1 Hamiltonian and demonstrate that the orbital degrees of freedom can remove the infinite spin-degeneracy of the "pyrochlore" structures and induce a spin dimerization. Moreover, we have shown that the residual orbital degeneracy can be lifted by the spin-lattice interaction forcing a tetragonal distortion to the chiral structure actually observed. We propose to investigate such a low-symmetry phase by means of x-ray natural circular dichroism. The work has been submitted to Phys. Rev. B [11)].

V_2O_3 has become one of the most famous transition metal oxide after its identification as the prototype of Mott-Hubbard systems at the beginning of the 70s. Beside the critical analysis of the RXS and linear dichroism experiments already introduced at item 1), we have also dealt with its electronic ground-state properties. About this problem, we have concluded the work already started two years ago and depicted its phase diagram also in the presence of a spin-orbit coupling, in order to describe its antiferromagnetic insulating properties. This analysis is summarized in [12, 13)].

Another field of growing interest is that of the so-called double perovskites, that are becoming more and more important after the discovery of their colossal magnetoresistance. We focused on the insulating double perovskite Sr_2FeWO_6, and derived its phase diagram on the basis of an effective spin-orbital Hamiltonian. The technique adopted for such a derivation and for the construction of the effective hamiltonian was borrowed from our previous experience on V_2O_3. In this case, anyway, we had to deal with the much more complicated case of 4 electrons in 5 Fe-orbitals and include the empty W-orbitals. Our results predicted predicted two transition temperatures, the higher to an antiferromagnetic state and the lower to an orbitally ordered state. We have suggested a possible experiment to detect them both. [14, 15]

In collaboration with the neutron diffraction group in Dubna, we also studied the compound $Nd_{1-x}Sr_xMn_{1-x}Ru_xO_3$. In this case, the correlated doping of A- and B-sites with Sr and Ru ions in $Nd_{1-x}Sr_xMn_{1-x}Ru_xO_3$ leads to long-range ferrimagnetic ordering but leaves the system insulating. Such an experimental fact has been observed for the first time and, in order to explain it, the role of Ru-doping has been analyzed under several aspects. The mean-field phase diagram of this compound has been studied as a function of the doping x. [16]

3 Improving the analysis of synchrotron radiation spectroscopies

3.1 Fitting of the XANES spectra by a full multiple scattering procedure

The fitting of XANES spectra to derive structural information, described in the 2002 report and summarized in ref.s [17, 18] has been applied to two problems: the study of redox-induced structural dynamics of Fe-heme ligand in myoglobin and a crystal-chemical investigation of Cr substitution in muscovite by x-ray absorption spectroscopy.

In the first case the Fe(III) –> Fe(II) reduction of the heme iron in aquomet-myoglobin, induced by x-rays at cryogenics temperatures, produces a thermally trapped nonequilibrium state in which a water molecule is still bound to the iron. Water dissociates at T > 160 K, when the protein can relax toward its new equilibrium, deoxy form. Synchrotron radiation x-ray absorption spectroscopy provides information on both the redox state and the Fe-heme structure. Using our method we obtain structural pictures of this photo-inducible, irreversible process, with 0.02-0.06-Angstrom accuracy, on the protein in solution as well as in crystal. After photo-reduction, the iron-proximal histidine bond is shortened by 0.15 Angstrom, a reinforcement that should destabilize the iron in-plane position favoring water dissociation. Moreover, we are able to get the distance of the water molecule even after dissociation from the iron, with a 0.16-Angstrom statistical error [19].

In the second case the procedure was applied and validated on a chromium-containing muscovite for which structural and crystal-chemical characterization is available from literature. The simulation, which involved clusters formed by up to 90 atoms, proved to be effective in representing the Cr local environment, even if the system is characterized by a very low metal content, as demonstrated by the extremely good correspondence with experimental data [20] (see figure 2).

This fitting method was presented by M. Benfatto as a plenary talk at the XAFS12 International Conference held in Malmo (Sweden) from the 22th to the 27th of June 2003.

3.2 Implementation of the GW approximation for the photo-electron optical potential.

As mentioned above a method for utilising the near edge part of the absorption spectrum (XANES) for structural analysis has been proposed by Benfatto *et al* [17, 18]. In this method hundreds of theoretical signals obtained by fully inverting the multiple scattering matrix are compared with the experimental data, until a best fit is obtained in the parameter space of the atomic positions. Very good results are obtained if in the course of the fitting procedure the optical potential used to generate the theoretical signal is taken as the real part of the local Hedin-Lundqvist (H-L) potential, whereas for the imaginary part, describing the damping of the excited photoelectron, a suitably parametrised functional form is fitted together with the structural parameters. Indeed the use of the imaginary part of the H-L potential usually leads to fits with bad R-factors. This is an indication that the fault might lie in the single plasmon pole approximation applied also to core electron densities, as usually done in the H-L potential (for more discussion on this point, see

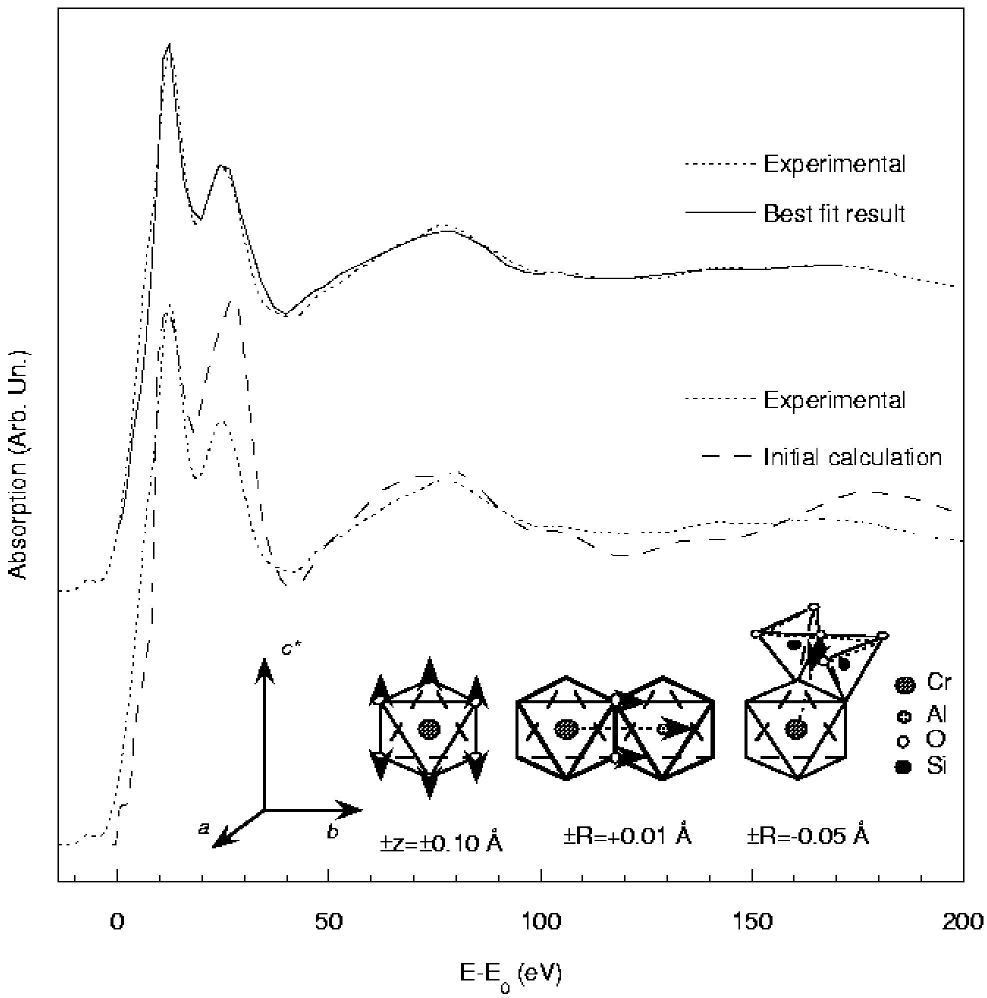

Figure 2: *Comparison between simulation and experimental data.*

ref.s [17, 18]). Clearly an *ab initio* potential wich corrects for this approximation would have both advantages of reducing the number of fitting parameters and improving the sensitivity of the fit to structural parameters.

As anticipated in previous reports, the non local optical potential based on the *GW* approximation for core electrons as developed by Fujikawa, Hatada and Hedin (Phys. Rev. B 62, 5387 (2001)) seems to be a good candidate for this kind of fitting. After solving the difficulties mentioned in the last report, we have studied the performance of this potential in a significant test case, namely the XANES of transition metal ions in water solution.

We tested our new optical potential by calculating the absorption spectrum in two significant model system, namely the Ni and Zn K-edge of $Ni(OH_2)_6$ and $Zn(OH_2)_6$ (Ni and Zn in water solution). Hydrogen atoms were included since they affect significantly the near edge structure. In these compound the spectrum calculated using the usual H-L potential shows significant discrepancy with the experimental data, which is recovered with the GW non local potential.

The results of this investigation were presented as an oral contribution at the XAFS12 International Conference held in Malmo (Sweden) from the 22th to the 27th of June 2003 [21].

3.3 Multichannel multiple scattering theory

The collaboration between the Frascati group and P. Kruger, now maitre de conference at the University of Bourgogne (Dijon), on a method that combines eigenchannel R-matrix and multiple scattering formalism to take into account multiplet-like electron correlation effects in condensed systems, has continued. Application of the theory to Ca $L_{2,3}$ edges in CaO and CaF_2 has led to very good agreement between theory and experiments. The novelty here is that each L-edge is split by crystal field effects, so that the theory is expected to recover *ab initio* not only the correct branching ratio (as in the same spectroscopy in Ca metal) but also the correct crystal field splitting, without adjustable parameters. [22)]

This finding opens the way to biological applications. In fact, many proteins interact strongly with certain heavy element, which act as cofactors or as part of substrate binding/utilisation sites. Calcium is almost ubiquitous in this respect, as well as many transition metal ions of the first series. X-ray absorption fine structure (XAFS) from such metal centres can provide valuable information about the local structural and binding properties around the metal centre and thereby about the bio-chemical action of the protein. So far, XAFS studies on Ca or transition metal centres in biological systems have considered almost exclusively the K-edge, due to the availability of numerical *ab initio* simulations based on the independent particle approach in the framework of multiple scattering theory. This is in contrast to the fact that the $L_{2,3}$ edges fine structure of these elements is known to be sensitive to local symmetry, coordination, valency and chemical binding. This is because the excited 2p electrons probe directly the empty 3-d-states on the metal site, which are the lowest unoccupied states. The neglect of these edges is probably due to the difficulty of their theoretical modelisation. Thus, a quantitative analysis of the $L_{2,3}$ edges would provide important complementary information to the K-edge XAFS. A future goal will be the investigation along the same lines of the L-edges of transition metal complexes in proteins.

4 Nanotubes and Nanostructures

We investigated the effects of a strong transverse magnetic field in 2DEG Quantum Wires and Quantum Dots in the presence of Rashba Spin Orbit coupling. As we know magnetic field enhances the spin selection in the current and also give very singular spin textures in the nanostructures [23)]. We propose these systems as possible devices for the spin filtering at low and intermediate temperature regime.

A scaling approach allows us to encompass the different values of the critical exponent α measured for the tunneling density of states in carbon nanotubes [24)]. Our results can be compared with those obtained from recent experiments, where measurements of the tunnelling conductance have been carried out in doped Multi Walled Carbon Nanotubes (MWNT), with a number of subbands at the Fermi level N_s=10 (in the outer layer). Our results show an overall agreement with the exponents measured in MWNT. We predict that further reduction of α should be observed in multi-walled nanotubes with a sizeable amount of doping. [25)]

Recent experiments about the low temperature behaviour of a Single Wall Carbon Nanotube (SWNT) showed typical Coulomb Blockade peaks in the zero bias conductance. We gave a theoretical explanation of this behaviour starting from a microscopic model of the many electron system, comparing results for SWCNT with those obtained for an ideal vertical Quantum Dot. [26)] Defects and doping can break some symmetries of the system, as revealed by the experimental data, so we introduce an appropriate model in order to approach this problem.

An important part of our activity concerned the modeling of the low dimensional structures considered, as well as the interpretation of different kinds of experiments. Recently we have investigated the X-ray absorption spectra at the K edge of C [27)] in SWNT samples. The surface structure and the bonding properties (the π^* and σ^* bands arising from the sp^2 bonding) can be identified by studying characteristic pre-edge features, while structural characteristics of nanostructured systems can be identified looking at the variation in the multiple-scattering region of the x-ray near dge spectra (XANES).

Channeling of a particle beam in straight and bent single-wall nanotubes, with a strong potential impact onto the accelerator world, has been studied in computer simulations (Monte Carlo). The first results identify the range of carbon nanotube parameters (diameter, length, curvature) suitable for channeling of GeV particles. This may be used to create a very elegant technique of beam handling at accelerators [28, 29]. Also, in [30] we studied the theory of processes accompanying the X-ray transmission by capillary structures, with potential technological applications in X-ray and neutron physics, as well as in chemistry, biology and medicine.

Exploratory investigations of toy-model realizations, capable of describing the physically measurable properties of low-dimensional correlated electron systems have been carried out. For instance, we apply nontrivial quantum mechanical systems (e.g. quantum mechanics on curved spaces, supersymmetric quantum mechanics and noncommutative quantum mechanics) to the excitonic effects in quantum dots where supersymmetric extensions allow us to take into account the interaction of the spin of system with a magnetic field, whereas non-commutativity describes collective effects in the lowest Landau levels. We studied in [31] the application of noncommutative theories to the Hall effect in its four-dimensional generalization. We also used, in connection the description of the optical properties of cylindrical and the spherical/parabolical quantum dots, the generalizations of two- and three-dimensional oscillator and Coulomb systems on the spheres and hyperboloids as well as their noncommutative and supersymmetric counterparts [32] in the presence of a magnetic field. Very recently we proposed an exactly-solvable model of a quantum oscillator on two-(complex) dimensional complex projective space (in its compact and noncompact versions), as well as on the related non-constant curvature Kahler spaces with conic singularities. [33]

References

1. S. Di Matteo, Y. Joly, A. Bombardi, L. Paolasini, F. de Bergevin and C.R. Natoli, Observation of local chiral-symmetry breaking in globally centrosymmetric crystals. - Phys. Rev. Lett. **91**, 257402 (2003)

2. S. Di Matteo, Y. Joly, and C.R. Natoli, The role of orbital and magnetic ordering in resonant anomalous scattering at the Vanadium K-edge in V_2O_3 Submitted for publication to Phys. Rev. B.

3. S. Di Matteo, Y. Joly, C.R. Natoli "A critical re-examination of the non-reciprocal x-ray gyrotropy in V_2O_3" - Phys. Rev. B **67**, 195105 (2003)

4. A. Bombardi, F. de Bergevin, S. Di Matteo, L. Paolasini, J.M. Honig, P. Metcalf, "Precursor symmetry breaking in Cr-doped V2O3." - accepted for publication in Physica B

5. S. Di Matteo, T. Chatterjee et al. "Resonant x-ray scattering from $LaSr_2Mn_2O_7$ at the Mn K edge" - Phys. Rev B **68**, 024414 (2003)

6. A. Marcelli, G. Cibin, S. Di Matteo, J. Chaboy et al. "Octahedral low spin symmetric configurations vs. high spin octahedral distorted configurations: The case of Fe in natural layered silicates" - accepted for publication in Jour. Phys. Chem. Solid

7. S. Di Matteo, C.M. Varma, "Symmetry considerations for detection of time-reversal breaking phases in cuprates by x-ray diffraction and absorption" - Phys. Rev. B **67**, 134502 (2003)

8. A. Bombardi, F. de Bergevin, S. Di Matteo, et al. "Direct determination of the magnetic ground state in the square lattice S=1/2 antiferromagnet Li_2VOSiO_4." - submitted to Phys. Rev. Lett.

9. S. Di Matteo, "Resonant x-ray scattering as a probe of toroidal moments in centrosymmetric systems." - submitted to Phys. Rev. Lett.

10. S. Burdin, N.B. Perkins and C. Lacroix, "Electronic states and magnetic excitations in LiV_2O_4", Journal of Physics: Condensed Matter **16**, xxxxx (2004)

11. S. Di Matteo, G Jackeli, N.B. Perkins and C. Lacroix, "Interplay of orbital, lattice and magnetic degrees of freedom in $MgTi_2O_4$: an orbital driven spin singlet ground state", submitted to Phys. Rev. B

12. S. Di Matteo, N.B. Perkins, C.R. Natoli "Open points on the nature of the antiferromagnetic ground state of V_2O_3" - Acta Physica Polonica B, **34** 775, (2003)

13. S. Di Matteo "On the nature of the magnetic space group in the monoclinic phase of V_2O_3" - submitted to Physica Scripta

14. S. Di Matteo, G. Jackeli, N.B. Perkins, "An effective spin-orbital Hamiltonian for the double perovskite Sr_2FeWO_6: Derivation of the phase diagram" - Phys. Rev B **67**, 184427 (2003)

15. N.B. Perkins, S. Di Matteo and G. Jackeli, "An effective spin-orbital Hamiltonian for Sr_2FeWO_6"- accepted for publication in Journal of Magnetism and Magnetic Materials (2004)

16. A.M. Balagurov,S.N. Bushmeleva,V.Yu. Pomjakushin,D.V. Sheptyakov, V.A. Amelichev, O.Yu. Gorbenko, A.R. Kaul, E.A. Gan'shina and N.B. Perkins, "Magnetic structure of $NdMnO_3$ consistently doped with Sr and Ru", Phys. Rev. B (2004).

17. C.R. Natoli, M. Benfatto, S. Della Longa and K. Hatada X-ray absorption spectroscopy: state-of-the-art analysis - J. Synchrotron Rad. **10**, 26-42, (2003)

18. M. Benfatto, S. Della Longa and C.R. Natoli The MXAN procedure: a new method for analysing the XANES spectra of metalloproteins to obtain structural quantitative information - J. Synchrotron Rad. **10**, 51-57, (2003)

19. Della Longa, S, Arcovito, A, Benfatto, M, et al. Redox-induced structural dynamics of Fe-heme ligand in myoglobin by x-ray absorption spectroscopy BIOPHYS J **85** (1): 549-558 (2003)

20. Cardelli, A, Cibin, G, Benfatto, M, et al. A crystal-chemical investigation of Cr substitution in muscovite by XANES spectroscopy PHYS CHEM MINER **30**(1): 54-58 (2003)

21. K. Hatada, M. Benfatto and C.R. Natoli Self-consistent non local potential for XANES Physica Scripta 2004 Conference Proceedings, XAFS12 International Conference, Malmo (Sweden) 22-27 June 2003.

22. P. Kruger and C. R. Natoli, Theory of Ca-L_{23} edges using a novel multichannel multiple scattering method. Invited presentation at the BIOXAS workshop held in Paris, 29-30 June 2003 and J. Synchrotr. Rad. **59**, xxx (2004).

23. S. Bellucci, P. Onorato, Rashba effect in two-dimensional mesoscopic systems with transverse magnetic field, Phys. Rev. B **68**, 245322 (2003).

24. S. Bellucci, J. Gonzalez, P. Onorato, Large N Effects and Renormalization of the Long-Range Coulomb Interaction in Carbon Nanotubes, Nucl. Phys. B **663**, 605 (2003).

25. S. Bellucci, J. Gonzalez, P. Onorato, Doping- and size-dependent suppression of tunneling in carbon nanotubes Phys. Rev. B (2004), cond-mat/0304079.

26. S. Bellucci and P. Onorato, Single-wall nanotubes: Atomic-like behavior and microscopic approach Phys. Rev. B (submitted).

27. S. Bellucci, S. Botti, A. Marcelli, K. Ibrahim, Z.Y. Wu, X-ray absorption spectroscopy study of nanotubes 19th Int. Conference on X-ray and inner-shell processes, A. Bianconi et al. editors, American Institute of Physics, Melville, New York 2003, p.355.

28. S. Bellucci, V. M. Biryukov, Yu. A. Chesnokov, V. Guidi, W. Scandale, Channeling of high energy beams in nanotubes, Nucl. Instrum. Meth. B **202**, 236 (2003).

29. S. Bellucci, V. M. Biryukov, Yu. A. Chesnokov, V. Guidi, W. Scandale, Making Micro- and Nano-beams by Channeling in Micro- and Nano-structures, Phys. Rev. ST Accel. Beams **6**, 033502 (2003).

30. S. Bellucci, S.B. Dabagov, On X-Ray Channeling in microcapillaries and nanocapillaries, J. Phys. Cond. Mat. **15**, 3171 (2003).

31. Stefano Bellucci, Pierre-Yves Casteill, Armen Nersessian, Four-dimensional Hall mechanics as a particle on CP3 Phys. Lett. B **574**, 121 (2003).

32. S. Bellucci, A. Nersessian, (Super)Oscillator on CP(N) and Constant Magnetic Field, Phys. Rev. D **67**, 065013 (2003).

33. S. Bellucci, A. Nersessian, A. Yeranyan, Quantum Mechanics Model on Kahler conifold, Phys. Rev. D (submitted), hep-th/0312323.

LF-21: PHENOMENOLOGY OF ELEMENTARY PARTICLE INTERACTIONS AT COLLIDERS

G. Isidori, G. Pancheri (Resp.), C. Smith (Bors. PD), R. Unterdorfer (Dott.)

1 Summary of the project

This project investigates two main research areas:

- Flavour physics.
- Quantum Chromodynamics and the rise of total cross-sections.

The first area, discussed in Section 2, concerns the possibility to perform new low-energy precision tests about the mechanism of quark-flavor mixing, by means of K and B meson decays. The second area, discussed in Section 3, is the project related to the QCD description of hadronic and photonic total cross-section at high energies.

2 Flavour Physics

Despite the fact so far that the Standard Model (SM) provides a successful description of particle interactions, it is natural to consider it only as the low-energy limit of a more general theory, or as the renormalizable part of an effective field theory valid up to some still undetermined cut-off scale Λ. Since the SM is renormalizable, we have no direct indications about the value of Λ. However, theoretical arguments based on a natural solution of the hierarchy problem suggest that Λ should not exceed a few TeV.

One of the strategies to obtain additional clues about the value of Λ is to constrain (or find evidence for) the effective non-renormalizable interactions, suppressed by inverse powers of Λ, which encode the presence of new degrees of freedom at high energies. These operators should naturally induce large effects in processes which are not mediated by tree-level SM amplitudes, such as $\Delta F = 1$ and $\Delta F = 2$ flavour-changing neutral current (FCNC) transitions. Up to now there is no evidence of these effects and this implies severe bounds on the effective scale of dimension-six FCNC operators. For instance the good agreement between SM expectations and experimental determinations of K^0–$\bar{K}^0$ mixing leads to bounds above 10^3 TeV for the effective scale of $\Delta S = 2$ operators, i.e. well above the few TeV range suggested by the Higgs sector.

The apparent contradiction between these two determinations of Λ is a manifestation of what in many specific frameworks (supersymmetry, techincolour, etc.) goes under the name of *flavour problem*: if we insist with the theoretical prejudice that new physics has to emerge in the TeV region, we have to conclude that the new theory possesses a highly non-generic flavour structure. Interestingly enough, this structure has not been clearly identified yet, mainly because the SM, *i.e.* the low-energy limit of the new theory, does not possess an exact flavour symmetry. The attempt to clarify this structure, both at the phenomenological level (with the help of precision data on rare decays) and at a more fundamental level (with the help of new symmetry principles), is one of the main activity of our group. [1)]

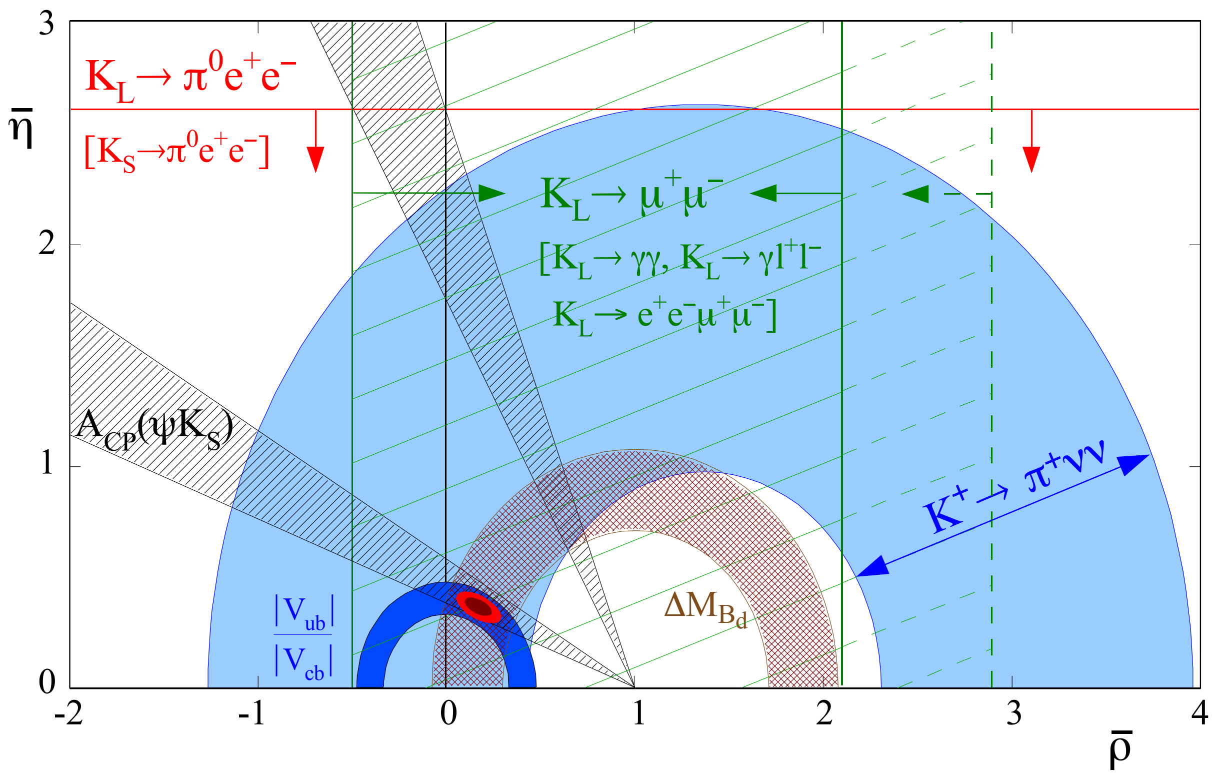

Figure 1: Summary of the present constraints in the $\bar{\rho}$–$\bar{\eta}$ plane from rare K decays: the $K_L \rightarrow \mu^+\mu^-$ bound on $\bar{\rho}$ [10], the $K_L \rightarrow \pi^0 e^+ e^-$ bound on $\bar{\eta}$ [9] and the $K^+ \rightarrow \pi^+ \nu\bar{\nu}$ ellipse [7]. The constraints on $|V_{ub}|$ and B–$\bar{B}$ mixing, from Ref. [11], are also shown for comparison.

In the last year we performed a series of studies on the rare decay $B \rightarrow X_s \ell^+ \ell^-$ [2, 3, 4] and other rare B decays [5, 6]; on the rare K decays $K_L \rightarrow \pi\nu\bar{\nu}$ [7, 8], $K_L \rightarrow \pi^0 e^+ e^-$ [9] and $K_L \rightarrow \mu^+\mu^-$ [10]; on the precise determination of the Cabbibo angle from $K_{\ell 3}$ decays [11, 12].

Concerning $K_L \rightarrow \mu^+\mu^-$, [10] our aim was the precise calculation of the long-distance two-photon amplitude, taking advantage of recent experimental results from KLOE, NA48 and KTeV. Our analysis allows to extract the conservative bounds on the Wolfenstein parameter shown in Fig. 1. Similarly, we performed a new analysis of the rare decay $K_L \rightarrow \pi^0 e^+ e^-$ taking into account important experimental progress that has recently been achieved in measuring $K_L \rightarrow \pi^0\gamma\gamma$ and $K_S \rightarrow \pi^0 e^+ e^-$. [9] As a result, we obtained the first reliable prediction of the total rate for this process: $B(K_L \rightarrow \pi^0 e^+ e^-) = (3.2^{+1.2}_{-0.8}) \times 10^{-11}$. The latter result turns out to be dominated by CP violation with a sizable contribution ($\sim 40\%$) from the direct-CP-violating amplitude (see Fig. 2).

3 Quantum Chromodynamics and the rise of total cross-sections

This project [13, 14, 15] is presently developed through collaborations between G. Pancheri and Rohini Godbole for what concerns the Eikonal Minijet Model, R. Godbole, A. Grau and Y.N. Srivastava for the studies of the effect of Soft Gluon Resummation on the taming of the rise of total cross-section, and with A. de Roeck for the study of total cross-sections at Linear Colliders.

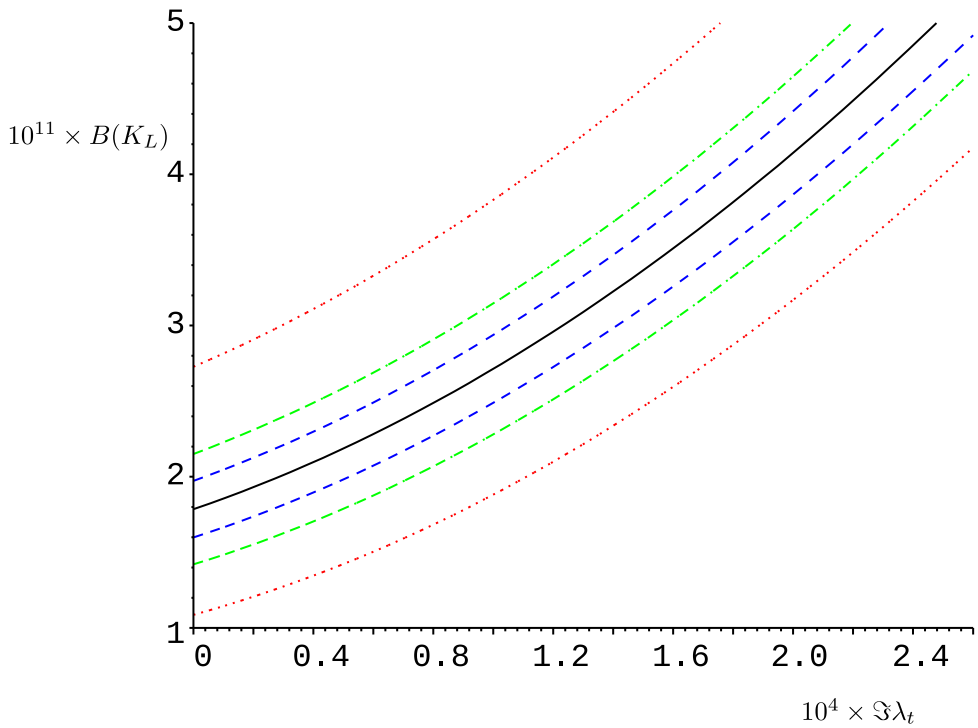

Figure 2: SM Prediction for $B(K_L \to \pi^0 e^+ e^-)$ as a function of $\Im\lambda_t = \Im(V_{ts}^* V_{td})$, assuming a positive interference between direct- and indirect-CP-violating components [9]. The three curves correspond to the central value of $B(K_S \to \pi^0 e^+ e^-)$ from NA48 and no error (central full line); 10% error (dashed blue lines); 20% error (dashed green lines); present error (red dotted lines).

The goal of this project is to obtain a QCD description of the initial decrease and the final increase of total cross-sections through soft gluon summation (via the Bloch-Nordsieck Model) and QCD calculable jet x-sections, also known as mini-jets in this context. Thus, the physical picture includes multiple parton collisions and soft gluons dressing each collision.

3.1 *The Eikonal Minijet Model for protons and photons*

In the Eikonal Minijet Model (EMM) the rise can be obtained using the QCD calculable contribution from the parton-parton cross-section, whose total yield increases with energy. For a unitary description, the jet cross-sections are embedded into the eikonal formalism, where the eikonal function contains both the energy and the impact parameter distribution in b-space. The simplest formulation with minijets to drive the rise, and hadronic form factors for the impact parameter distribution, can be applied to all the available x-sections. One finds that proton-antiproton high energy data can be reproduced by this model. However it is not possible to describe both the early rise, which in proton-antiproton scattering takes place around $10 \div 50\, GeV$, and the Tevatron data, with a single set of parameters.

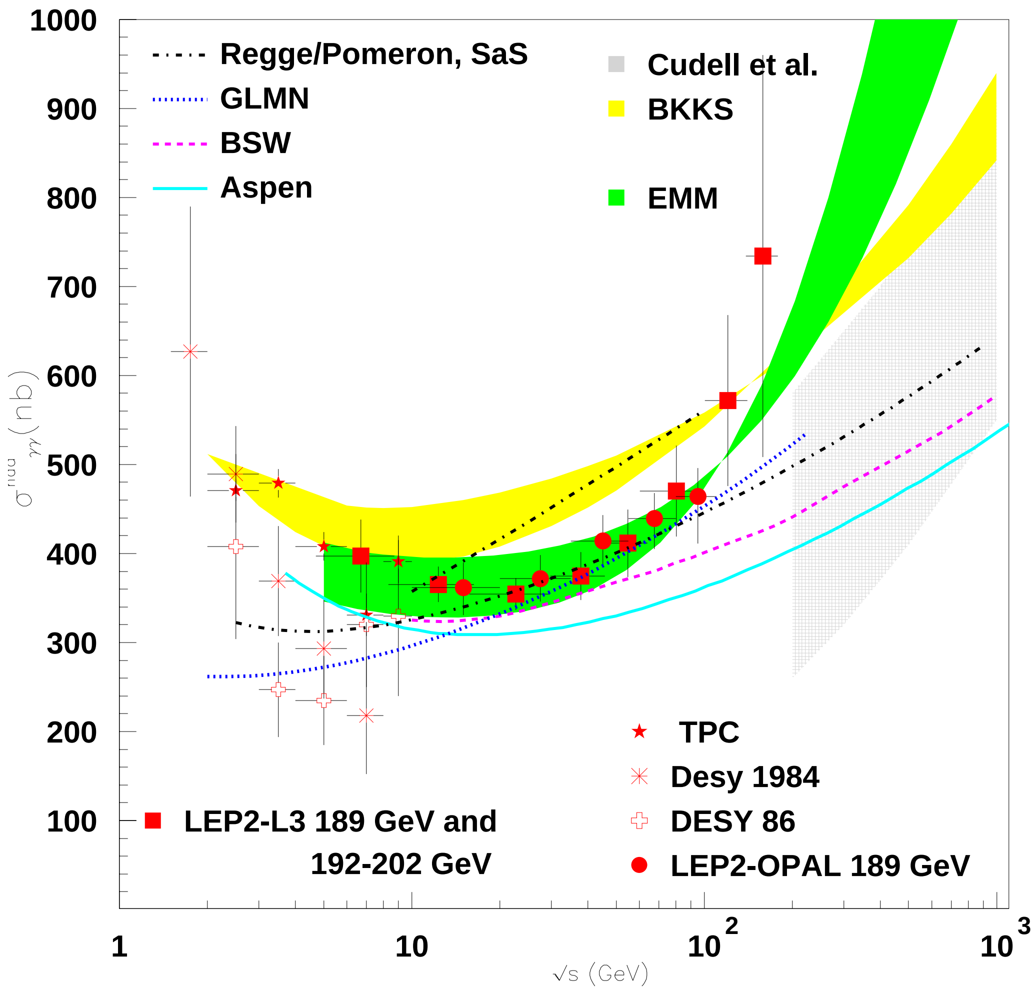

Figure 3: *The predictions from factorization (proton-like) models, Regge-Pomeron exchange and a QCD structure function model together with those from the EMM are compared with the data.*

Photo-production data can be described through the same simple eikonal minijet model, with the relevant parton densities for the jet cross-sections, scaling the non perturbative part with VMD and quark counting factors. However, just like in the proton-proton case and in the gamma-gamma case, the case for extrapolation of the EMM to higher energies is not convincing. A compilation of $\gamma\gamma$ data, including present LEP data, done for future Linear Collider indicated that the EMM describes quite well the rise at present energies, but the extrapolation to even higher energies appears unrealistic and may need to be modified, as found in the proton case. In the figure from [14] we show the predictions of this model for photon-photon collisions in comparison with predictions from different models and with the available data.

A possible way to decrease the uncertainty in the predictions is to refine the QCD analysis, through resummation of soft gluon emission from the initial state partons, a feature absent from most simple EMM.

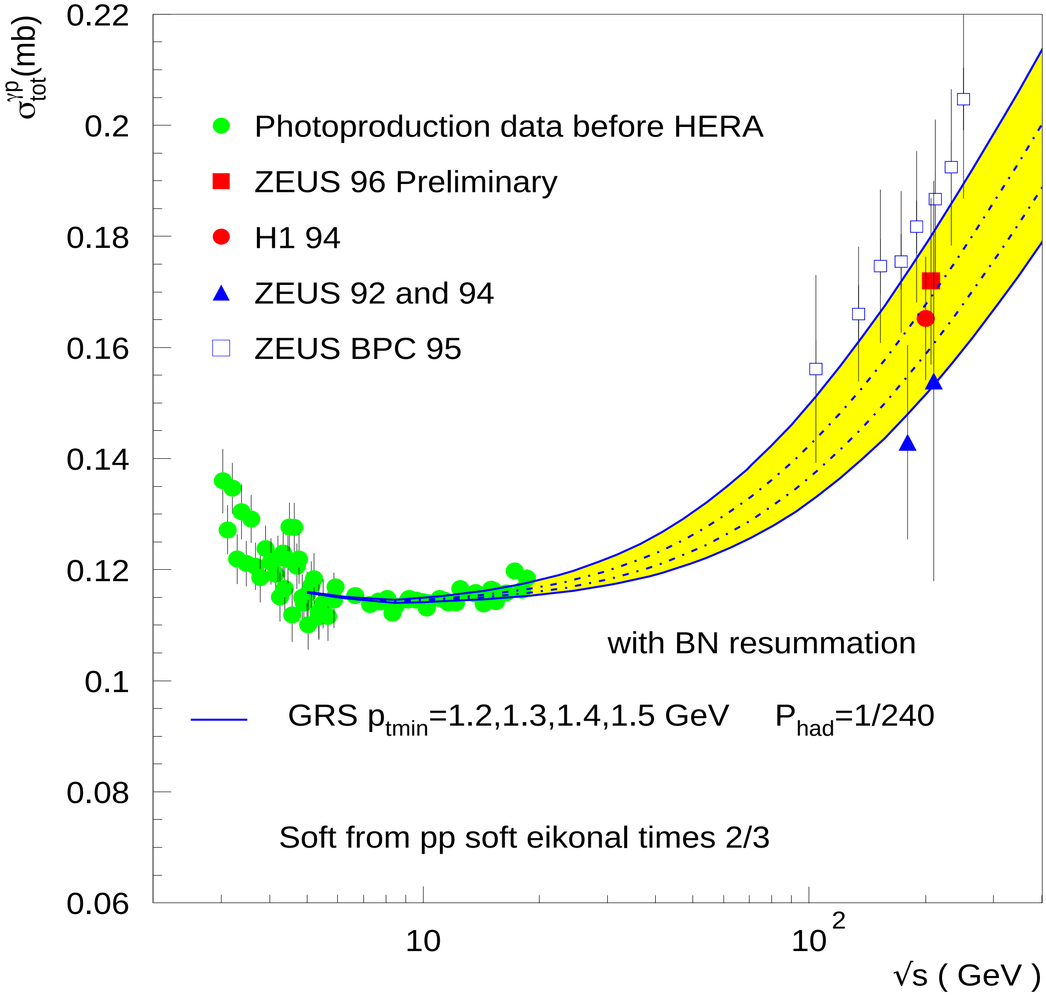

Figure 4: *Total γp cross-section, with soft gluon resummation (BN) and GRS densities in the mini-jet cross-section, for an indicative set of values for p_{tmin}.*

3.2 *Soft Gluon Summation and the impact parameter distribution of partons*

A model for the impact parameter space distribution of parton in the hadrons has been developed and applied to the proton and photon cross-sections in order to obtain a better description of total cross-section. The physical picture underlying this model is that the fast rise due to mini-jets and the increasing number of gluon-gluon collisions as the energy increases, can be reduced if one takes into account that soft gluons, emitted mostly by the initial state valence quarks, determine an acollinearity between the partons which reduces the overall parton-parton luminosity. This model can describe very well all available data for proton collisions and appears very flexible when applied to photon processes. We show next a representative figure from [13].

4 Work Program for the year 2004

Most of the activity previously described in hadronic physics will be continued into the year 2004. The work on QCD and total cross-sections, a long term project, will focus mainly on discussing the complementarity between the coming measurements at LHC and the prospects of measuring total cross-sections at the Lineaar Colliders.

References

1. G. Isidori, *Kaon decays and the flavour problem,* Annales Henri Poincare **4** (2003) S97.

2. A. Ghinculov, T. Hurth, G. Isidori and Y. P. Yao, *Forward-backward asymmetry in* $B \to X_s l^+ l^-$ *at the NNLL level,* Nucl. Phys. B **648** (2003) 254.

3. A. Ghinculov, T. Hurth, G. Isidori and Y. P. Yao, *NNLL QCD corrections to the decay* $B \to X_s l^+ l^-$. Nucl. Phys. Proc. Suppl. **116** (2003) 284.

4. A. Ghinculov, T. Hurth, G. Isidori and Y. P. Yao, *New NNLL QCD results on the decay* $B \to X_s l^+ l^-$, hep-ph/0310187, to appear in Nucl. Phys. B.

5. G. Isidori, *Theory of radiative and rare B decays*, hep-ph/0401079; invited review talk at BEAUTY 2003 (C.M.U. Pittsburg, Oct. 2003).

6. R. Fleischer, G. Isidori and J. Matias, *Shedding light on the dark side of* B–$\bar{B}$ *mixing through* $B \to \pi^+\pi^-$, $K \to \pi\nu\bar{\nu}$ *and* $B \to \mu^+\mu^-$. JHEP **0305** (2003) 053.

7. G. Isidori, $K \to \pi\nu\bar{\nu}$ *decays and CKM fits,* eConf **C0304052** (2003) WG304 [hep-ph/0307014].

8. Y. Grossman, G. Isidori and H. Murayama, *Lepton flavor mixing and* $K \to \pi\nu\bar{\nu}$ *decays,* hep-ph/0311353, to appear in Phys. Lett. B.

9. G. Buchalla, G. D'Ambrosio and G. Isidori, *Extracting short-distance physics from* $K_L \to \pi^0 e^+ e^-$ *decays,* Nucl. Phys. B **672** (2003) 387

10. G. Isidori and R. Unterdorfer, *On the short-distance constraints from* $K_{L,S} \to \mu^+ mu^-$, JHEP **0401** (2004) 009.

11. M. Battaglia *et al.*, *The CKM matrix and the unitarity triangle*, hep-ph/0304132 (CERN Yellow Book).

12. G. Isidori, *Summary and overview of working group VI:* V_{us} *and* V_{ud}, eConf **C0304052** (2003) WG601.

13. R.M. Godbole, A. Grau, G. Pancheri, Y.N. Srivastava, *Photon Total Cross-sections* IISC-CTS-10-03, LNF-03-20-P, Nov 2003. Talk given at Photon 2003: International Conference on the Structure and Interactions of the Photon and 15th International Workshop on Photon-Photon Collisions, Frascati, Italy, 7-11 Apr 2003. e-Print Archive: hep-ph/0311211

14. R.M. Godbole, A. De Roeck, A. Grau, G. Pancheri, *Hadronic Cross-sections in two photon proceses at a future Linear Collider*, DESY-03-054, May 2003. Published in JHEP 0306:061,2003 e-Print Archive: hep-ph/0305071

15. R.M. Godbole, A. Grau, G. Pancheri, A. De Roeck, *Predictions for the* $\gamma\gamma$ *total cross-section in the TeV region : un update*, CERN-TH-2002-338, Mar 2003. Presented at International Workshop on Linear Colliders (LCWS 2002), Jeju Island, Korea, 26-30 Aug 2002. e-Print Archive: hep-ph/0303018

MI-11: QCD at finite temperature and density. Lattice studies

M.-P. Lombardo, F. Palumbo (Resp.)

1 Introduction

Our work focuses on strong interactions in different thermodynamics conditions, including the quark gluon plasma, where confinement is lost and the hadron spectrum is heavily modified. As this regime is outside the reach of perturbative domain we use the lattice approach: we are interested in its formal aspects as well as in applications, with emphasis on the physics of ongoing experiments at RHIC and ALICE and CMS (and perhaps ATLAS) at LHC [1].

QCD at finite temperature is easily dealt with on the lattice. On the contrary, QCD at finite density presents specific challenges [2]. Nonetheless, a region of the QCD phase diagram up to moderately large baryon chemical potentials has been successfully explored on the lattice. All in all, QCD at finite temperature and density is nowadays an active field of research, with many overlaps with other aspects of particle physics, astrophysics, and even condensed matter theory.

2 Formal developments

2.1 Different actions with identical partition function in theories regularized on a lattice (FP)

In the action of theories defined on a lattice the fields and their conjugates are generally time-split, both in the relativistic and non-relativistic case. Such time splitting makes the action somewhat more complicated. In particular in gauge theories it generates a coupling of the chemical potential to the temporal links.

We found a general procedure to avoid the time splitting without changing the partition function and applied it to QCD at finite baryon density [3] and to many-body theories (in progress).

2.2 Fermionic composites in many-body systems and relativistic field theories (FP with S.Caracciolo)

The lowest lying excitations of fermionic systems can often be described in terms of bosons. Familiar examples in Many-Body systems are the Cooper pairs of Superconductivity in metals and the s- and d-bosons in the Interacting Boson Model of atomic Nuclei. The obvious example in relativistic field theories is provided by mesons in QCD.

From the technical point of view relativistic and nonrelativistic theories look very different. In the first case the fermion interaction is quartic, and it can be made quadratic by the Hubbard-Stratonovich transformation introducing bosonic auxiliary fields which are then naturally promoted to dynamical fields, which can describe the bosonic excitations, provided they are sufficiently collective. Such an approach, however, is not general enough. In particular we are unable to treat at the same time bosons which “condense” and bosons which do not. In renormalizable relativistic theories the situation is even worse, because the fermion interaction is quadratic to start with, and to our knowledge there is no way to introduce analytically bosonic fields.

We are studying a new approach where in the evaluation of the partition function the trace of the transfer matrix is restricted to coherent states of fermionic composites. The bosonic functions appearing in such coherent states are then naturally promoted to dynamical bosonic fields. The method has been satisfactorily tested on simple nonrelativistic models and we are now considering the case of QCD.

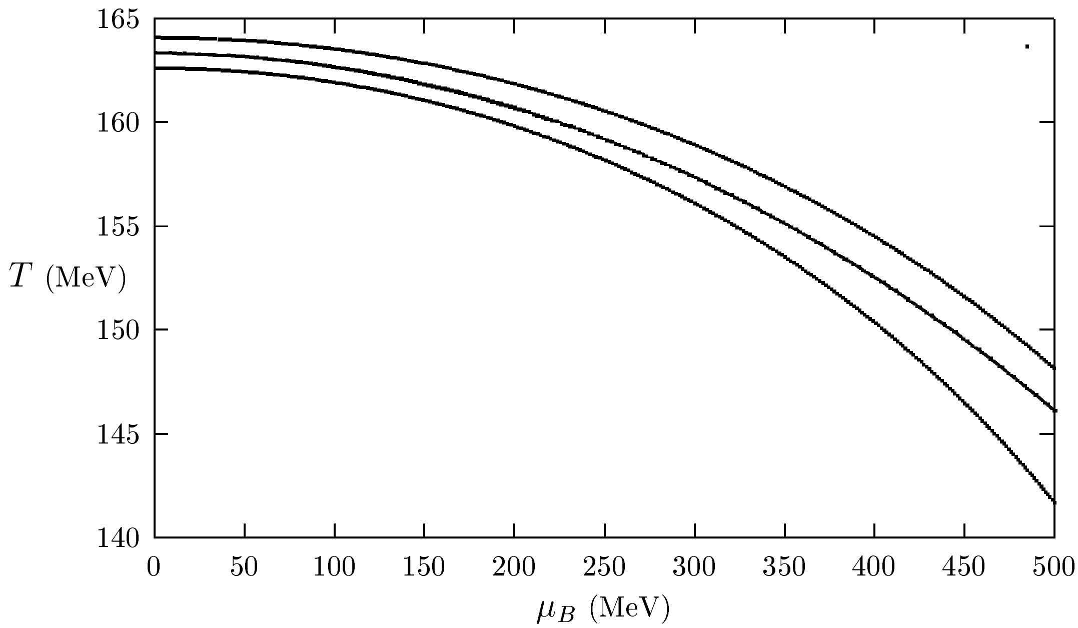

Figure 1: *Phase diagram of four-flavor QCD in the temperature-baryochemical potential plane* [4]. *The central line* $T = T_c\sqrt{(1 - \frac{0.021}{2}\frac{\mu^2}{T_c^2})}$ *is the result, the dotted lines limit the errorband.*

3 Results

3.1 Phase diagram (MPL with Massimo D'Elia)

We have studied [4] QCD at nonzero temperature and baryon density in the framework of the analytic continuation from imaginary chemical potential. We carried out simulations of QCD with four flavor of staggered fermions, and reconstructed the phase diagram in the temperature-imaginary μ plane. We have considered ansätze for the analytic continuation of the critical line and other observables motivated both by theoretical considerations and mean field calculations in four fermion models and random matrix theory. We have determined the critical line, and the analytic continuation of the chiral condensate, up to $\mu_B \simeq 500MeV$, which is the region of interest of current experiments. The results are in qualitative agreement with the predictions of model field theories, and consistent with a first order chiral transition. The correlation between the chiral transition and the deconfinement transition observed at $\mu = 0$ persists at nonzero density.

3.2 Lattice and phenomenological models (MPL with Massimo D'Elia)

More recently, we [5] presented results in the different phases and we did show that our method is ideally suited for a comparison between lattice data and phenomenological models. This is also relevant in view of nonequilibrium studies, which are restricted to simple models: hence, is very important to assess their validity. An extended writeup shall appear soon.

3.3 Hadrons in media (MPL with M. Paciello, S. Petrarca and B. Taglienti)

The important physics of scalar and glueballs has been studied within the two-color model. We [6] have established the level ordering in the scalar/pseudoscalar sector, and found that it changes from $m_\pi < m_S \simeq m_{0^{++}}$ in the normal phase to $m_{0^{++}} < m_S \simeq m_\pi$ in the dense medium. Moreover, our results suggest that the vector particle becomes heavier in the medium. Also in this case we are working on a lengthier publication.

4 List of conference talks

1. M.-P. Lombardo *QCD critical region and quark gluon plasma from an imaginary* μ_B talk at LATTICE 2003. *The XXI International Symposium on Lattice Field Theory* Tsukuba , Ibaraki , Japan , July 15-19, 2003.
2. M.-P. Lombardo *Lattice QCD at Finite Density - a primer* review at FINITE DENSITY QCD AT NARA, Nara, Japan,July 10-12, 2003.
3. M.-P. Lombardo *Results on the QCD Phase Diagram from the Lattice* talk at THE STRUCTURE OF MANY-BODY SYSTEMS AT DIFFERENT SCALES", Catania,October 6-8, 2003.

5 Conference and school organization, membership of EU programs

1. *Il Quark Gluon Plasma e gli Ioni Pesanti Relativistici:Passato, Presente,Futuro* Torino,1-5 Dicembre 2003 `http://www.infn.it/conference/qgp2003`.
2. *Quarkonium Working Group* `http://www.qwg.to.infn.it/`. Convenor for the *In Media* topic.
3. *The Strongly Interacting Matter - Network of the HadronPhysics I3.* Coordinator of the Frascati node.

References

1. See e.g. F. Wilczek' speech in acceptance of 2003 EPS prize *From concept to reality to vision* [arXiv:hep-ph/0401035] for a quick introduction framed in a general HEP context; *ALICE Physics Performace Report* http://alice.web.cern.ch/Alice/ppr/web/CurrentVersion.html for an experimental perspective; E. Laermann and O. Philipsen, *Status of lattice QCD at finite temperature* [arXiv:hep-ph/0303042], to appear in *Annual Review of Nuclear and Particle Science, 2003*, for a lattice introduction aimed at non–lattice experts.
2. M. P. Lombardo, *Lattice QCD at finite density: A primer* [arXiv:hep-lat/0401021], Prog. Theor. Phys. Suppl., to appear.
3. F.Palumbo, *Different definitions of the chemical potential in the action with identica partition function in QCD on a lattice* [arXiv:hep-lat/0210045], Phys.Rev.D, in press.
4. M. D'Elia and M. P. Lombardo, Phys. Rev. D **67** (2003) 014505.
5. M. D'Elia and M. P. Lombardo, *QCD critical region and quark gluon plasma from an imaginary* μ_B, [arXiv:hep-lat/0309114] .
6. M. P. Lombardo, M. L. Paciello, S. Petrarca and B. Taglienti, *SU(2) glueballs, diquarks and mesons in dense matter* [arXiv:hep-lat/0309110].

MI-12

S. Bellucci (Resp.), P.-Y. Casteill, S. Ferrara (Ass.), A. Galajinsky, E. Latini, F. Morales, E. Orazi (Laur.), C. Sochichiu

1 Research Activity

The group in Frascati made important contributions to gauged supergravity and duality symmetry, supersymmetry algebras in diverse dimensions, super Higgs effect, supersymmetric theories in non-commutative superspaces, classification of operators in the AdS/CFT correspondence, supergravity interpretation of flux compactification, supersymmetric Born-Infeld actions, gauge theories in non-compact spaces.

2 Activity on pp-wave duality and AdS/CFT correspondence

It was shown in Frascati that the string bit model suffers from doubling in the fermionic sector, leading to a strong violation of supersymmetry in the limit $N \to \infty$. Since there is an exact correspondence between string bits and the algebra of BMN operators, doubling is expected also in the latter. The origin of doubling in the BMN sector was discussed. In Frascati a simple conformal mechanics model was proposed, which is classically equivalent to a charged massive particle propagating near the AdS2 x S2 horizon of an extreme Reissner-Nordstrom black hole. The equivalence, which holds for any finite value of the black hole mass and with both the radial and angular degrees of freedom of the particle taken into account, is ensured by the existence of a canonical transformation in the Hamiltonian formalism. Using this transformation, the Hamiltonian of a N=4 superparticle was constructed on a AdS2 x S2 background.

3 Other developments

Nonlinear realizations superfield techniques, pertinent to the description of partial breaking of global N=2 supersymmetry in a flat d=4 super Minkowski background, were generalized in Frascati to the case of partially broken N=1 AdS5 supersymmetry SU(2,2—1). Off-shell manifestly N=1, d=4 supersymmetric minimal Goldstone superfield actions were presented, in an explicit form, for two patterns of partial breaking of SU(2,2—1) supersymmetry. They correspond to two different nonlinear realizations of the latter, in the supercosets with the AdS5 and AdS5 x S1 bosonic parts. The relevant worldvolume Goldstone supermultiplets were accommodated, respectively, by improved tensor and chiral N=1, d=4 superfields. The second action was obtained from the first one by dualizing the improved tensor Goldstone multiple into a chiral Goldstone one. In the bosonic sectors, the first and second actions yield static-gauge Nambu-Goto actions for a L3-brane on AdS5 and a scalar 3-brane on AdS5 x S1.

In Frascati the one-loop renormalization of dimension four composite operators and the energy-momentum tensor in noncommutative phi 4 scalar field theory was considered. Proper operator bases were constructed and it was proved that the bare composite operators are expressed via renormalized ones, with the help of a mixing matrix, whose explicit form was calculated. The corresponding matrix elements turn out to differ from the commutative theory. The canonically defined energy-momentum tensor is not finite and must be replaced by the "improved" one, in order to provide finiteness. The suitable "improving" terms were found. A two-dimensional non-commutative inverted oscillator in the presence of a constant magnetic field, coupled to the system in a “symplectic” and “Poisson” way was also analyzed in Frascati. It was shown that it has a discrete energy spectrum for some value of the magnetic field.

4 List of Conference Talks by LNF Authors in Year 2003

1. S. Bellucci, Frascati, Congresso di Fisica Teorica ”Cortona 2003”, Cortona, Italy

References

1. ”ADS / CFT EQUIVALENCE TRANSFORMATION”, S. Bellucci, E. Ivanov e S. Krivonos, hep-th/0206126, Phys. Rev. D 66 (2002) 086001.

2. CAN STRING BITS BE SUPERSYMMETRIC? By Stefano Bellucci, Corneliu Sochichiu (Frascati). Jul 2003. 8pp. Published in Phys.Lett.B571:92-96,2003 e-Print Archive: hep-th/0307253.

3. RENORMALIZATION OF THE ENERGY MOMENTUM TENSOR IN NONCOMMUTATIVE SCALAR FIELD THEORY. By S. Bellucci (Frascati), I.L. Buchbinder (Tomsk Pedagogical Inst.), V.A. Krykhtin (Tomsk Polytechnic U.). Mar 2003. 21pp. Published in Nucl.Phys.B665:402-424,2003 e-Print Archive: hep-th/0303186.

4. FERMION DOUBLING AND BERENSTEIN-MALDACENA-NASTASE CORRESPONDENCE. By Stefano Bellucci, Corneliu Sochichiu (Frascati). Feb 2003. 12pp. Published in Phys.Lett.B564:115-122,2003 e-Print Archive: hep-th/0302104.

5. CONSTANT MAGNETIC FIELD AND 2-D NONCOMMUTATIVE INVERTED OSCILLATOR. By Stefano Bellucci (Frascati). Jan 2003. 7pp. Published in Phys.Rev.D67:105014,2003 e-Print Archive: hep-th/0301227.

6. GOLDSTONE SUPERFIELD ACTIONS IN ADS(5) BACKGROUNDS. By S. Bellucci (Frascati), E. Ivanov, S. Krivonos (Dubna, JINR) Nuclear Physics B 672:123, (2003).

7. ADS(2) / CFT(1), CANONICAL TRANSFORMATIONS AND SUPERCONFORMAL MECHANICS. By S. Bellucci (Frascati), A. Galajinsky (Frascati and Tomsk Polytechnic U.), E. Ivanov, S. Krivonos (Dubna, JINR). 10pp. Published in Phys.Lett.B555:99-106,2003.

8. GOLDSTONE SUPERFIELD ACTIONS FOR PARTIALLY BROKEN ADS(5) SUPERSYMMETRY. By S. Bellucci (Frascati), E. Ivanov, S. Krivonos (Dubna, JINR). Published in Phys.Lett.B558:182-190,2003

9. K3 X T**2 / Z(2) ORIENTIFOLDS WITH FLUXES, OPEN STRING MODULI AND CRITICAL POINTS. By C. Angelantonj (CERN), R. D’Auria (Turin Polytechnic and INFN, Turin), S. Ferrara (CERN and Frascati and UCLA), M. Trigiante (Turin Polytechnic),. CERN-TH-2003-295, Dec 2003. 10pp. e-Print Archive: hep-th/0312019

10. UNUSUAL GAUGED SUPERGRAVITIES FROM TYPE IIA AND TYPE IIB ORIENTIFOLDS. By Carlo Angelantonj (CERN), Sergio Ferrara (CERN and Frascati and UCLA), Mario Trigiante (Utrecht U.),. CERN-TH-2003-248, SPIN-03-31, ITP-03-50, UCLA-03-TEP-28, Oct 2003. 12pp.

    e-Print Archive: hep-th/0310136

11. NON-ANTICOMMUTATIVE N=2 SUPERYANG-MILLS THEORY WITH SINGLET DEFORMATION.

    By Sergio Ferrara (CERN and Frascati), Emery Sokatchev (Annecy, LAPTH),. CERN-TH-2003-180, LAPTH-992-03, Aug 2003. 10pp. Published in Phys.Lett.B579:226-234,2004 e-Print Archive: hep-th/0308021

12. FLUXES, SUPERSYMMETRY BREAKING AND GAUGED SUPERGRAVITY. By Laura Andrianopoli (CERN), Sergio Ferrara (CERN and Frascati), Mario Trigiante (Utrecht U.),. CERN-TH-2003-163, SPIN-03-24, ITP-UU-03-38, Jul 2003. 14pp. Contributed to International Conference on 20 Years of SUGRA and Search for SUSY and Unification (SUGRA 20), Boston, Massachusetts, 17-20 Mar 2003. e-Print Archive: hep-th/0307139

13. SUPERSYMMETRY IN NONCOMMUTATIVE SUPERSPACES. By S. Ferrara (CERN and Frascati), M.A. Lledo (INFN, Turin and Turin Polytechnic), O. Macia (Valencia U.),. CERN-TH-2003-150, IFIC-03-32, FTUV-03-0602, Jul 2003. 23pp. Published in JHEP 0309:068,2003 e-Print Archive: hep-th/0307039

14. NEW D = 4 GAUGED SUPERGRAVITIES FROM N=4 ORIENTIFOLDS WITH FLUXES. By Carlo Angelantonj (CERN), Sergio Ferrara (CERN and Frascati), Mario Trigiante (Utrecht U.),. CERN-TH-2003-136, SPIN-03-19, ITP-03-31, Jun 2003. 51pp. Published in JHEP 0310:015,2003 e-Print Archive: hep-th/0306185

15. N=4 SUPERGRAVITY LAGRANGIAN FOR TYPE IIB ON T**6 / Z(2) IN PRESENCE OF FLUXES AND D3-BRANES. By Riccardo D'Auria (Turin Polytechnic and INFN, Turin), Sergio Ferrara (CERN and Frascati), Floriana Gargiulo (INFN, Turin and Turin U.), Mario Trigiante (Utrecht U.), Silvia Vaula (Turin Polytechnic and INFN, Turin),. CERN-TH-2003-046, DFTT-3-2003, SPIN-03-03, ITP-UU-03-03, Mar 2003. 47pp. Published in JHEP 0306:045,2003 e-Print Archive: hep-th/0303049

16. U-DUALITY, ATTRACTORS AND BEKENSTEIN-HAWKING ENTROPY IN FOUR AND FIVE DIMENSIONAL SUPERGRAVITIES. By L. Andrianopoli, R. D'Auria (Genoa U. and INFN, Turin and Turin Polytechnic), S. Ferrara (CERN),. 1998. Prepared for Spring School and Workshop on String Theory, Gauge Theory and Quantum Gravity, Trieste, Italy, 7-18 Apr 1997. Published in Nucl.Phys.Proc.Suppl.67:17-24,1998 Also in *Trieste 1997, String theory, gauge theory and quantum gravity* 17-24

17. 4-D GAUGED SUPERGRAVITY ANALYSIS OF TYPE IIB VACUA ON K3 X T**2 / Z(2).

    By L. Andrianopoli (CERN), R D'Auria (Turin Polytechnic and INFN, Turin), S Ferrara (CERN and Frascati), M A Lledo (Turin Polytechnic and INFN, Turin),. CERN-TH-2003-037, Feb 2003. 29pp. Published in JHEP 0303:044,2003 e-Print Archive: hep-th/0302174

18. ON THE SPECTRUM OF ADS / CFT BEYOND SUPERGRAVITY. By N. Beisert (Potsdam, Max Planck Inst.), M. Bianchi (Rome U., Tor Vergata and INFN, Rome), J.F. Morales (Frascati), H. Samtleben (Utrecht U.),. AEI-2003-084, ROM2F-03-28, ITP-UU-03-56, SPIN-03-37, Oct 2003. 28pp. e-Print Archive: hep-th/0310292

19. ON STRINGY ADS(5) X S**5 AND HIGHER SPIN HOLOGRAPHY. By Massimo Bianchi (Rome U., Tor Vergata and INFN, Rome), Jose F. Morales (Frascati), Henning Samtleben (Utrecht U.),. ROM2F-2003-08, ITPUU-03-22, SPIN-03-12, May 2003. 37pp. Published in JHEP 0307:062,2003 e-Print Archive: hep-th/0305052

PI-31

F. Palumbo (Resp.)

As a first approach to a derivation of the IBM (Interacting Boson Model) from a microscopic nuclear hamiltonian, we bosonized the pairing hamiltonian in the framework of the path integral formalism respecting both the particle number conservation and the Pauli principle. Special attention was payed to the role of the Goldstone bosons. We constructed the saddle point expansion which reproduces the sector of the spectrum associated to the addition or removal of nucleon pairs [1) 2)].

This project is a collaboration with M. B. Barbaro, A. Molinari and M. R. Quaglia.

References

1. F. Palumbo, *Derivation of the IBM from an effective nuclear hamiltonian*, talk at "The structure of many-body systems at different scales", Catania,October 6-8, 2003.
2. M. B. Barbaro, A. Molinari, F. Palumbo and M. R. Quaglia, nucl-th/0304028, submitted to Nucl.Phys. A.

ALFAP

A. La Monaca (Resp.), G. Cappuccio (Ass.), E. Costa,G. Di Persio,
L. Pacciani, G. Patria, A. Rubini, P. Soffitta, N. Zema

1 Introduction

ALFAP is an experiment of X-ray Astronomy, which aims to build an advanced large field and wide area astronomical polarimeter for detecting polarized X-rays, emitted from extreme compact astronomic sources as black holes and gamma ray bursts (GRB). The pertinent physics ranges from the X-ray afterglow sources to the cosmic rays ($>10^{19}$ eV) and neutrinos of very high energy ($\sim 10^{14}$ eV).

ALFAP project differs from traditional polarimeters. It is based on X-ray photoelectron gas effect and can get a very high sensibility (>3 order of magnitude). When an X-ray photon is absorbed in the gas a photoelectron is ejected that, interacting with the gas, produces an ionization track. Under the effect of an electric field the track drifts toward a Gas Electron Multiplier (GEM) where each piece of the track is multiplied yielding at the rear of the GEM an intensified charge and a light signal. The GEM is in the focus of an optical system and the intensified track is imaged on an optical CCD. From this image of the track the original direction of the photoelectron is derived. In a polarized beam these directions are clustered on the plane of the electric vector of the beam. This concept compared with similar devices that collect the charge on a micropattern anode has different capabilities because of the smaller size of the CCD pixels that, combined with the possible demagnification of the optical system can afford to handle a larger detecting area with a single read-out chain. While the charge collecting system is suited in the focus of an X-ray optics the ALFAP system is suitable for a large area system combined with a collimator (for the study of bright sources such as X-ray black hole binaries) or in a wide field experiment for gamma-ray bursts. Moreover the system can be further extended by implementing an array of CCDs. Such a GRB instrument, without focusing optics, can cover up to 1.8 steradiants measuring about 4 brighter GRBs/month.

However, because of high cost of the project (including 25 backside illuminated CCD matrix), a minimal configuration, using two CCD matrixes, was funded by GR V of INFN. ALFAP activity has been carried out at LNF in collaboration with CNR-IASF, which has also contributed to partial funding, CNR-ISM (Roma - Tor Vergata) and CNR-ISMN (Montelibretti).

The dramatic assigned funding cut-off suffered by ALFAP during 2002 caused a partial modification of the original project. In 2003, therefore, the experiment, receiving only a little funding from common funding of LNF GR V, has further reduced its activity, but the new polarimeter has been realized, even if in reduced form.

2 Activities

During the 2003 year our group has completed the mechanical assembly of the rotating table using an aluminum crystal at 45° to give a 4 KeV X-ray polarized source for laboratory tests, and realized a new version of electronics control trigger system of the polarimeter. The GEM synchronization circuitry to the CCD read out system foresees two modes of operations. In the first mode the CCD is forced in an integration state. In this condition both vertical and horizontal CCD control phases are locked and the image is integrated in the focal plane. As soon as the GEM detects a valid event a pulse is propagated to the acquisition front-end synchronization flip-flop, which resumes the CCD from the integration state into the readout mode. So far the first image collected by the

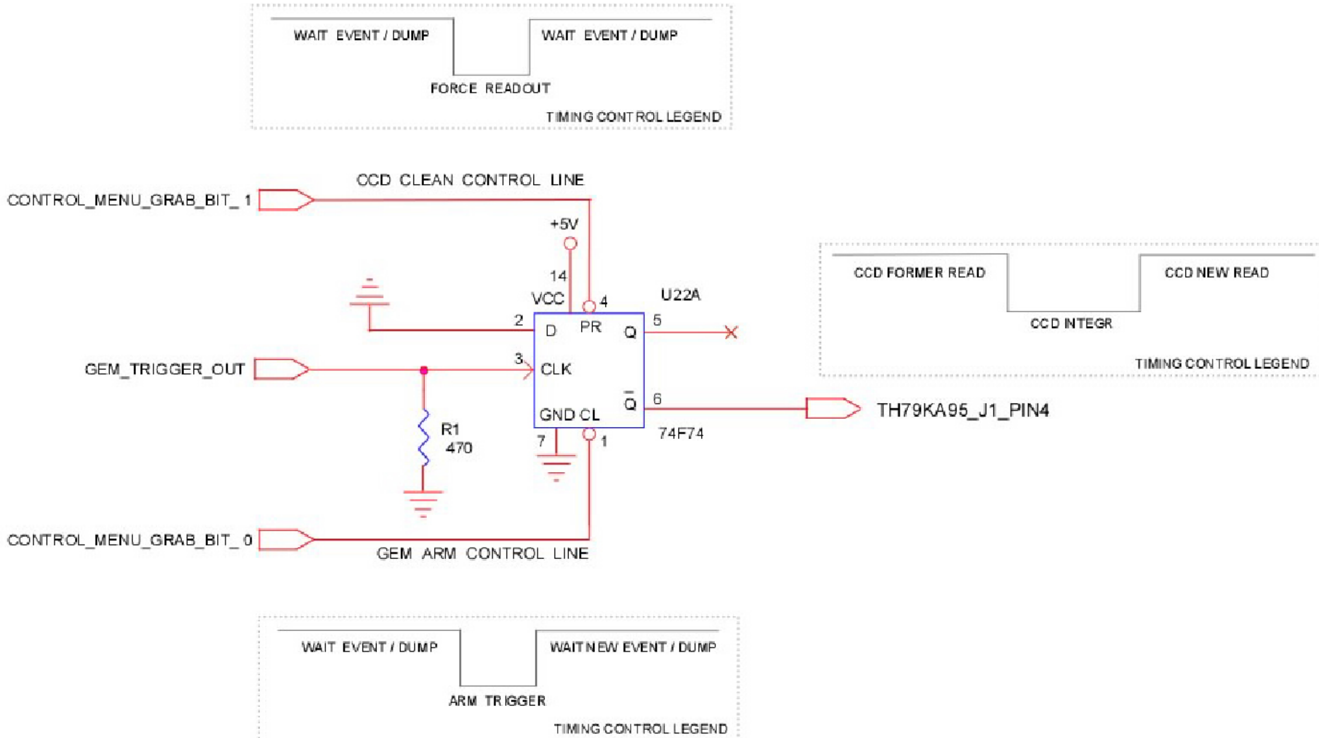

Figure 1: *Schematics of the new trigger concept.*

frame grabber hosted in the acquisition PC contains the optical footprint of the event recorded by the GEM. The footprint is not affected by a position displacement because it was collected while the CCD was in its ground state and thus the readout charge scrolling was not activated. Remote host resets and controls the front end flip-flop by the I/O lines shown in the annexed figure. This synchronization method, even if in principle correct, has been upgraded because, the TH79KA95 unit in which the CCD is hosted is operated around 18°C and the detector cannot be more significantly cooled down. Therefore the thermally generated leakage charges collected during the integration period were exceeding the signal event charges.

The second synchronization mode leaves the CCD continuously running alternating integration and readout cycles, therefore the thermally generated charges can be removed (see Fig.1). In order to avoid footprint displacement for the event occurring during the time in which the CCD is scrolling the charges, the trigger is inhibited during the readout cycles. Conversely the events are propagated to the frame grabber trigger while they are occurring during the integration cycle. In this way the acquisition mode is fully automated and it is arrested only after the read out of the image following an event occurring during the related integration time window. The operator can decide to save or discharge the frozen frame and resuming the automated acquisition process. In this mode, apart the operator evaluation time, the duty cycle is essentially given by the ratio of the integration time period, which can be adjusted by the user, and the integration period itself plus the read-out time, which is of the order of 40 ms. Therefore for long integration periods, but still compatible with the thermal environment, the duty cycle can approach the 100%.

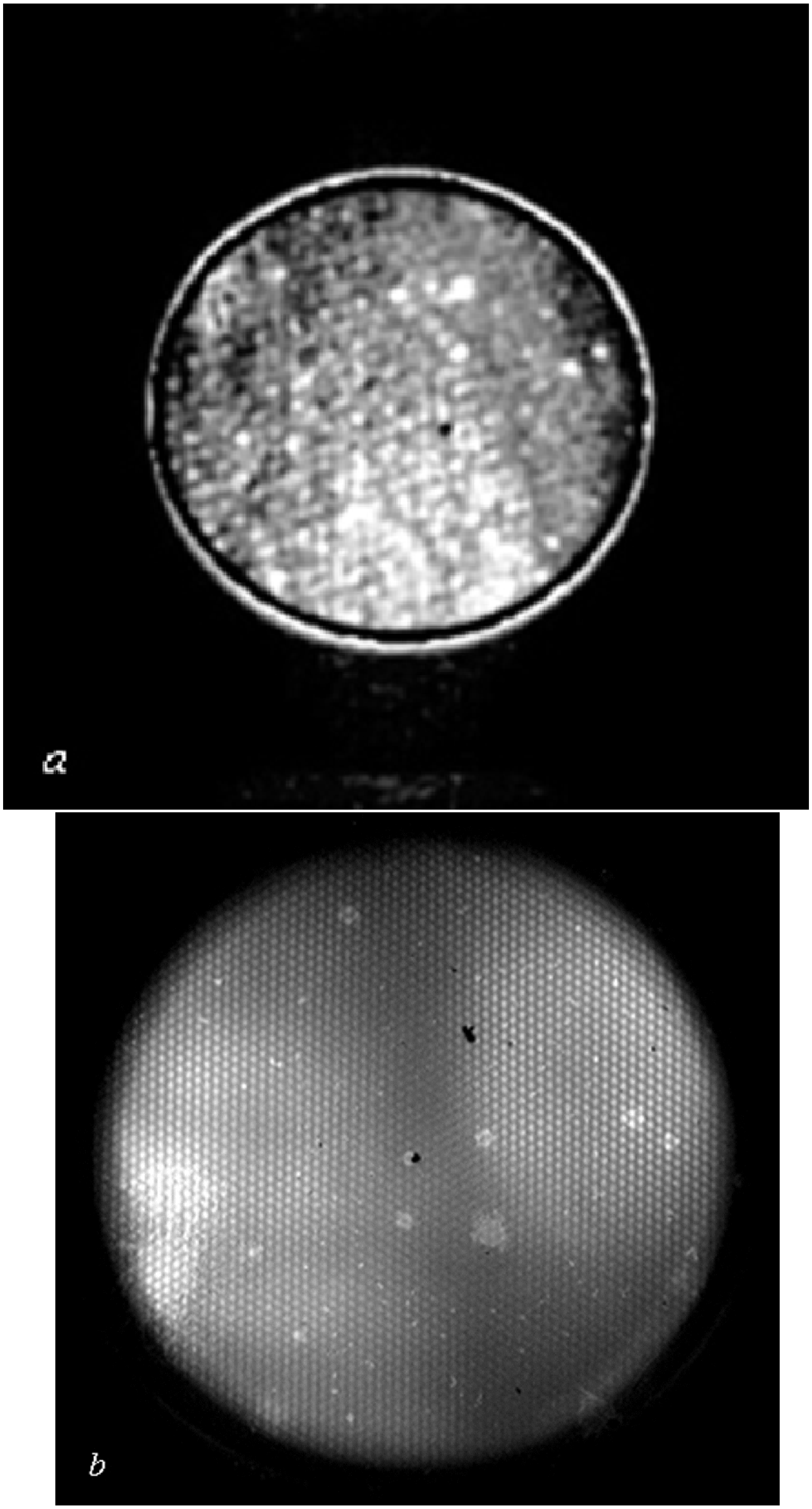

Figure 2: *Comparison between pictures of GEM structures with $\sim 50\mu m$ pinholes resolved by the CCD matrix, whose pixel structure is $\sim 20\mu m$ pixel size. (top is the old version, bottom is the new version). The improvement of polarimeter appear immediately comparing the GEM structures.*

ARCO

F. Tazzioli (Resp.), R. Sorchetti (Tecn.)

Participant Institutions: Università Roma2 and INFN, IPJ Swierk

1 Introduction

Implementation of superconducting RF cavities with thin Nb films on copper is a very interesting alternative to bulk Nb since copper is cheaper than Nb, has higher thermal conductivity and better mechanical stability. The vacuum arc coating method, as compared to the standard sputtering process, has several advantages, i.e. absence of gases to sustain the discharge, higher energy of the atoms reaching the substrate and higher deposition rates. Filtering of macroparticles is essential for avoiding surface roughness. Three different cathodic arc sources, planar, filtered and cylindrical, all working under UHV conditions, have been built and operated at Roma2 and INFN.The cylindrical geometry is the best suited for coating multicell structures.

2 Results

We have shown that high quality Nb films can be deposited. The measured RRR values reach as high as 80 for films deposited at 200 C.The critical temperature of film samples coated in plane geometry is very close to the bulk values and the narrow transition(about 0.01 K), together with X-ray diffraction patterns, indicate that the films are little stressed and very homogeneous. Filtering of the macroparticles in the planar arc proved to be very effective. To eliminate all possible sources of contaminants we have implemented an arc triggering system based on a Nd-Yag pulsed laser.

Detailed information can be found on the web site :
http://ares.roma2.infn.it/ARCO/arcoHome.html

References

1. A.Cianchi, L.Catani, R.Russo, S.Tazzari, F.Tazzioli, J.Langner, M.J. Sadowski, N.N. Koval, “UHV Arc Deposition for RF Superconducting Cavity: Samples Characterization”.

   Proc. International Symp. PLASMA-2003 on “Research and Application of Plasmas”, Warsaw (Poland) Sept. 2003.

2. R.Russo, L.Catani, A.Cianchi, S.Tazzari, R.Polini, F.Tazzioli, J.Langner, N.N. Koval, “UHV Arc For Superconducting Niobium Film Deposition”.

   Proc. XI Workshop on RF superconductivity, 8-12 Sept. 2003 Travemünde/Lübeck (Germany).

3. R.Russo, L.Catani, A.Cianchi, S.Tazzari, F.Tazzioli, J.Langner, “UHV Arc Deposition for RF Superconducting Cavities”.

   Proc. XI Workshop on RF superconductivity, 8-12 Sept. 2003 Travemünde/Lübeck (Germany).

CAERES

F.Tazzioli (Resp.), C.Vicario(Dott.)

Participant Institutions:
Univ. Roma1-Dip. Energetica and INFM; Univ. Roma2-Dip. Scienze e Tecnologie Chimiche; Univ. Milano-Dip. Fisica e INFN

1 Introduction

The CAERES experiment has the aim of studying robust photo-cathodes, both non-metallic and metallic, for applications in advanced particle accelerators. The diamond CVD films that are currently tested have given interesting results. Some films have shown a single-photon emission process at 266 nm laser wavelenghth excitation (4.7 eV) with relatively high quatum efficiency (Q.E.). A further stimulus to continue in the development of cathodes has been given by a possible application to the SPARC project of the LNF, which foresees the employment of "state of the art" bulk Cu and Mg cathodes. Our research activity has been extended to metal films, in particular Magnesium films. These films, deposited by laser ablation or sputtering, are expected to show a high quantum efficiency and more uniform emission than bulk material.

2 Activity

In 2003 we have improved the Q.E. of diamond films by varying the deposition parameters and by terminating the surface with Hydrogen. Emission efficiencies up to 10^{-5} at 266 nm laser wavelenth (4.7 eV photon energy) have been obtained. This efficiency is comparable with that of Copper , but diamond has the advantage of requiring much less severe vacuum conditions. A strategy to improve the efficiency has been devised. Some diamond film cathodes have been exposed to very high RF fields inside an RF Gun cavity at UCLA Los Angeles University (USA). A new collaboration with Lecce University has been established to develop metal film cathodes. As metals require a better vacuum, a new chamber for UHV tests has been designed and built.

3 References

References

1. S. Orlanducci et al, "Structural features of diamond layers photo-emitting at sub-band gap energies". Diamond and Rel. Mat. Vol. 12/12, 2186-2194 (2003).

2. I. Boscolo *et al*, "Photo-emission from diamond films illuminated by intense Nd:Yag laser harmonics". Applied Physics A, 77, 805-809 (2003).

CAPIRE

A. Calcaterra, L. Daniello (Tecn.), R. de Sangro, G. Mannocchi (Ass.)
P. Patteri, M.Piccolo (Resp.), L. Satta (Ass.)

1 Introduction

Among gas detectors, parallel plate counters are the ones that, in principle, should be the easiest to built and sturdiest to operate. Recent experience with large systems have not yielded the expected performances: a needed R& D program was started by the CAPIRE collaboration (LNF-Milan-Turin) to understand performances and limitations of these devices both with Bakelite and glass electrodes. The LNF BTF (Beam Test Facility) turns out to be a very appropriate test facility for these detectors: results from data collected at the linac beam show the great potential of this line of testing/development.

2 The experimental program

The development of parallel (resistive) plate counters plays an important role in many programs both for particle and astro-particle physics. General purpose detectors require large area inexpensive devices to be used in the hadronic calorimeter and/or muon identifier compartment. Lately the idea of digital calorimetry has been proposed [1]: such an application would call for a low cost large area device; RPCs would fit very well the specifications required.

Neutrino Physics, both accelerator and atmospheric could also benefit very much from an inexpensive easy to operate detector, such as a reliable RPC.

Two materials have been used up to now to build large area detectors, Bakelite and glass. While the Bakelite has the advantage of a relatively easy tuning of the resistivity, it requires a long and critical surface treatment with leen-seed oil. On the other hand, glass, that is not easily resistivity tunable, has good mechanical properties, does not require surface treatments and could benefit from silk printing technology, which, in turn, might cut substantially construction time and upgrade the overall reliability.

Within this framework, the CAPIRE collaboration has built and operated both Bakelite and glass RPCs based on the technique developed at General Tecnica, that is with the Bakelite/glass planes that act both as electrodes and gas containers; they are kept at the nominal distance (2 mm.) with Lex an spacers layed out on a square grid of 10 cm side. Tyical dimensions of glass RPC electrodes are 1.1 m^2.

The glass and/or Bakelite chambers have been tested at the BTF and in a cosmic test facility. During the latter phase a complete monitoring of the environmental conditions has been implemented so that detector behavior can be correlated with such variables as temperature, relative humidity etc.

The cosmic testing facility at LNF (a second one is active at University of Milan "Bicocca") includes triggering and tracking. Efficiency maps can be obtained with a spatial resolution of about 1 cm, so that few cm size trouble areas can be spotted.

The runs at the LNF-BTF are extremely useful in determining the time/space performances of the detectors. As a matter of fact the capability of the facility, to ship a tunable number of particles in a given RF bucket and in a given (tunable) spatial spot result in the possibility of performing a direct measurement of the recovery time and the local rate capability of the RPCs.

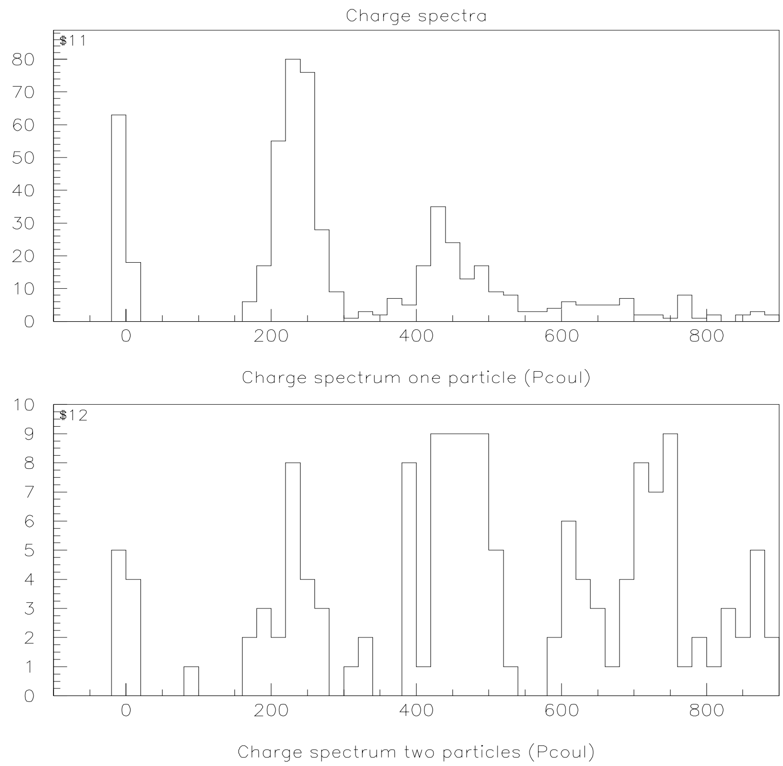

Figure 1: *Charge spectra from a glass silk-printed RPC: the upper plot is obtained requiring one and only one particle hitting the detector. The lower plot refers to events in which two particles hit the detector within the beam spot (2×2 mm^2)*

3 Preliminary results

The collaboration has collected data at the LNF-TBF in spring 2003: five different large area chambers have been exposed to the beams. The particular arrangement allowed a "no-bias" trigger arrangement based only on external detectors. Read out electronics included both digital and analog circuitry so that the performances of the RPCs could be understood in depth. Pulse height spectra from a glass, silk printed RPC can be seen in fig 1. The two spectra refers to one or two particles impinging on the detector. Double pulse probability as well as double particles efficiency can be obtained from these spectra. Changing the linac frequency one can directly measure the recovery time of the detectors: in fig. 2 the detector efficiency vs the linac frequency is depicted. Recovery time of this glass detector can be evaluated to be ≈ 2.5 sec.

Data have been collected in a variety of configurations both for what the beam condition were concerned and the detectors: different linac frequency, different beam dimensions, different particles density contents in the beam as well as different operating conditions (H.V. and gas mixes) for the detector. Data are being analyzed; results of preliminary analysis have been already presented [2)] and will be published shortly.

As mentioned before, long term tests for the detectors are carried out on cosmic ray test-benches both at LNF and in Milan. To have an idea of the diagnostic power of the setup in fig 3 where the bidimensional efficiency map for one of the old and slightly damaged BaBar Bakelite RPC is shown: few bad spots can be noticed.

Extensive monitoring is implemented on the LNF setup, like the time evolution of current and temperature over a period of few days for three of the detectors under long term test.

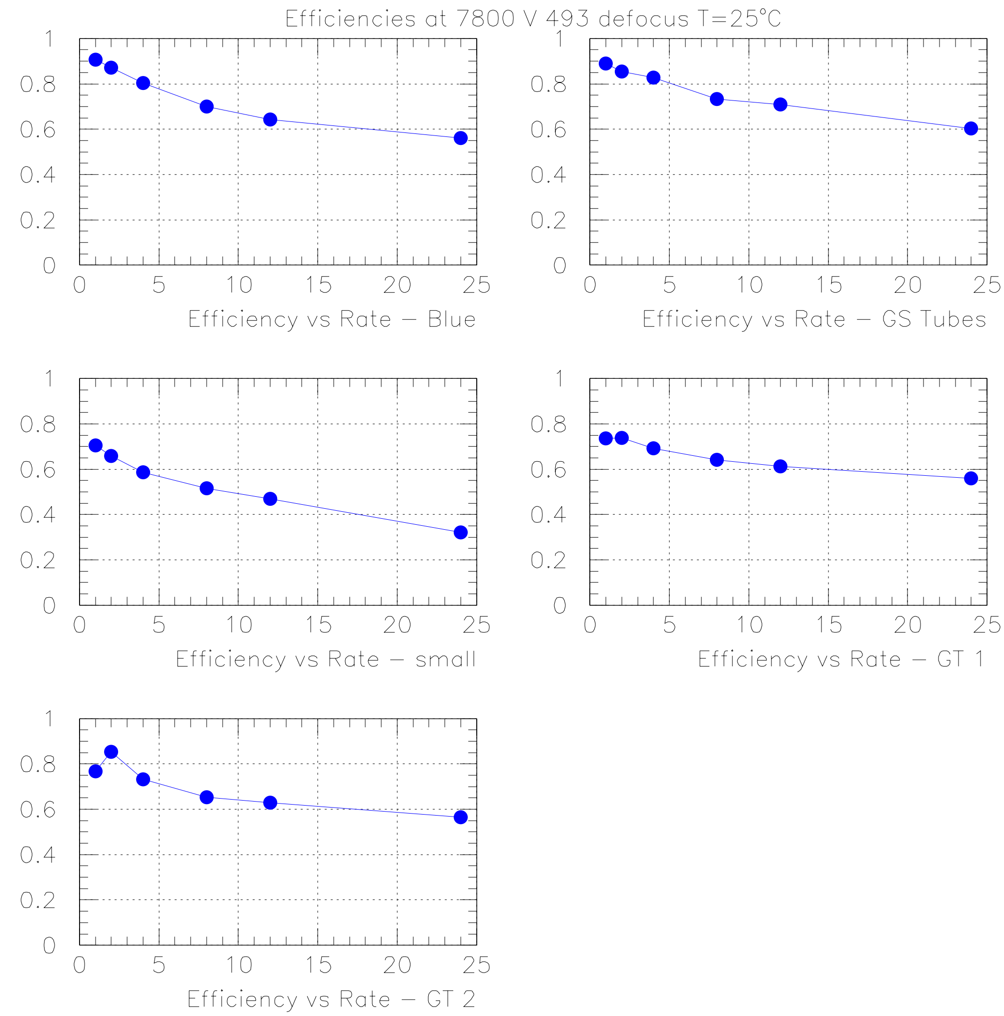

Figure 2: *Efficiency vs linac frequency for the different detectors at the BFT beams. The five plot refer respectively to (upper left) a silk printed RPC, (upper right) a LNGS "tube detector", a 0.5× 0.5 m^2 graphite coated chamber and (middle right and lower left) two standard General Tecnica 1.1 m^2 graphite coated chambers.*

References

1. Tesla technical design report Part IV 'A Detector for TESLA' R.D. Heuer, D. Miller, F. Richard, P. Zerwas editors.

2. A. Calcaterra et al. "Test of large area glass RPCs at the DAΦNE Beam Test Facility" Contribution to RPC2003, Montpellier, Oct 2003.

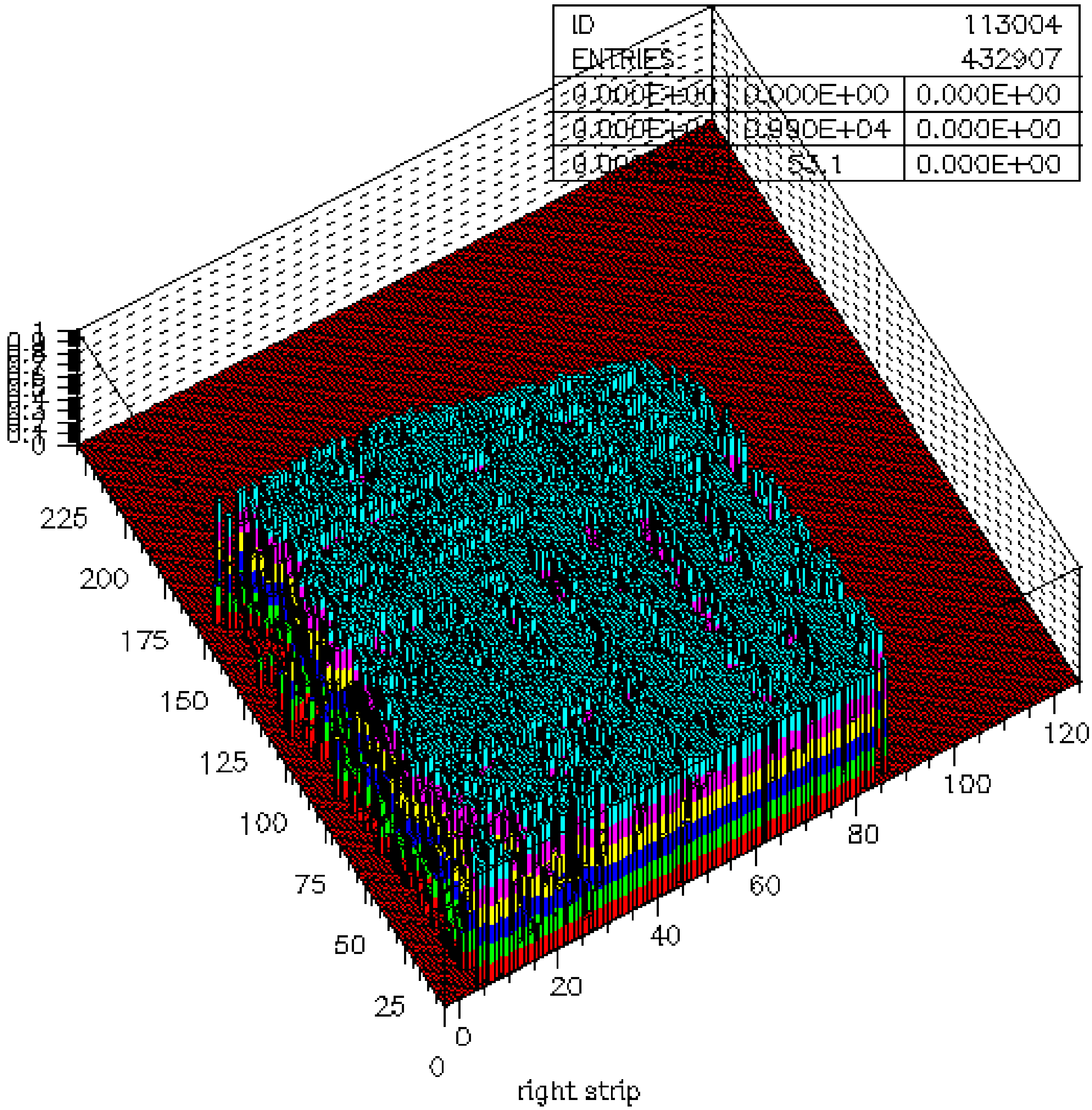

Figure 3: *Efficiency map for a 2 m^2 Bakelite chamber. Few low efficiency spots are evident.*

CORA

D. Alesini (Art. 23), R. Boni, M. Ferrario, A. Gallo (Resp.), F. Marcellini, M. Vescovi

1 Activity

The object of the CORA experiment is the study and fabrication of RF accelerating structure prototypes aimed to the particle bunch length reduction by means of the "RF compression" technique. In particular, the LNF group inside the CORA collaboration is studying the application of such a technique to the S-band electron Linac beams to be used for SASE-FEL radiation production.

The velocity buncher concept is based on the longitudinal focussing properties of the slow waves, and allows compressing the bunch length up to a factor 20. The obtainable rms longitudinal dimensions of the bunches are of the order of few 100^{th} μm with a controllable effect on the bunch emittance being the compression process completely integrated in emittance correction process which is accomplished in the first 150 MeV of acceleration. The velocity buncher is a modified accelerating structure to allow the inside propagation of a wave whose phase velocity v_{ph} is close to but slightly less than the light velocity c (slow wave, $v_{ph}/c = 0.999 \div 1$). The required gradients are similar to that of the standard S-band structures, that means about 20-25 MV/m.

During year 2003 the LNF group has proceeded in the work, in collaboration with the INFN Milan group, according to the guidelines defined in year 2002. An accelerating slow wave can be obtained by linearly scaling the dimensions of a standard, synchronous RF accelerating structure ($v_{ph} = c$). In this case the relative phase velocity variation is proportional to the scaling factor $\Delta f/f$ through a constant equal to the ratio between the phase and the group velocity of the structure:

$$\Delta\, v_{ph}/v_{ph}=\Delta f/f\,(1\text{-}v_{ph}/v_g) \approx -\, \Delta f/f \cdot v_{ph}/v_g \quad (1)$$

In a SLAC type section the value of the ratio is $v_{ph}/v_g \approx 100$, which means that deformations of the order of 10^{-5} are sufficient to produce phase velocity variation of the order of 10^{-3}. Since the Copper linear thermal expansion coefficient is $\approx$1.6 $10^{-5}/^o$C, a variation of 1^{o}C of the operating temperature of the structure produces a variation of the structure phase velocity larger than desired. This means that a special accelerating section equipped with a thermal regulation system capable to stabilize the section temperature at a small fraction of 1^{o}C can be used as a slow wave velocity buncher. The phase velocity in the buncher can be tuned by changing the temperature set point of the thermal regulation system, assuming that the real section temperature can be maintained equal to the set value within a very narrow range (of the order of 0.1^{o}C). Since the all cell dimensions change with temperature, the cell-to-cell phase advance in the buncher will not be in general equal to an integer fraction of 2π as in the standard case ($2\pi/3$ for a SLAC structure). But, being the structure of TW type, any cell-to-cell phase advance is allowed, and this does not affect the accelerating structure operation at all. The CORA experimental activity is mainly orientated to the demonstration of the feasibility and reliability of such a temperature regulation system to precisely control the phase velocity in the RF compressor.

The stability specifications of the temperature control system can be relaxed if the basic cell of the RF accelerating structure is re-designed to obtain a larger group velocity with respect to a SLAC structure. In this case the phase velocity variation associated to a given temperature fluctuation is smaller since the magnification factor v_{ph}/v_g of eq. 1 is reduced. The use of a standard SLAC accelerating sections as velocity buncher has another potential drawback since this structure is of "constant gradient" type. This means that the iris diameter decreases along

Table 1: *Characteristics of different cell design.*

	Mark IV (SLAC)	Alma2	Alma3	Alma4
Cavity radius [cm]	4.124	4.21	4.26	4.27
Iris radius [cm]	1.130	1.38	1.54	1.59
Septum thickness [cm]	0.584	0.59	0.59	0.45
Cell length [cm]	3.5	3.5	3.5	3.5
Mode	$2\pi/3$	$2\pi/3$	$2\pi/3$	$2\pi/3$
Frequency [MHz]	2856	2856	2856	2856
Q	13200	12936	13084	13205
Shunt imp. [MΩ/m]	53	45	41	41
Vg/c	0.012	0.023	0.034	0.043
ΔT[^{o}C]	0.6	1.3	1.9	2.5

the section to compensate the wave attenuation keeping the accelerating E-field constant. As a consequence, the group velocity has a significant variation along the structure and, in the thermal deformation regime, the phase velocity will not be perfectly uniform. The impact of such effect on the longitudinal dynamics and on the compression process has not been evaluated by means of numerical simulations so far. On the contrary the structures of "constant impedance" type, with constant iris diameter along the structure and no modulation of the group velocity, will still show a uniform phase velocity even in presence of thermal deformation. In order to relax the temperature stability specifications of the regulation system and to maintain the uniformity of the phase velocity along the structure, special high group velocity, constant impedance accelerating sections have been designed. The various designs are compared in Table I.

The so called "Alma" cells have a larger iris with respect to a typical SLAC cell (the one named "Mark IV"). The resulting shunt impedance is marginally lower (about 20% in the worst case) but the group velocity is about 3.5 times larger. The reduced shunt impedance is not an issue since the maximum required gradient of 20 MV/m is achievable with a reasonable RF power dissipation. On the other hand, the larger group velocity reduces the criticality of the phase velocity control. In fact, the temperature interval corresponding to a v_{ph}/c value in the $0.999 \div 1$ range is only 0.6 ^{o}C wide for a MarkIV structure, while it is 2.5 ^{o}C wide for an Alma4 structure.

The sensitivity of phase velocity on the temperature fluctuations is proportionally decreased. A 3-cells Aluminium prototype of the Alma3 structure has been manufactured and tested. The dispersion curve as sampled by the resonant coupled modes of the 3-cells is in a good agreement with the expectations.

A complete mechanical design of a 9-cells copper prototype of the Alma3 structure has been produced, including the cooling channels and the cell tuning tools. This prototype is in fabrication and will be brazed at CERN and tested in Milan by the end of March 2004.

The mechanical design of an Alma4 structure is in progress. The design of the RF input/output couplers is also in progress. Tests on the control of the temperature stability of a full scale SLAC structure using a sophisticated temperature control system (0.1 ^{o}C stability) will be also performed starting in April 2004.

The phase velocity tuning has to be accomplished by changing the structure temperature if operating the RF compressor at constant frequency is mandatory. If this constraint could be removed, the phase velocity could be controlled by simply changing the RF driving frequency. In this case eq. 1 still holds, with Δf referring to the variation of the driving frequency instead of the variation of the resonant frequency of the structure itself. Since variations of the phase velocity can be easily and efficiently detected by monitoring the whole in-out phase delay of the structure, the phase velocity can be controlled by a "phase locked loop" looking at the phase insertion of the structure and acting on a VCO (voltage controlled oscillator) generating the RF driving tone. This method will guarantee a much better stability of the phase velocity, because a pure electronic control loop is certainly more precise and effective than a thermal stabilization system. Unfortunately, being a part of a LINAC, the RF compressor can be hardly operated at a variable frequency, unless all the LINAC RF is operated with the same variable frequency, that would affect all the timing and synchronization systems. Nevertheless, the variable frequency option is of general interest, and will be experimentally tested during year 2004 on the SLAC-type structure available at the Milano INFN Labs. Part of the devices and instrumentation needed for this test is already available in the LNF as Laboratory equipment. The remaining part (in particular the VCOs) has been ordered by the LNF group during year 2003 and will be delivered about February 2004.

2 Publications

D. Alesini et al., "Study and Design of Room Temperature Cavities for an RF Compressor Prototype", Proc. of the 2003 Particle Accelerator Conference, Portland (Oregon), May 12-16, p. 2080.

E-cloud

R. Cimino (Resp.), A. Clozza, C. Vaccarezza

In the vacuum science community, it is now commonly accepted that, for the present and next generation accelerators, the surface electronic properties of the vacuum chamber material have to be studied in detail. Moreover, such studies are of valuable help to define the cleaning procedures of the chosen materials and to identify the most efficient vacuum commissioning. Most of the studies done in this project are oriented to study the Large Hadron Collider (LHC) to be built at CERN (Geneve), but are applicable and of importance to other accelerators machines like GSI, NLS and Tesla Damping Rings, DAΦNE etc. For such machines the beam stability, in the presence of an electron cloud, is analysed using Beam Induced Electron Multipacting (BIEM) simulations requiring a number of surface related properties, such as photon reflectivity, electron and photon induced electron emission, heat load, etc. and their modification during machine commissioning and operation. Such simulation codes base their validity on the completeness and reliability of the aforementioned input data. In 2003, we mainly addressed two separate items: i) how synchrotron radiation (SR) can been used to measure the reflectivities (forward, backscattered and diffuse), using white light SR similar to the one emitted by LHC; ii) how a Surface Science approach can be applied to measure, total electron yield (SEY) as well as energy distribution curves excited by a very low energy electron beam (0-320 eV), from the industrially prepared Cu co-laminated material, the adopted LHC beam screen material, held at cryogenic temperatures (about 10K).

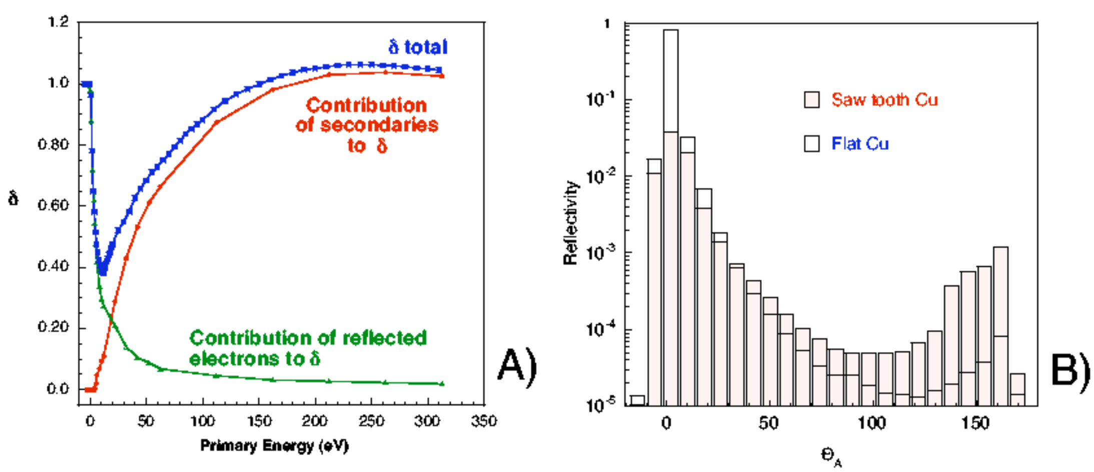

Figure 1: *A) Total SEY(δ) and contribution to it of secondaries and reflected electrons from a Cu surface at $\sim 10K$ as a function of primary electron energy. B) Measured reflectivity, on the scattering plane, from a flat Cu sample (blue empty bars) and from the saw-tooth sample (red bars).*

When present, synchrotron radiation (SR) may generate a significant number of photoelectrons, that may play a role in determining the onset and the detailed properties of the electron-cloud related instability. Since electrons are constrained to move along field lines, those created on the accelerator equator in a strong vertical (dipole) field cannot participate in the e-cloud build-up. Therefore, for the LHC there has been a continuous effort to find solutions to absorb the photons on the equator. The solution adopted for the LHC dipole beam screens is a saw-tooth structure on the illuminated equator. SR from a bending magnet beamline has been used to measure the reflectivities (forward, backscattered and diffuse), for a flat and a saw-tooth structured Cu co-laminated surface using both white light SR (as shown in fig. 1 B)), similar to the one emitted by LHC, and monochromatic light [2].

Than, we studied electron induced electron Energy Distribution Curves (EDC) from low temperature surfaces ($\sim 10K$) to try to disentangle in those EDC the percentage of reflected electrons contributing to the total SEY [1]. We show in fig. 1 A) SEY measurements on the LHC type beam-screen Cu surface. Such SEY data and the EDC analysis, here not shown, make possible to conclude that, at low energy most of the impinging electrons are reflected by the Cu surface, giving a SEY close to unity approaching primary electron beam zero energy. Our data shows, for the first time in this context, that very low electrons may have long survival time inside the accelerator vacuum chamber due to their high reflectivity. This notion may well explain why in the KEK B factory and SPS a memory effect has been observed. Preliminary results obtained by implementing these experimental data into BIEM simulations indicate an increased heat load for the LHC and significant variation in the e-cloud build-up predictions for different accelerators suggesting that the high electron reflectivity at low energy presented here could also be of relevance to electron cloud effects on damping rings and more in general on future accelerators.

In conclusion our reflectivity study show that the saw-tooth structure adopted for LHC does reduce, but not to zero, the total reflectivity and modifies the photon energy distribution of the reflected photons. The implications of these results on the LHC arc vacuum system need to be analyzed in more details with the aid of computer codes. The study of electron induced electron emission shows that the SEY converges to unity at zero primary electron energy and that the ratio of reflected to secondary electrons increases for decreasing energy below about 70 eV, and becomes dominant below electron energies of about 20 eV. These observations lead to the notion of longlived low-energy electrons in the accelerator vacuum chamber, which could be an issue for the LHC, damping rings and future accelerators.

1 List of Conference Talks by LNF Authors in Year 2003

1. R. Cimino (Invited) : Workshop on "Damping Rings and Associated Physics" January 27-29, 2003 at Daresbury LaboratoryUK.
2. R Cimino: Workshop on "Fisica e tecnologia degli acceleratori e tecniche correlate", 2-4 Giugno 2003, Villa Orlandi, Capri
3. R. Cimino: Workshop on "e^+ e^- in the 1-2 GeV range: Physics and accelerator prospects", 10-13 September 2003 Alghero (SS), Italy.
4. R. Cimino: European Vacuum Conference 8, 23-26 June 2003, Berlin Germany.

2 Publications

References

1. R. Cimino and I. R. Collins, Applied Surface Science, to be published (2004) and CERN-LHC-Project-Report-669; (2003).
2. R. Cimino, V. Baglin, I. R. Collins, N.Mahne, A.Giglia, L.Pasquali, M.Pedio ed S.Nannarone; Applied Surface Science, to be published (2004) and LHC-Project-Report-668; (2003).
3. Arduini *et al*, CERN-LHC-Project-Report-645 (2003).

FLUKA

M. Carboni, M. Pelliccioni (Resp.), S. Villari (Perfez.)

1 Report year 2003

In order to investigate the influence of the aircraft shielding on the galactic component of cosmic rays, an aircraft mathematical model has been developed by the combinatorial geometry package of the Monte Carlo transport code FLUKA. The model is constituted by 162 regions and includes 17 different materials. The isotropic irradiation of the aircraft in the cosmic ray environment has been simulated. Effective dose and ambient dose equivalent rates have been determined inside the aircraft at several locations along the fuselage for typical civil aviation altitudes.

Assistance has been ensured to Milano group for the FLUKA web server and to study the thecnical aspects of a possible CVS distribution.

2 Program for 2004

The penetration of cosmic rays in atmosphere will be simulated by the FLUKA code in order to study the angular distribution of the particles at various altitudes and geographical positions.

Further calculations on aircraft shielding effect are in program with the aim to investigate the dependence of the doses on the various parameters of interest (type of aircraft, internal configuration, route, etc.). A more realistic angular distribution of the incident cosmic ray will be considered.

Like in 2003, assistance will be still ensured to Milano group for the web server and for the preparation of the full FLUKA release through CVS.

3 Conference Talks in 2003

1. M. Pelliccioni, Simulation: Presentations and Discussion, TEPC Workshop, Vienna 10-13/03/03.
2. M. Pelliccioni, FLUKA Simulations, 1st ATPROMO, Roma-Tor Vergata 7-8/05/03.
3. M. Pelliccioni, Dosimetria dei raggi cosmici, Seminario, CCR Ispra, 19/11/03.
4. M. Pelliccioni, Il problema del personale navigante ad alta quota, Scuola Superiore di Fisica Sanitaria, Villa Olmo (Como), 20/11/03.
5. M. Pelliccioni, Criteri di valutazione della dose nell'esposizione ai raggi cosmici, Scuola Superiore di Fisica Sanitaria, Villa Olmo (Como), 20/11/03.

4 List of Publications 2003

1. A. Fasso' et al, "The FLUKA Code", paper presented at the CHEP03, March 24-28, 2003, La Jolla, California (USA).
2. A. Ferrari and M. Pelliccioni, "On the Conversion Coefficients for Cosmic Ray Dosimetry", Rad. Prot. Dosim. 104, 211-220, 2003.
3. A. Ferrari, M. Pelliccioni and R. Villari, "Evaluation of the Influence of Aircraft Shielding on the Aircrew Exposure through an Aircraft Mathematical Model", accepted for publication on Rad. Prot. Dosim.

FREETHAI

F. Celani (Resp.), A. Spallone (Ass. Res.), E. Righi (Ass. Res.), G. Trenta (Ass. Res.), C. Catena (Ass. Res.), P. Quercia (Guest Res.), V. Andreassi

Collaboration with Companies:
EURESYS (Rome), Pirelli Labs (Milan), Centro Sviluppo Materiali (Castel Romano), CESI (Milan), ORIM (Macerata), STMicroelectronics (Cornaredo, Milan), Mitsubishi Heavy Industries (Yokohama-Japan)

1 Introduction

The experimental task of FREETHAI (Fusion Research by Electrolytic Experiments: Tritium and Heat Anomalous Increase) is to develop innovative and reproducible techniques to maximise the values of Hydrogen (H) and Deuterium (D) concentrations in Palladium (Pd), i.e. the so-called "overloading", ($H,D/Pd \gg 0.95$) through light (H) or heavy (D) electrolytic solutions (water and/or hydro-alcoholic) through electrolysis with short waiting times for the overloading ($\ll$50 hours) and long time stability (> 4 hours). It is a "further developing" of the **FREEDOM** experiment ended in December 2002; (see the Activity Report-A.R.- of such experiment for further details).
* Our experimental pathway consists in the development of very innovative methods of overloading of Pd (surface and/or bulk) using light H and, later on, in the transfer and adaptation of the successful methods to the use of heavy (water, alcohol) solutions. Such two steps procedure was demonstrated to be overall quite efficient because the experiments using light H didn't need particularly sophisticated cares (for example the solutions are insensible to ambient humidity). The employment of heavy H solutions is, on the contrary, very time consuming and experimentally complex because all the deuterated compounds are strongly igroscopic: the H contamination of D solutions (with H arising from ambient humidity), was an uncontrollable parameter in our D-based experiments and it could work as a "poison" with respect to the heavy H electrolyte. The resulting main drawback of such a procedure is that it is necessary to build at least a twin experimental set-up, electronic data acquisition system together with full-time dedicated people.
* In the case of the D based experiments, we were looking for "the anomalous production" of excess heat, tritium and "transmutations" also, i.e. the quite "strange" and unusual thermal and/or nuclear ashes related to the so-called, and still now very controversial, "Cold Fusion" (CF) phenomenology.

During the overloading experiments we changed from water based electrolyte to hydro-alcoholic solution. The scientific explanations for the use of such an unconventional electrolyte are stated in detail in our previous A.R. In short, we used a main solution made of heavy ethyl alcohol (C_2H_5OD) and heavy water (D_2O) with a ratio 90-95% to 10-5%. The main dissolved cations were Strontium (as $SrCl_2$) and Mercury (as $HgCl_2$) ions, at a typical concentration as low as 10 micromolar and 1 micromolar respectively. The pH, "mild", was kept at about 4 (acidic). For the sake of comparison, most of the electrolytic "Cold Fusion" experiments (several thousands) performed in the world use pure D_2O and LiOD at a concentration of $0.1 \div 1$ molar, i.e. giving strongly basic solutions ($pH \simeq 13 \div 14$). Solutions of the latter type follow the "teachings" of M. Fleischmann and S. Pons (Utah University-USA) who in 1989 first showed the possible "nuclear" origin of some anomalous heat in their electrolytic cell.

We stress that, thank to the mild pH (4), it is possible to reduce etching of the components of electrolytic cell typical of "conventional" electrolytic experiments: it is possible to make elemental composition analysis of cell residual poweders (by Inductively Coupled Plasma-Mass Spectroscopy ICP-MS) remained, after electrolysis, in a quite reliable way.

We use as cathode Pd electrodes consisting of wires 50 to 100cm long with diameter as thin as 50 microns instead of the most diffused rods (according to Fleischmann and Pons) or plates (according to Akito Takahashi, Osaka University-Japan, 1992). We experienced that some suggestions from Giuliano Preparata and Emilio Del Giudice (University and INFN Milan, 1994) about the peculiarity of long-thin wires are substantially effective.

* As referred in detail in the papers quoted in our A.R., we performed a series of experiments with hydro-alcoholic solutions containing small amounts of Sr salts and Hg ions during which we found excess heat (see ref. 22 in Pub.1) and tritium (see ref. 24 in Pub.1) well above background. We found that in the hydro-alcoholic environment, during the anodic phases (that is for some hours every 1-3 days) of our loading cycles, the Pd electrode is eroded. Significant amounts of very fine Pd particles are found at the bottom of the cell at the end of the experiments. ICP-MS analysis after electrolysis showed the presence of Pd in this black powder (see ref. 26 in Pub. 1). Moreover, after several electrolytic loading-deloading cycles, the Pd wire eroded surface could absorb the D dissolved in the solution (whose maximum overpressure is only 50mbar in our experimental apparatus), quickly and without applied electrolysis current so as to yield a mean D/Pd ratio up to 0.75. Such a behavior could result from an increase of the catalytic activity of the Pd surface. We would like to point out that Yoshiaki Arata (University of Osaka- Japan) has stressed the importance of nano-structures in order to get loading of D in Pd (even over 1/1). Accordingly, very large amounts of anomalous excess heat and ^{4}He (see ref. 27 in Pub. 1) were observed in some of his experiments when a proper "trigger" was applied. It is reasonable to suggest that the increased activity exhibited by our Pd wires is caused by the formation of nano-structures on its surface, similar to those obtained by Y. Arata in a more elaborated way.

* Y. Iwamura, at Mitsubishi Heavy Industries (Yokohama-Japan); (see ref. 25 in Pub. 1) first showed that Sr is apparently transmuted into Molybdenum (Mo), or Cesium (Cs) into the rare heart Praseodymium (Pr) when a proper multilayer of Pd/Pd-CaO/Sr or Pr is forced to be flown at high rate ($>$2 SCCM), by D gas for enough long time (several hundred of hours). We tried to check whether such a "transmutation" could occur also after the repeated D-Pd loading/deloading/loading cycles in our experimental set-up. In July 2002 we were ready to perform an independent variant of the Iwamura experiment.

Before starting, we analysed by ICP-MS, all the components present in the cell (C_2H_5OD, D_2O, $SrCl_2$, DCl, $HgCl_2$, Pd), and pieces of 2 Pt wires (anode and reference electrodes). At the end of the repeated D-Pd loading/deloading experiment, the electrolytic solution was vacuum dried, the residue was collected and again analysed by ICP-MS together with the Pd cathode (all dissolved in hot-concentrate daqua regia). Mo was found in excess of any conceivable contamination, its isotopic composition of the Mo was different from the natural one (see ref. 26 in Pub.1).

It appears that the phenomenon first discovered by Y. Iwamura in a flowing deuterium gas system also occurs in our electrolytic cell when it is operated according to our loading-deloading-loading procedure for a time length of the order of 500-1000 hours.

2 Experimental activity: Thorium salts as electrolyte

In January 2003 we substituted Th salts for the Sr salts used previously.

The reason for such kind of experiments were mainly two, as following:

a) based on some results (published also from our group) on 1997-1998, indicating possible Th "transmutations" during high-electric power (and high-temperature, high-pressure) AC (50Hz) electrolysis with massive zirconium electrodes (both anode and cathode, see ref. 28 in

Pub.1), we decided to test whether something similar could happen in our new experimental apparatus based on thin Pd wires and a very strict control of impurities;

b) like Sr, Th ions can form an inorganic precipitate on the cathode surface as $Th(OH)_4$ (solubility product Ks = 10^{-50}), by action of the current density. Another similarity to Sr^{+2} is that Th^{+4} ions are difficult to be galvanically deposited because of the high negative value of their standard potential (E_0 = -1.899V). Even if Th is co-deposited on Pd surface through some unknown process, it can form a stable hydride-deuteride compound with no incompatibility with the aim of our specific experiment. According to such chemical-physical characteristics, it is possible to deposit the proper $Th(OD)_4$ and/or ThD_x layer(s) on the Pd cathode surface at a value of the current density lower than that required for Sr salts: the input power to the cell is reduced and anomalous excess heat, if any, can be more easily detected

Accordingly, with the present work we intended to essay the following:

c) The occurrence of anomalous excess heat.

d) The presence, if any, of foreign elements in both the cathode and the cell after electrolytic loading.

The operations were performed with electrolytes containing small amounts of Th and Hg salts.

* *Experimental set- up: electrolytic cell and flow calorimeter*

The cell configuration is shown in Fig. 1 of Pub. 1. The sample holder, a PTFE tube, is placed in a 1000ml borosilikat glass (type 3.3) cylinder (diameter 67mm, height 460mm). The cathode and anode are both "U" shaped and are located on the opposite walls of the holder, facing each other. The cathode is a thin (diameter 0.050mm) long (60cm) Pd wire (total surface about 1cm^2). In the lower part of the "U", at its center, a small weight (6g PTFE cylinder) keeps the wire tense during the Pd loading so as to compensate its 4-6% elongation. The anode is a Pt wire (diameter 0.250mm, length 60 cm, purity 99.99%). A third Pt wire (diameter 0.250mm, length 30cm) is put exactly in the middle of the "U" shaped cathode for reference purposes.

To measure the cathode resistance, an AC current (16mA, 10KHz, square wave: equivalent to a current density along the wire as high as 800A/cm^2) is superimposed to the (low intensity) electrolysis DC current (2-20mA): the AC resistance value is continuously measured.

A high quality LM135H thermometer (sensitivity 0.05°C), inserted in a PTFE tube, is placed in the middle of the cell, perpendicular to the cathode and anode. A Joule heater (max. 20W) is used to calibrate the calorimeter and is located between the electrodes in a peripheral position. It is inserted in a PTFE tube, (diameter 8mm, length 30cm). The cell is pressurized (50mbar) and thermally insulated. The electrolysis gases and vapors are allowed to flow through both twin cold-traps and silicon oil bubblier before reaching the atmosphere. Corrections for these losses of energy are not yet applied, consequently all the data about excess heat are under-estimated.

The heat exchanger within the cell consists of a 500cm long PTFE pipe, outer/inner diameter 4/2mm, wound around the PTFE holder through which water flows. Temperature of the distilled water flowing in the pipe is continuously measured at the inlet and outlet of the heat exchanger with two LM135H thermometers. A computerized peristaltic pump (Masterflex 7550-62) provides a constant flow of distilled water (0.200ml/sec, with day-to-day stability of ± 1%, routinely measured every 12 hours). Water is picked up by the pump from a 2-liter reservoir to which it returns from the cell. The cell, water reservoir, and pump are placed in a container held constant at 24°C: we continue (since 1992) to use the, very reliable, flow calorimetric measurement method.

Composition of the electrolyte, cleaning procedure

A typical 93 to 7 % by volume mixture of heavy ethyl alcohol (C_2H_5OD) and water (D_2O) respectively was used as the electrolyte, having a total volume of 750 ml.

* The ethyl alcohol was previously vacuum distilled at 35°C (by a vacuum distillation system Buchi 134) in order to eliminate mainly sodium and iron and ultra-filtered on-line using a 100nm, MILLIPORE PTFE filter: all distillation system deeply modified in our Frascati Laboratory. The density was routinely measured (Mettler Toledo DA-110M) before and after distillation, to confirm that no significant H_2O contamination occurred during the operations.
* The heavy water, 99.97% isotopic purity (reactor grade from Ontario-Hydro, Canada), was distilled at 45°C under vacuum and ultra-filtered before use, similarly to alcohol. Density was measured before and after distillation.
* $Th(NO_3)_4$, (5÷15mg) was added to the electrolyte and the pH of the resulting hydro-alcoholic solution was adjusted to a value of about 3 by adding few drops of concentrated HNO_3, in order to avoid uncontrolled precipitation of $Th(OD)_4$.
* The cell was cleaned after each experiment using repeated cycles of water / organic solvents / water / nitric acid / water in an ultrasonic warm bath. After Experiment ♯2 (Feb. 14, 2003; see Table 1 in Pub. 4), we increased the duration of the immersion in concentrated (65%) warm (60°C) HNO_3, from 2 minutes to 14 hours because we suspected that a residual amount of Cs might be hidden somewhere in the cell. As a consequence, the final washing cycles with distilled water were increased from 4 to over 10 because we experienced that warm, long time lasting, HNO_3 is absorbed by the non-glass parts of the cell.

3 Experimental results

In short, we got both excess heat (best result was an energy gain of about 10 for several days) and several strong indications of the "production" of new elements, some of these with an isotopic composition different from the natural one.
* About the new elements "produced", some (Cu, Zn) are the same as those obtained by using Sr as the main electrolyte, others are peculiar respectively of Strontium (i.e. Mo) or of the Thorium addition (i.e. Pb). Further details can be found in the papers published (Pub.1, 4).
* Surprisingly, we found that the electrolyte consumption was much larger than could be expected according to the Faraday's law. We suspect that this loss is caused by the heat being generated in a few hot spots at wire surface, where the temperature might raise to rather high values. This local over-heating could evaporate the solution so that gaseous D_2O and C_2H_5OD are lost in addition to D_2 and O_2. We plan to build a new cell made out of PTFE, quartz, HDPE, and use an IR thermo-camera in order to detect the IR radiation that might issue from the deuterated Pd wire surface.

3.1 ICP-MS Measurements

Because the ICP-MS measurements are both unusual in our Institute and the results obtained are crucial for our experiments, we will spend few words in order to explain the adopted procedure. Anyway, we suggest, strongly, to read the paper at Pub. 1 for key details.

ICP-MS measurements were performed in a chemistry laboratory operating under the ISO 9001 quality control protocol. The laboratory is located in the Interdisciplinary Research Area of Castel Romano (Rome), in the "Centro Sviluppo Materiali" building. The ICP-MS used is from HP & YOKOGAWA Analytical Systems, model 4500. It has been in operation since 1996. Calibrations with Atomic Absorption Standards are made every day before starting analysis. Sensitivity is about 6E10 Atoms/count. Typical background is 10 - 80 counts, depending both on the mass analyzed and the "overall condition" of the instrument (mainly HV setting and the Ar carrier gas flow intensity).

3.2 Comments on ICP-MS experimental result

The ICP-MS results are shown in Tab.1 and Tab 2 of Pub. 4. In short, we studied 3 main reactions: Sr→ Mo, Cs→ Pr, Th→ Pb (+other).

$$Sr \rightarrow Mo$$

Results using Sr within the electrolyte were reported in Ref.26 of Pub.1. We observed that some of the Sr was transmuted to elements with mass 94 and 96, qualitatively in agreement with the Y. Iwamura results. Moreover, the total amount of Mo atoms we found (1-2E15), normalized to Pd electrode surface (about 1cm^2), is very similar to the Iwamura gas experiments.

$$Cs \rightarrow Pr$$

Transmutation of Cs to Pr (according to Y. Iwamura) was not observed in our experiments when we used concentrated Cs solutions, because in the ensuing conditions we were not able to achieve a sufficiently high deuterium concentrations within the cathode. Much to our surprise, results were better when a Th salt, at very low concentration, was used with a "proper mixture" of Ca and Sr salts. Using these mixtures, we apparently transmuted Cs and Pr, although in smaller amounts in respect to Iwamura procedure. We noticed that the thorium salt did not contain measurable impurities of Cs or Pr, according to both the assay from the chemical company (Aldrich) and our routine analysis by ICP-MS. In the best experiment in which apparent transmutations have been detected, the signal is nine times the background.

Later (in experiments ♯5 and ♯6) we used only Th and Hg salts to increase the deuterium concentration in Pd. Surprisingly in experiment ♯6 we observed for Pr a signal to background ratio as large as 21. Experiment ♯4 did not achieve the necessary deuterium concentration, making it a very useful blank for ICP-MS analysis. In other words, apparent transmutations of Th to Cs (like "fission") and later Cs to Pr (like "fusion" of Cs+2^{4}He) occurred in an electrochemical environment, similar to those reported by Y. Iwamura in a gaseous environment (see ref. 25 and 29 in Pub.1) and recently confirmed by A. Takahashi et. al. (see ref. 30 in Pub.1). Such kind of, very surprising, 2-steps reactions needed more experiments and cross-check by other kind of analysis.

$$Th \rightarrow Pb\,(+other)$$

We performed a total of 4 experiments with Th salts, in amounts ranging from 8x10^{-6} to 6.5x10^{-5} moles in the total volume of electrolyte. The pH for the Th solution was $\simeq$3 compared to $\simeq$4 for the Sr containing solution.

3.2.1 Details on ICP-MS results

In Table 1 and 2 of Pub. 4 are reported a list of the masses which are relatively easy to interpret and for which reproducible results were obtained. We observed several other anomalies that are not yet fully understood. We anticipate that most of such anomalies are in the range of masses 46 - 60, 107 - 116, along with some isotopic anomaly for Pd.

4 Conclusions

After a large number of experiments performed during 14 years of research work aimed at finding anomalous effects in systems forced to a high concentration of deuterium, we are confident that most of the observed effects occur at the interface between the solution and the Pd bulk. A properly thin formed layer of a third element is necessary. Non-equilibrium situations are also necessary to trigger the effects. Recently, we found that deuterated hydro-alcoholic, slightly acidic solutions, works very well at producing the so called "anomalous effects". Additions of Th and Hg salts within the micromolar concentration range improves the effects even at very low electrolytic current density ($<10mA/cm^2$). We think that the model developed by Akito Takahashi about multi-body resonance fusion of deuterons (see ref. 31 in Pub.1) can explain most of the thermal and isotopic anomalies, including foreign elements that we too have recently observed. Further work is necessary to fully characterise the system and increase the magnitude of the effects.

About the Publications, we would like to inform that our paper, Pub. 3, presented at LXXXIX Congress of Italian Physical Society, held in Parma on September 2003, get the 1st Price in the Section of "General Physics, Teaching and History of Physics".

5 Publications

1. Thermal and Isotopic Anomalies when Pd Cathodes are Electrolysed in Elecrolytes Containing Th-Hg Salts Dissolved at Micromolar Concentration in C_2H_5OD/D_2O Mixtures.

   F. Celani, A. Spallone, E. Righi, G. Trenta, C. Catena, G.D'Agostaro, P. Quercia, V. Andreassi, P. Marini, V. Di Stefano, M. Nakamura, A. Mancini, P.G. Sona, F. Fontana, L.Gamberale, D. Garbelli, F. Falcioni, M.Marchesini, E. Novaro, U. Mastromatteo.

   Invited Paper at the ICCF10, Cambridge (USA), 23-29 August 2003; To be published, as Conference Proceedings, by World Scientific. http://www.lenr-canr.org

   Also INFN-LNF Report 03/21 (P) December 12, 2003; http://www.lnf.infn.it

2. Anomalie termiche ed isotopiche in compositi deuterati per via elettrolitica.

   F. Celani, A. Spallone, E. Righi, G. Trenta, C. Catena, G.D'Agostaro, P. Quercia, V. Andreassi, P. Marini, V. Di Stefano, M. Nakamura, A. Mancini, P.G. Sona, F. Fontana, L.Gamberale, D. Garbelli, F. Falcioni, M.Marchesini, E. Novaro. Contributed Paper at "LXXXIX Congresso Nazionale Societá Italiana di Fisica". Parma, 17-22 September 2003;

   http://www.sif.it

3. Analisi critica risultati presentati a "Decima Conferenza Internazionale sulla Fusione Fredda"

   F. Celani, A. Spallone, P. Marini, V. Di Stefano, M. Nakamura, Contributed Paper at "LXXXIX Congresso Nazionale Societá Italiana di Fisica". Parma, 17-22 September 2003; ***Talk winner of 1st Price, Section 6. SIF LXXXIX Annual Congress***.

   http://www.sif.it

4. Further tests on composition and isotopic anomalies when Pd thin cathodes are electrolysed in acidic C_2H_5OD/D_2O mixtures added with Th-Hg salts at micromolar concentration.

   F. Celani, A. Spallone, E. Righi, G. Trenta, C. Catena, G. D'Agostaro, P. Quercia, V. Andreassi, P. Marini, V. Di Stefano, M. Nakamura, A. Mancini, P.G. Sona, F. Fontana, L. Gamberale, D. Garbelli, E. Celia, F. Falcioni, M. Marchesini, E. Novaro, U. Mastromatteo: Invited Paper at the "5th Meeting of Japan CF-Research Society", Kobe University, December 15-16, 2003. To be published by: Japan CF-Research Society; JCF5 Meeting series, 2003.

   http://www.eng.osaka-u.ac.jp/nuc/03/nuc03web/JCF/.

INTRABIO

E. Righi (Resp.), C. Catena (Ass.), F. Celani, D. Pomponi, G. Trenta (Ass.)

1 Introduction

The heavy water, since its discovery, was tested even to evaluate its eventual biological effects. Those studies hardly ever turned out to be in depth. Particularly it was impossible to find data in the scientific literature on the biological effects due to the heavy irradiated water. The last aspect was the investigation object of the INTRABIO which initiated this study at end of 2001 year.

2 Experiment purpose

The experimental evidences reached during 2002 year on the effects of heavy water irradiated (D_2O R) at high dose on some cell lineages, got us to probe into a phenomenon which could have important consequences from experimental oncology point of view. The programming of the experimental activity for the 2003 year was therefore mainly addressed to verify in a more concrete way the effects, their trends versus the D_2O R concentration and its entity on various "in vitro" cultured cell lineages utilizing:

* not irradiated heavy water at various concentrations,
* heavy water irradiated at high dose (17 kGy from γ ray of ^{60}Co),
* light water irradiated at high dose (17 kGy from γ ray of ^{60}Co).

Therefore the main purpose of the INTRABIO research group in the 2003 year was the validation of the outcomes of a fortuitous result of an interesting serendipity event shown in the previous year.

Results

The experiments were curried out on three stabilized cell lineages: RPMI 1788 (normal leucocytes), CCRF-CEM (lymphoblastic leukaemia) and DAUDI (Burkitt lymphoma). In a first time they were cultivated with different concentrations of not irradiated heavy water and we valued: the surviving fraction (SF) and the apoptosis (A). The figure 1 shows the log of SF vs. the D_2O concentration. It indicates a 50% SF for a 20% concentration of not irradiated heavy water in the culture medium.

The general trend is well fitted by the following polinomial curve:

$$\log(\mathrm{SF})=\mathrm{k}+\alpha\mathrm{C}+\beta\mathrm{C}_2$$

Where k, α, β are suitable constants and C is the D_2O concentration.

Similarly for the apoptosis we get the results of figure 2. It indicates a more spread behaviour for the various cell lineage and a greater sensibility for the DAUDI cells.

The same three stabilized cell lineages were then treated in a culture medium with a different concentrations of heavy water irradiated at 17 kGy of γ dose. The results are shown in figure 3. It is self evident the effect of the irradiated water on the SF.

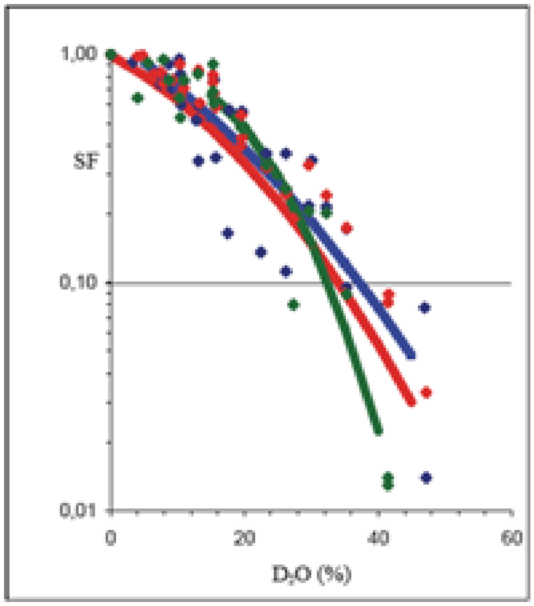

Figure 1: *Surviving fraction (RPMI bleu, CEM read, DAUDI green) vs. D_2O in culture medium.*

A similar evidence is coming out by the comparison of the results of figure 4 and those of figure 2 as far as the apoptosis is concerned.

We repeated the same experiments with light water irradiated at high dose (H_2O R), and a similar but a lower effect on SF was observed (see figure 5). Nevertheless it was also observed, 6 months after the water γ treatment, a dip in the effectiveness of citotoxic effect by the light irradiated water with respect to the heavy irradiated water. It is amazing the long surviving time of the citotoxic effects that, for the irradiated heavy water is longer than one year.

At the moment, we suspect the effects are due to the reactive oxygen species (ROS) produced by radiolysis in the irradiated water and/or to some other chemical species and we are investigating in this direction.

Moreover we are carrying out a similar experiment, on other kinds of oncological and onco-haematological cell lineages. At the same time a collaboration is starting with Prof. G. De Rossi, Director of the Haematological Division of the Bambino Gesú Hospital (Rome). Furthermore the INTRABIO (now DEUTER) group is developing a research project on an "in vivo" experiment on laboratory animals with heavy irradiated water with the aim to propose it to same qualified scientific Institutions.

Up to now, we were unable to use the infrared beam from DAΦNE-Luce (e^+e- collider ring at Frascati National Laboratories) and could not initiate the research on numerical and conformational protein alterations following the action of a physical stressor; but we intend to undertake this objective in the near future.

Also the foreseen researches on the investigations on the features of the *Ralstonia detusculanense* bacteria are at moment deferred because we are waiting for the response of the quilified Institute on the environmental biocompatibility of the bacterium.

At the same time the DEUTER is collaborating with the FREETHAI Group (see details in this activity Report) on bacteriological and chemical aspects of heavy water used in overloading the deuterium concentration into palladium lattice.

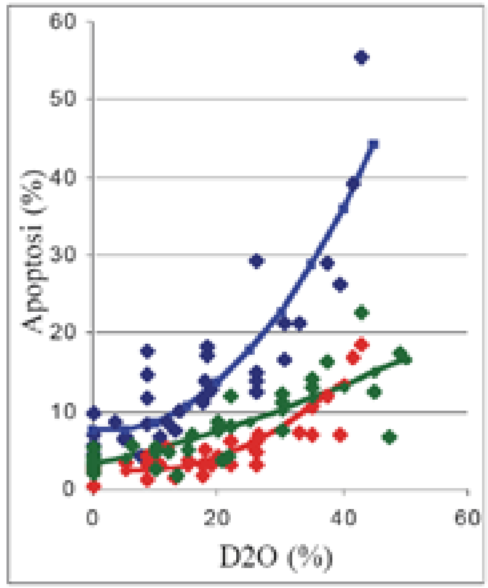

Figure 2: *Apoptosis percent (RPMI blue, CEM read, DAUDI green) vs. D_2O in culture medium.*

3 Publications and Conferences

1. Master di II livello - Tecniche nucleari per industria, ambiente e beni culturali. Gennaio 2003 E. Righi - Danno da radiazioni ionizzanti. G. Trenta - Radiazioni ionizzanti: il rischio sanitario, la contaminazione dell'ambiente, l'informazione, gli aspetti medico-legali.
2. Seminario LNF 21/2/2003 c/o LNF su "Oncologia sperimentale: citotossicitá "in vitro" dell'acqua pesante irradiata e non".
3. Seminario ristretto LNF 14/7/2003 con Ematologia Ospedale Bambino Gesú su: "La citotossicit dell'acqua pesante in oncologia sperimentale".
4. Convegno Ispettorato logistico dell'Esercito: Le emergenze radiologiche - LNF 13 maggio 2003 Righi E. - Le irradiazioni parziali, triage, primo soccorso e clinica della panirradiazione. Trenta G. - Radiocontaminazione esterna e interna: diagnosi strumentale e di laboratorio, criteri e mezzi di decontaminazione.
5. Convegno Nazionale FIRR - Radiazioni in Medicina e Biologia: stato delle ricerche ed applicazioni cliniche. LNL-INFN 20-22 Novembre 2003. Trenta G. - Tavola rotonda: Il Laboratorio di biologia in radioterapia.
6. 17° Corso Avanzato di Radioprotezione Medica 1- 5 settembre 2003, Righi E. - Le nuove linee guida AIRM. Trenta G. - Le basse dosi: aggiornamenti e considerazioni. Trenta G. - Il principio di cautela in Radioprotezione. Trenta G. - Radiocontaminazione ambientale: ritorno all'uomo.
7. 18° Congresso Nazionale AIRM - Riva del Garda, 4-7 giugno 2003, Tenta G. - La radioinducibilitá nelle varie forme tumorali.
8. Seminario sulla valutazione del rischio radon: implicazioni sulla tutela della salute negli ambienti di vita e di lavoro - Genova, 14 aprile 2003. Trenta G. - Effetti del radon sulla salute, dati epidemiologici.
9. Master in Tecnologie nucleari e radiazioni ionizzanti, Univ. Pavia 15 luglio 2003. Trenta G. - Danni da radiazioni ionizzanti, sorveglianza medica, compiti del medico autorizzato/competente, visite mediche di radioprotezione, aspetti medico-legali e probability of causation.

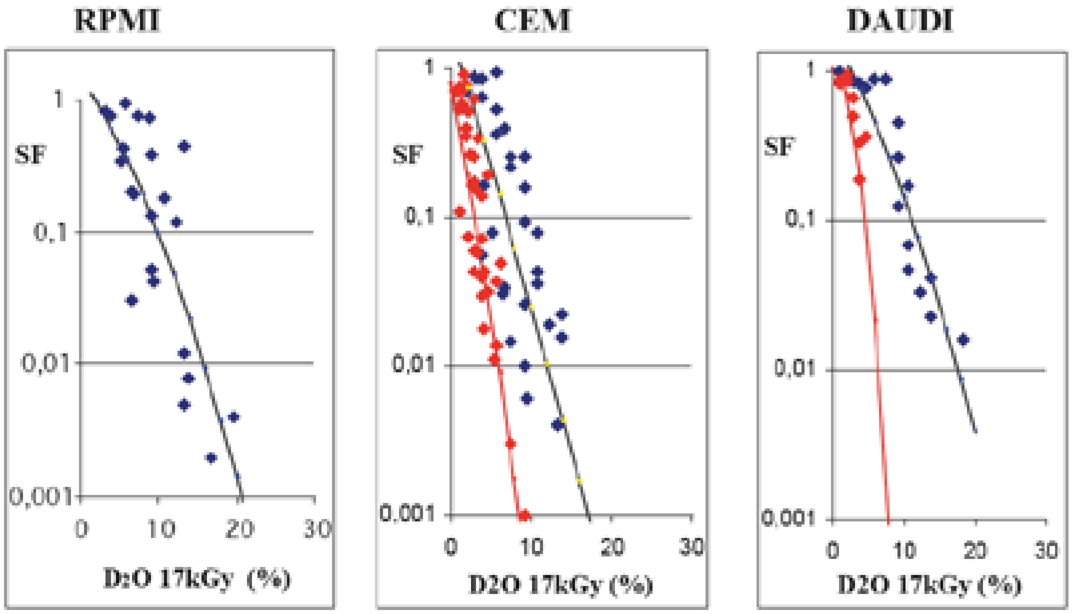

Figure 3: *Surviving fraction vs. D_2O R in culture medium 1-6 (red) and 20-36 months after irradiation.*

10. Corso di Radioprotezione Univ. Napoli, 12 maggio 2003. Trenta G. - Fisica e metrologia delle radiazioni.
11. Convegno Nazionale Univ. Foggia - Nuove prospettive medico legali nella patologia oncologica, 16-17 maggio 2003. Trenta G. - La probabilitá causale.
12. Convegno Regione Valle d'Aosta/CABLIT - Misure di protezione civile ed interventi sanitari nelle emergenze NBC, 1-2 febbraio 2003. Righi E. - Interventi nella irradiazione esterna. Trenta G. - Interventi nella contaminazione radioattiva.
13. Corso Centro Alti Studi della Difesa (CASD)/Associazione Italiana degli Operatori di Pace Nazioni Unite (CABLIT) - Corso avanzato per addetti al coordinamento degli interventi nelle emergenze NBC, 20 maggio 2003. Righi E. - Interventi nella irradiazione esterna. Trenta G. - Interventi nella contaminazione radioattiva.
14. F. Ottenga, A. Giovanazzi, N. L'Abbate, E. Righi, T. Terrana, G. Trenta - Linee guida per la sorveglianza sanitaria degli esposti a radiazioni non ionizzanti - Societá Italiana di Medicina del Lavoro ed Igiene industriale. pime Editrice, Pavia (2003).
15. 66° Congresso Nazionale di Medicina del Lavoro e Igiene Industriale - Epidemiologia occupazionale, ed ambientale: valutazione del rischio in tossicologia occupazionale 15-18 ottobre 2003 Trenta G. - Epidemiologia dei tumori radioinducibili.
16. Convegno ASL 5 Spezzina/Prefettura La Spezia/Marina Militare - Emergenza nucleare biologica chimica radiologica: organizzazione degli interventi e convergenza di professionalitá - Lerici 5 dicembre 2003. Trenta G. - Analisi dei rischi.
17. F. Celani, A. Spallone, P. Marini, V. di Stefano, M. Nakamura. E. Righi, G. Trenta, P. Quercia, A. Mancini, G. D'Agostaro, C. Catena, V. Andreassi. Evidence of anomalous tritium excess in D/Pd overloading experiments. Condensed Matter Nuclear Science ICCF9 19-25 May 2002, Beijing (China); pp.36-41. ISBN 7-302-06489-X.
18. F. Celani, A. Spallone, P. Marini, V. di Stefano, M. Nakamura, A. Mancini, G. D' Agostaro, E. Righi, G. Trenta, P. Quercia, C. Catena, V. Andreassi, F. Fontana, D. Garbelli, L. Gamberale,

D. Azzarone, E.Celia, F .Falcioni, M. Marchesini, E. Novaro. Unexpected detection of new elements in electrolytic experiments with deuterated ethyl-alcohol, Pd wire, Sr and Hg salts. "The 4th Meeting of Japan CF-Research Society" Oct ,2002, Iwate Univ. (Japan).

19. 89° Congresso Nazionale di Fisica Parma, 17-22 settembre 2003. C. Catena, F. Celani, E. Righi, G. Trenta - Ambiente e protezione radiologica. C. Catena, D. Pomponi, F. Celani, P. Marini, M. Nakamura, E. Righi, G. Trenta - Citotossicitá dell'acqua pesante irradiata su cellule coltivate in vitro. F. Celani, A. Spallone, P. Marini, V. Di Stefano, M. Nakamura, A. Mancini, P. Sona, E. Righi, G. Trenta, C. Catena, G. D'Agostaro, P. Quercia, V. Andreassi, F. Fontana, L. Gamberale, D. Gabelli, F. Falcioni, M. Marchesini, E. Novaro - Anomalie termiche ed isotopiche in composti deuterati per via elettrolitica. G. Moschini, E. Righi - Nuove tecniche fisiche nello sminamento umanitario.

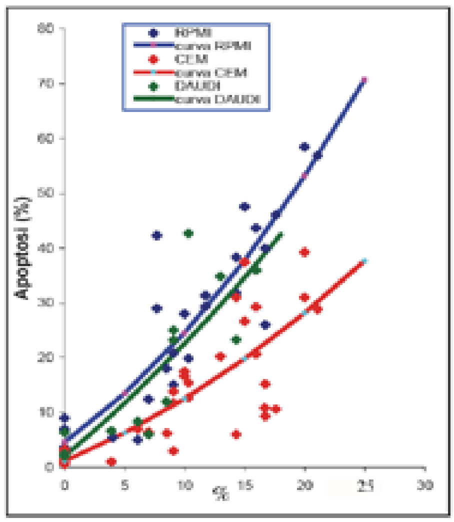

Figure 4: *Apoptosis (percent) vs.* D_2OR *concentration added to the culture medium* (D_2O *was irradiated 20-36 months before).*

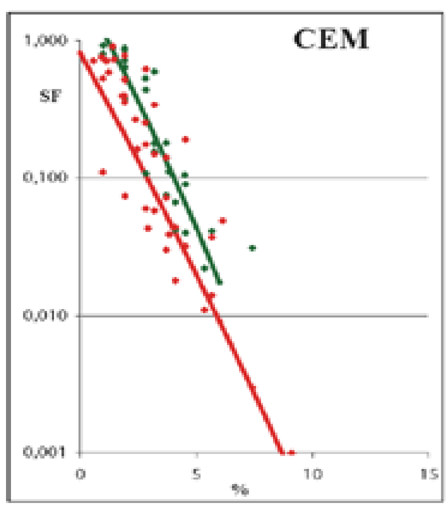

Figure 5: *Surviving fraction vs.* D_2OR *(red) and* H_2O *R (green) in culture medium.*

LCCAL

S. Bertolucci, S. Miscetti (Resp.)

1 Introduction

An excellent jet energy reconstruction is an important requirement for a Linear Collider Detector [1]. The capability to separate the contributions due to charged or neutral particles in the calorimeters is mandatory for jet measurements. In order to achieve this, the calorimeters have to be designed with the highest granularity compatible with costs and technical feasibility. To fulfill those requirements, we propose a solution consisting of a sampling calorimeter made by absorber and scintillator tiles interleaved by three planes of silicon pads at differente positions along the shower development.

2 The prototype

The proposed prototype consists of 45 layers of lead planes $25 \times 25 \times 0.3$ cm^3 (~ 24 X_0 in total) coupled to 45 layers of scintillator slabs subdivided in cells of $5 \times 5 \times 0.3$ cm^3 with a green WLS fiber inserted in circular grooves. The scintillator tiles (SCSN-61 from Kuraray and BC-408 from Bicron) were machined, with a vacuum plate as a holder, in order to produce circular grooves for the fiber insertion and linear grooves for cell light separation. The linear grooves were filled by Tyvec paper. All the WLS fibers (40 cm in length) were polished and aluminised on one face by sputtering. A middle temperature oven (about $60°C$) was used to curl the fibers before their insertion into the 2.25 cm radius groove. The WLS fibers are connected to clear fibers to transport the light signal at large distance. In the region of the 3×3 central scintillator cells, the fibers corresponding to the cells placed at the same lateral position are grouped into 4 bundles, each connected to a PM, thus obtaining a 4-fold longitudinal segmentation. All the longitudinal sectors, of the 16 border cells, are instead grouped into a single bundle to recover the lateral energy leakage.

Three planes of 252 Silicon diode pads (0.9×0.9 cm^2) are inserted at a depth of 2, 6 and 12 X_0 from the calorimeter front face. Each plane consists of 3×2 detectors of 6×7 pads. Each pad is connected, through a conductive glue, to a PCB where the front-end ASIC VAHDR9c from Ideas is mounted. The Silicon pads production was much slower than foreseen. After one single detector was mounted and fully tested, a set of 20 detectors was delivered in autumn 2002. Only two planes could be fully equipped for the first low energy test beams. More recently (June 2003) a different and simpler production (DC detectors) for additional 12 detectors was successfully accomplished allowing to complete the three Silicon planes.

3 Test beam results

In summer 2002, we have tested at SPS the first calorimeter segment (4 Pb-Sci layers $= 2X_0$) and a single Si detector to determine the light yield (~ 5.1 ph.e./m.i.p./scintillator tile) and to check the Si pads behaviour.

The complete prototype (excluding the third Si plane) was exposed twice to the Frascati Beam Test Facility (BTF) in December 2002 and April 2003. At BTF we used low energy electron beams (50 to 750 MeV) with a variable multiplicity of particles ($0.2 \div 3$). To calibrate the PM response an iterative procedure, based on the minimization of the energy resolution, was applied.

A good linearity in response and an energy resolution of $\sim 11.5\ \%/\sqrt{E}$ was obtained in agreement with Monte Carlo expectations.

A high-energy run ($5 \div 40$ GeV) with electron and pion beams was then carried out at the CERN SPS H6 beam in August 2003 where a fully equipped detector was in place. The BTF results are confirmed by a preliminary analysis of this high-energy test: a good linearity in response below 30 GeV [1] and an energy resolution [2] of $11.1\%/\sqrt{E}$.

The detector has a high redundancy in the measurements of the longitudinal and lateral shower development thanks to the four calorimetric longitudinal samplings and to the three planes of high granularity Si pads. The electron-hadron separation achieved is excellent. The overall rejection factor was evaluated to be better than 10^{-3}. The measurement was limited by the contamination of electrons in the pion beams.

The shower position is determined through the centre of gravity of the energy released on the pads. The position resolution is obtained by comparing the reconstructed position with the particle impact point provided (with a resolution of 50 μ) by an external microstrip telescope. We achieve a position resolution of 2.5 mm for 10 GeV electrons. Given the good position resolution, it is also possible to measure the dependence of the energy response on the particle impact point as determined by the external telescope or by the internal pad information. The dependence is small ($< 2\%$) over the whole detector thus proving the good uniformity in the light collection.

The capability of this detector to separate the contributions of two close showers is a complex pattern recognition problem which is still under study.

4 Acknowledgments

This work has been done in the framework of the LCCAL *R&D* project (Como, ITE-Warsaw, LNF, Padova and Trieste). We want to thank the whole INFN mechanical shop, and in particular G. Bisogni, which helped us in assemblying the prototype and installing it at BTF. M. Anelli was also giving us a really valuable help during the SPS test-beam.

5 List of Conference Talks by LNF Authors in

1. S. Miscetti, *First test of LCCAL prototype at BTF*, ECFA-DESY: LC workshop, 02/04/2003, Amsterdam, the Netherlands.
2. S. Miscetti, *Status report from LCCAL*, World Wide Calorimetry for LC, 12/11/2003, Montpellier, France.
3. S. Miscetti, *Status report from LCCAL*, ECFA-Study: Physics and Detectors for LC, 13/11/2003, Montpellier, France.

6 Publications during 2003

1. LC note LC-DET-2003-014.

References

1. TESLA Technical Design Report DESY 2001-011 ECFA 2001-209, Part IV.

[1]Above 30 GeV the PMs with largest gain were showing clear evidence of saturation but time-constraints did not allow us to repeat the measurement with lowered PM gains.

[2]From the fit we also obtained a constant term compatible with the beam momentum spread.

Ma - Bo

D. Di Gioacchino, U. Gambardella (Resp.) G. Celentano, A. Mancini, P. Tripodi, S. Pace

1 Purposes of the project

The *Ma-Bo* experiment is devoted to analyze the use of the magnesium diboride MgB_2 compound. As it becomes superconducting at temperatures below 39 K, its potentiality either in wire applications (magnets) or in thin films applications (RF applications or electronics) will be investigated. Six INFN sections are involved: Genova (group leader), Milano, Torino, LNF, LNL, and Napoli, in collaboration with INFM Genova, CNR Genova, and ENEA Frascati.

2 The Frascati group activity

The Frascati group, composed by LNF and ENEA, takes care of studying the process of thin film depositions, their structural and morphological properties, as well as to analyze the MgB_2 superconducting properties by means of current transport and *ac* susceptibility measurements in high magnetic fields.

2.1 Thin film sinthesis

The activity carried out in this field was devoted to study the process to realize MgB_2 superconducting thin films. During 2003 we mainly focused on the sputtering processes assisted by pure Mg co-evaporation, either in one deposition step [1)] or alternate layer depositions MgB_2/Mg, with different heat treatments [2)]. Samples have been grown on [111] MgO, or Al_2O_3 *r*-cut substrates. As before we used *dc* magnetron sputtering deposition technique from commercial stoichiometric MgB_2 targets, and thermal evaporation from pure Mg. The growth process is then followed by an *insitu* annealing at moderate temperatures, in the range of 500 C. The aim of the work is to achieve the optimized Mg phase diagram pressure to promote MgB_2 phase sinthesis. The annealing temperatures and the annealing time have been investigated to achieve the highest critical temperature in one structure of ~ 30 layers MgB_2/Mg. The highest critical temperature obtained so far is 31 K. To study the effect of the annealing in the multilayer structure samples have been analysed in Genova by means of XPS. Further samples have been provided to Torino group for their programs in thin films superconducting detectors.

2.2 AC susceptibility measurements

We carried out further investigations on the vortex dynamics in MgB_2 bulk samples. We have computed the irreversibility line using the onset of the measured third harmonic amplitude of *ac* susceptibility in *dc* magnetic field [3)]. The analysis of magnetic behavior of the MgB_2 bulk samples has also included magnetization cycles measured in an high field vibrating sample magnetometer, to gather further information on the fluxon dynamics at lower frequencies. Magnetization cycles at different temperatures have been compared to the 3rd harmonic amplitude of the *ac* susceptibility measurements at comparable fields. Moreover the Cole-Cole plots of third harmonic have been analyzed, with the support of numerical simulation: the fits suggest the occurrence of a 3D glass collective pinning behaviour [4)].

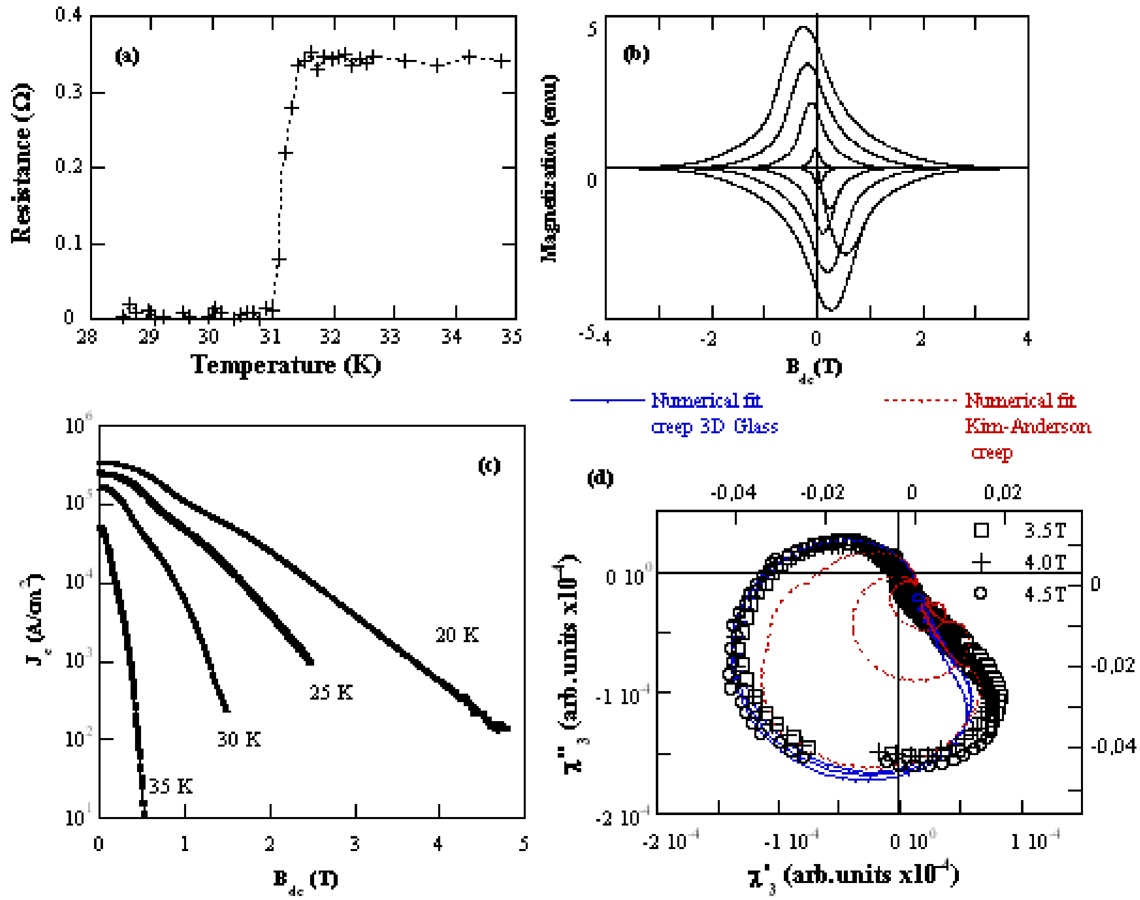

Figure 1: *a) improved resistive superconducting transition in our MgB_2 film; b) VSM magnetization cycles of a bulk MgB_2 sample; c) $J_c(B)$ derived from magnetization; d) Cole-Cole plot representing the imaginary part of the $\chi_3(T)$ -vs- $\chi_3(T)$ real part, measured in a MgB_2 bulk sample. The continuous and dotted lines represent the numerical analysis using the 3D pinning vortex-glass and the Kim-Anderson model, respectively.*

References

1. A. Mancini, V. Galluzzi, U. Besi Vetrella, V. Boffa, G. Celentano, L. Ciontea, U. Gambardella, G. Grassano, T. Petrisor, A. Rufoloni, S. Sprio, M. Vadrucci, "Properties of MgB_2 films grown by means of different vapour phase techniques", IEEE Applied Superconductivity **13** (2003), 3305

2. R. Rogai, V. Galluzzi, A. Mancini, G. Celentano, T. Petrisor, A. Rufoloni, E. Varesi, G. Grassano, V. Boffa, U. Gambardella, "Growth of MgB_2 thin films by means of *insitu* deposition techniques", Int. J. of Modern Physics B **17** (2003) 703

3. D. Di Gioacchino, P. Tripodi, U. Gambardella, "Third harmonic ac susceptibility measurements on MgB_2 bulk: irreversibility line and frequency dynamic behaviour", Physica C: Superconductivity **388-389** (2003), 175

4. D. Di Gioacchino, U. Gambardella, P. Tripodi, G. Grimaldi, "Irreversibility line and magnetic field dependence of the critical current in superconducting MgB_2 bulk samples", Superconducting Science and Technology **16** (2003), 534

MORDILLO - ARCHIMEDE

G. Cinque (Resp.), A. Marcelli, M. Piccinini (Bors.), S. Bellucci, A. Raco (Tecn.), A. Soldatov (Osp.) and M. Matzuritsky (Osp.)

1 Summary

The experiment Multistep Optics ReDesIgned as Layer by Layer Optics (MORDILLO), concerns the study of new optical systems with high reflectivity for soft X-rays at quasi-normal incidence. Designed for the so-called water window, i.e. in between oxygen and carbon absorption edges, such devices have to be used and characterized by synchrotron radiation at the DAΦNE- Light facility. This multidisciplinary research combines both know-how and technologies developed within INFN laboratories, namely the construction of multistep optical devices in cylindrical and pseudo-spherical geometry by the group of LNF (MUST experiment) with the growing of multilayered diffracting systems at LNL (ARCHIMEDE experiment). Since 2003 the MORDILLO proposal merged into the existing ARCHItects of Mirror Extreme ultraviolet DEvices experiment (ARCHIMEDE) experiment as further development.

2 Activity

The ARCHIMEDE project originally aimed to grow multilayer mirrors, with high normal incidence reflectivity, for X-ray and Extreme Ultra Violet (EUV) wavelengths in the spectral region from 24 to 300 Å. In this range the foreseen applications in astrophysics and in projection nano-lithography are strategically important. On including MORDILLO's goals, the interest of lower wavelengths, from about 24 to 40 Å, has raised up since the scientific importance of X-ray microscopy on organic structures, e.g. cells and their organelles, in aqueous environment, as well as of X-ray microprobe spectroscopy in general. Such envisaged applications necessarily require both collecting the X-ray radiation emitted from a source and refocusing onto an object. This can be accomplished by depositing X-ray multilayer mirrors and by their multiple assembly onto large substrates, shaped according to focusing geometries, offering the advantage of larger optical aperture in quasi normal incidence without increase aberrations.

Consisting in alternating high/low refractive index layers with a minimum absorption, the maximum reflectivity of multilayers requires abrupt and flat interfaces. In charge of the LNL group, the design and deposition of these optical systems is under progress: the process needs the optimization since the deposition conditions crucially balance cinematic growth rate and surface roughness, the latter dominating the overall device reflectivity. In the case of extreme UV and soft X-ray Ni/Ti e Ni/TiO_2 o NiO_y/TiO_x have been identified as good material candidates (Fig. 1). The problems reside in depositing about 500 layers while achieving minimal bulk diffusion and interface mixing. Being never done before, especially challenging are the technological aspects of growing a pure metal (Ni) on a different metal oxide (TiO_2).

The research activity at the DAΦNE-Light facility includes a preliminar characterization of the multilayered materials by X-ray Absorption Spectroscopy (XAS): this technique probes both the physical and local structure of the atoms within different material layers. As soon as the first optical-grade multilayers will be available, they will be characterized in terms of X-ray reflectivity and energy bandwidth. This in view of setting up the test procedure of the final optical devices, which will be constructed, on multistep planar and/or spherical supports, on fixing the multilayers by optical contact, i.e. without gluing, a procedure that may deform the diffracting surfaces.

In December 2002, the preliminary issue of commissioning the X-ray beamline has been ended with the calibration and put into work of the double-crystal monochromator in the soft X-ray energy range. X-ray Absorption Spectroscopy (XAS) has been implemented on exploiting measurements in transmission of thin samples from lighter elements (K-edges) and transition metal (L-edges) standards. A Peltier cooled PIN Si detector is now available for the detection of X ray fluorescence from thick samples: this will access the characterization of inter- and intra-atomic layer structure within the optical devices by such XAS analysis. Since the reduced fluorescence yield of the low Z elements, a channeltron system is also available, including its low noise electronic chain and power supply, to allow the detection of photoelectrons in total yield.

Until September 2003 the DAΦNE storage ring was not operational with a consequent significant delay of all synchrotron radiation activities. Within this time a further improvement of the beamline equipment, has been performed, based on i) new crystal pair set with large lattice spacing (KAP(100) with 2d$\sim$27 Å), and ii) new vacuum tight ultrathin windows with high X-ray transmission (10 $\div$ 0,1 μm). These changes extend the working region to the lower energy side of X-rays closer to the oxygen K-edge. Thus, the direct measure of the multiplayer reflectivity will be possible in the water window working with monochromatic beams of synchrotron radiation on test samples. Due to the spectral range (EUV/soft X-ray) and the kind of test (detection of direct and reflected/diffracted radiation beams), a high vacuum regime is sufficient to perform the experiments by a preamplified photodiode (already present) set up and an external acquisition system (under development). The optical techniques to be used follow two modalities:

1) energy resolved assessment of reflectivity with fixed detector and sample position;

2) rocking curve determination or θ-θ diffraction measurement at fixed energy.

On purpose, a remotelly controlled system of goniometers is to be acquired: it guarantees angular precision and accuracy better than 1/1000 of degree. After the first multilayer tests of their soft X-ray reflectivity, multistep support prototypes could be designed with curved surfaces where to fix the optical mirrors. This part of the project benefits from the experience acquired by the LNF group during the collaboration with the Rostov University in the framework of the MUST experiment (INFN Gr V). Such experiment designed and manufactured multistep optical systems made by a few diffraction crystals aligned and fixed by optical contact technique of cylindrically or spherically shaped supports, according to different grazing angle focusing geometries. Because of the limited size of the multilayers, the project intend to test the feasibility design of multistep devices consisting of several multilayer elements, to cover X-ray energy ranges not accessible by crystals, working at quasi-normal incidence to the beam, allowing full exploitation of angular aperture, in a focusing geometry.

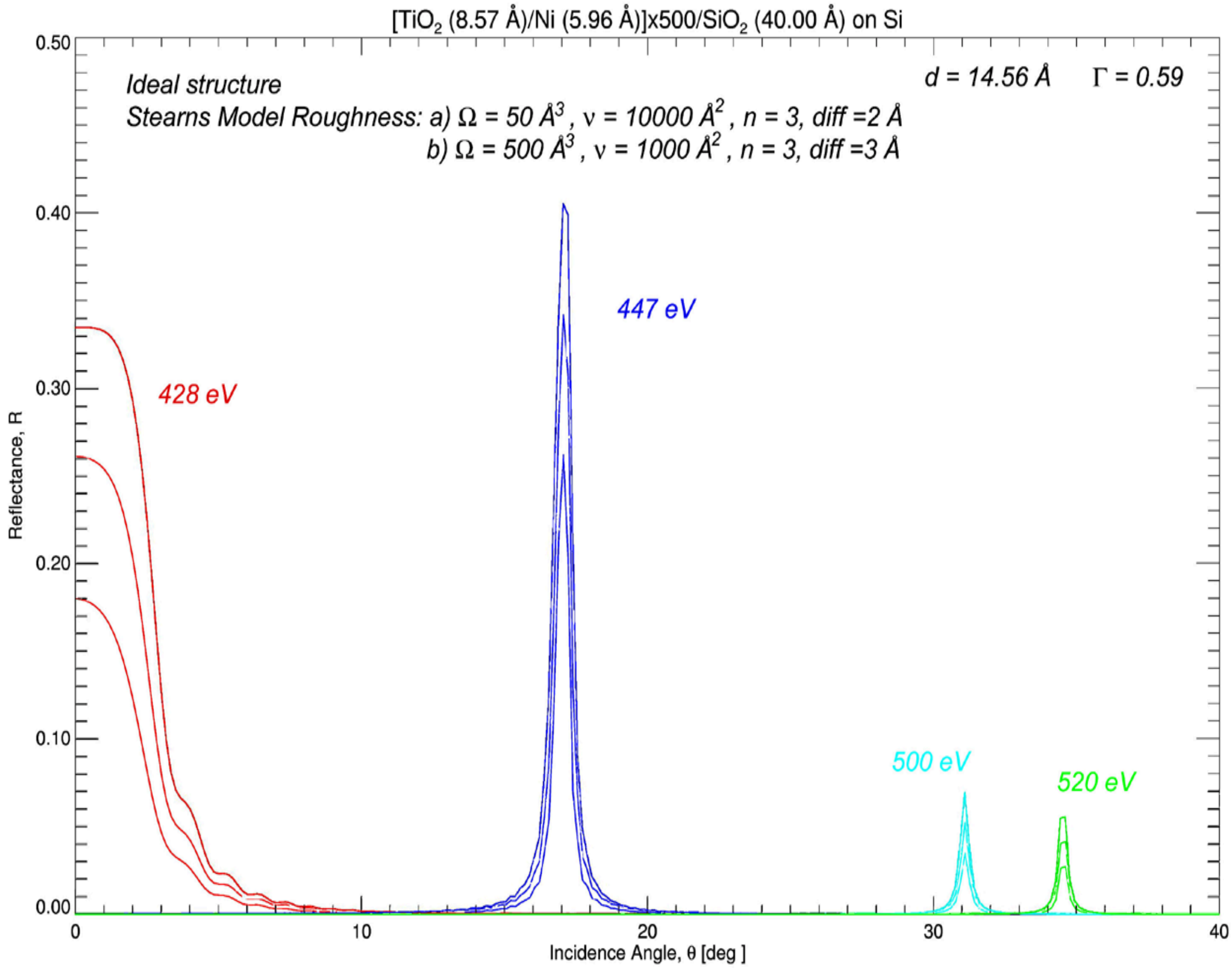

Figure 1: *Expected reflectivity of the multilayer (plane) mirror taylored for the X-ray water window. The curves refer to different working energies/angles taking into account some surface roughness (by Alessandro Patelli).*

NANO

S. Bellucci (Resp.), S. Bini, C. Balasubramanian, G. Giannini, A. Marcelli,
A. Raco (Tecn.), F. Tombolini (Dott.), Z. Wu (Ass.).

1 External collaborating Institutions

Univ. Roma La Sapienza, Univ. Modena, Univ. Roma Tre, Univ. Perugia, IHEP-Protvino (Russia), CNR-IFN (Roma), VARIAN (Torino), CSM (Pomezia), HITESYS (Aprilia), Univ. Pune (India), Burnham Institute (La Jolla, CA, USA), IMM-CSIC (Madrid, Spain), ILL (Grenoble, France).

2 Relevant results achieved

Good quality samples of: a) aligned ropes of SWNT, with the average tube diameter of 1.3 nm and a bundle diameter of 20-40 nm, as well as MWNT with diameter of 20-60 nm; b) high yield in terms of C nanotube density in the sample (above 50%). The electron microscopy characterization for a typical sample we produced by arc discharge is carried out in collaboration CNR-IFN. The result of another deposition by arc discharge, obtained using a different experimental setup, has also been obtained. It looks very promising for a higher yield in nanotubes and a higher purity of the sample. The SEM characterization is however not sufficient to establish the very nature of such nanostructures, i.e. it is impossible to say only on the basis of SEM observations whether the tubular structures are empty or full, hence distinguishing C nanotubes from nanofibers. Thus, we proceed to a TEM analysis of the samples, with the result obtained in collaboration with Univ. Pune where a bundle of about 10 micron long SWNT without closures at their ends is observed on a scale of 1m. We also obtained TEM images of a MWNT we manufactured, where the coaxial cylinders and the central channel in the tube are clearly seen. This images have been taken on a scale of 5 nm at the Univ. of Modena and shows clearly a structure closing one end of the nanotube. In this case one can estimate the diameter of such structure to be approximately 20 nm. Atomic Force Microscopy (AFM) studies of the carbon nanotubes that were synthesized by arc discharge have been carried out at IMM-CSIC, Madrid. The imaging was carried out to determine (a) the morphology and dimensions of the CNT and (b) to evaluate the friction coefficient of the nanotube with the substrate surface. Contact mode AFM was used for the imaging under a constant force. The images reconfirmed the dimensions of our nanotubes to be approximately 30 - 60 nm as detected from the SEM images earlier (Fig. 10). The samples of the nanotubes were initially dispersed in isopropyl alcohol and sonicated for a few hours. Drops of this were then suspended on three different substrates, namely HOPG, silicon wafer and mica sheet. The adhesion of nanotubes was found to be highest for HOPG, as compared to mica and silicon (where the nanotubes got displaced easily by the AFM tip). Also it was observed that the nanotubes got laterally compressed on a HOPG surface (due to Van der Waals interaction of the nanotubes with the substrate) to a ratio of 0.5. For mica and silicon there was lateral elongation of the order of nearly 3 times, indicating that the interaction of the tube with tip was far greater than the interaction of the tube surface with substrate. The study of these results should be further continued and is quite interesting from the point of application-oriented studies of nanotubes. From such results we can say e.g. that mica and silicon can be used for nanomechanics and HOPG for applications where strong bonding of nanotubes to substrates is required, as it is the case for field emitting devices. Good field emission properties of the samples, with activation fields of 0.4 V/micron and a typical current emission of about 10 m A/ cm2 (for a voltage of 1 V/micron: I-V measurements). These results are competitive with the best results reported by Saito, Carbon 38 (2000) 169. We started to study the stability of the emitted current, which is a very important constraint for the proposed applications. We also repeated the measurements of the emitted current for samples obtained using different conditions, The data collected show a 40% increase in the current density, which is a likely consequence of the higher purity of the new sample, compared to the old, implying a higher density of nanotubes in the sample.

3 Level of leadership in the international context, competing experiments

In SWNT synthesis and field emission studies, we confirmed that our experimental parameters are in line with the best achievements in the international community active on this topic. Our group organizes since 2000 a series of international meetings in the area of nanotechnology www.lnf.infn.it/conference/nn2003. Part of the yearly event consists in a school dedicated to training of Ph.D. students and young postdocs in the basics of nanoscience. Also, our group in Frascati has been selected as the host of the 2004 international conference on relativistic channeling and coherent phenomena in strong fields www.lnf.infn.it/conference/rc2004.

4 Potential relevance for other INFN experiments

The enhancement in the efficiency and stability of directional electron emission in cold cathods, for the production of interesting electron sources, at low cost and with a long lifetime. Potential applications of field emitters producing a stable current of low energy electrons can have a big impact on the monitoring of purity of the liquid Ar inside neutrino detectors (such as for the ICARUS or the OPERA experiments). As it is well known, there are methods developed for measuring the electronegative contamination of liquid Ar, based on the transport of electrons emitted from a metallic photocathode (see G. Carugno, et al., Nucl. Instr. Meth. A 292, 580 (1990)). In principle, one could replace the emitters with low-cost C nanotube based ones, measuring the purity through the observed ratio of collected to emitted charges, as in the standard case. We plan to develop this application in collaboration with research groups at the Univ. of L'Aquila. Also, our results based on field emission effects from C nanotubes can be useful for benchmarking with other techniques developed at INFN, based on high temperature diamond emission (ad es. DIAMANTE3). C nanotube based table-top low-energy X-ray sources can be of interest for groups with an interest in national security, artistic and archeological patrimony protection, bio-medical and environmental applications.

5 Potential relevance for other scientific disciplines

Production of micro and nanostructured films, as promising candidates for producing X-ray sources and gas discharge tubes, for potential applications in radiotherapy, as well as for biological and space research applications.

6 Impact for applied research and industrial applications

Our activity attracts interest from collaborating enterprises, including large companies (VARIAN, CSM) which are world leaders in their fields (vacuum technology, sensors), as well as SME (HITESYS) with an eminent position in the market of electro-medical devices.

7 List of conference talks by LNF authors in 2003

1. S. Bellucci, Frascati, International Symposium on Channeling-Bent Crystals-Radiation Processes, Eds. W. Greiner, A Solov'yov and S. Misicu, Frankfurt am Main, 5-6 June 2003.

References

1. S. Bellucci et al., 19th Int. Conference on X-ray and inner-shell processes, A. Bianconi et al. editors, American Institute of Physics, Melville, New York 2003, p.355.
2. Z.Y. Wu, 19th Int. Conference on X-ray and inner-shell processes, A. Bianconi et al. editors, American Institute of Physics, Melville, New York 2003, p.497.
3. F. Tombolini, 19th Int. Conference on X-ray and inner-shell processes, A. Bianconi et al. editors, American Institute of Physics, Melville, New York 2003, p. 481
4. S. Bellucci, S. Bini, V.M. Biryukov, Yu.A. Chesnokov, S. Dabagov, et al, Phys. Rev. Lett. 90 (2003) 034801.
5. S. Bellucci, V.M. Biryukov, Yu.A. Chesnokov, V. Guidi and W. Scandale, Nucl. Instr. Meth. B202 (2003) 236.
6. S. Bellucci, V.M. Biryukov, Yu.A. Chesnokov, V. Guidi and W. Scandale, Phys. Rev. Special Topics AB 6 (2003) 033502.
7. S. Bellucci and S.B. Dabagov, Journal of Physics: Condensed Matter 15, 3171 (2003).
8. S. Bellucci, P. Onorato, Phys. Rev. B 68, 245322 (2003).
9. S. Bellucci, J. Gonzalez, P. Onorato, Nucl. Phys. B 663 [FS], 605 (2003).
10. S. Bellucci, Proceedings of the International Symposium on Channeling-Bent Crystals-Radiation Processes, Eds. W. Greiner, A Solov'yov and S. Misicu, Frankfurt am Main, 5-6 June 2003, p. 171.

POLYX

G. Cappuccio (Resp., Ass.), S. Dabagov, D. Hampai, A. Marcelli,
V. Sessa, C. Veroli (Tecn.), M. Kumakhov, R. Fedorchuk

1 Experiment aims

The main aim of the POLYX project is to study and to utilize polycapillary optics in X-ray applications, using both conventional X-ray sources (Cu tube) and synchrotron radiation. The implementation of polycapillary lenses makes it possible to increase the radiation density in the focal spot position, while with polycapillary semi-lenses, parallel X-ray beams can be obtained from divergent sources, or convergent beams from parallel sources. Finally, by using cylindrical polycapillaries, we can match parallel beams with X-ray detectors, monochromators, etc. One of the purposes of the project is to insert polycapillary optics in the X-ray diffractometer at the Dafne Light Laboratory. The advantages in using polycapillary lenses for diffraction measurements will be a net increase in the spot density on the samples and a decrease in peak profile width, which corresponds to an increase in spectral resolution.

2 2003 Activities

To improve the analysis of thin solid films by X-ray diffraction (XRD) it is extremely useful to utilize a "quasi" parallel X-ray beam. Hence, when synchrotron radiation is not available for experimental activities at the Dafne Light Laboratory, the divergent beam from the Cu X-ray tube could be transformed into a parallel beam by using a polycapillary semi-lens. Moreover, to improve the scintillation detector response, a cylindrical polycapillary lens, instead of the classical "Soller slit", should be put in front of the detector.

During 2003 the mechanical statives that support the Gimbal mounts with the polycapillary lens holders were placed on the diffractometer (Fig.1), while the "LabView" was used to develop a program to control the micrometric linear transducers that actuate the Gimbal mounts. Due to the extremely high precision required for positioning the polycapillary lenses, the subsequent tests brought to light a failure, so the design of the statives was partially revised and mechanically upgraded. For the final test, a diffraction spectrum was collected, using a Si wafer as a standard sample. The Si [111] diffraction peak at $2\theta = 28.443°$ showed a slight decrease in the FWHM value, as expected, but its shape was asymmetric, proving that the alignment procedure of the optical parts remains the most critical aspect in the use of polycapillary lenses. Further work in this direction will be carried out during 2004.

In order to increase our knowledge in the field of polycapillary optics and our understanding in the design of polycapillary optical systems, we decided also to develop a CAD program, named "PolyCAD". As a first step, we used the software package, to predict the spot shape on a screen located at the exit of a single cylindrical or conical capillary for different types of X-ray sources. Figure 2 shows the images formed on the screen by the two capillaries, for a point X-ray source located at finite distance from the optics entrance. The focusing effect due to the conical capillary is evident. During 2004 the PolyCAD program will be extended to dealing with the polycapillary lenses and half-lenses.

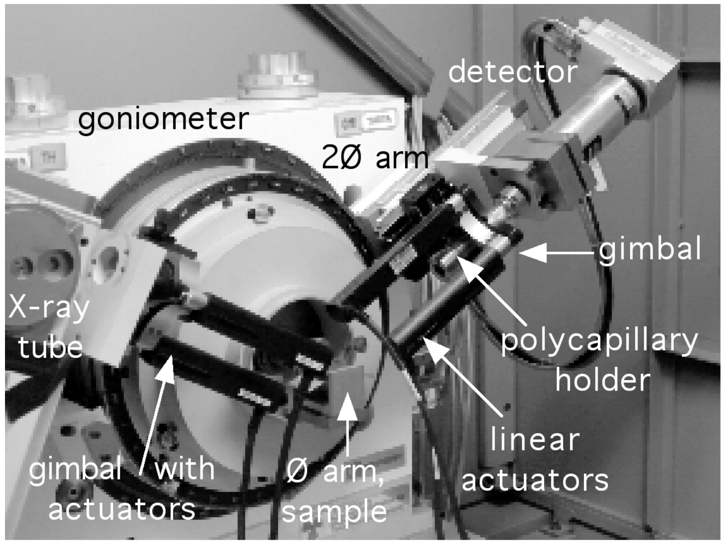

Figure 1: Polycapillary lenses mounted on the x-ray diffractometer.

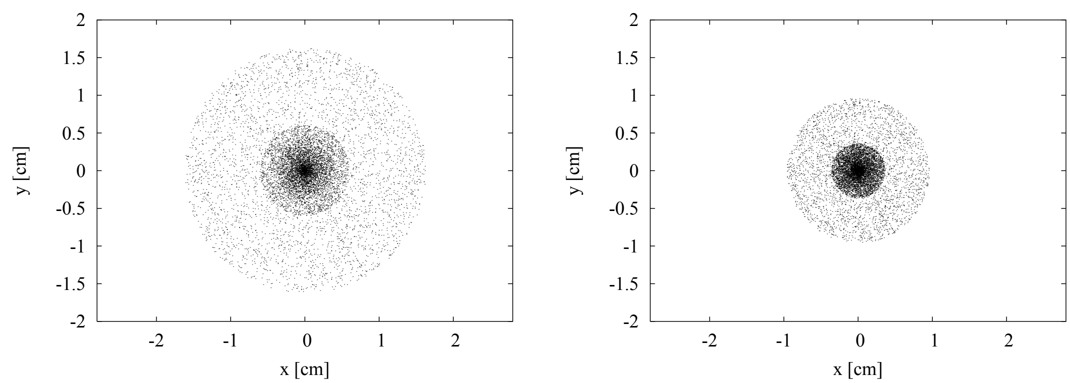

Figure 2: CAD simulation of X-ray propagation from a point source through a cylindrical (left) and conical (right) single capillary. The conical focusing effect is evident.

3 Conferences

1. G. Cappuccio, "Ottiche policapillari in applicazioni strumentali", Meeting FISR Project, Pisa, February 6-7 (2003).
2. S. B. Dabagov, "Coherent Scattering of X-Rays in Micro- and Nano-capillaries", International Congress on X-Ray Optics and Microanalysis, Chamonix, September 22-26, (2003).

References

1. S. B. Dabagov, X-Ray Spectrometry **32**, 3 (2003)

SAFTA2

D. Alesini (Art. 23), V. Fusco (Dott.), M. Migliorati (Ass.),
A. Mostacci (Ass.), L. Palumbo (Ass.), B. Spataro (Resp.)

1 Aim of the experiment

The aim of SAFTA2 group is mainly related to the study of the electromagnetic interaction between a particle beam and the accelerator pipe wall, the generation of the parasitic fields, the related energy loss and the instability effects. The main investigated subjects are: the coupling impedance of the LHC and SPS machines and hybrid beam position monitor for LHC machine, parasitic diagnostic device for bunch length-position monitoring, the realization of a standing wave accelerating structure. The first activity, done in collaboration with AB/ABP group at CERN, consists of estimating the longitudinal and transverse impedance budget of the LHC and SPS rings in order to evaluate the instability thresholds. Results obtained from simulations have been cross-checked with analytical estimations and whenever possible with experimental results. The second activity has been focused to completely characterize a new promising bunch-length position monitor for ultra-short bunches in term of theoretical analysis, numerical simulations and measurements. The third activity has been the design, realization and measurements of a prototype compact standing wave accelerating structure operating at 11 GHz to be used for linearizing the longitudinal space phase in the Frascati Linac Coherent Light Source.

2 Main results of 2003

The energy losses, the parasitic resonances and the longitudinal and transverse impedances of several beam pipe components and the standing wave accelerating structure have been studied with the MAFIA3D, HFSS, ABCI, OSCAR2D and SUPERFISH codes:

- cold to warm transitions with different geometries for the SPS machine;
- hybrid beam position monitor for LHC;
- standing wave accelerating structure working on π mode.

In all cases the analysis of the results have suggested an optimization of the design in order to obtain acceptable values of the coupling impedance and energy loss. In order to reduce strongly the heating of the cold section the change of the shape and sizes of the previous installed vacuum chamber inside the SPS machine has been required. As a final design study result, the new and innovative cold transition proposed is in Cu OFHC with inner diameter 67 mm and 2232 mm long. The slots are 2 mm wide, 9.5 mm long with a 1 mm radius at the extremity. The longitudinal distance between the slots axes is 16.3 mm. There are two rows of 132 slots each. In a cross-sectional view the slots are located at -42 and +42 degrees. The numerical calculations have been carried out by using the MAFIA3D code in time domain by carrying out the Fourier transform of the wake potential for the impedance estimations. Measurements have shown a good agreement with the predictions of the simulation results. The shape of the warm transition is again like the previous one since from the study results no specific problem was determined. It has been completed the investigation of the special type beam position monitor, which will be installed in some dedicated positions of the LHC straight sections. It is referred to as "hybrid monitor" in the sense that the BPM's body is equipped with both the conventional button electrodes, and, in addition to it, also contains strip lines. The bunch length-position monitor consists of a small coaxial cavity coupled to the beam pipe through four slots (see Fig.1). If the length of the cavity is properly chosen, the beam power spectrum lines can excite the resonant longitudinal or transverse modes in the cavity resonator. Probing the field by a small antenna it is possible to measure the amplitudes of the beam power spectrum lines and to calculate the bunch length and the position. The theoretical and numerical study was carried out by using the Bethe s theory and by performing electromagnetic simulations with MAFIA3D and HFSS. Wire measurements have been made on the aluminum prototype shown on Figs.2 and 3. In particular to excite the dipolar modes the wire inside the beam pipe has been properly displaced from the axis of the beam pipe with a thin nylon wire connected to the central wire and displaced from the beam pipe axis in a controlled way. The comparison between the theoretical and the experimental results confirm the potential application of this device as a bunch-length position monitor. The very low coupling impedance of the device and the possibility of a calibration by simply wire measurements make the device hopefully usable in the accelerators machines. In order to linearize the longitudinal space phase and obtain a 5 MeV energy gain for the X-FEL project to be at Frascati Laboratories, we have chosen an X band accelerating structure operating on π mode as possible candidate . It has carried out the theoretical study by calculating the dispersion curve and the relevant RF parameters of the working mode. In this case the codes OSCAR2D and SUPERFISH have been used for designing the structure. A thermal analysis of the structure has been determined by means of the ANSYS software. To compare the numerical results with the experimental one a prototype has been realized. Preliminary results at room temperature on the copper prototype are in progress.

3 Publications

1. B. Spataro et al., *On trapped modes in the LHC recombination chambers: numerical and experimental results*, NIMA 42319, 3 September 2003.

2. B. Spataro et al., *Impedance of the LHC hybrid Beam Position Monitor BPMC*, LHC Project Note 315, March 17, 2003.

3. B. Spataro et al., *Study of a low impedance beam position monitor for short bunches*, 2003 Part. Acc. Conf., Portland (Oregon).

4. A. Mostacci et al., *Bench measurements of low frequency transverse impedance*, 2003 Part. Acc. Conf., Portland (Oregon).

5. B. Spataro et al., *An X-band structure for a longitudinal emittance correction at SPARC*, LNF-03/008 (R), May 6, 2003.

6. L. Palumbo et al., *Longitudinal beam dynamics in the Frascati DAΦNE e^+ e^- collider with a passive third harmonic cavity in the lengthening regime*, Physical Review Special Topics - Accelerators and Beams, 6, 074401 (2003).

7. M. Migliorati et al., *Muon phase rotation and cooling: simulation work at CERN*, Journal of Physics G: Nuclear and Particle Physics, 29 (2003), pp. 1649-1651.

8. M. Migliorati et al., *Evolution operators and Euler angles*, Il Nuovo Cimento, Vol. 118 B N. 5 (2003), pp. 493-4988.

9. M. Migliorati et al., *On new families of summation formulae of ordinary and generalized Bessel functions*, International Mathematical Journal, Vol. 4, N. 3 (2003), pp. 239-246.

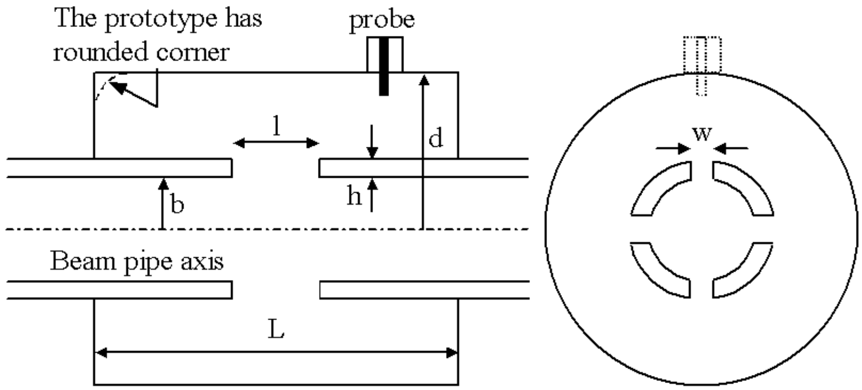

Fig. 1

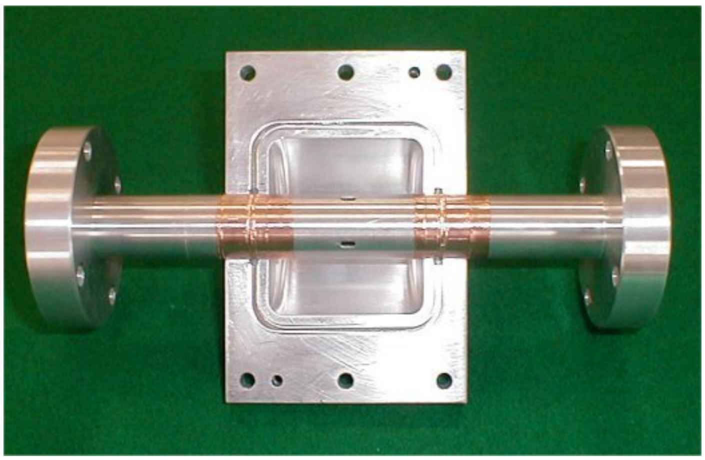

Fig. 2

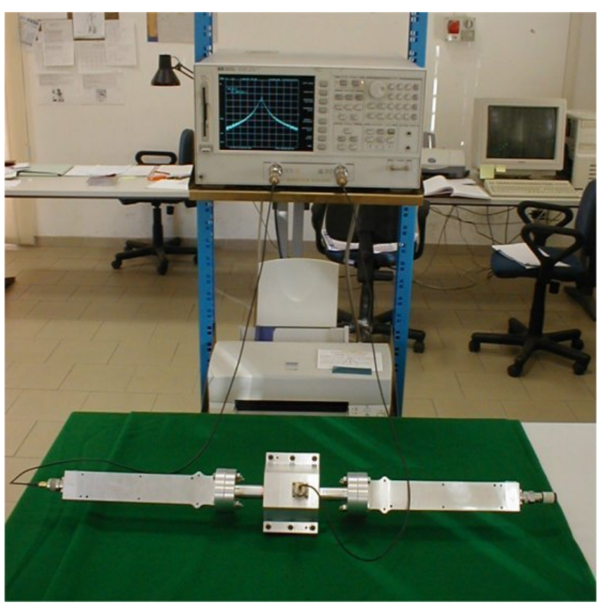

Fig. 3

SI-RAD

L.Bongiorno (Ass. Ric.), G.Mazzenga (Tecn.), M.Ricci (Resp.), B.Spataro

Participant Institutions:

ITALY: INFN LNF, Firenze, Roma2, Trieste;
RUSSIA: MePhi, IBMP, RKK"Energia" (Moscow)
SWEDEN: KTH (Stockholm)

1 Introduction

The SI-RAD experiment is a continuation of the activity that the Collaboration has carried out for the experiments SIEYE1 and SIEYE2 on board the Russian Space Station MIR and SIEYE3/ALTEINO on board ISS in the years 1995-2002 [1, 2, 3, 4, 5, 6, 7, 8, 9]. Si-RAD will be installed on board the International Space Station (ISS) to study and monitor the radioactive environment internally and externally of ISS. At the same time, the investigation, with a more sophisticated instrument, of the "Light Flashes" phenomenon [10], will be conducted to improve and refine the results obtained with the previous SIEYE experiments. The instrument will consist of a 16-plane tower of double-sided silicon detectors (8x8 cm^2 area) equipped with trigger and anticoincidence counters. The total weight is 13 kg and the total power consumption should not exceed 30 W. The experimental program will be completed through three steps by the construction of a laboratory prototype model, an engineering model and the final flight, space-qualified model. In 2003, the laboratory model has been completed with five silicon planes, a read-out card and front-end electronics for testing purposes. At the same time, the prototype of a new, space qualified CPU (wich also includes DSP operations) has been designed and tested. In 2004, work on the engineering model will start with the the following program:

- completion of a tower of at least 12 silicon planes
- trigger system
- vibration tests of 4 planes
- read-out system implemented with the new CPU
- servicing systems (power supply, thermal regulations, interfaces with ISS, Ground Support Equipment and onboard simulators)
- support mechanics
- beam tests at TSL/Uppsala and GSI/Darmstadt.

2 Activity of the LNF group

The LNF group has taken the responsibility of the design, construction and test of the mechanical structures and interfaces of the three models of the detector. The group will also contribute to the integration of the mechanical support for the DAQ. This activity is carried out with the support of the LNF Service of Development and Costruction of Detectors. In 2003, first mechanical supports for the laboratory model have produced, tested and integrated. Activity in 2004 will be mainly devoted to the mechanical support of the engineering model and to the interfaces of front-end and

DAQ with the detector. The LNF group will also participate in the beam test activities at GSI and TSL having the responsibility of the beam trigger counters.

3 List of publications in 2003

1) "Dual origin of light flashes in space"; V.Bidoli et al., Nature 422 (2003)680

2) "ALTEA: Anomalous Long Term Effects in Astronauts. A probe on the influence of cosmic radiation and microgravity on the central nervous system during long flights"; L.Narici et al., Adv.Space Res. vol 31 n.1 (2003)141

3) "Study of the radiation environment on MIR Space Station with SILEYE2 experiment"; M.Casolino et al., Adv.Space Res. vol 31 n.1 (2003)135

4) "Relative nuclear abundances measurements inside MIR and ISS with Sileye2 and Sileye3 experiments"; Proc. 28th International Cosmic Ray Conference (Tsukuba, Japan, 2003) SH 3.6 p.4245

5) "Light flashes observations on board MIR and ISS with Sileye experiments"; Proc. 28th International Cosmic Ray Conference (Tsukuba, Japan, 2003) SH 3.6 p.4161

References

1. G.Furano et al.: "Measurement of Nuclear Mass Distribution of Primary and Recoil Heavy Ions inside MIR Space Station with SilEye Silicon Detector", Proc. XXVI ICRC, Salt Lake City vol.5 p128 (1999).
2. S.Avdeev et al.:"The SilEye nuclei cosmic ray and eye light flash experiment onboard the Mir Space Station", Proc. XXVII ICRC, Hamburg (2001) p.1745.
3. M.Casolino et al.:"Cosmic ray measurements on board space station MIR with SILEYE-2 experiment", Proc. XXVII ICRC, Hamburg (2001) p.4011.
4. V.Bidoli et al.:"In-flight performances of SilEye-2 Experiment and cosmic ray abundances inside space station MIR"; Journal of Physics G: Nuclear and Particle Physics 27, 2051 (2001).
5. S.Avdeev et al.:"Eye light flashes on the Mir Space Station"; Acta Astronautica, 50, 511 (2002).
6. L.Narici et al.:"The ALTEA facility on the International Space Station"; Physica Medica Suppl. 1 17, 255 (2001).
7. M.Casolino et al.:"The Sileye/3-Alteino experiment on board the International Space Station"; Nucl.Phys. 113B, 88 (2002).
8. V.Bidoli et al.: "Dual origin of light flashes in space"; Nature 422 (2003)680.
9. P.Maponi et al.:"A syncitium model for the interpretation of the phenomenon of anomalous light flashes occurring in the human eye during space missions"; Nuovo Cim., 116B, 1173 (2001).
10. G. Horneck: "Radiobiological experiments in space: a review", Nucl. Tracks Radiat. Meas., 20, 185 (1992).

SUE

E. Burattini(Resp.), A. Grilli(Tecn.), F. Belloni(Bors.), D. Bettega (Ass.), P. Calzolari(Ass.), F. Malvezzi Campeggi(Ass.), F. Monti(Ass.), L. Tallone(Ass.), S. Crema, L. Doneda

The variation of the ozone layer observed in the last decades can lead to an increase in the UVB component of the solar spectrum transmitted onto the earth surface. Since the biological effectiveness of UV radiation is strongly wavelength dependent, even a low increase in the UVB irradiance can lead to a significant increase of its biological effects, especially at shorter wavelengths. It is then important to evaluate their dependence as a function of the dose at each wavelength. To this aim, in the framework of the SUE (Solar Ultraviolet Effects) experiment, we are carrying out a sistematic study of early and delayed biological effects induced in *in vitro* human cell cultures by monochromatic radiation in the UVB band (280÷320 nm) at the UV beamline of the DAΦNE-Light Synchrotron Radiation Facility.

The experimental hutch is equipped with a Jobin-Yvon monochromator where a holographic diffraction grating blazed at 250 nm allows to select photons in the range 200÷600 nm within a 0.1÷0.3% spectral band. The beam travels in air after a 38 mm diameter, 2 mm thick sapphire window and is focussed on the entrance slits of the monochromator by two remotely controlled Al-coated mirrors. Photons of wavelength shorter than 180 nm are not transmitted through the sapphire window, ensuring the absence of higher order contamination in the monochromatic beam at the exit of the monochromator.

The cell cultures are grown on the quartz base (13 mmm diameter) of small teflon cylinders. After the exit slits of the monochromator, a suitable sample holder allows to fix the teflon cylinder at the right distance for uniform (within 10%) spatial exposure. The photon distribution at the sample position is determined by microdensitometry on UV sensitive photographic plates.

Dosimetry is accomplished using a calibrated Hamamatsu Silicon photodiode sensitive in the range 200÷1200 nm whose active area is 1 cm^2. Before irradiation, at each wavelength, the power and the irradiance on the sample per unit of the current circulating in the DAΦNE electron ring are determined. During irradiation, the circulating current $I(t)$ is continuously monitored and the dose is calculated as the irradiance per unit of the circulating current multiplied by the $\int I(t)dt$. The linearity of the photodiode response versus $I(t)$ has been verified in the range 0.1÷1A.

In the two irradiation sessions perfomed, cultures of human hybrid cells CGL1 (HeLa x human skin fibroblast) were exposed to monochromatic beams of three different wavelenghts (285, 292 and 295 nm) in the dose range between 5 and 55 J/m^2.The power on the sample area per unit of the circulating current in a 2.5÷3 nm bandwidth was around 4 mW/A; the average irradiance during an exposure was 20 mW/m^2.

Treatment of the cell cultures after irradiation was performed at the Radiobiology Laboratory of the Department of Physics of the University of Milan. Three different biological effects have been studied as a function of the dose at each wavelength: survival of the irradiated cells, delayed reproductive death (i.e. cloning efficiency of the survived cells) and neoplastic transformation. We have found that the radiation effectiveness depends on the wavelength and increases at decreasing wavelength at all wavelengths (Fig.1, Fig.2, Fig.3).

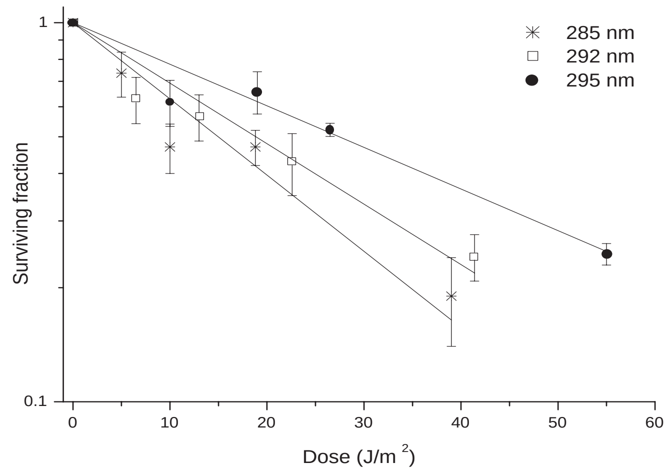

Figure 1: *Survival of the irradiated cells vs the dose.*

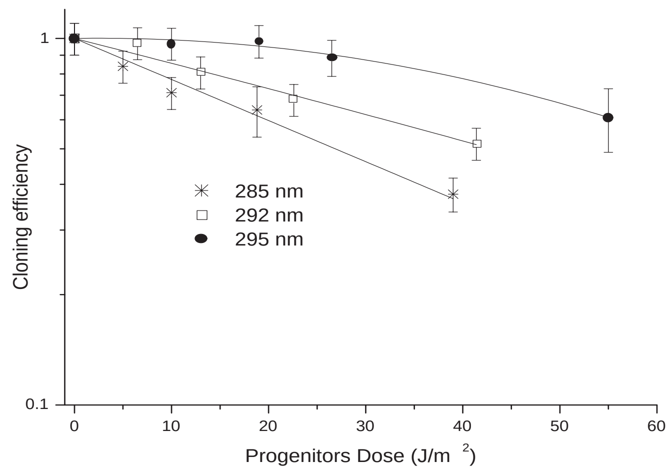

Figure 2: *Cloning efficiency of the survived cells vs the dose.*

Very interestingly, the rate at which the radiation effectiveness increases at decreasing wavelength is higher for the two delayed effects (delayed reproductive death and neoplastic transformation) than for the early effect (cell survival) (Fig.4). These results suggest that the action spectrum of UVB radiation may be different for delayed and early biological effects.

1 List of conference talks in 2003

1. P. Calzolari, F. Monti, *Studio di Effetti Biologici a Lungo Termine Indotti in cellule umane della linea CGL1 con fasci UVB monocromatici presso la linea UV di Luce di Sincrotrone dei LNF*, I Convegno Nazionale della Federazione Italiana per le ricerche sulle Radiazioni - Radiazioni in medicina e biologia: stato delle ricerche e applicazioni cliniche. Legnaro (Padova), 20-22 November 2003

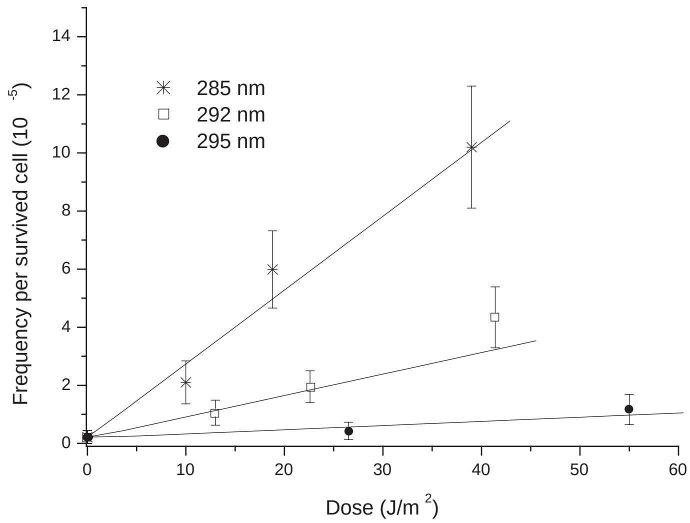

Figure 3: *Neoplastic transformation per survived cell vs the dose.*

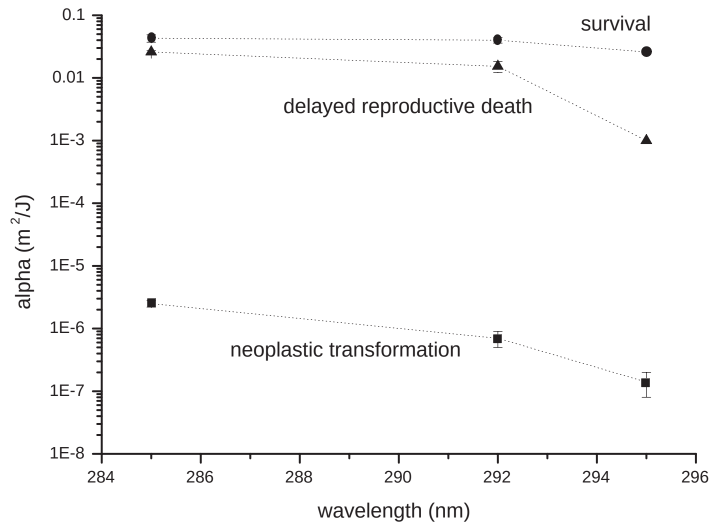

Figure 4: *Slope (*alpha*) of the curves for each biological effect vs wavelength.*

References

1. Stanbridge *et al*, Science **215**, 252 (1982)
2. J.L. Redpath *et al*, Rad. Res. **110**, 468 (1987)
3. Mendonca *et al*, Rad. Res. **131**, 345 (1992)
4. D. Bettega *et al*, Int. J. of Rad. Biol. **72**, 523 (1997)
5. J. Little *et al*, Int. J. of Rad. Biol. **74**, 663 (1998)
6. D. Bettega *et al*, Int. J. of Rad. Biol. **77**, 963 (2003)

TIBET

A. Balerna, E. Bernieri (Resp.), U. Denni (Tecn.) A. Esposito

1 Introduction

The TIBET (Tibet Investigation Base for Environmental Transformation studies) experiment is a feasibility study whose goal is to verify the possibility to install at the ARGO INFN laboratory in Tibet also a permanent laboratory where chemical and physical measurements related to climate and environment can be performed.
The Asian continent is one of Earth's areas where in the last decades a great economical and demographic growth has been observed. The environmental consequences of this growth are very complex and involve many different aspects among which the increase of pollution problems at a local and global scale. A given example is the immission into the atmosphere of aerosol and greenhouse gases and macroscopic events like ABC (Atmospheric Brown Cloud) that is a cloud composed by carbon particles, sulfates and other minor substances, able to modify atmosphere's transparency and light's spectral composition.
The effects due to pollution are not only local because, due to transport and circulation phenomena in the atmosphere, they can effectively influence the atmosphere and the environment of the whole Planet. The Central Himalayan range, the Karakoram range and the Tibetan plateau are very important regions from an environmental point of view and suitable for monitoring the health status of Earth.
In these regions it becomes very important to have different points where meteo-climatic monitoring can be performed and the chemical composition of the atmosphere studied, in order to follow, using also other instruments like mathematical and computer methods, the complex interactions related to transport mechanism of pollutants.
In the last few years many international programs like the United Nations Environment Programme (UNEP) and national institutions like the Comitato Ev-K2-Cnr and the INRM (Istituto Nazionale per la Ricerca Scientifica e Tecnologica sulla Montagna) have been working to realize a wide network to monitor environmental changes.
ARGO can probably be included as one of the main components of this network.
The TIBET experiment, which follows the previous experiment GEDI (Gamma Emission in Deep Ice) is a collaboration among INFN, INRM, Ev-K2-CNR, ISPESL, the University of Milano and University of Milano Bicocca. The experimental program is to perform a survey mission at the ARGO laboratory and some environmental measurements near the Nyenchen Thangla mountain chain, which is in the near northern side of the ARGO laboratory. In this program also in situ radioactivity measurements, using the detector and the whole system developed by the GEDI experiment, are included.

2 Activity in 2003

In 2003 using the portable gamma-ray spectrometer developed by the GEDI experiment, in situ radioactivity measurements where performed during a glacial perforation at the Lys glacier (Colle del Lys 4240 m a.s.l.- Monte Rosa, Alps) which has reached a depth of about 110 m.
During these measurements, the layer corresponding to the Chernobyl's accident in 1986 was probably found at a depth of about 30 m due to the presence of gamma emission from Cs-137 and the presence of Bi-214 at different depths probably related to some huge Saharian dust depositions

was also detected.
Due to the short time given for the in situ measurements (bad signal to noise ratios) new measurements on the ice cores corresponding to the found depths will be performed. If the results will be confirmed these will be the first in situ radioactivity measurements in ice core drillings which gave in real time the depths of the layers that can be used as time markers for glaciological studies.

3 Work program for the year 2004

In April and May 2004 our group will be involved in in situ radioactivity measurements on the northern side of the Everest mountain during a scientific-mountaineering expedition organized to celebrate the 50th anniversary of K2 mountain first summit by an Italian team. The huge scientific activity, linked to this and other two expeditions that will be realized during the 2004 and that involves more than 50 researchers coming from different Italian Insitutes and Universities, will be financed by the INRM. INRM charged the TIBET experiment with the responsibility of technical coordination of the scientific part af all these expeditions.
In autumn 2004 the survey mission to the ARGO laboratory will be performed.

4 Talks by LNF authors in 2003

1. E. Bernieri, Invited talk on “Chemical Pollution in the Cryosphere” at the GDIN (Global Disaster International Network) International Conference, Rome 17-21 June 2003

References

1. A. Balerna, E. Bernieri, M. Chiti, U. Denni, A. Esposito, M. A. Frani and V. Tullio, Nuclear Instrum. and Meth. **A 512**, 631 (2003).
2. A. Balerna, E. Bernieri, M. Pecci, S. Polesello, C. Smiraglia and S. Valsecchi, Atmospheric Environment **37**, 1573 (2003).

BTF

B. Buonomo (Bors.), G. Mazzitelli (Resp.), P. Valente (Art.23)

1 Description of the DAΦNE BTF 2003 Activities

The Beam Test Facility (BTF) has been commissioned in 2002 and started first regular data taking with users from the end of 2002 [1]. The facility, optimized for the production of single electron-positron, has been operated in a wide range of multiplicity and energy. The beam characteristics, the operation mode, and the main diagnostics tools and detectors are described with some details elsewhere [2, 3]. The operated parameters (in year 2003) of the facility are summarized in Tab. 1.

Parameter	Value
Energy range	50÷750 MeV (e^-/e^+)
n_{average}	$1 \div 10^7$
Pulse Duration	1-10 ns
Repetition Rate	0÷50 Hz
Energy Resolution	$\simeq 1\%$
Spot Size	$\simeq 2 \times 2$ mm

Table 1: The year 2003 operated parameters of the DAΦNE BTF.

The 2003 has been divided in three periods:

- During the DAΦNE **LINAC mantenance**, a number of tools and facilities were installed in the BTF area: a complete GAS system; a motorized trolley moving on rails, that can be operated remotely from the BTF control room; a permanent DAQ system for the main diagnostics devices (calorimeter, Cerenkov counter, scintillating fiber profilometer); a remotely controlled High Voltage power supply; structural intranet networking and DAΦNE control system consoles and PC's. Some of this improvements will be briefly described in Sec. 3.
- **Dedicated runs**, from March the 17^{th} to June the 18^{th} during DAΦNE main rings upgrade: in this period only the DAΦNE LINAC and BTF were operated. The beam was delivered up to 69% of the time, while the 26% has been dedicated to installation/disinstallation of the experiments. Only a 5% of this period was lost for faults or operation problems. Due to problems with the water for the cooling system of DAΦNE, this dedicated period was extended to the end of August.
- **Parasitic runs**, from September the 18^{th} to the end of the year, during the data taking with FINUDA: the priority for the LINAC was the injection in the DAΦNE main rings, so that the maximum time delivered to experiments during this period was around the 50%.

2 Users Experience

During year 2003 many different test-beams and experiments have been operational at the BTF, with very different requirements and beam conditions, as briefly reported below:

AIRFLY [4]: this experiment is dedicated to the measurement of AIR FLourescence Yield and lifetime; it requires a multiplicity around 10^3 electrons per pulse, 1 ns pulse-length, variable energy in the range 50-700 MeV, with as low as possible contamination from the low energy particles background to the main beam. Beam has been delivered for two weeks in the dedicated period, and one during parasitic operation (this work was partially funded by Transnational Access to major Research Infrastructures, TARI, project 29 and 42).

LCCal [5]: energy resolution and linearity study of a hybrid electromagnetic calorimeter. A single electron distribution has been provided in a wide range of energy. One week of dedicated beam-time has been allocated. The remote-controlled trolley has been effectively used to map calorimeters cells equalization.

AGILE [6]: performances study of the silicon tracker device installed in the "Astro-rivelatore Gamma a Immagini LEggero" gamma ray detector. A multiplicity of a few electron/positron has been delivered for a week of dedicated runs. An example of the beam bidimensional profile measured by this device, using a silicon strip readout of 242 μm pitch, is shown in Fig. 1: the beam has a nearly Gaussian distribution in both x and y with $\sigma \approx 2$ mm.

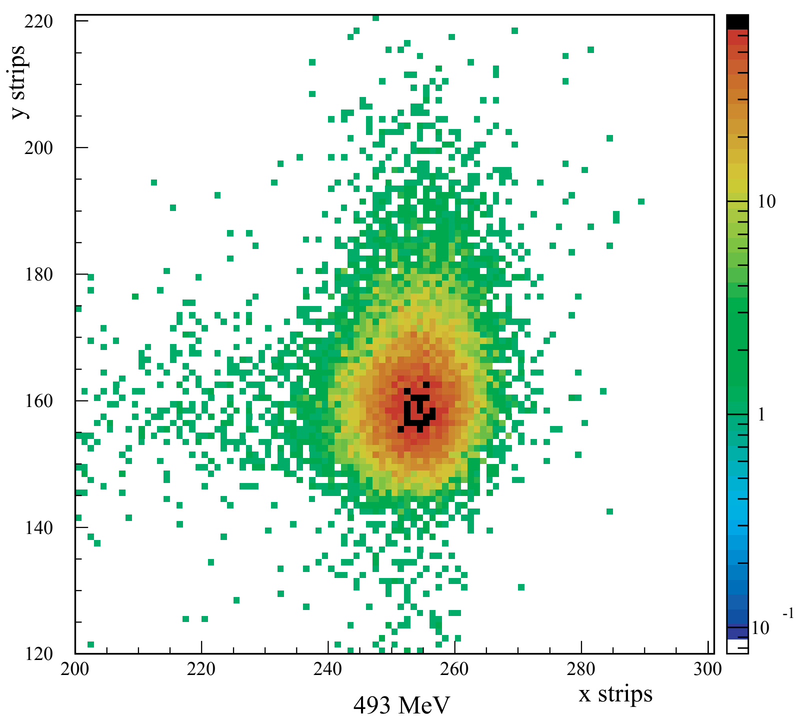

Figure 1: The beam profile as measured by the AGILE silicon strip tracker for a low multiplicity, E =493 MeV, electron beam with optimized focussing of the line. The strip pitch is 121 μm, the readout pitch is 242 μm corresponding to one pixel in the plot: the beam spot size is of order $\sigma_x \approx \sigma_y \approx 2$ mm.

LHCb [7]: test of efficiency for the MWPC and GEM detectors that will be installed in

Large Hadron Collider beauty experiment. A multiplicity of a few electrons has been delivered at the maximum repetition rate of 49 Hz. Four weeks of beam-time, two in the dedicated period and two in the parasitic operation, were allocated.

CaPiRe [8]: the test consists in mapping the efficiency of large glass chamber as a function of the beam impinging position, gas mixture and repetition rate. Beam has been delivered for two weeks in dedicated mode and one week during the parasitic operation.

RAP [9]: measurement of particle energy conversion efficiency in acoustic vibration of the fundamental modes of a cryogenic detector, as a function of its thermodinamic temperature. "Rivelazione Acustica di Particelle" needs a large number of particles in the beam, in order to release more then 100 TeV energy in the detector. Two weeks of parasitics runs have been allocated. The experiment also took data sharing beam-time with other two experiments (SIDDHARTA, FLAG) simultaneously installed in the facility.

SIDDHARTA [10]: test of triggerable Silicon Drift Detector in order to replace the standard CCD detector in nuclear physics and avoid the asynchronous background. A few tens of electrons impingin a target of different materials were used to produce synchronous background. Fe and Sr sources were instead used to produce the asynchronous background. This experiment has been operational for three weeks of dedicated runs and two weeks of parasitics runs (work partially funded by Transnational Access to major Research Infrastructures, TARI, project 40). The experiment was installed on the remotely controlled table and have been in time-sharing operation with the RAP and FLAG experiments.

FLAG [11]: test of very high sensitivity beam fluorescence detector. Different fluorescence targets were tested in very low current beam conditions. The experiment has been installed in the second (straight) beam line of the BTF, and is able to run in a parasitic way together with any experiment installed on the main beam line.

NANO [12]: study of the particle channeling effect via a bent nanotube. Well collimated positron were sent to a nanotube sample optimally aligned by a goniometer system. The profile of channeled positrons was monitored 5 meters far from the sample, by means of the scintillating fiber hodoscope (see in the following section) installed on the beam line. One week of dedicated runs has been allocated (work partially funded by Transnational Access to major Research Infrastructures, TARI, project 23).

CRYSTAL [13]: study of the particle channeling effect via a bent crystal. Positrons were sent to a crystal sample optimally aligned (with as setup similar to the one of the NANO experiment). The profile of channeled positrons was monitored 5 meters far from the sample, by means of the BTF scintillating fiber hodoscope. Four weeks of parasitic runs have been allocated (work partialy funded by Transnational Access to major Research Infrastructures, TARI, project 35).

3 Diagnostics and Facility Improvements

The large spectra of applications of the BTF pushed us to improve both the infrastructure and the diagnostics devices of the facility.

Tools and infrastructure improvements. Some new tools were installed during year 2003 to improve the facility capabilities:

- a GAS system composed of four independent stainless steel lines, connecting to a gas-packs area, located just outside the experimental area, providing four pressure-reduced heads dedicated to different kind of gases: carbon dioxide, isobutan, ethane and argon (or noble gases).
- A motorized, remotely controlled trolley (2×1 m^2 area). The table is camera monitored, and can perform two kinds of movements, with a millimiter positioning accuracy: horizontally,

on two rails running transversally with respect to the beam direction, in order to move the installed apparata in and out from the beam-line; and vertically, in order to center the beam position or to perform position scans.

- A permanent DAQ system, consisting of 64 TDC and ADC channels, acquired by a dedicated, fast, VME CPU. The acquisition is embedded in the DAΦNE control system so that the beam properties can be easily monitored on-line using dedicated tools, fully integrated in the DAΦNE control environment. The data on the beam characteristics can also be easily accessed through the DAΦNE data-logging system.
- 48 channel High Voltage CAEN SY2527 for negative powering and 40 channel CAEN SY127 for positive powering.
- Dedicated switched intranet for users device connection, LNF-LAN and WAN connection is also available; two DAΦNE control system consoles and three general purpose PC's.

New diagnostic devices. The main upgrade to the diagnostics of the BTF beam was the design, construction, test and operation of a scintillating fiber hodoscope for the monitoring of the beam spot size and position with millimetric accuracy [14)]. Since high-fluorescence metallic flags are not sensitive at very low beam intensities, a position sensitive particle detector is needed, in particular for the single particle operation mode. The detector was conceived keeping in mind the wide range of beam conditions (in energy and multiplicity), the typical beam spot characteristics (with an optimum size of 2×2 mm^2), and the need for a non-destructive, easy to implement and compact detector.

The hodoscope is composed by two stacks of 1 mm diameter cladded scintillating fibers (Pol.Hi.Tech 0046), to have the x and y beam profile. Each stack is composed by four layers, staggered by half fiber diameter, in order to minimize dead-zones and to have a good light yield even with a non-optimal coupling to the photocathode. Each view of the two views is composed by 16 bundles of three aligned four-layers fiber stacks, for a total active area of 48×48 mm^2; the fibers are glued with optical cement BICRON BC600. Each bundle of fibers is then coupled, by means of a grooved PVC mask, to the surface of a 16 pixels (4.2×4.2 mm^2 each) multi-anode photomultiplier tube (Hamamatsu H6568), operated at a typical gain of 2×10^6 and read-out by a charge-integrating ADC in the BTF acquisition system (a picture of the assembled detector is shown in Fig. 2).

An example of the transverse beam profile distribution, obtained with the two detectors mounted with the fibers running along the horizontal and vertical directions is shown in Fig. 2, for a well focussed, 493 MeV, electron beam, with an average of 1-2 particles per pulse.

4 Future Plans and Conclusions

The Beam Test Facility showed very good performances, both from the point of view of operation reliability and of the flexibility in order to answer very different experimental needs: electron and positron beams were produced in the energy range from 50 to 700 MeV, in single particle mode as well as in at high intensity. Moreover, the improved beam diagnostics was effectively exploited both to monitor the beam conditions and to adjust them to the experimental requests. In some cases, the BTF diagnostics detectors have been fully used by the experimental groups to get informations on the beam properties. All the experiments were satisfied, as testified by the publication of their first results [4, 5, 7, 8, 9, 10)].

In order to improve the facility duty-cycle an upgrade [15)] has been planned for March 2004 during the FINUDA experiment rollout. The installation of a berillium tiny window is also planned in order to decrease the beam divergence at very low energy introduced by the present

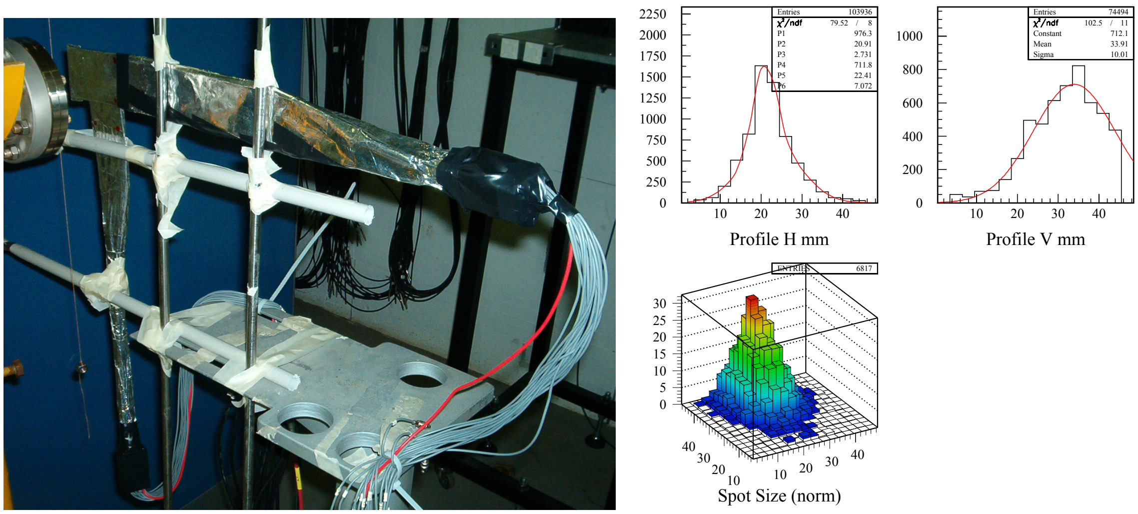

Figure 2: Left: photograph of the two-view scintillating fibers hodoscope mounted at the exit of the BTF vacuum pipe. Right: the horizontal (top left), vertical (top right) and two-dimensional (bottom) beam profile as measured by the scintillating fiber hodoscope for a low multiplicity, 493 MeV, electron beam (units are mm).

output window (1.5 mm thick aluminum). In order to improve the multiplicity tuning capability, vertical slits will be added to the BTF line. In order to improve the beam diagnostics at high intensity, an high sensitivity toroidal beam current monitor will be mounted.

Finally, a collaboration with the AGILE group started in order to install a **photon tagged source** and a permanent silicon beam profile monitor. A collaboration also started in order to study a **linac-based neutron source** (work partialy founded by Transnational Access to major Research Infrastructures, TARI, project 44) and the first test wil be performed during 2004.

5 List of Conference Talks by LNF Authors in Year 2003

1. P. Valente, Seminario generale presso LNF, Jan. 11, 2003, Frascati, Italy.
2. P. Valente, Seminario generale presso “La Sapienza”, Jan. 16, 2003, Roma, Italy.
3. P. Valente, Seminario generale presso Roma III, Jan. 11, 2003, Roma, Italy.
4. G. Mazzitelli, DIPAC 2003 , May 23, 2003, Mainz, Germany.
5. G. Mazzitelli, 26^{th} Meeting of the LNF Scientific Committee, May 30, 2003, Frascati, Italy.
6. G. Mazzitelli, PAC 2003 , May 12-16, 2003, Portland, USA.
7. P. Valente, Frontier Detector for Frontier Physics 2003 , Jun. 18, 2003, Elba, Italy.
8. G. Mazzitelli, SIDDHARTA Collaboration Meeting, Jun. 27, 2003, Frascati, Italy.
9. G. Mazzitelli, Rapporto Attivita' Consiglio dei Laboratori, Jul. 8, 2003, Frascati, Italy.
10. P. Valente, Commissione Nazionale I, Sep. 22, 2003, Lecce, Italy.
11. G. Mazzitelli, Commissione Nazionale II, Nov. 19, 2003, Roma, Italy.

References

1. G. Mazzitelli *et al.*, BTF report in *LNF Annual Report 2002*, LNF-03-010(IR).

2. G. Mazzitelli and P. Valente, *Commissioning of the DAFNE Beam Test Facility*, LNF-03-003(P).

3. G. Mazzitelli *et al.*, *Commissioning of the DAFNE Beam Test Facility*, Nucl. Instrum. Meth. A **515** (2003) 516-534.

4. F. Arciprete *et al.*, *Air Fluorescence Induced by Electrons in a Wide Energy Range*, in proceding of 28^{th} ICRC (2003).

5. S. Bertolucci *et al.*, *First tests of LCCAL prototype at BTF*, ECFA/DESY Workshop (2003).

6. M. Prest *et al.*, *The AGILE silicon tracker: an innovative γ-ray instrument for space*, Nucl. Instrum. Meth. A **501** (2003) 280-287.

7. M. Alfonsi *et al.*, *Triple GEM detector operation for high rate particle triggering*, Frontier Detector for Frontier Physics (2003), Elba, Italy. Nucl. Instrum. Meth. A **518** (2004) 106-112

8. S. Calcaterra *et al.*, *Test of large area glass RPCs at the DAFNE Test Beam Facility (BTF)*, submitted to Nucl. Instr. and Meth. A.

9. S. Bertolucci *et al.*, *RAP: Acoustic detection of particles at the DAΦNE BTF*, Frontier Detector for Frontier Physics (2003), Elba, Italy. Nucl. Instrum. Meth. A **518** (2004) 261-263.

10. C. Curceano (Petrascu) *et al.*, *Future precision measurements on kaonic hydrogen and kaonic deuterium with SIDDHARTA*, in proceeding of Workshop on Hadronic Atoms, Trento, Italy (2003).

11. D. Filippetto, *Studio sperimentale della radiazione emessa da schermi fluorescenti attraversati da fasci di elettroni relativistici*, Tesi di Laurea in Ingegneria Elettronica (2003), Universita degli Studi di Roma "La Sapienza".

12. V Biryukov *et al.*, *Tari 23 project*, Private Comunication.

13. V Biryukov *et al.*, *Tari 35 project*, Private Comunication.

14. M. Anelli, G. Mazzitelli, P. Valente, *A scintillating fiber beam profile monitor for the DAΦNE BTF*, LNF Note in preparation.

15. G. Mazzitelli *et al.*, *DAΦNE Beam Test Facility Upgrade Proposal*, DAFNE Technical Note BTF-1 (2003).

DAΦNE

The DAΦNE Team: D. Alesini, G. Benedetti, M.E. Biagini, C. Biscari, R. Boni, M. Boscolo,A. Clozza, G. Delle Monache, G. Di Pirro, A. Drago, A. Gallo, A Ghigo, S. Guiducci, M. Incurvati,C. Ligi,F. Marcellini, G. Mazzitelli, C. Milardi, L Pellegrino, M. Preger, P. Raimondi (Resp), R. Ricci, C. Sanelli, M. Serio, F. Sgamma, A. Stecchi, A. Stella, C. Vaccarezza, M. Vescovi, M. Zobov

The DAΦNE Technical Staff: G. Baccarelli, G. Baldini, P. Baldini, A. Battisti, A. Beatrici, M. Belli, B. Bolli, G. Ceccarelli, R. Ceccarelli, A. Cecchinelli, S. Ceravolo, R.Clementi, O.Coiro, S.De Biase, M.De Giorgi, N.De Sanctis, R.Di Raddo, M.Di Virgilio, G.Ermini, G.Fontana, U.Frasacco, C.Fusco, F.Galletti, O.Giacinti, E.Grossi, F.Iungo, R.Lanzi, V.Lollo, V.Luppino, C.Marchetti, M.Marchetti, C.Marini, M.Martinelli, M.Masciarelli, A.Mazzenga, M.Monteduro, A.Palleschi, M.Paris, E.Passarelli, V.Pavan, S.Pella, D.Pellegrini, R.Pieri, G.Piermarini, S.Quaglia, F.Ronci, M.Rondinelli, F.Rubeo, M.Sardone, M.Scampati, G.Sensolini, A.Sorgi, M.Sperati, A.Sprecacenere, P.Tiseo, R.Tonus, T.Tranquilli, M.Troiani, V.Valtriani, R.Zarlenga, A.Zolla

1 Introduction

DAΦNE has been the first "electron-positron factory" in operation. With this name we call the storage rings for electrons and positrons delivering a high rate of mesons for high resolution experiments requiring an extremely large number of events. In order to reach such high rates, the factories are designed to work at the energies of the meson resonances, where the production cross section peaks. Examples of such resonances are the Φ near 1 GeV, the J/ψ around 3 GeV and the Υ near 10 GeV, which decay into mesons containing the "strange", "charm" and "beauty" quarks respectively. However, it is not sufficient to exploit the high cross section to obtain the required production rate: it is also necessary that the collider luminosity (the number of events per unit time of the reaction under investigation divided by its cross section weighted by the acceptance of the detector) is very high, between one and two orders of magnitude larger than that obtained in the conventional colliders with a single ring where electrons and positrons run on the same orbit in opposite directions.

DAΦNE is the heart of a system consisting of a double ring collider, a linear accelerator (LINAC) an intermediate damping ring to make injection easier and faster and 180 m of transfer lines connecting these machines. The geometry of this accelerator complex has been designed to reuse the buildings hosting ADONE (the 3 GeV center of mass electron-positron collider in operation at LNF from 1969 to 1993) and its injector, a LINAC used both to refill the collider and to perform nuclear physics experiments. The complex is shown schematically in Fig. 1.

The reason why a double ring collider can deliver a much larger luminosity than a single ring one is the following: in an electron-positron storage ring both beams consist of a number N of short "bunches". Since in a single ring the bunches, due to the invariance of the Lorentz force in the absence of electric fields with respect to particles of opposite charge and velocity, follow the same trajectory, they cross in 2N points. The maximum obtainable luminosity is limited by the electromagnetic beam-beam interaction. The effects of this interaction can be reduced with a very strong focussing (called "low-β") at the points where the beams cross, obtained by means of quadrupole doublets or triplets in the Interaction Region (IR). These magnetic structures require space and excite chromatic aberrations which must be corrected elsewhere in the ring. It is clear that in a small machine like DAΦNE only two of these regions can be realized, and therefore only a single electron bunch and a single positron one could be stored in a single ring. A larger number of

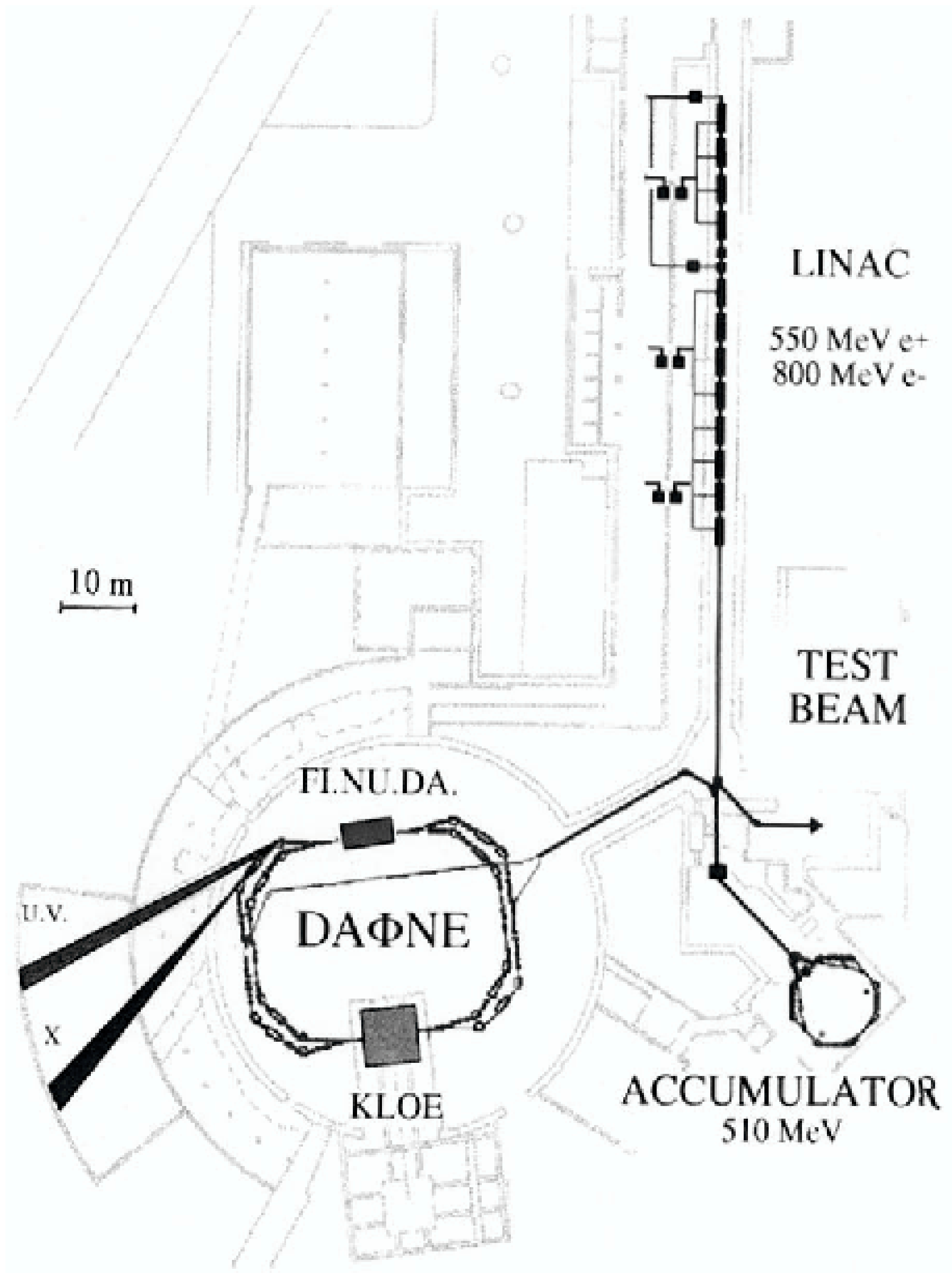

Figure 1: *The layout of the DAΦNE accelerator complex inside its buildings.*

bunches could be stored only if more low-β points would be available, twice the number of bunches stored in each beam.

This limitation does not hold for a double ring collider, consisting in two separate rings crossing in two low-β points. The number of bunches that can be stored in such a collider is limited only by the geometry of the IR's.

In DAΦNE the trajectories followed by the two beams cross at the interaction point (IP) at an angle of 1.5 degrees in the horizontal plane. A positron bunch leaving the IP after crossing an electron one will reach the following electron bunch at a distance of half the longitudinal separation between bunches from the IP. However, due to the horizontal angle between the trajectories of the two beams, the distance in the horizontal direction between the two bunches is equal to the horizontal angle times half the longitudinal distance between the bunches in the beam. The beam-beam interaction can be harmful to beam stability even if the distance in the horizontal direction between bunches of opposite charge is of the order of few bunch widths at points where the β function is high and this sets a lower limit on the bunch longitudinal separation and therefore on the number of bunches which can be stored in the collider. For DAΦNE the minimum separation is 80 cm, and the maximum number of bunches to be stored in each ring is 120. This number determines the frequency of the radiofrequency cavity which replaces at each turn the energy lost in synchrotron radiation, which must be 120 times the revolution frequency. The luminosity of the collider can therefore be up to 120 times larger than that obtainable in a single ring with the same size and optical functions.

Crossing at an angle could in principle be a limitation to the maximum single bunch luminosity. In order to make the beam-beam interaction less sensitive to this parameter and similar to the case of single ring colliders where the bunches cross head-on, the shape of the bunches at the IP is made very flat (typical r.m.s. sizes are 30 mm in the longitudinal direction, 2 mm in the horizontal and 0,02 mm in the vertical one).

Of course the double ring scheme with many bunches has also important drawbacks: the total current in the ring reaches extremely high values (5 A in the DAΦNE design) and the high power emitted as synchrotron radiation ($\approx$50 KW) needs to be absorbed by a complicated structure of vacuum chambers and pumping systems in order to reach the very low residual gas pressure levels necessary to avoid beam loss. In addition, the number of possible oscillation modes of the beam increases with the number of bunches, calling for sophisticated bunch-to-bunch feedback systems.

The structure of the collider consists of two rings, shown schematically in Fig. 2.

Both rings lay in the same horizontal plane and each one consists of a long external arc and a short internal one. Starting from the IP the two beams travel together inside a common vacuum chamber and their distance increases until it becomes $\approx$12 cm at the level of the magnetic separators called "splitters" (SPL). These are special magnets with two regions of opposite field which deflect the two beams in opposite directions, allowing them to reach the separate vacuum chambers of the long and short arcs. Each arc consists of two "almost achromatic" bends (deflecting the beam by 81 degrees in the short arc and 99 degrees in the long one) similar to those frequently used in synchrotron radiation sources, with a long straight section in between. Each bend consists of two dipoles, three quadrupoles, two sextupoles and a wiggler. This structure is used for the first time in an electron-positron collider and it has been designed for the particular requirements of DAΦNE: the amount of synchrotron radiation power emitted in the wigglers is the same as in the bending magnets and the wigglers can be used to change the transverse size of the beams. The increase of emitted power doubles the damping rates for betatron and synchrotron oscillations, thus making the beam dynamics more stable, while the possibility of changing the beam sizes makes the beam-beam interaction parameters more flexible.

The straight section in the long arc houses the pulsed magnets used to store into the rings the bunches coming from the injection system, while in the short arc straight there are the radiofrequency cavity and the equipment for the feedback systems which are used to damp longitudinal and transverse instabilities.

The most delicate part of the whole structure are the IR's. The collider can host two experiments, even if up to now only one at a time can get useful luminosity. Three detectors have been realized, KLOE, DEAR and FINUDA. The first two have been installed in the two IP's, while the third has been assembled in its pit inside the DAΦNE hall and has been installed this year in the IR that was occupied by DEAR. The detectors of KLOE and FINUDA are surrounded by large superconducting solenoid magnets for the momentum analysis of the decay particles and their magnetic fields represent a strong perturbation on the beam dynamics. This perturbation tends to induce an effect called "beam coupling", consisting in the transfer of the betatron oscillations from the horizontal plane to the vertical one. If the coupling is not properly corrected, it would give a significant increase of the vertical beam size and a corresponding reduction of luminosity. For this reason a superconducting solenoid magnet with half the field integral of the detector one and of opposite direction is placed near each splitter in such a way that the overall field integral in the IR's vanishes. However, this is not sufficient to obtain full compensation of the beam coupling induced by the main solenoids. In the case of KLOE the low-β at the IP was originally designed with two quadrupole triplets. Due to the flat shape of the beam at the IP, the low-β is realized only in the vertical plane. The quadrupole cannot be of the conventional electromagnetic type for two reasons: the first is that the iron of the joke would degrade the flatness of the magnetic field in the detector and the second is that the overall transverse size of a conventional quadrupole is at least twice its useful aperture. Therefore quadrupoles realized with permanent magnets have been built, which exhibit a surprisingly good field quality, very small transverse size and are fully transparent to external fields. The region of space around the IP occupied by machine elements, which is unavailable for the detection of decay particles by the experiment consists in two cones with the vertex at the IP and a half aperture of only 9 degrees. In order to obtain a good compensation of the above mentioned coupling effects induced by the solenoids, these quadrupoles are rotated around their longitudinal axis by angles between 10 and 20 degrees and are provided with actuators to finely adjust their position and rotation.

The structure of the FINUDA IR is quite similar. Since its superconducting solenoid magnet has half the length (but twice the field) of the KLOE one, the low-β focusing at the IP is obtained by means of two permanent magnet quadrupole doublets inside the detector and completed with two other conventional doublets outside. Both the IR's have been further modified during the 2003 shutdown, as will be described in detail in the following sections.

The DEAR experiment, which is was installed on the IR opposite to KLOE, took data during the years 2002-2003 and was dismounted to allow for the roll-in of FINUDA. The DEAR detector did not need magnetic field and therefore only conventional quadrupoles were used.

Two synchrotron radiation lines, one from a bending dipole and the other from the wiggler have also been realized by the DAΦNE-LUCE group.

The vacuum chambers of the arcs have been designed to stand the high level of radiation power emitted by the beams (up to 50 KW per ring): they consist of 10 m long aluminum structures built in a single piece: its cross section exhibits a central region around the beam and two external ones, called the antechambers, connected to the central one by means of a narrow slot. In this way the synchrotron radiation hits the vacuum chamber walls far from the beam and the desorbed gas particles can be easily pumped away. The chambers contain water cooled copper absorbers placed where the radiation flux is maximum: each absorber has a sputter ion pump below and a titanium sublimation pump above.

The single cell copper radiofrequency cavities, one in each ring, are capable of running at 250 KV and are designed with particular care to avoid high order modes which could induce longitudinal instabilities in the particular multibunch structure of the beams. This is obtained by means of external waveguides terminated on 50Ω loads. A sophisticated longitudinal feedback has however been built to mantain a reasonable safety margin on the threshold of multibunch instabilities. The system is based on the digital signal processing technique and acts on each single bunch individually. Additional feedback systems on the vertical betatron motion have been also realized following the observation of coherent instabilities during the collider operation.

The correct superposition of the beams at the IP is of course of critical importance for the luminosity of the ring. For this reason, 46 beam position monitors are available in each ring and 31 small dipoles can be used to steer the beam and correct orbit distortions caused by alignment errors or wrong currents in the magnetic elements by means of sophisticated software procedures implemented in the Control System of the collider. Additional beam diagnostics are two synchrotron radiation outputs, from which the transverse and longitudinal size of the beam can be measured, total beam current monitors and strip-line pickups delivering the charge of each bunch.

In a low energy electron-positron collider, such as DAΦNE, the lifetime of the stored current is mainly limited by the Touschek effect, namely the particle loss due to the scattering of the particles inside the bunches. In the present operating conditions it is of the order of half an hour. It is therefore necessary to have a powerful injection system, capable of refilling the beam without dumping the already stored one. In addition, flexibility of operation requires that any bunch pattern can be stored among the 120 available buckets. The injection system of DAΦNE is therefore designed to deliver a large rate of particles in a single bunch at the working energy of the collider.

It consists of a linear accelerator (LINAC, see Fig. 1) with a total accelerating voltage of 800 MV. In the first section, electrons are accelerated to ≈250 MeV before hitting a tungsten target (called positron converter) where positrons are generated by bremsstrahlung and pair production with an efficiency of ≈1%. The positrons exit from the target with an energy of few MeV and are then accelerated by the second section of the LINAC to their final energy of ≈0.51 GeV. The positrons are then driven along a transfer line and injected into a small storage ring, called Accumulator, at a frequency of 25 Hz. Up to 19 positron pulses are stacked into a single bucket of the Accumulator, then injection stops and the bunch damps down to its equilibrium beam size and energy spread, which are much smaller than the LINAC ones. Damping takes ≈0.1 seconds and then the beam is extracted from the Accumulator and injected into the positron main ring at an overall repetition rate of 1 Hz. A powerful and flexible timing system allows the storage of any desired bunch pattern in the collider. In the electron mode, the converter is extracted from the LINAC and electrons are directly accelerated to 0.51 GeV and injected into the Accumulator in the opposite direction with respect to positron operation. They are then extracted like in the positron case and injected into the electron main ring through the second transfer line.

The Accumulator has been introduced for the following reasons. The first is that the LINAC can deliver pulses of 10 ns with a charge of ≈1 nC. Since the design charge of the main ring at the maximum luminosity is 1.5 μC and the longitudinal acceptance of the main rings is only 2 ns, the number of pulses necessary to fill the ring is of the order of 104. In order to avoid saturation it is therefore necessary that at each injection pulse a fraction smaller than 10^{-4} of the already stored beam is lost, and this is not easy to achieve. The Accumulator instead can work with a lower frequency RF cavity and therefore with a larger longitudinal acceptance. In this way the full charge coming from the LINAC can be stored. The number of pulses into the Accumulator is only 19, and after damping the whole charge stacked into an Accumulator bunch can be stored into the main ring. In this way a single main ring bucket can be filled with only one pulse from the Accumulator, reducing to 120 the number of injection pulses into each main ring. As an additional benefit, the transverse beam size and energy spread of the beam coming from the Accumulator are at least one order of magnitude smaller than those of the LINAC beam, and this strongly reduces the aperture requirements of the main ring and, as a consequence, the overall cost of the collider.

In the following section the activities carried on during the year 2003 are described in detail.

2 Year 2003 activity

In 2003 a long shutdown (from January 2003 to July 2003) was devoted to important modifications of the rings hardware. New assemblies were realized for both IR's and the FINUDA magnetic detector was rolled in into IR2. Two superconducting solenoids, equal to the KLOE IR ones, have been installed in IR2 to cancel out the overall field integral. In summary, the following items have been addressed:

- new KLOE IR;
- new FINUDA IR;
- better detector shielding;
- additional quadrupoles for machine tunability;
- improved injection kickers;
- ion clearing electrodes modifications;
- bellows and scrapers modifications;
- magnetic measurements on a new spare wiggler and subsequent modifications on the 8 wigglers;
- 3rd harmonic cavity test.

2.1 KLOE IR

Major modifications to the KLOE IR have taken place. It has been extracted from the detector and reassembled according to a new design, with a modified optics and supports in order to decrease the IP β functions, optimize background rejection and provide variable quadrupole rotation to operate at different magnetic fields (from 0 to maximum) in the solenoids. This will allow obtaining a better correction of coupling in the machine for any value of the KLOE solenoidal field. It makes also possible to run the machine with the KLOE solenoid off, in order to guarantee the maximum flexibility to the collider operation. The mechanics has been modified in order to allow for the four PM quadrupoles to rotate by 135 degrees, so that it will be possible to run DAΦNE with the KLOE solenoid off and to change the sign of the quadrupole focusing. This allows realizing a detuned lattice, similar to that used for the 2001-2002 operation, when running with a single IP. This rotation is performed by stepping motors and remotely controlled. The vacuum chamber has been modified with a new structure in beryllium alloy (AlBeMet) similar to the existing one but shorter, in order to allow for the insertion of two new beam position monitors. Tungsten masks have also been installed to better shield the detector from machine background. The IR lattice has also been changed: from a triplet to a doublet structure. The first quadrupole (QF i.e. focusing in the horizontal plane) of the old triplet has been removed and the third one has been reinforced with another quadrupole to get a factor 1.5 higher integrated gradient. In such a way the old FDF triplet has been converted into a DF doublet. The DF scheme allows obtaining the same IP β_y^* with a lower chromaticity, leading to longer beam lifetimes and better beam-beam performances. Moreover it will be possible to decrease in the future the IP β_x^* from the present value of 2.7 m down to 1.5 m. This is needed to double the number of colliding bunches (from 50 to 100) in the KLOE configuration without losing luminosity because of the parasitic crossings. The FDF scheme was adopted in the original DAΦNE design in order to allow for a good beam separation at the splitter magnets with a low value of the horizontal crossing angle (about 12.5 mrad), while the DF solution needs an angle of the order of 15 mrad. However, during recent runs, it has been shown that a crossing angle as large as 15 mrad can be used without performance limitations. Fig. 3 shows the new KLOE IR PM quadrupoles under assembly.

2.2 FINUDA IR

For what concerns IR2, where the FINUDA detector has been installed, a new thin Be chamber with four PM quadrupoles has been inserted in the detector. The original design has been improved by adopting some of the solutions used for the KLOE IR. As for the KLOE IR the mechanics has been modified in order to allow for full rotation of the PM quadrupoles. The four conventional quadrupoles outside the detector have also been equipped with rotating supports, allowing rotation in a range of 23 degrees, corresponding to the difference between the solenoidal field on and off. Fig. 4 is a picture of the present IR during its insertion into the detector.

2.3 Wiggler modifications

Since the first operation of DAΦNE, it appeared clearly that the wigglers were a strong source of non linearities in the machine lattice. The dependence of the betatron tunes on the RF frequency with all sextupoles off, expected to be linear for an ideal machine, exhibited a strong curvature, which almost disappeared when the rings were tuned on a configuration with sextupoles off. Moreover, in fall 2002, an experiment was performed by measuring the tunes as a function of beam displacement in the wigglers realized with localized orbit bumps in the horizontal plane. The result was the the wigglers contribute a strong octupole term to the beam dynamics, due to the combination of a decapole term in the wiggler field and the wiggling trajectory of the beam inside it. Since all the wigglers are operational in DAΦNE, the decision was taken to purchase from the same factory a spare wiggler built on the same design and with the same materials together with 14 mm thick plates of the the same rectangular shape of the poles. The goal was to machine the plates with a shape capable of increasing the width of the good field region, thus reducing the higher order terms in the wiggler field and substantially increasing the dynamic aperture of the ring. The wiggler was built by Danfysik and shipped to LNF in December 2002. Figs. 5 and 6 show the wiggler inside the magnetic measurements hall, equipped with a Hall probe positioning system with 4 degrees of freedom and an accuracy of 10 m.

The structure of the magnet, consisting of two C-shaped supports on each side, does not allow the measurement of a complete map in the horizontal symmetry plane with a single probe, as in the case of the measurements performed on all DAΦNE magnets. The system was therefore modified with a T-shape support (see Fig. 6) with two probes placed at a such a distance that the zones outside the range of the first probe could be always reached by the second one and the other way round. Using the modified system it was possible to obtain a complete map of the vertical field component on the horizontal symmetry plane, which, due to the symmetry of the magnet and by integrating Maxwell equations, yields the full knowledge of the magnetic field. A first measurement of the field in the central pole with the additional plates glued on the poles was performed after inserting 28 mm thick diamagnetic plates between the two halves of the C-shaped supports (see Fig. 6) in order to preserve the original value of the wiggler gap. At the operating current of the wigglers in DAΦNE, due to the longer magnetic structure, a reduction by $\approx$6% in the peak field was observed. Several shapes for the additional plates have been realized and the corresponding field me asured. The final result was obtained with a concavity of $\approx$2 mm on each plate. This

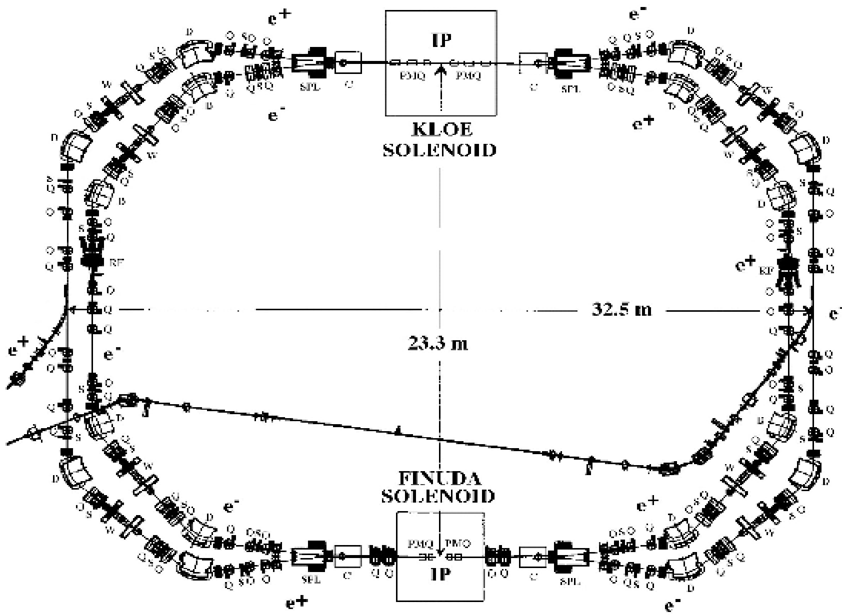

Figure 2: *The DAΦNE Main Rings.*

Figure 3: *The new KLOE IR quadrupole assembly.*

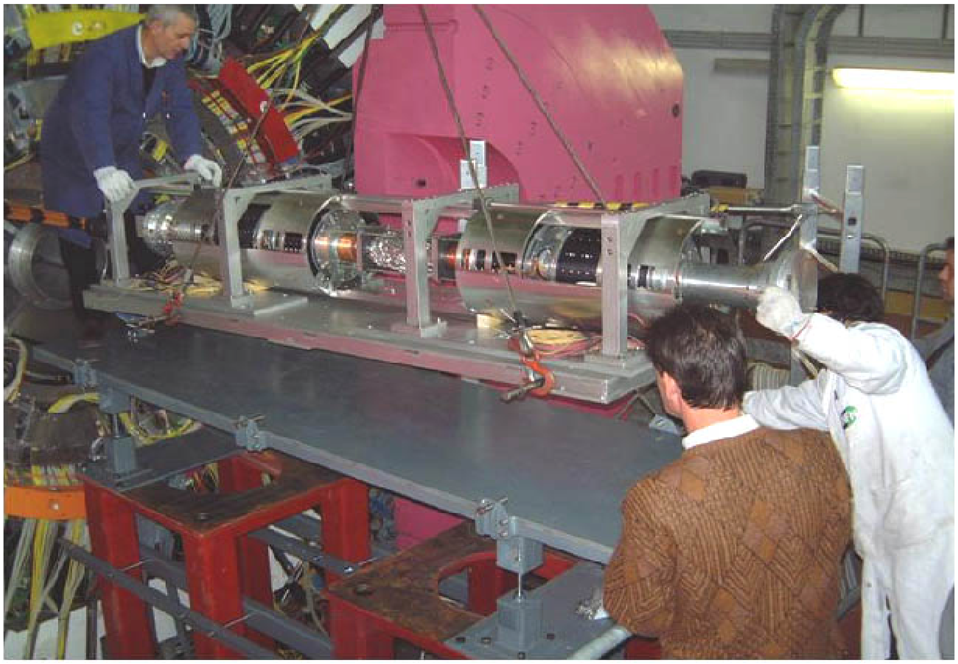

Figure 4: *FINUDA IR during installation.*

Figure 5: *The spare wiggler in the Magnetic Measurement Hall.*

shape balances the natural trend of the field to decrease towards the pole boundary. Fig. 7 shows a comparison between the field measured at the pole center in the original configuration, with the flat poles and after pole shaping. The overall reduction in peak field after shaping increased to ≈11%. The dotted line in Fig. 7 gives the field after pole shaping, normalized at the original one in the pole center, in order to show the improvement in the good field region.

As shown in Fig. 7, the curvature of the field at the pole center is slightly overcompensated. This is due to the fact that the curvature of the field in the original configuration increases with the distance from the pole center along the wiggler axis, reaching its maximum value at the pole end. Due to the complexity of a three dimensional shaping of the pole, it was decided to apply a constant profile to the plates with an additional correction obtained by changing the length of the plate as a function of the distance from the wiggler axis in the horizontal direction. The resulting curvature of the field (i.e. the second derivative of the field with respect to the horizontal position) is shown in Fig. 8, compared to the original configuration. It can be observed that the peak curvature has been reduced and that its average value is very small. This also reduces the additional focusing in the wiggler created by the wiggling trajectory of the beam together with the field curvature inside the poles.

In order to reduce the loss in peak field due to the longer magnetic circuit and to the concavity of the plates, their thickness has been decreased by 7 mm. In addition, the wiggler gap has been reduced from the original 40 mm to 37 mm, at the limit imposed by the vacuum chamber. As a consequence, the thickness of the spacer inserted between the two halves of the C-shaped support structure was reduced to 11 mm. The overall loss in peak field was finally limited to ≈4%. The additional plates in their final configuration were glued on all the five full poles of the wiggler and on one of the terminals. The other terminal pole was instead modified to increase its natural field curvature, creating an additional sextupole term. This was required by numerical simulations of the dynamic aperture of the machine. Of course, this additional sextupole is not tunable, but it turns out that the strength of all other sextupoles in the ring required to correct the cromaticity in both planes can be significantly reduced, with a beneficial effect on the overall non-linearity of the machine. The field map in the horizontal symmetry plane has been measured in the final configuration with the double Hall probe system. A numerical code was written to track the trajectory followed by the beam in the measured field. The results of this procedure have been used to find the current in the terminal poles which makes the field integral on the trajectory vanish. The vertical position of the field clamp at the end of the wiggler (see Fig. 6) has also been optimized to make the field distribution as simmetrical as possible in the longitudinal direction with respect to the wiggler center. During the shutdown of DAΦNE for the installation of the FINUDA detector all the wigglers in the two rings have been modified by glueing the additional plates on the poles. After commissioning the ring for FINUDA the measurement of the tune as a function of the horizontal position of the beam in the wigglers has been repeated, finding a reduction of the octupole term by a factor ≈2.5.

2.4 Scrapers, Bellows and Ion Clearing Electrodes

Scrapers were very useful in reducing the beam backgrounds for both experiments. However few jaws were not properly working. They were inspected during the shutdown and it was found that they were protuding into the beam pipe. It was decided to remove the horizontal tapers, that are the least critical to the ring impedance, and to modify the vertical ones, that were intercepting the beam instead of the jaws.

Some copper bellows were found to be distorted and have been flattened with the insertion of pins, as shown in Fig. 9.

About 50% of the Ion Clearing Electrodes installed in the electron ring were broken due to faulty welding. Most of them were replaced with welding-free electrodes (shown in Fig. 10).

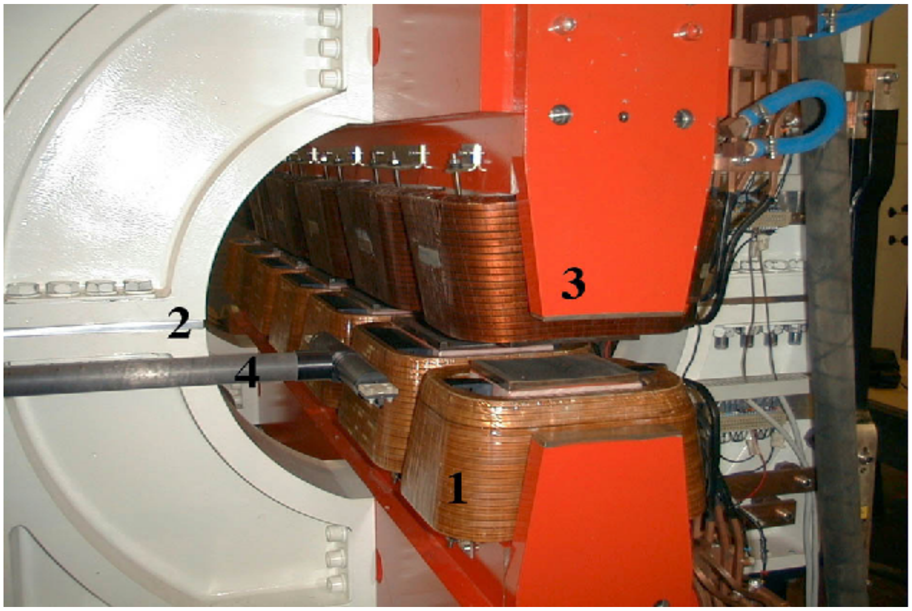

Figure 6: *Particular of the wiggler showing the terminal pole with the glued plate (1), the spacer between the two halves of the C-shaped support structure (2), the field clamp (3) and the modified support of the double Hall probesystem (4).*

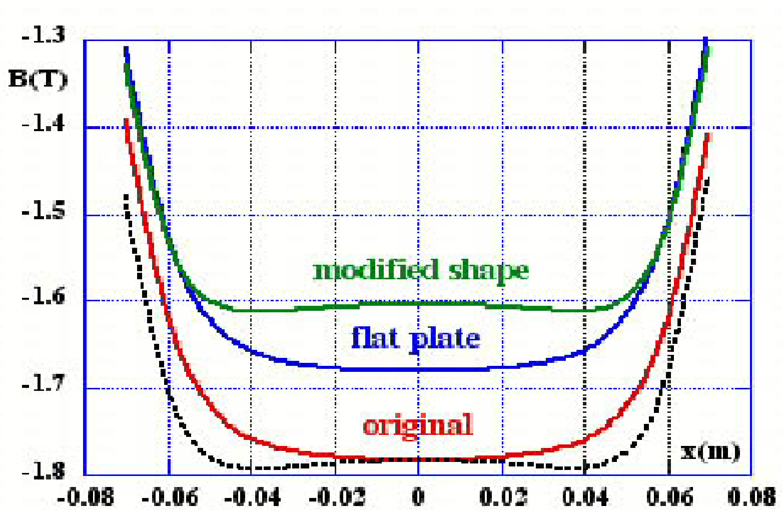

Figure 7: *Field at magnet center versus distance from the wiggler axis in the three configurations. The dotted line is the field after pole shaping normalized to the value measured in the original configuration at the pole center.*

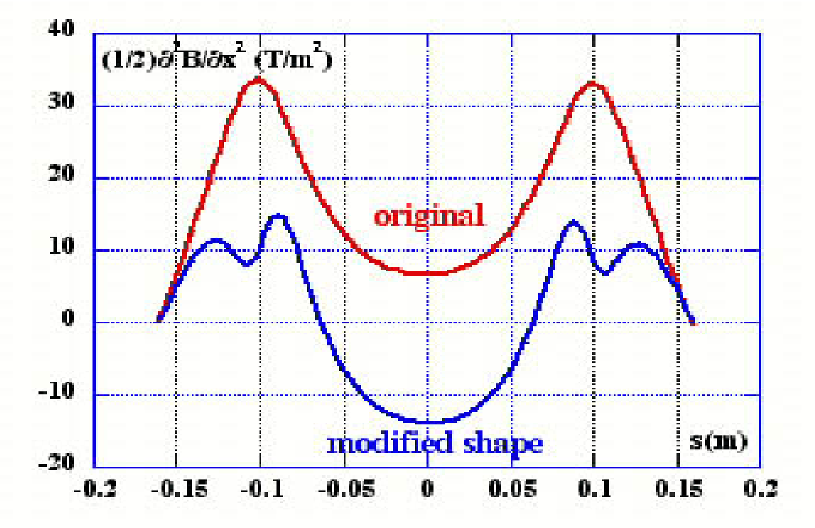

Figure 8: *Second derivative of the field with respect to the horizonl position as a function of the longitudinal position along the wiggler axis in the central pole.*

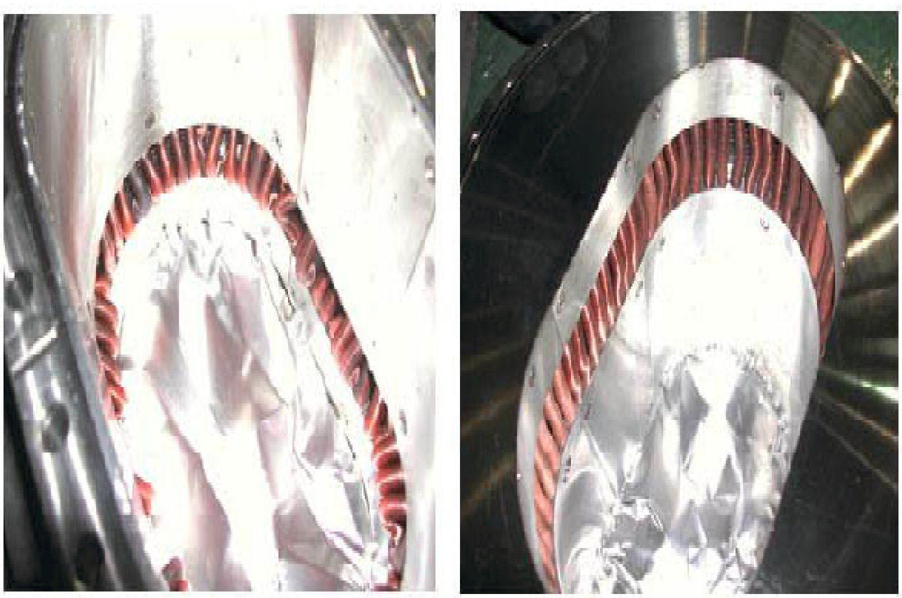

Figure 9: *Damaged bellow: as found (left) and after pin insertion (right).*

2.5 Injection Straight Sections

The "long" straight sections, where beams are injected, have been rearranged, by adding two quadrupoles and one sextupole and removing one out of the three kicker magnets, in order to:

- improve injection efficiency;
- decrease the effect of the injection kick on the already stored beam, by reducing the pulse duration by 50%;
- reduce dispersion at the septum;
- optimize optical functions and phase advance in the section with respect to the dynamic aperture.

2.6 3rd Harmonic Cavity

The installation of a passive 3rd harmonic cavity in each DAΦNE ring has been proposed to control the bunch length and therefore the Touschek lifetime and the coherent instabilities by increasing the Landau damping due to the non-linearity of the longitudinal potential well. Due to the peculiarity of the DAΦNE parameters (low RF voltage, high beam current), powering the cavity in a passive way is the simplest and the most effective choice. The required harmonic voltage can be obtained with modest cavity shunt impedance and over a wide range of beam currents. The choice of the harmonic number 3 is a compromise between beam dynamics requirements and constraints related to the space available for the cavity installation. A picture of the actual cavity is shown in Fig. 11. The damping of the cavity HOM has been obtained by means of a special ferrite ring developed for the superconducting cavities installed on the High Energy Ring (HER) of the KEK-B collider in Japan. The cavity has been designed by means of an extensive use of the e.m. codes MAFIA and HFSS. The measurements performed on the real cavities are in good agreement with the results obtained by e.m. simulations. Two harmonic cavities have been fully tested on bench. One cavity has been also installed in one ring to check beam pipe and connections, and disinstalled before the operation resumed.

2.7 Additional hardware modifications

Many other hardware modifications and upgrades were performed during the shutdown. Briefly:

- increased horizontal feedback power;
- two valves and two bellows in each IR removed to further reduce ring impedance;
- a faulty injection kicker found (in the last days of the DEAR run) and repaired, source of the e- current limit;
- a faulty power supply and bend coil found and repaired, responsible for horizontal drifts of the positron beam;
- new cameras for the Synchrotron Light Monitor for better emittance diagnostic;
- new electronics for the Transfer Lines BPMs to read position and optimize the beam transmission in non-invasive mode;
- 50 Hz linac operation in order to inject positrons at 2 Hz (electron injection is at 2 Hz already);
- new (custom) Helium transfer lines to cool the solenoidal compensators with the existing crio-plant.

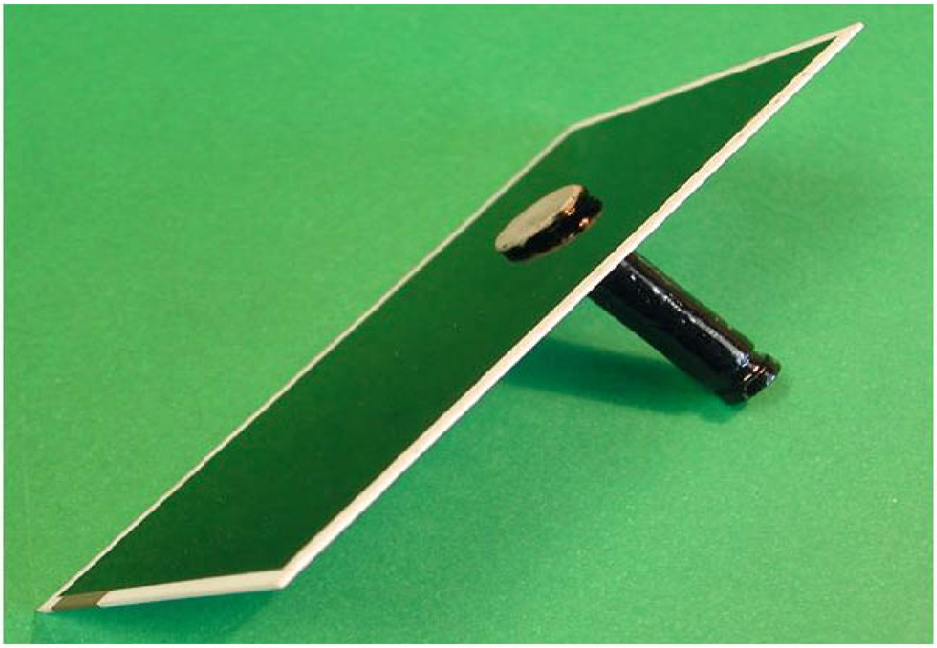

Figure 10: *New Ion Clearing Electrode.*

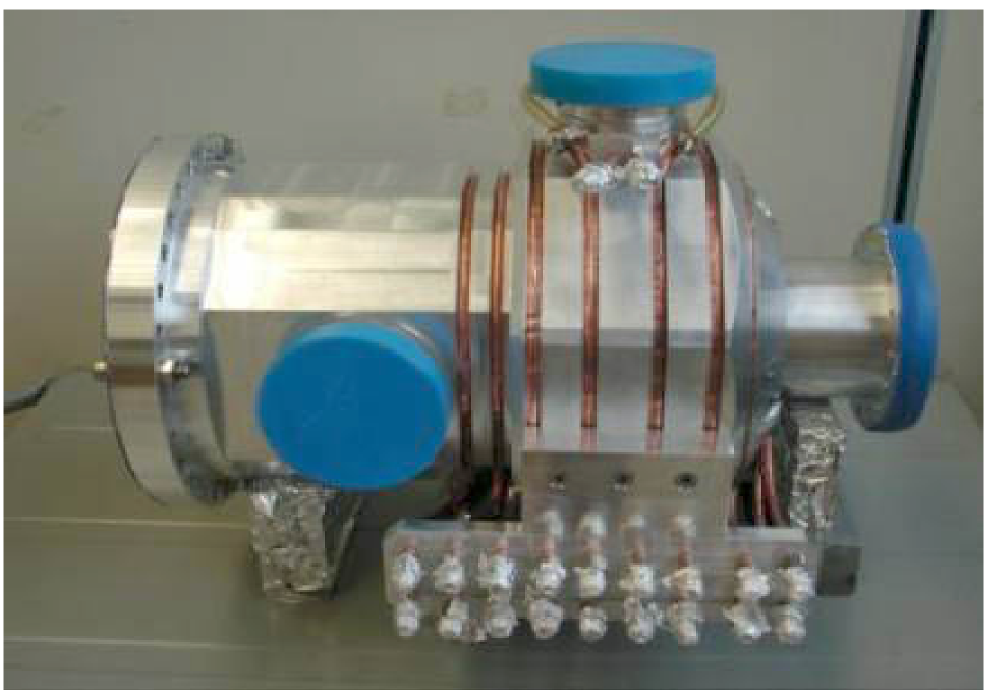

Figure 11: *3rd harmonic cavity on bench.*

3 Optics modifications

A new lattice for the FINUDA operation in IR2 has been designed by taking into account all the hardware modifications. Its main characteristics are summarized in the following:

- lower emittance (0.42 mm mrad);
- lower β in the wigglers to minimize the effect of non-linearities;
- $\beta_x^* = 1.7$ m to allow for the minimum bunch spacing;
- $\beta_y^* = 27$ mm, close to the bunch length;
- additional sextupoles in the wigglers and at the septum;
- optimized phase advance between sextupoles for chromaticity correction and dynamic aperture optimization;
- low beam invariants to minimize background;
- straight sections optimized for injection efficiency and dynamic aperture.

The lattice for the KLOE operation in IR1 will have the same characteristics, but the low-β in IR2 will be removed, thus lowering the ring chromaticity and allowing for a larger beam separation in IR2 during collision in IR1.

4 FINUDA Operation

The shutdown for the installation of FINUDA was completed mid-July, but unfortunately a severe water shortage in the whole Frascati area caused by the extremely hot summer made the operation of DAΦNE so troublesome that it was decided to interrupt the commissioning while modifying the cooling water supply system. Operations resumed at the beginning of September with a tank used as a buffer with water being collected during the night and consumed during the day.

About one month was required to complete commissioning of the rings. The main items were:

- the vacuum chamber conditioning with beam to achieve a pressure level yielding reasonable lifetime and background in the detector.
- tuning of the new lattice, strongly changed with respect to the one used for DEAR at the end of 2002, because of the different magnetic structure of the two interaction regions and the modifications to the wigglers and to the injection sections;
- the optimization of the coupling with the new remote-controlled rotation of the quadrupoles in the interaction regions of KLOE and FINUDA;

Coupling correction required rather long adjustment procedures since the involved parameters are four indipendent rotations in KLOE, eight in FINUDA, the magnetic field in the main solenoids and in the two compensators. Measurements of the coupled horizontal/vertical response matrix together with an algorithm for correction have been particularly useful to reach a satisfactory residual value of ≈0.5% for the coupling. A strong transverse instability was observed in the positron ring with a sharp threshold depending on the injected bunch pattern, which limited the storable current to ≈600 mA in the typical operating conditions for FINUDA, with 90 adjacent bunches in both beams. Investigations with beam about the possible sources did not give significant results. X-ray pictures will be taken during the Christmas shutdown on the most sensitive elements inside the vacuum chamber (bellows etc.) to search for damages occurred during the installations of the long shutdown. A first period, from mid-October to the beginning of November, was dedicated to the first tests with beam of the FINUDA detector. After it the experiment has run for 47 days until the Christmas shutdown of the Lab, collecting ≈70 inverse picobarns. The peak luminosity reached $\approx 5\text{x}\,10^{31}\text{cm}^{-2}\text{s}^{-1}$ and the maximum integrated luminosity per day exceeded 3 pb^{-1} in the last runs. Fig. 12 shows the integrated luminosity per day from mid-October to Christmas.

The FINUDA achievements for the 2 months of operation are the following:

- number of bunches per beam: 90 + 90;
- total current per beam e-/e+: 1./0.6 A;
- peak luminosity $\approx 0.5 \text{ x } 10^{32}\text{cm}^{-2}\text{s}^{-1}$;
- average luminosity during runs $\approx 0.3 \text{ x } 10^{32}\text{cm}^{-2}\text{s}^{-1}$;
- maximum integrated luminosity per day $\approx 3.\, pb^{-1}$;
- luminosity lifetime: 0.6 h;
- number of fillings per hour: 2;
- injection frequency e-/e+: 2/1 Hz;
- data acquisition during injection: OFF.

5 Future Plans

The original physics program of DAΦNE should be completed in 2-3 years and which future is expected for the collider has been discussed. Physics measurement in the 1-2 GeV range will be competitive in next decade, provided the luminosity increases by at least one order of magnitude with respect to what has been obtained up to now. Two possibilities have been envisaged for the DAΦNE upgrade:

- to transform the collider in a light quark factory by increasing the maximum center of mass energy from 1.4 GeV to ≈ 2.2 GeV;
- to upgrade it to a super-regime factory with a luminosity by a factor 100 with respect to the present best performances, namely in the $10^{34}\text{cm}^{-2}\text{s}^{-1}$ range.

A joint Physics and Accelerator Workshop was held in Alghero (Sardinia, Italy) in September to study both the machine feasibility and the physics cases. The Workshop on "e^+e^- in the 1-2 GeV range: Physics and Accelerator Prospects" was organized by INFN and also sponsored as an ICFA Beam Dynamics Panel Miniworkshop, by the working group on High Luminosity e^+e^- colliders. Participation was shared between Experimental and Theoretical Physics and Accelerator Physics, attending the two different working groups on the Physics Case for the c.m. energy between 1 and 2 GeV and the luminosity issues at these energies.

The first option, the increase in energy by at least a factor 2, needs changes of some of the present systems: essentially the dipoles, the Interaction Region and the injection. All the other systems, RF, feedback, vacuum, quadrupoles, sextupoles, correction coils, diagnostics, are already dimensioned for the higher energy. The requested luminosity is similar to the one already achieved in DAΦNE at the lowest energy, $10^{32}\text{cm}^{-2}\text{s}^{-1}$. The project for this upgrade is named

DAFNE2, where the ”F” stays for Frascati and the ”2” for the c.m. energy in GeV. The dipole preliminary designs, fitting the present vacuum chambers, are based on the use of two materials, steel and permendur. This last one, having a higher saturation field, will be used on the pole in order to increase the magnetic field on the beam axis, up to the necessary 2.2 T. The luminosity requirements can be achieved with a total current of 0.5 A in 30 bunches. The corresponding beam-beam tune shifts are $\xi_x/\xi_y = 0.014/0.024$, below the limit already achieved in DAΦNE. The IR design, based on the same principles of the present ones, could use superconducting quadrupoles very similar to those used at CESR. Two possibilities are being considered for the injection: a Linac upgrade to 1 GeV for on-energy injection, or the collider ramping, the first one optimizes the average luminosity, while the second one optimizes the costs.

The second option, named DAΦNE-II, on which a preliminary conceptual design has been presented at Alghero, is based on the ”strong RF focusing” principle, very high radiation emission and negative momentum compaction ring configuration. The strong RF focusing is a modulation of the bunch length along the ring, obtained by a very large longitudinal phase advance, corresponding to synchrotron tune near the half integer. The minimum of the bunch length occurs at the IP, while the maximum occurs at the RF cavity position. Such a scheme needs a large absolute value of the momentum compaction and a high RF voltage, and the ring acts as a magnetic compressor. The high radiation emission can be obtained with a new lattice based on cells with positive and negative dipoles, in which the damping time is of the order of few msec, about a factor 5 less than the present DAΦNE one. In this lattice the dispersion self solution oscillates around zero and in each dipole has the sign opposite to the bending angle and has a high value, so that its contribution to the momentum compaction is always negative and high, almost an order of magnitude with respect to the present DAΦNE one. The advantages of the negative momentum compaction regime, like shorter bunches, and more regular bunch shape are therefore included in the design. An RF system at 500 MHz, with voltage of the order of 10 MV, for a 100m long ring, and momentum compaction near -0.2, will give bunch lengths at the IP near 2 mm. The IR fitting the existing KLOE detector is based on low-β quadrupoles very close to the IP, to focus the β_y^* to few millimeters.

The preliminary collider layout fits the existing DAΦNE hall (see Fig. 13) and could utilize all existing infrastructures and sub-systems. The collider should have only one IR, while the opposite section could be used for the injection and the RF system. The elements introducing impedance should be placed in the sections where the bunch length is longer, so that the perturbation to the bunch distribution is minimized.

Both options seem to be appealing to the Physics community. DAΦNE is the only e^+e^- collider in Europe, and the only one in the world, at present, operating at such a low energy. Its upgrade, both towards higher luminosity or energy, would allow continuing the tradition of the Frascati Laboratories in designing, building and operating e^+e^- storage rings.

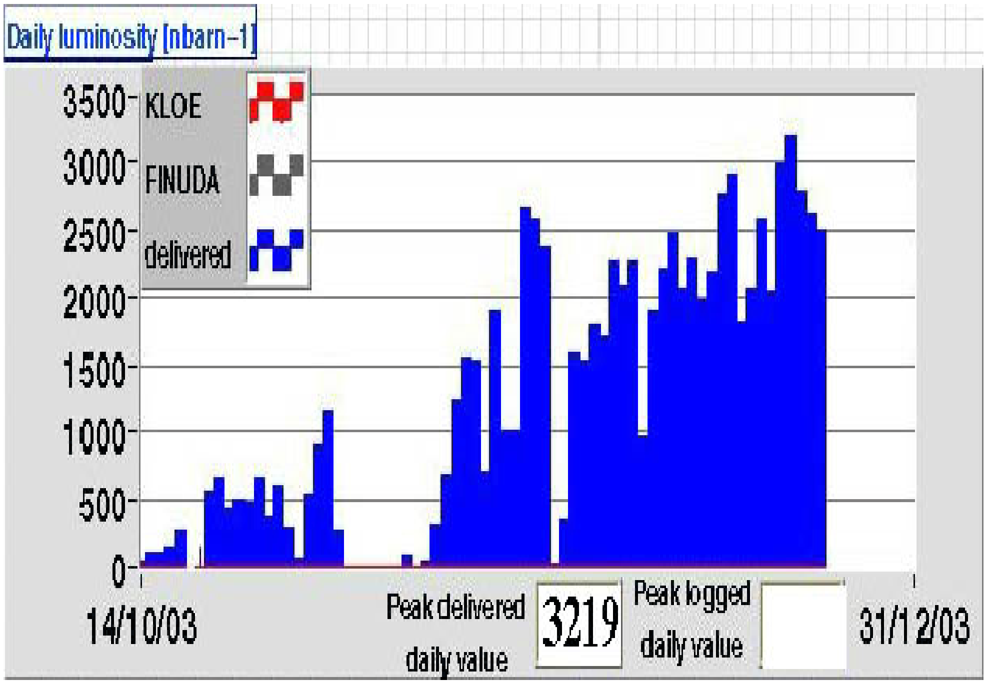

Figure 12: *Integrated luminosity per day delivered to FINUDA.*

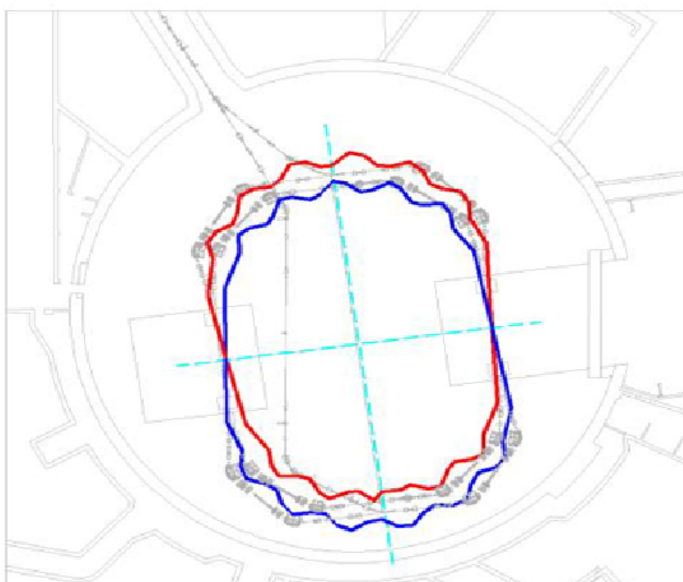

Figure 13: *Layout of DAΦNE-II in the DAΦNE Hall.*

6 Publications

1. A. Drago, D. Alesini, G. Benedetti, M.E. Biagini, C. Biscari, R. Boni, M. Boscolo, A. Clozza, G. Delle Monache, G. Di Pirro, A. Gallo, A. Ghigo, S. Guiducci, F. Marcellini, G. Mazzitelli, C. Milardi, L. Pellegrino, M.A. Preger, P. Raimondi, R. Ricci, C. Sanelli, M. Serio, F. Sgamma, A. Stecchi, C. Vaccarezza, M. Zobov: "100 Bunches DAΦNE Operation", Presented at PAC2003, Portland, Oregon, May 12-16, 2003. LNF-03/012 (P), 11/07/03.

2. G. Benedetti, D. Alesini, M.E. Biagini, C. Biscari, R. Boni, M. Boscolo, A. Clozza, G. Delle Monache, G. Di Pirro, A. Drago, A. Gallo, A. Ghigo, S. Guiducci, M. Incurvati, C. Ligi, F. Marcellini, G. Mazzitelli, C. Milardi, L. Pellegrino, M.A. Preger, P. Raimondi, R. Ricci, C. Sanelli, M. Serio, F. Sgamma, A. Stecchi, A. Stella, C. Vaccarezza, M. Vescovi, M. Zobov: "Feasibility Study of a 2 GeV Lepton Collider at DAΦNE", Presented at PAC2003, Portland, Oregon, May 12-16, 2003. LNF-03/012 (P), 11/07/03

3. C. Milardi, G. Benedetti, M.E. Biagini, C. Biscari, M. Boscolo, S. Guiducci, M. Preger, P. Raimondi, C. Vaccarezza, M. Zobov: "Developments in Linear and Non-Linear DAΦNE Lattice", Presented at PAC2003, Portland, Oregon, May 12-16, 2003. LNF-03/012 (P), 11/07/03.

4. A. Drago, A. Gallo, A. Ghigo, M. Zobov, INFN-LNF; J.D. Fox, D. Teytelman, SLAC: "Longitudinal Quadrupole Instability and Control in the Frascati DAΦNE Electron Ring", Physical Review Special Topics - Accelerators and Beams, Volume 6, 052801 (2003).

5. S. Guiducci for the DAΦNE Team, "Status of DAΦNE", Proceedings of the ICFA Mini Workshop on "e+e- in the 1-2 GeV energy range: Physics and Accelerator Prospects", Alghero (SS), Italy, Sep. 10-13 2003.

6. A. Gallo, P. Raimondi, M. Zobov, "Strong RF Focusing for Luminosity Increase", Proceedings of the ICFA Mini Workshop on "e+e- in the 1-2 GeV energy range: Physics and Accelerator Prospects", Alghero (SS), Italy, Sep. 10-13 2003. DAΦNE Technical Note G-60, 18/8/03

7. P. Raimondi, "Luminosity and beam-beam for very large crossing angles", Proceedings of the ICFA Mini Workshop on "e+e- in the 1-2 GeV energy range: Physics and Accelerator Prospects", Alghero (SS), Italy, Sep. 10-13 2003. DAΦNE Technical Note G-60, 18/8/03

8. M. Zobov, "Negative Momentum Compaction at DAΦNE", Proceedings of the ICFA Mini Workshop on "e+e- in the 1-2 GeV energy range: Physics and Accelerator Prospects", Alghero (SS), Italy, Sep. 10-13 2003.

9. M.E. Biagini, "Interaction Region Design: Preliminary Considerations", Proceedings of the ICFA Mini Workshop on "e+e- in the 1-2 GeV energy range: Physics and Accelerator Prospects", Alghero (SS), Italy, Sep. 10-13 2003.

10. C. Biscari, "Lattice for Longitudinal Low Beta", Proceedings of the ICFA Mini Workshop on "e+e- in the 1-2 GeV energy range: Physics and Accelerator Prospects", Alghero (SS), Italy, Sep. 10-13 2003.

11. S. Guiducci, "Touschek Beam Lifetime", Proceedings of the ICFA Mini Workshop on "e+e- in the 1-2 GeV energy range: Physics and Accelerator Prospects", Alghero (SS), Italy, Sep. 10-13 2003.

12. M. Boscolo, "Background Issues at Super DAΦNE", Proceedings of the ICFA Mini Workshop on "e+e- in the 1-2 GeV energy range: Physics and Accelerator Prospects", Alghero (SS), Italy, Sep. 10-13 2003.

13. C. Ligi, R. Ricci, "Preliminary feasibility study on 1.1-2.3 T ramping dipoles for DAFNE2", Proceedings of the ICFA Mini Workshop on "e+e- in the 1-2 GeV energy range: Physics and Accelerator Prospects", Alghero (SS), Italy, Sep. 10-13 2003.

14. R. Ricci, "Super DAΦNE Dipoles First Evaluation", Proceedings of the ICFA Mini Workshop on "e+e- in the 1-2 GeV energy range: Physics and Accelerator Prospects", Alghero (SS), Italy, Sep. 10-13 2003.

15. A. Clozza, "Vacuum: From DAΦNE to DAΦNE-II", Proceedings of the ICFA Mini Workshop on "e+e- in the 1-2 GeV energy range: Physics and Accelerator Prospects", Alghero (SS), Italy, Sep. 10-13 2003.

16. C. Milardi, "Energy ramping for DAΦNE-II", Proceedings of the ICFA Mini Workshop on "e+e- in the 1-2 GeV energy range: Physics and Accelerator Prospects", Alghero (SS), Italy, Sep. 10-13 2003.

17. G. Benedetti, "DAFNE2: lattice for a 2 GeV e+e- collider", Proceedings of the ICFA Mini Workshop on "e+e- in the 1-2 GeV energy range: Physics and Accelerator Prospects", Alghero (SS), Italy, Sep. 10-13 2003.

18. R. Boni, "Proposal of doubling the DAΦNE-Linac energy", Proceedings of the ICFA Mini Workshop on "e+e- in the 1-2 GeV energy range: Physics and Accelerator Prospects", Alghero (SS), Italy, Sep. 10-13 2003.

19. F. Ruggiero, M.Zobov, "Summary of the Working Group on High Luminosity Issues" Proceedings of the ICFA Mini Workshop on "e+e- in the 1-2 GeV energy range: Physics and Accelerator Prospects", Alghero (SS), Italy, Sep. 10-13 2003.

20. S. Guiducci, C. Zhang, "Summary of the Working Group on Single Beam High Luminosity Issues", Proceedings of the ICFA Mini Workshop on "e+e- in the 1-2 GeV energy range: Physics and Accelerator Prospects", Alghero (SS), Italy, Sep. 10-13 2003.

21. C. Biscari, "Results from the Alghero Workshop on e+e- in the 1-2 GeV range", Proceedings of the ICFA Workshop on "e+e- Factories 2003", SLAC, USA, Oct. 13-16 2003.

22. M.E. Biagini for the DAΦNE Team, "The DAΦNE Phi-Factory status and perspectives", Proceedings of the ICFA Workshop on "e+e- Factories 2003", SLAC, USA, Oct. 13-16 2003.

23. A. Gallo, P. Raimondi, M. Zobov, "Strong RF Focusing: a possible approach to get short bunches at the IP", Proceedings of the ICFA Workshop on "e+e- Factories 2003", SLAC, USA, Oct. 13-16 2003.

DAΦNE-Light

E. Burattini (Resp.), P. Calvani (Ass.), G. Cappuccio (Ass.), G. Cavallo (Ass.),
G. Cinque (Art.23), S. Dabagov (Art.23), M. Guidi Cestelli (Ass.), A. Grilli (Tec.),
A. Marcelli, F. Monti (Ass.), A. Nucara (Ass.), E. Pace, M. Piccinini (Bors.), A. Raco (Tec.)

1 Summary

During the 2003 long shutdown of DAΦNE, the DAΦNE-Light Laboratory attained a series of scheduled improvements on all the three Synchrotron Radiation beamlines, in particular on the optical system of the Synchrotron INfrared Beamline at Daϕne (SINBAD), as well as on upgrading the soft X-Ray beamline and UltraViolet (UV) branch line. After the restart of DAΦNE machine in September, we began operating the SR Facility in full parasitic mode with respect to the new collider experiment FINUDA. Being fully operative in the whole IR range, SINBAD completed several of the European users' experimental projects within the LNF Transnational Access to Research Infrastructure (TARI) program, while the soft X-Ray beamline hosted its first researchers, within the same European program, still allowing new characterization of the wiggler source in the energy region 2,1-3,6 keV. Devoted to the Solar Ultraviolet Effects (SUE) experiment, the UV line carried out further investigations on the effects induced by irradiations of biological specimens with the UVB-band light during few hours of dedicated beamtime.

2 Activity

2.1 SINBAD

The infrared beamline SINBAD makes use of the radiation emitted by one of the eight bending magnets on the electron ring, having a critical wavelength of ~60 Å (208 eV). The front end, 3 m far from the source, collects a SR fan under a solid angle of (v x h) 45 x 18 mrad^2, and the SR beam size is defined through a set of four remotely controlled slits; on changing the accepted angle over the vertical quote, either linear (in plane) or circular (out of orbit plane) IR polarization can be selected. The IR optical line, under UHV to minimize absorption by residual gas, consists of six gold-plated mirrors (one ellipsoidal, two toroidal and three plane mirrors), all remotely controlled in angle and monitored by CCD cameras. By this system, the SR beam is refocused into a final spot of about 1 x 2 mm^2 at a CVD diamond wedged window 25 m afterward. This is the effective source of an interferometer BRUKER Equinox 55, modified to work under vacuum, which allows both transmission and reflectivity IR experiments. The wavenumber range of the instruments is 10 - 10000 cm^{-1}, covered with different detectors and beamsplitters for a maximum resolution of 0,5 cm^{-1}. The instrument is equipped with a cryogenic apparatus for low temperature experiments in the range T = 20 - 300 K. A top view of the instrumentations at the end of the beamline is shown in Figure 1. In addition, a BRUKER Irscope 1 microscope (from Roma University *La Sapienza*) is connected to an exit port of the interferometer (see Fig. 1).The microscope has a spatial resolution of ~10 μm and works in the mid IR range, i.e. 500 - 8000 cm^{-1}. In November, we also started the first phase of the commissioning of this dedicated instrument. Its performances have been measured in terms of intensity ratio between SR and glow-bar versus the pinhole diameter at sample position. Fig. 2 shown the preliminary data of the SR gain inside the microscope, after normalization to an electron current of 1 A.

Within this period several experiments of the TARI program has been performed with success. In particular, we may mention the research on IR reflectivity as a function of the temperature, an experimental program devoted to the analysis of the phonon spectra of semiconductor solid

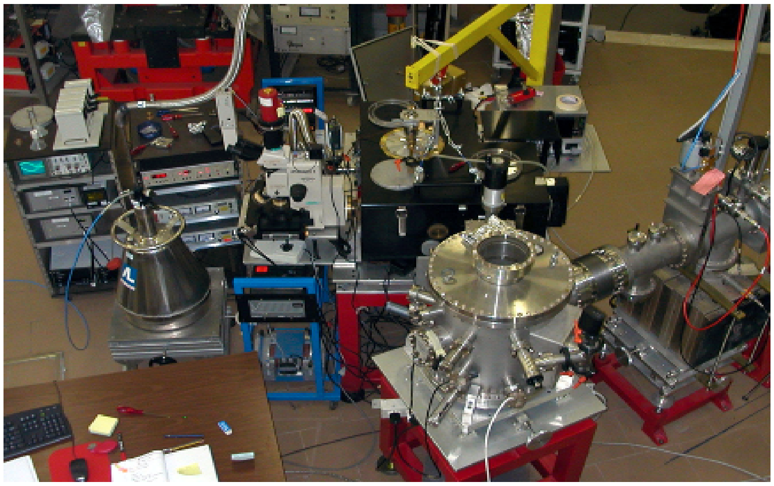

Figure 1: *Top view of the infrared experimental station. At the end of the beamline is clearly visible the vacuum chamber of the last toroidal mirror and the vacuum chamber hosting the BRUKER interferometer.*

solutions, based on HgTe systems, that are the main materials of infrared detectors. Several compositions of ternary CdHgTe, ZnHgTe and ZnCdTe systems as well as of quaternary ZnCdHgTe compound were investigated. Using SINBAD at DAΦNE as an intense and brilliant IR source, we were able to resolve the fine multimode structure of the phonon spectra of these compositions. (see Fig. 3)

2.2 Soft X-Ray Beamline

The X-ray source is one of the 6-pole equivalent planar wiggler installed on the electron ring for vertical beam compaction. Since the large e^- deflection in this insertion device (K=107), the electromagnetic radiation is emitted in a wide fan, mostly horizontally polarized, and with a continuous spectral distribution around the critical energy of 310 eV. By over 1 A of circulating current in DAΦNE, the intense flux of soft X-rays available makes this beamline unique for the experimental researches and technological applications in the energy window around few keV. The front-end accepts about 15 mrad of the photon fan in the orbit plane. Beyond the DAΦNE hall, a beam size of 50 x 20 mm^2 is allowed through a set of horizontal-vertical slits in the UHV pipe: about 5 mrad in horizontal and the full SR vertical divergence ($\sim$1 mrad) encounter an Au-coated Si-mirror (80 cm long), deflecting half of the SR fan circa 80 mrad sideway in the UV line. To guarantee the UHV machine environment, the X-rays proceed straightforwardly through new high transmittance thin windows: either a 1000 Å polyamide film or an 8 μm Be foil can be choose for, respectively, selecting the softer (T$\sim$80 % at the oxygen K-edge) or harder (T$\sim$80% at $\sim$2 keV) photon energy range. Micrometric resolution slits defines the beam entering the monochromator, which is a double-crystal fixed-exit device (by Toyama) working in the *boomerang* geometry with Bragg's angles from 15° to 75°. The original equipment of Si(111), α-Quartz(10-10) crystals has been completed with the new KTP(011) and KAP(100) materials to match the spectrum of wavelengths above 10 Å with resolution $\Delta\lambda/\lambda$=10^{-4}. Here, a HV experimental chamber with two ionization chambers (ICs) is used for X-ray Absorption Spectroscopy (XAS) on thin samples. Over the standard kapton windows for transmission measures, new ultra-thin polyamide films with Si mesh allow the spectroscopy even below the phosphor K-edge. In the experimental area, a Clean Room (class A100) is available to apply lithographic and micro-engineering techniques on soft X-ray photoresists by a micro-controlled stepper device. Furthermore, investigations on policapillary systems are in due course to provide X-ray focusing for the planned activity with SR microbeams.

The X-ray beamline has restarted its activity the long DAΦNE shutdown: X-ray Absorption Near Edge Spectroscopy technique was carried on in the range below 4 keV, i.e. a decade higher than the wiggler critical energy, using Si(111) crystals for high energy resolution. Since the parasitic operation mode, the spectra acquisitions were constrained in runs of circa 20 min, but at an average circulating current of 500 mA in DAΦNE e^- ring. Energy calibration was obtained using as reference the Rydberg-like peak of the Ar K-edge (see Fig. 4). XANES technique was successfully applied on the analysis of K-edge from low Z elements and L-edges from transition metals (e.g. see Fig. 5). Some biological samples underwent preliminary XAS measures to optimize the set up for their analysis by elemental contrast X-ray microscopy (TARI experiment on leaves accumulating toxic metals). To extend the XAS analysis also on thick samples, the experimental equipment was enriched with solid state detectors like PIN Si devices, photodiodes and channeltrons to perform, respectively, both X-ray Fluorescence, total yield and secondary electron detection. Once widen the spectral range to the lighter element side (Mg K-edge), further improvements on the monochromator system and control are expected to open the soft X-rays energy upper limit.

3 Conference Proceedings

1. A. Marcelli and P. Calvani, Nucl. Sci. Tech. 14, 93 (2003);
2. E. Burattini, F. Monti, F. Belloni, G. Cinque, S. Dabagov, A. Grilli, A. Marcelli, E. Pace, M. Piccinini, A. Raco, P. Calvani, M. Cestelli Guidi and A. Nucara , Frascati Physics Serie XXXII, 243 (2003);
3. G. Cinque, E. Burattini, F. Monti, G. Bellisola, G. Fracasso, M. Colombatti and A. Simionovici, Frascati Physics Series XXVI, 275 (2003);
4. S. Agrestini, A. Marcelli, G. Cibin, Z. Wu and A. Bianconi, Frascati Physics Serie XXXII, 61 (2003);
5. G. Cibin, A. Marcelli, A. Mottana, G. Giuli, G. Della Ventura, C. Romano, E. Paris, A. Cardelli and F. Tombolini, Frascati Physics Serie XXXII, 95 (2003);
6. E. Burattini, G. Cinque, G. Bellisola, G. Fracasso, F. Monti and M. Colombatti, AIP Conference Proceedings 652, 515 (2003);
7. Z. Y. Wu, C. R. Natoli, A. Marcelli, E. Paris, A. Bianconi, and N. L. Saini, AIP Conference Proceedings 652, 497 (2003);
8. F. Tombolini, G. Cibin, A. Marcelli, A. Mottana, M. F. Brigatti, and G. Giuli, AIP Conference Proceedings 652, 481 (2003);
9. S. Bellucci, S. Botti, A. Marcelli, K. Ibrahim, and Z. Y. Wu, AIP Conference Proceedings 652, 355 (2003);
10. S.B. Dabagov, AIP Conference Proceedings 652, 89 (2003);
11. O.V. Mikhin, S.B. Dabagov, V.D. Gelver and A.V. Priladyshev, LNF-03-16 (P);
12. I. Titkova, M. Zobov and S. Dabagov, LNF-03-002(IR);

13. F. Bonfigli, B. Jacquier, R.M. Montereali, P. Moretti, E. Nichelatti, M. Piccinini, H. Rigneault and F. Somma, Proceedings SPIE 5131, 139 (2003);

14. F. Bonfigli, B. Jacquier, F. Menchini, R.M. Montereali, P. Moretti, E. Nichelatti, M. Piccinini, H. Rigneault and F. Somma, Proceedings Int. School Atomic and Mol. Spectroscopy, 697 (2003);

15. R.M. Montereali, A. Pace, M. Montecchi, E. Nichelatti, A. Grilli and M. Piccinini, Proceedings ECIO 2003, 1, 241 (2003);

16. E. Burattini, G. Cinque, S. Dabagov, A. Grilli, A. Marcelli, F. Monti, E. Pace, M. Piccinini and A. Raco, AIP Proceedings SRI2003, in press.

4 Seminars

1. A. Marcelli, BioSR 2003, Frascati;
2. M. A. Cestelli, WIRMS 2003, Lake Tahoe - CA;
3. A. Marcelli, Euroclay 2003, Modena;
4. A. Marcelli, 1^{st} BASIE Workshop 2003, Karlsruhe;
5. S. Dabagov, Int. Congress on X-Ray Optics and Microanalysis 2003, Chamonix;
6. S. Dabagov, 5^{th} Italian-Russian Laser Symposium 2003, Moscow;
7. F. Monti, P. Calzolari, I Convegno Nazionale Federazione Italiana per le Ricerche sulle Radiazioni 2003, Legnaro;

5 Publications

1. Z. Y. Wu *et al.*, J. Phys.: Cond. Matter **15**, 7139 (2003);
2. A. Cardelli *et al.*, Phys. Chem. Miner. **30**, 54 (2003);
3. S.B. Dabagov (*et al.), Physics Uspekhi* **173**, *1083 (2003);*
4. *S. Bellucci et al., Phys. Rev. Lett.* **90**, *034801 (2003);*
5. *S. Dabagov and S. Bellucci, J. Physics: Cond. Matter* **15**, *3171 (2003);*
6. *S.B. Dabagov, X-Ray Spectrometry* **32**, *3 (2003);*
7. *F. Bonfigli et al., Rad. Effects and Defects in Solids* **185**, *1580 (2003);*
8. *M.A. Forastiere et al., Optics Comm.* **217**, *249 (2003);*
9. *G. Dalba et al., Phys. Chem. Glasses* **44** *(82), 75 (2003);*
10. *F. Rocca et al., J. Sol-Gel Science and Tech.* **26**, *267 (2003);*
11. *J.J. Polit et al., J. Alloys and Compounds (2003), in press;*
12. *A. Marcelli et al., J. Phys. Chem. Sol. (2003) in press;*

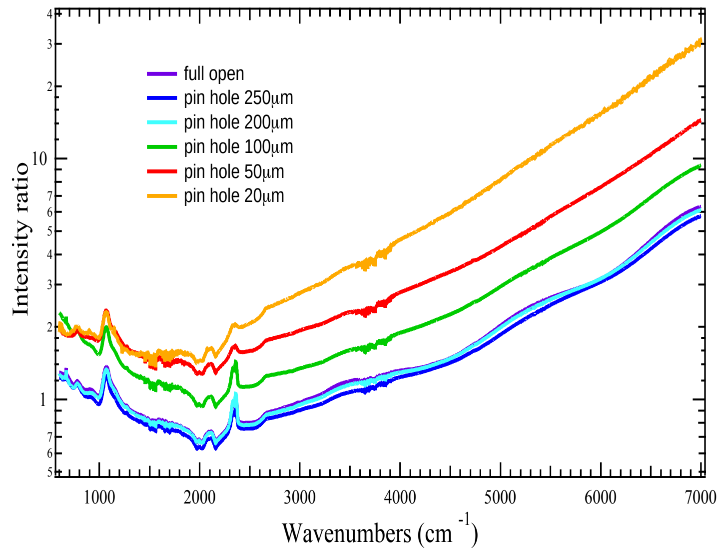

Figure 2: *Experimental ratio of the SR intensity and the glowbar source installed in the interferometer vs. different pinhole (from full aperture to 20 micron of diameter). These preliminary data, normalized to a beam current of 1 A, already show the significant advantage of SR for IR microscopy.*

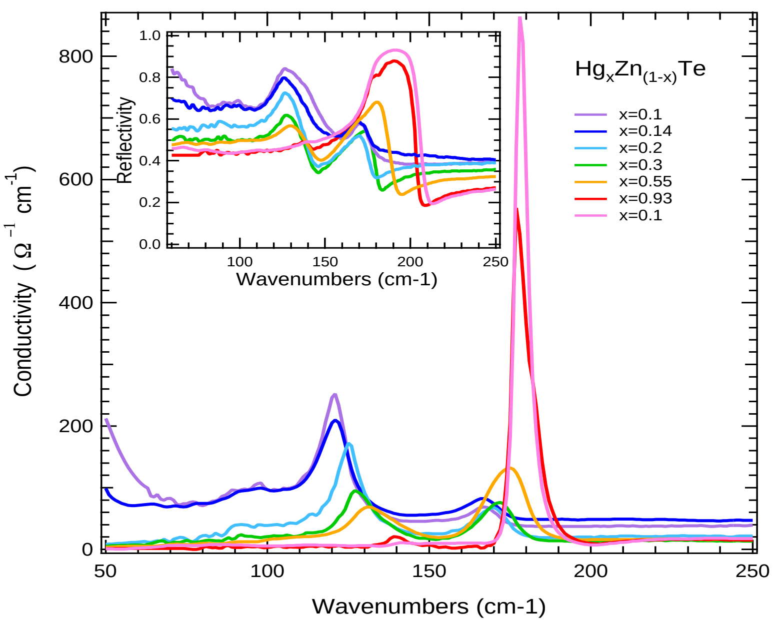

Figure 3: *Conductivity data vs. wavenumber in the far IR region for a series of ternary compounds $Hg_xZn_{(1-x)}Te$. After Kramers-Kronig transformation of the data, a clear fine structure was resolved in the phonon bands as shown by the reflectivity curves plotted in the inset.*

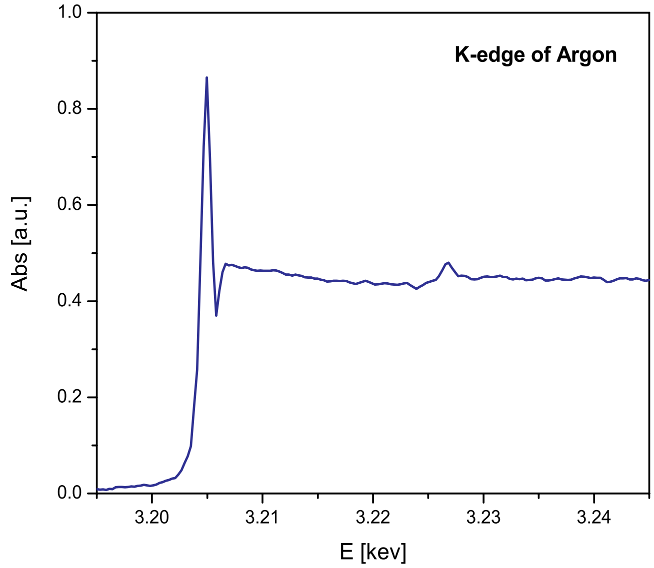

Figure 4: *Spectrum of argon K-edge acquired in transmission by ICs with Kr gas at 250V and 10^9 V/A of pramplifier gain; the energy resolution is 0,25 eV using Si(111) crystals. After the Rydberg peak, also the second excitation was detected at the higher energy side.*

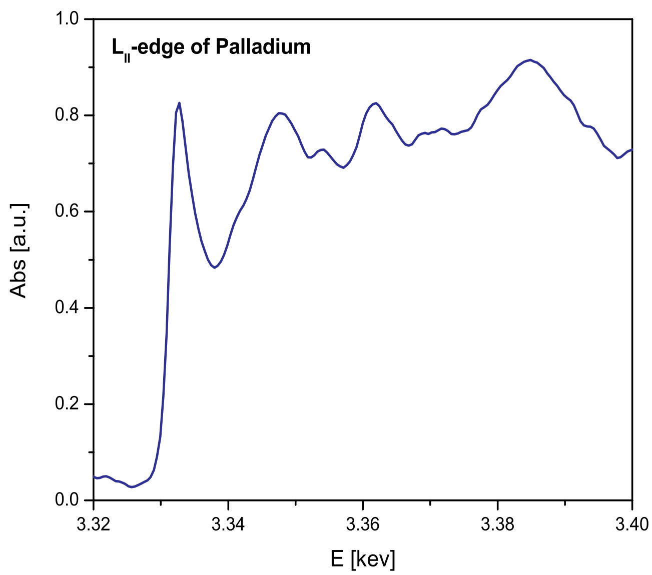

Figure 5: *XANES spectrum of palladium L_{II} absorption edge acquired in transmission by ICs with Kr gas at 250V and 10^9 V/A of pramplifier gain. The energy resolution is 0,25 eV using Si(111) crystals.*

GILDA

A. Balerna, F. Campolungo (Tecn.), S. Mobilio (Resp.), V. Sciarra (Tecn.), V. Tullio (Tecn.)

1 Introduction

GILDA (General Purpose Italian BeamLine for Diffraction and Absorption), is the Italian CRG beamline, built to provide the Italian scientific community with an easy access to the European Synchrotron Radiation Facility to perform experiments with a high energy and brilliance X-ray photon beam. GILDA is funded by the three Italian public research Institutes: Consiglio Nazionale delle Ricerche (CNR), Istituto Nazionale per la Fisica della Materia (INFM) and Istituto Nazionale di Fisica Nucleare (INFN). Experimental stations for X-ray Absorption Spectroscopy, Anomalous X-ray Scattering and X-ray Diffraction (XRD) are present at the GILDA beamline.

2 Activity on the GILDA beamline during 2003

1) The support for the second mirror was designed and at the moment is under construction; this support is necessary for installing the new second mirror of the beamline, bought to minimize the focus dimension of the X-ray beam in the three experimental hutches. 2) The new support of the monochromator first crystal was realized; slight modifications are under development in order to improve its mechanical stability. 3) The installation of new hardware control system, fully compatible with the ESRF standards was extended to the third experimental hutch; the corresponding software was developed using LABVIEW. 4) A new software for a fast and easy alignment of the double mirrors for harmonic rejection was developed and tested. 5) A first X-ray diffraction experiment in grazing incidence geometry was performed; a new sample holder to optimise this kind of experiments is now under development. 6) A system for the growth and characterization of metal clusters was designed. The system will be installed at the LNF laboratory and will be used to prepare samples to measure at Grenoble on GILDA. 7) Concerning the MANU-2 experiment of the INFN Group II, the measurements performed with a micro-colorimeter based on a Transition Edge Sensor working at 150mK, which has a very high energy resolution, were fully analysed; the results were presented at the 10th international Workshop on "Low Temperature Detectors (LTD10)". The proceedings will be published on Nuclear Instruments and Method A.

3 Beamtime use during 2003 and scientific outcomes

During 2003 ESRF delivered beam for about 5000 hours; about 3200 hours were used for user's experiments, about 650 hours for in-house research, 600 hours for beamline improvement, maintenance and alignment; about 500 hours were delivered in single bunch mode and therefore used for tests. A total of 37 experiments were performed, 27 of Italian users and 10 of European users. Studies and results to be mentioned are the following:

1. Study of dilute nitrides: these are III-V semiconductor alloys with a few percent of N included in the anion sublattice. This inclusion causes an a-priori unexpected decrease of the band gap, which has been understood as due to the creation of states at the bottom of the conduction band. On the GILDA beamline XAFS measurements have been performed on Ga(AsN) and (InGa)(AsN), to verify the theoretical prediction of Kim and Zunger

[Phys. Rev. Lett. 86, 2609 (2001)] of the existence of a significant deviation from the random arrangement of the constituent atoms on lattice sites, with a strong prevalence of In-N bonds over Ga-N bonds. Indium K-edge XAFS measurements were performed which have shown that chemical ordering is present but it is significantly weaker than the one predicted.

2. Study of the Ti-silicalite (TS-1) systems. These are catalysts with a remarkable high efficiency and molecular selectivity in oxidation reactions such as the conversions of ammonia to hydroxylamine, of secondary alcohols to ketones, of secondary amines to dialkylhydroxylamines; for these reasons TS-1 is one of the most relevant industrial catalysts in the last twenty years. Silicalite, which is the parent Ti-free material, is catalytically inactive and therefore Ti atoms have been immediately designed as the catalytic centers of the material. At GILDA the Ti sites were studied by XAFS spectroscopy measuring for the first time the catalytic interaction with water peroxide in the absence of water, ruling out the important effect of the reaction conditions in the chemistry of TS-1. The data have shown the existence of two different peroxy species formed on the Ti in TS-1: the first one in the presence of water and the second one in the absence of water, giving new possibilities in the comprehension of the real active species in the partial oxidation reactions.

3. Zn site in photosynthetic reaction centres. Photosynthetic reaction centers are pigment membrane protein complexes which catalyse the photosynthetic process. The binding of heavy metals slows down the light-induced charge separation across the membrane which is the primary event occurring during the photosynthesis. Diffraction indicates that Cd and Zn bind in the same way to AspH124, HisH126 and HisH128. In the case of Zn also a water molecule interacts with the metal. The local structure around the Zn was investigated at GILDA by X-ray Absorption Spectroscopy. Results indicate that the Zn atom binds two O atoms and two N atoms in first coordination shell. The two N atoms come from His, and only one of the two O atoms come from an amino acid (presumably Asp or Glu). The second oxygen is due to a coordinating water molecule.

4 2004 - GILDA Forseen Activity

During the 2004, the activity foresees: 1) the optical tests of the new second mirror, its installation and commissioning; 2) software control of the machine parameters, in order to stop the data acquisition during injections; 3) development of a standard catalytic cell for XAS measurements at low temperature and in fluorescence mode; 4) development of a total electron yield detector to measure thin films on crystalline substrates; 5) commissioning of the system for the production of nanocluster samples and start of their production

References

1. A. Martorana, G. Deganello, A. Longo, F. Deganello, L. Liotta, A. Macaluso, G. Pantaleo, A. Balerna, C. Meneghini, and S. Mobilio, J. Synch. Rad. **10**, 177 (2003)

2. G. Ciatto, F. D'Acapito, L. Grenouillet, H. Mariette, D. De Salvador, Bisognin, R. Carboni, L. Floreano, R. Gotter, S. Mobilio, and F. Boscherini Phys. Rev. **B 68**, 161201 (2003)

3. A. Garca Prieto, M. L. Fdez-Gubieda, C. Meneghini, A. Garca-Arribas, and S. Mobilio, Phys. Rev. **B 67**, 224415 (2003)

NTA-CTF

D. Alesini, C. Biscari, G. Benedetti (Dott.), R. Boni, A. Clozza, G. Delle Monache,
A. Drago, A. Gallo, A. Ghigo (Resp.), M. Incurvati (Ass.), F. Marcellini, C. Milardi, L. Pellegrino,
M.A. Preger, R. Ricci, C. Sanelli, M. Serio, F. Sgamma, A. Stecchi, A. Stella, M. Zobov

1 Introduction

The design of the Compact Linear Collider (CLIC) aims at a centre-of-mass energy in the multi TeV range. It is based on a two beam scheme: a drive beam running parallel to the main beam, whose bunch structure carries a 30 GHz component, provides the RF power to the main beam.

CLIC Test Facility 3 is being realized as an intermediate step to demonstrate the technical feasibility of RF power generation scheme, to produce 30 GHz RF power at the nominal peak power and pulse length, such that all 30 GHz components for CLIC can be tested at nominal parameters.

The facility will be built in the existing infrastructure of the LPI as a collaboration between CERN, INFN LNF, LAL (France), SLAC (USA) and Uppsala University (Sweden).

2 Activity of the LNF group in year 2003

The INFN Frascati laboratories will provide the design and realization of the transfer lines from the linac and the first of the two rings of the compressor system called Delay Loop (DL). At the exit of this ring the frequency of the bunches coming from the Linac (1.5GHz) will be doubled with an increment of the current by a factor two.

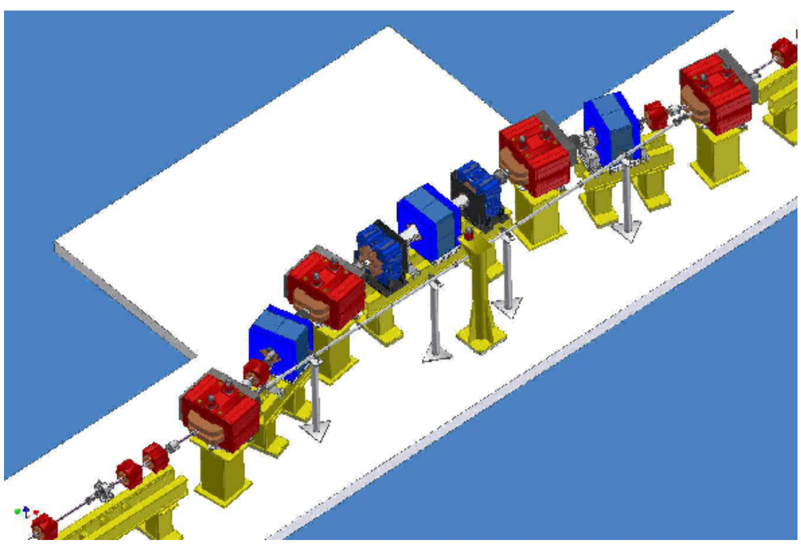

Figure 1: Layout of the transfer line chicane

During year 2002 the final Design Report has been completed and prototypes of the main parts of the vacuum chamber have been designed. Two deflectors to be used in CTF3 combiner rings have been built and tested in the preliminary phase. The CTF3 preliminary phase has been completed with the collaboration of the INFN-LNF group.

Activity during year 2003 has been focused on the completion of the final layout of the Delay Loop and Transfer Line. The first part of the CTF3 transfer line is in the installation phase, it includes a chicane (Fig.1) in which, because of the very flexible lattice and large aperture vacuum chamber, it is possible to change the bunch length in a wide range by tuning the R56 element of the transfer matrix. The chicane can be used as a stretcher to lengthen the pulses coming from the linac in order to reduce their energy spread created by the coherent synchrotron radiation (CSR) in the bunch trains recombination rings. A possible use as a bunch compressor is also foreseen in order to make CSR experiments and to characterize beam instrumentation .

Design and construction of the vacuum chamber components, including pump ports, shielded bellows and beam position monitors, have been completed and vacuum tests are in progress.

The magnetic layout of the Delay Loop (Fig.2) has been completed using existing dipole and quadrupole magnets of the EPA complex at CERN together with the injection extraction septa magnet.

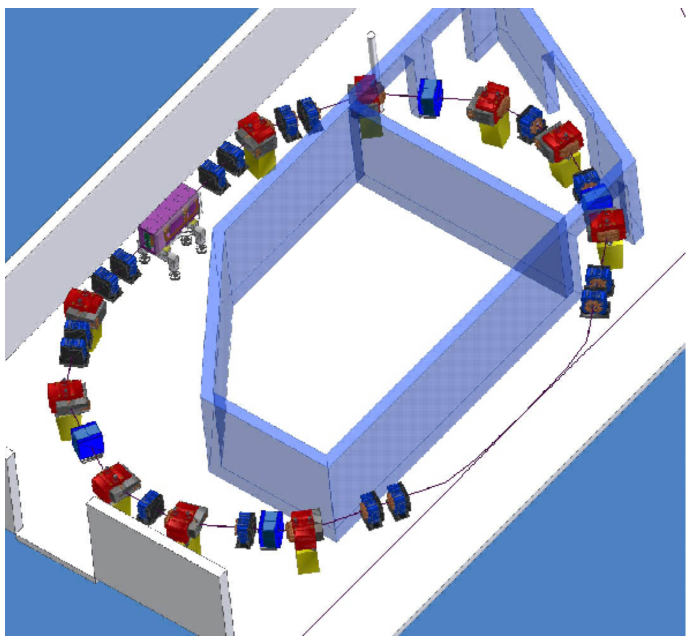

Figure 2: Layout of the delay loop

Final design of the missing magnets (sextupoles, correctors and wiggler magnets) has been completed and the tender request started. Sextupoles and correctors design have been designed following the same configuration adopted for the DAFNE damping ring and the realization has been assigned to Ansaldo.

Injection and extraction of bunch trains in the CTF3 Delay Loop for the recombination with the contiguous bunch trains, is performed by a dedicated RF deflector. Differently from the device realized for Combiner Ring, a standing wave structure has been preferred in this case, to limit its dimension. Three possible solutions have been studied and their design together with a comparative cost-effectiveness analysis have been started.

The first solution considered is the most standard one. A single cell is excited through a coupling hole. The hole dimensions set the external Q of the cavity and its filling time as a consequence. A circulator has to be foreseen to protect the klystron from the power reflected at

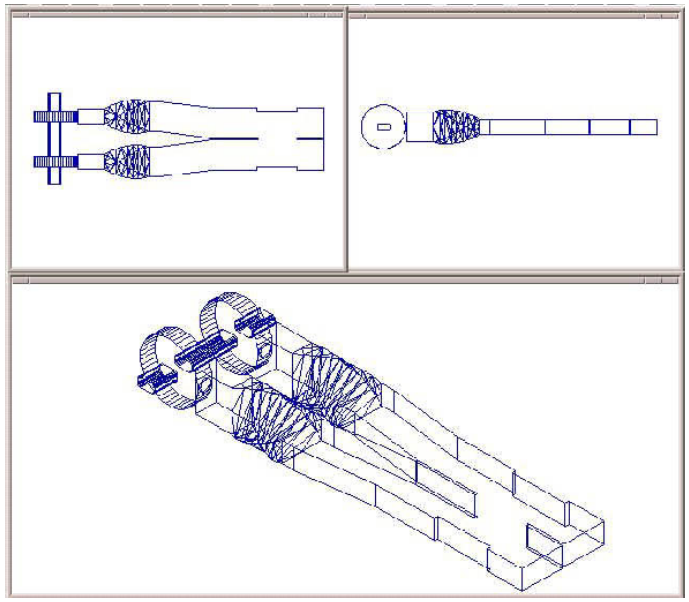

Figure 3: HFSS model of the DL deflector

the cavity input. The second solution (Fig.3) consists of two cavities coupled through an hybrid junction (HJ). The power reflected by the cavities adds out of phase at the klystron port of the HJ, so there is no need of circulator, and in phase at its fourth port, where it is dissipated on an external load. As third solution, a single cell is provided with two coupling holes of different size. On the side of the larger hole is connected the klystron, while on the other side is connected a load. Tuning separately the size of the two holes it is possible to have no reflection at the klystron port therefore also in this case the circulator is unnecessary.

Each of the three structure proposed seems to be able to satisfy the essential requirements of the system. Driving the deflectors with the already commissioned klystron, the right angle of deflection can be obtained for beams of energy up to twice the nominal energy.

All the presented work has been strongly supported by the DAFNE Technical Staff, drawings of machine layout have been realized by G.Fontana and A.Zolla.

References

1. CTF3 Prototypes: Design, Tests and Measurements in Proc. Of Particle Accelerator Conference (Portland USA) 2003 A. Ghigo, D. Alesini, C. Biscari, R. Boni, A. Clozza, G. Delle Monache, A. Drago, A. Gallo, F. Marcellini, C. Milardi, C. Sanelli, M. Serio, F. Sgamma A. Stecchi, A. Stella, M. Zobov

2. Bunch Frequency Multiplication In The CLIC Test Facility CTF3 in Proc. Of Particle Accelerator Conference (Portland USA) 2003; F. Tecker, R. Corsini, L. Rinolfi, C. Biscari, A. Ghigo, M. Preger,P. Royer,A. Ferrari, F. Marcellini, C. Milardi, C. Sanelli, M. Serio, F. Sgamma A. Stecchi, A. Stella, M. Zobov

3. Report on the Third Operation of the CTF3 Preliminary Phase in CERN CTF3 Note 054 (Feb, 2003); C. Biscari, R. Corsini, A. Ferrari, A. Gallo, A. Ghigo,L. Rinolfi, P. Royer

NTA-TTF

L. Cacciotti (Tecn), M. Castellano (Resp), A. Clozza, G. Di Pirro,
M. Ferrario, O. Giacinti (Tecn), S. Guiducci, C. Milardi,
R. Sorchetti (Tecn), F. Tazzioli, M. Zobov

1 Introduction

The TESLA Test Facility (TTF) is an international effort, based at Desy (Hamburg), aiming at the development of the technologies required for a Superconducting e+e- Linear Collider. High gradient superconducting RF cavities, with their high power coupling and tuning device, and low cost cryostats were the main goal of the project, but also the production of a high power, long pulse electron beam from a RF gun was required. This involved the development of new photocathode, an adequate laser source and new beam diagnostics. In addition to prove the possibility of producing and accelerating the kind of beam required for the TESLA Lineal Collider, TTF has also demonstrated that this beam was of enough good quality to be successfully used for the production of UV coherent radiation with the Self Amplified Spontaneous Emission (SASE) Free Electron Laser process, that is an important part of the TESLA project. INFN contribution comes from LNF, LNL, Sezione di Milano and Sezione di Roma2.

2 Activity in 2003

The 2003 was completely dedicated to the installation of the so called TTF2. The goal is the operating of a 1 GeV machine, with the same beam parameters of TTF, apart from a somewhat smaller emittance. Eventually, the machine will become an "user facility" for the FEL radiation, whose wavelength should reach 6 nm, but in the first stage other experiments testing components for the TESLA Linear Collider will be performed.

Among others, the tests of the new high gradient SC cavities, with their new tuning system, the powering of many cryostats and the control of the full power, high energy beam. The development of a new, non-intercepting, diagnostic instrument for emittance measurement, proposed by LNF and Roma2, has been funded by EU under the 6th FP.

All the 23 Optical Transition Radiation (OTR) screens have been installed and aligned in the vacuum chambers. The first 15 optical systems have been aligned and calibrated in laboratory, and 6 of them was already installed and aligned on the beam pipe. The alignment procedure is now well established, and a complete installation and alignment can be performed in less than two days.

Installation will continue in the first months of 2004, when, at the end or March, the commissioning of the injector will start. The image acquisition and its analysis is a responsibility of LNF and Roma2, together with the real time publishing of the images to allow a remote control of the linac. The image acquisition from the distributed digital camera will be performed by an adequate number of low cost industrial PC, equipped with direct firewire connection to the camera. Each PC will transmit the images, and a preliminary elaboration of them, to a server via ethernet connection. On the server the complete analysis of the images will be performed, and information sent to the operators, published on the web and stored for off line analysis. Hardware and software for the control of the injector will be installed in February 2004. The extension to the whole system will follow the first tests. (see Fig. 1)

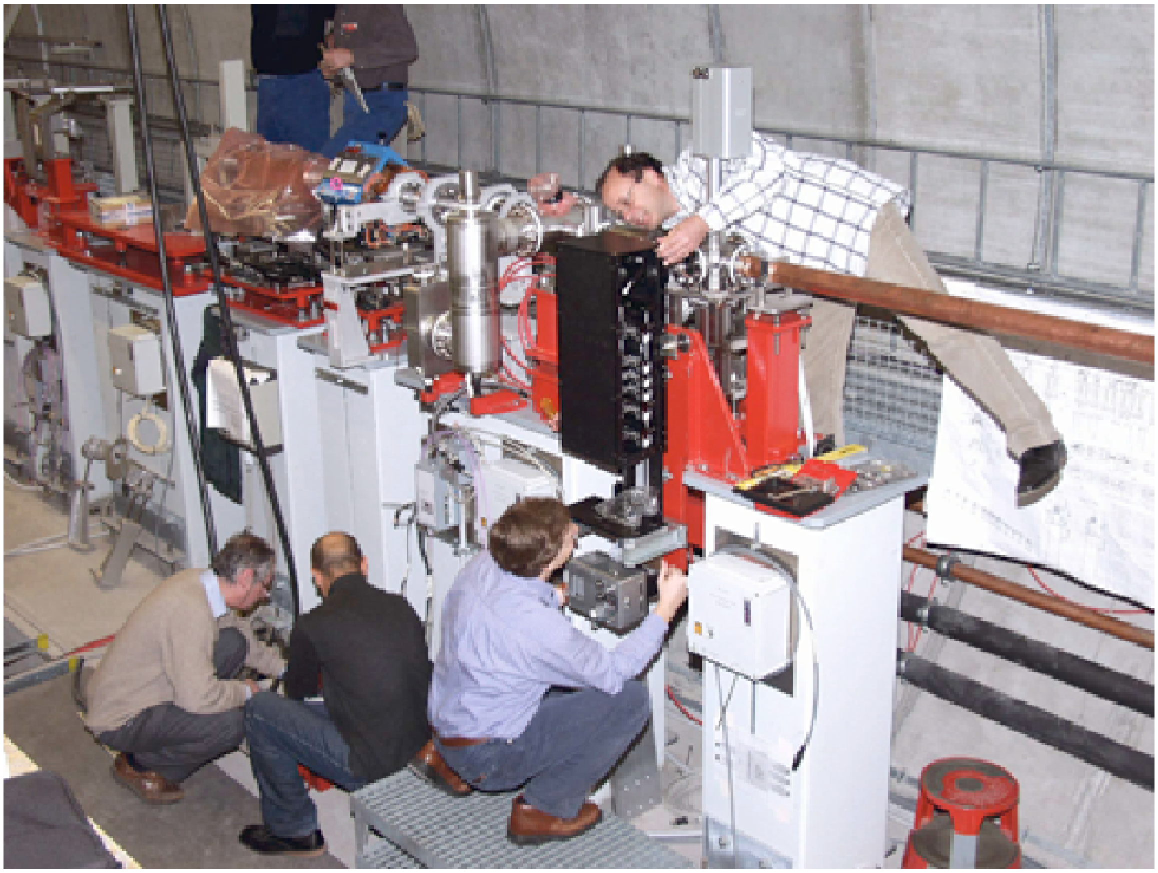

Figure 1: *Installation of an optical system on the TTF beam pipe.*

3 Publications

1. K. Honkavaara, A. Brenger, R. Fischer, D. Nolle, K. Rehlich, DESY, Hamburg, L. Cacciotti, M. Castellano, G. DiPirro, M. Raparelli, R. Sorchetti, INFN-LNF, Frascati, L. Catani, A. Cianchi, INFN-Roma 2, Roma.

2. Design of otr beam profile monitors for the tesla test Facility, phase 2 (ttf2).

3. Proceedings of PAC2003 Conference, 2476, (2003).

SPARC

D. Alesini, S. Bertolucci, M.E. Biagini, C. Biscari, R. Boni, M. Boscolo,
M. Castellano, A. Clozza, G. Di Pirro, A. Drago, A. Esposito, M. Ferrario,
V. Fusco, A. Gallo, A. Ghigo, S. Guiducci, M. Incurvati, C. Ligi, F. Marcellini,
M. Migliorati, C. Milardi, A. Mostacci, L. Palumbo (Resp.), L. Pellegrino,
M. Preger, P. Raimondi, R. Ricci, C. Sanelli, M. Serio, F. Sgamma,
B. Spataro, A. Stecchi, A. Stella, F. Tazzioli, C.Vaccarezza,
M. Vescovi, C. Vicario, M. Zobov **(INFN /LNF);**

F. Alessandria, A. Bacci, I. Boscolo, F. Broggi, S.Cialdi, C. DeMartinis,
D. Giove, C. Maroli, V. Petrillo, M. Romè, L. Serafini **(INFN /Milano);**

D. Levi, M. Mattioli, P. Musumeci, G. Medici **(INFN /Roma1);**

L. Catani, E. Chiadroni, A. Cianchi, C. Schaerf, S. Tazzari **(INFN /Roma2) ;**

F. Ciocci, G. Dattoli, A. Doria, F. Flora, G. P. Gallerano, L. Giannessi,
E. Giovenale, G. Messina, L. Mezi, P. L. Ottaviani, L. Picardi, M. Quattromini,
A.Renieri, C. Ronsivalle **(ENEA/FIS);**

S. De Silvestri, M. Nisoli, S. Stagira **(Politecnico /Milano)**

1 Aim of the experiment

The aim of the SPARC project (Phase 1) is to promote an R&D on high brightness photo-injector to drive SASE-FEL experiments. It has been proposed by a collaboration including ENEA, INFN, CNR, University of Roma Tor Vergata, INFM, ST, funded jointly by the Italian Government and INFN with a 3-year time schedule (Phase 1). The main goals of the SPARC project are:

- the generation of a high brightness electron beam able to drive a self-amplified spontaneous free-electron laser (SASE FEL) experiment in the green visible light and higher harmonics generation,
- the development of an ultra-brilliant beam photo-injector needed for future SASE FEL-based X-ray sources.

The machine will be installed at LNF, inside an existing underground bunker, see Fig. 1. We foresee conducting investigations on the emittance correction and on the rf compression techniques up to kA level. The SPARC photo-injector can be used also to investigate beam physics issues like surface-roughness-induced wake fields, bunch-length measurements in the sub-ps range, emittance degradation in magnetic compressors due to CSR (SPARC Phase 2). Beams with the features anticipated in the SPARC project are also of strong interest for experiments in other cutting edge fields. The SPARC injector may allow investigations into the physics of ultra-short beams, plasma wave-based acceleration, and production of Compton back-scattered X-rays (PLASMON/MAMBO activities).

In this report we present the status of the injector design that is under the INFN responsibility. In the past year the design of the experiment and the main technological choices have been set up as follows. The proposed system to be built consists of: a 1.6 cell RF gun operated at S-band (2.856 GHz, of the BNL/UCLA/SLAC type) and high peak field on the cathode (120 MV/m)

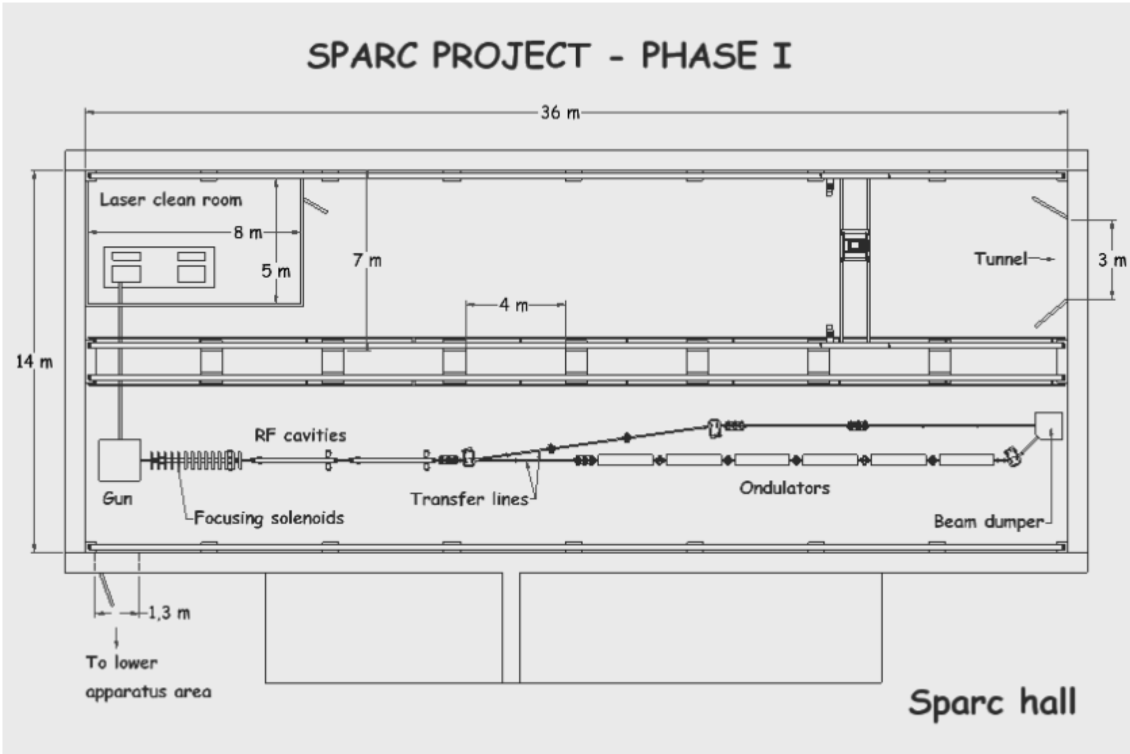

Figure 1: *Schematic layout of the SPARC photo-injector complex inside the SPARC experimental hall, including undulator, and by-pass line (Phase 1).*

with incorporated metallic photo-cathode (Copper or Mg), generating a 5.6 MeV beam which is properly focused and matched into 3 accelerating sections of the SLAC type (S-band, travelling wave) which accelerate the bunch up to 150-200 MeV.

The choice of the S-band Linac with respect to an L-band is due to compactness of the system, the lower cost, and the existence at LNF of an 800 MeV Linac based on the same technology (with obvious advantages regarding expertise and availability of spare components). Morover, the higher RF frequency leads to a higher peak brightness attainable by an optimized photo-injector. In our case we expect a projected emittance < 2 mm-mrad, a slice emittance ~ 1 mm-mrad with a slice peak current of 100 A.

The production of highest brightness electron beams in the photo-injector requires that a temporally-flat, picosecond laser source be used to drive the photo-cathode. The laser system driving the photocathode will therefore employ wide-band Ti:Sa technologies with the oscillator pulse train locked to the RF. The Ti:Sa mode locked oscillator and amplifiers able to produce the requested energy per pulse (500 μJ at 266 nm) are commercially available. To obtain the desired time pulse shape we will test the manipulation of frequency lines in the large bandwidth of Ti:Sa, in order to produce the 10 ps long flat-top shape. We plan to use a liquid crystal mask in the Fourier plane of the non-dispersive optic arrangement or a collinear acousto-optic modulator (Dazzler crystal) for linear frequency manipulation.

2 Group activity in 2003

The preparation of a Technical Design Report submitted to the Referee Review Committee has been one of the major achievements of the group in the year 2003. This work includes the optimization of the machine layout, start to end simulations and optimization of the beam working point, simulations of beam measurements (virtual experiments' program), the design of the main components of the injector, such as laser, radiofrequency, magnetic, control and vacuum systems. In addition the tender for the main components of the machine have been completed.

The experimental activity has also began with the laser pulse shaping measurements and the rf deflector cavity tests.

Memorandum of Understanding have been signed with UCLA and SLAC and collaborations through EU programs have started with DESY and other European institutions.

In the next sub-sections we discuss a restricted number of achievements. A more complete documentation about the SPARC activities, including the Preliminary Technical Design Report and the SPARC technical notes, can be found at the following dedicated web page:
http://www.lnf.infn.it/acceleratori/SPARC

2.1 Working point optimization and tolerance studies

A new optimization of the SPARC photo-injector, aiming to reduce the FEL saturation length, has been done. As the SPARC injector is the first one driving a saturating FEL without the use of a compressor scheme - either chicane or velocity bunching - the FEL requirements concerning the beam current have moved the design towards the limits of the state-of-art for pulse charge and pulse shape. In order to reach the goal with a good level of confidence we have explored a range of parameters that are not far from the previous best performances obtained in photo-injector labs. At present the best experimental results for a flat pulse with a FWHM=9 psec give an emittance of 1.2 mm-mrad at Q=1 nC and an emittance of 1.5 mm-mrad at Q=1.2 nC. Keeping in mind these results, we restricted the studies of operating point to a region of charge between 1-1.2 nC and a range of pulse lengths of 9-10 psec (FWHM). A detailed parametric investigation of these options was performed using the PARMELA code.

The results of this study led to a new working point optimization with 1.1 nC and a pulse length of 10 psec. A slice length defining the slice emittance and current of 300 μm has been considered.

The plots of figure 2 refer to the slice analysis for this case: 85% of the particles are in slices with an emittance smaller than 0.7 mm mrad, 54% have current $\geq$100 A and 70% have a current $\geq$90 A.

One of the major goals of the SPARC project is to experimentally explore the stability and robustness of the ultra-high brightness beam/SASE FEL systems.

In order to investigate the stability of the SPARC working point and to predict the most probable values of the projected and slice emittance in realistic conditions, a sensitivity study to various types of random errors in the SPARC accelerator was performed. The study was divided in two steps. In the first step the tolerances of the main tuning parameters were set with the criterium of having a maximum increase of the projected emittance of 10% respect to the nominal case (0.71 mm mrad). In the second step the errors were combined in the defined tolerance ranges and a statistical analysis has been performed in order to study the effect of the combination of errors on the projected and slice emittance and on the mismatching at the entrance of the undulator.

The reference case of 10 psec FWHM, 1.1 nC beam with a laser pulse rise time of 1 psec and a thermal emittance of 0.34 mm mrad was considered. The resulting tolerances on the different tuning parameters are listed in Table 1. It can be seen that the most critical parameters are the electric field amplitude and the spot ellipticity.

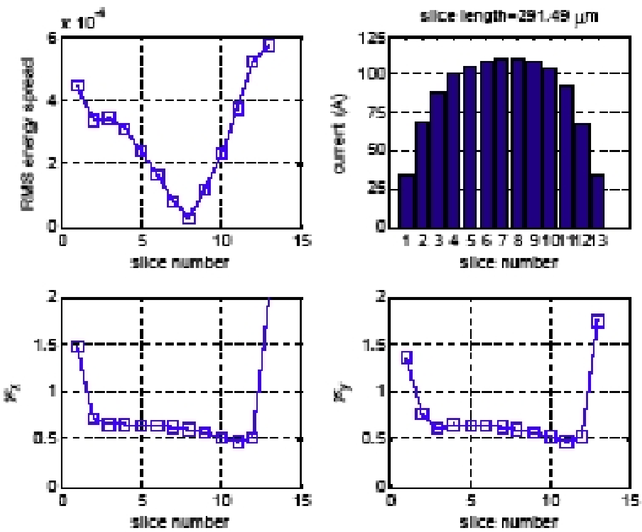

Figure 2: *Computed slice parameters for Q=1.1 nC, τ=10 psec.*

Table 1: *Minimum variation of the single parameters value for a 10% emittance increase.*

Phase jitter	$\pm 3°$
Charge fluctuation	+ 10%
Gun magnetic field	*pm* 0.4 %
Gun electric field	*pm* 0.5 %
Spot radius dimension	*pm* 10 %
Spot ellipticity	3.5 % (xmax/ymax=1.035)

One hundred PARMELA simulations runs have been performed, each with errors set randomly within the tolerance limits. In particular PARMELA was interfaced with a MATLAB-based program that accepts as input the limits of variation of the single parameters and generates a number of output files in which the six parameters of our interest are varied randomly in the pre-defined ranges according to the sampling technique of the 'latin hypercube' (as this algorithm is implemented in MATLAB statistical toolbox).

The results of the simulations were used to construct the curve plotted in Fig. 3, that gives the probability to obtain an emittance greater or equal than the corresponding value on the abscissa: for example, the probability to get a normalized projected emittance ≥ 1 mm mrad is only around 10%.

Concerning the slice emittance, in the 100 simulations it does not exceed 0.9 mm-mrad for the 9 central slices out of 13 slices.

2.2 Manipulation of the pulse energy and distribution in time

The need to minimize nonlinearities in the space charge field of the electron bunch, in particular during the early stages of acceleration from the photo-cathode surface, leads to a request for shaping the time profile of the laser pulse as it strikes the photo-cathode. The required shape is

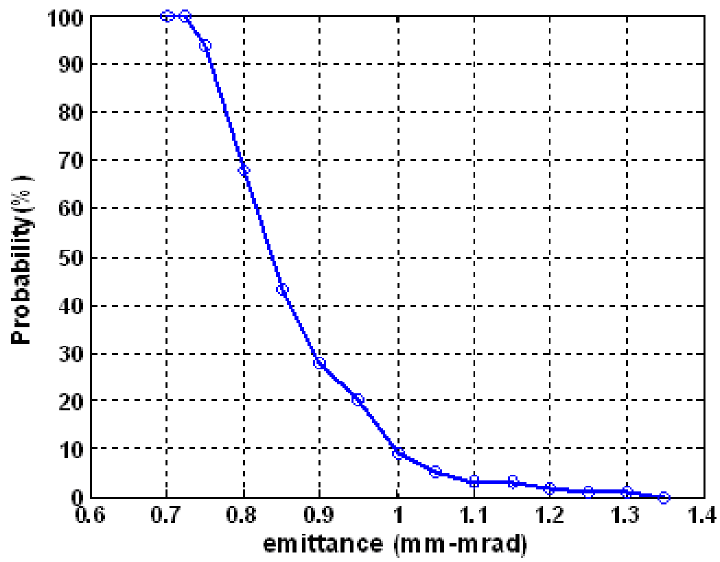

Figure 3: *Probability vs emittance over 100 simulations.*

a uniform intensity distribution in time, often called a flat-top time distribution. Beam dynamics simulations show that flat-top profile should exhibit very sharp edges in the head and tail of the pulse: the associated rise times must be at least shorter than 1 ps, with 0.5 ps being a desirable optimum value.

In collaboration with the Milano Politecnico ultrafast laser laboratory, we have conducted a series of tests to demonstrate the pulse shaping with the Dazzler crystal. The preliminary results are of great interest to the SPARC laser pulse shaper design.

The Dazzler crystal has been placed near a mirror and the optical laser pulse sent through the crystal for two passes, as seen in Fig. 4. This was prompted by the fact that the Dazzler can introduce a stretching only up to 6 ps in a single pass, a limitation caused by the length of the crystal. The obtained time intensity was measured by sampling the flat top pulse with the 20 fs reference pulses, delayed varying the optical path length by a translation stage with 100 nm resolution. The very short reference pulse assures a very precise measurement of the shaped pulse. The shaped and unshaped pulses overlapped in a BBO non-linear crystal, producing a frequency-doubled pulse proportional to the shaped pulse intensity. To improve the signal to noise ratio we used a light chopper at 472 Hz and a lock-in amplifier.

An interferometric filter was used to reduce the bandwidth of the incoming pulse. In fact it turned out that the optimal input pulse for the acoustic-optics crystal should have 10 nm bandwidth. For larger bandwidth optical pulses the Dazzler crystal shows a reduction of the spectral resolution.

The measurements indicated that the acoustic-optics crystal could produce pulses with duration up to 12 ps. Figure 5 reports the measurement of shaped intensity profiles that approach the required pulse for the SPARC photo-injector.

As shown in the plot, the pulse rise and fall time is less than 0.7 ps and the peak-to-peak ripple is less than 20% and the pulse duration is about 11 ps FWHM. These preliminary results are very promising for producing the flat-top time profile required in the SPARC photo-injector.

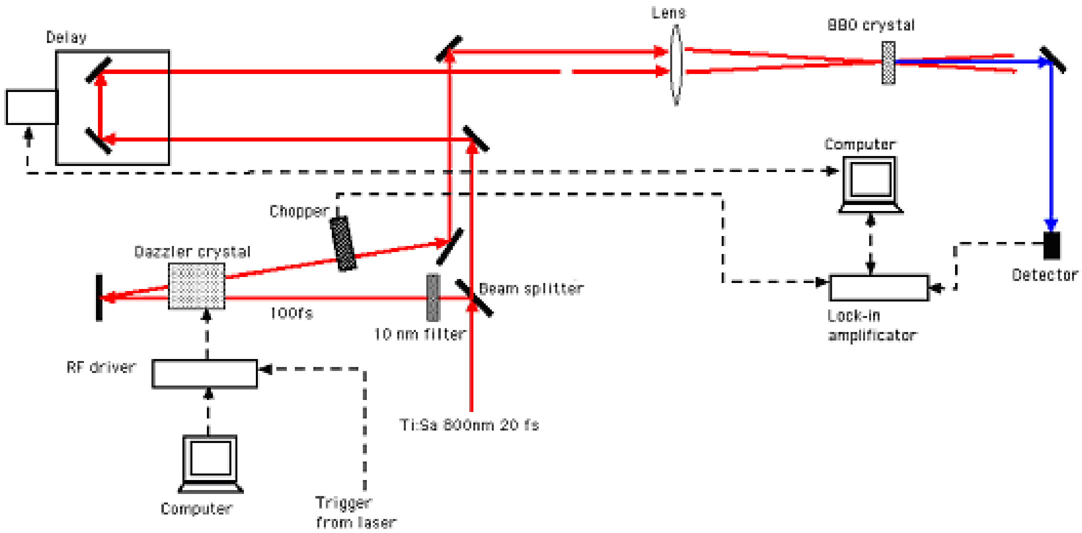

Figure 4: *Experimental setup used for pulse shaping with the acousto-optic crystal.*

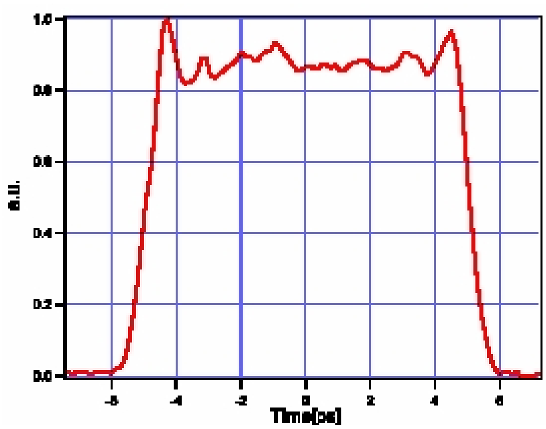

Figure 5: *Cross-correlation measurement of a 12 ps shaped pulse.*

2.3 Design of a movable emittance meter

Preliminary studies of the SPARC RF gun are planned to accurately analyse and optimize the emittance compensation scheme by measuring the beam emittance evolution downstream of the RF gun with an appropriate diagnostic system. Since with a space charge dominated beam the quad-scan can not be performed a 1D pepper-pot device will be used instead. A mask with narrow slits will be mounted on a movable support, spanning a 1.5 m region to measure the emittance at several positions and reconstruct its behaviour in the section following the gun (see figure 6).

Numerical simulations of the measurement process, mainly based on PARMELA and TREDI, have been done to estimate the achievable accuracy and to optimize the experimental setup, see

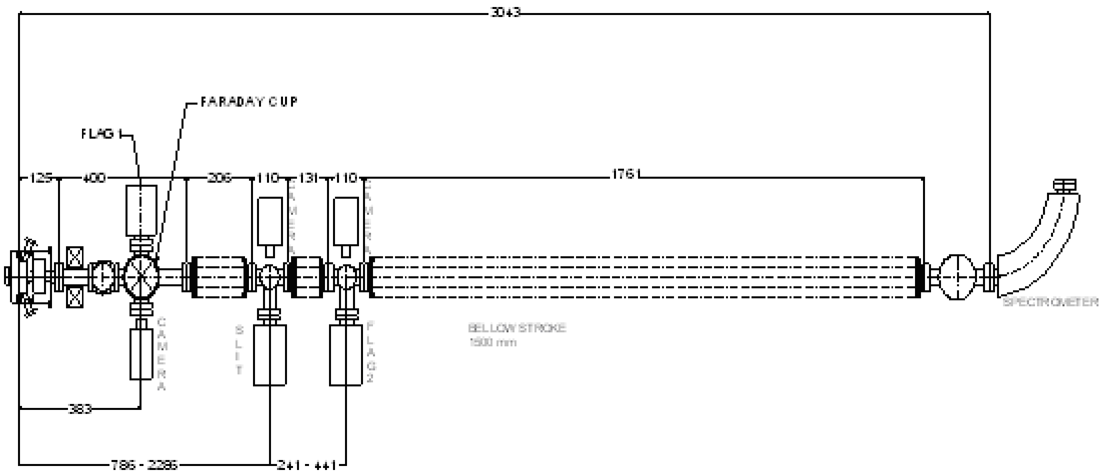

Figure 6: *Movable system for emittance measurement.*

fig. 7. Wake field effects induced by the beam propagation through the long bellows have been also investigated with HOMDYN. Based on these simulations the design of the apparatus, called emittance-meter, has been realized and is under construction at LNF.

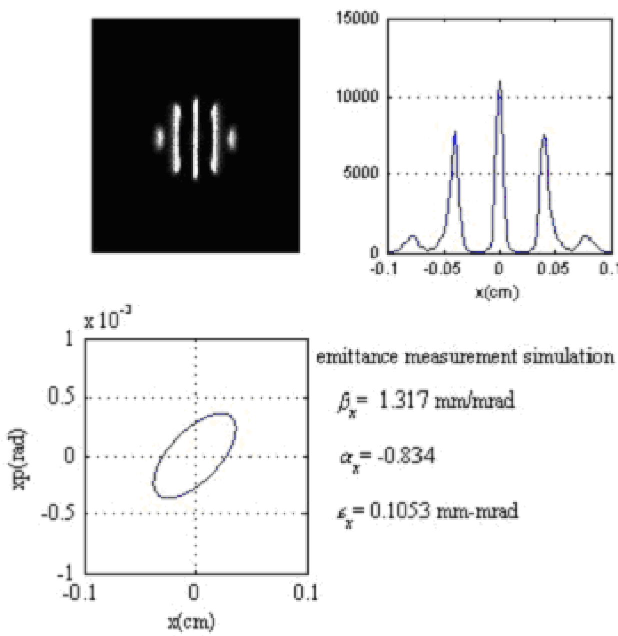

Figure 7: *Output of the MATLAB program analysing the PARMELA distribution on the output screen (L=20 cm).*

2.4 Rf deflector design and prototype tests

The characterization of the longitudinal and transverse phase space of the beam provided by the SPARC photo-injector at 150 MeV is a crucial point to establish the performance quality of the photo-injector itself. By means of an RF deflector and a dispersive system, the six dimensional beam phase space can be analyzed.

An aluminum cold test model of the 5-cell π-mode RF deflector has been manufactured to LNF specifications and tested by LNF and the University of Rome 'La Sapienza' by members of the SPARC team. A photograph of the device during its testing is shown in Fig. 8.

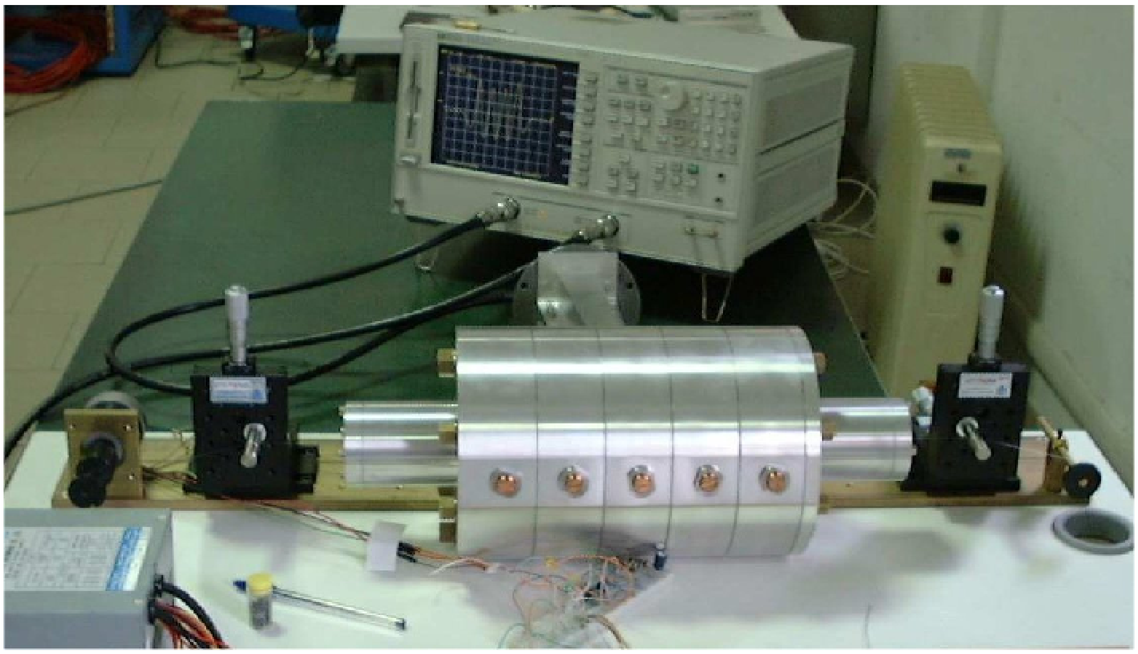

Figure 8: *Aluminum cold test model of 5-cell rf deflector.*

The RF deflector was tested for mode frequencies and for field flatness of the various modes. The S11 frequency spectrum for the device shows that the predicted π-mode frequency is directly at the design value of 2856 MHz. The results of the bead pull tests on the field profile of the RF deflector π-mode reveal a good level of magnetic field flatness.

3 Publications

1. M. Biagini, et al. : 'Beam Dynamics Studies for the SPARC Project', presented at PAC2003, 12-16/5/2003, Portland, Oregon, USA.

2. D. Alesini et al.: 'The SPARC Project: A High Brightness Electron Beam Source at LNF to Drive a SASE-FEL Experiment', presented at PAC2003, 12-16/5/2003, Portland, Oregon, USA.

3. M. Biagini et al.: 'Start to End Simulations for the SPARX Proposal', presented at PAC2003, 12-16/5/2003, Portland, Oregon, USA.

4. C. Limborg et al.: 'Code Comparison for Simulations of Photo-Injectors', presented at PAC2003, 12-16/5/2003, Portland, Oregon, USA.

5. D. Alesini et al.: 'Study of a Low Impedance Beam Position Monitor for Short Bunches', presented at PAC2003, 12-16/5/2003, Portland, Oregon, USA.

6. D.H. Dowell et al.: 'A Two-Frequency RF Photocathode Gun', presented at PAC2003, 12-16/5/2003, Portland, Oregon, USA.

7. H. Iijima et al.: 'Experimental verification of velocity bunching at the S-band photoinjector and Linac', Proc. of FEL Conference 2003, 8-12/9/2003, Tsukuba, Japan.

8. D. Alesini et al.: 'Status of the SPARC project', Proc. of FEL Conference 2003, 8-12/9/2003, Tsukuba, Japan.

9. D. Alesini et al.: 'Status of the SPARC project and Perspectives of Advanced Acceleration @ LNF', presented at ICFA Workshop on 'Laser and Plasma Accelerators', 29-9/3-10/2003, PortoVenere, Italy.

10. L. Serafini: 'Issues of Matching Extreme/Bright Beams into Transport Channels and/or Post-Accelerators', presented at ICFA Workshop on 'Laser and Plasma Accelerators', 29-9/3-10/2003, PortoVenere, Italy.

11. D. Alesini et al.: 'The SPARC/X Projects @ LNF', Proc. of Conference on 'Ultra-Short High-Energy Radiation and Matter', October 2003, Varenna, Italy.

12. L. Serafini et al.: 'Laser Systems for High Brightness Electron Beams', presented at ITARUS-2003, 5th Italian Russian Laser Symposium, Mosca, October 2003.

13. D. Alesini et al., 'Status of the Beam Dynamics Studies for the SPARC Project', BD-03/001, 08/04/2003.

14. M. Ferrario, V. Fusco, M. Megliorati: 'Electric Field for a Uniformly Charged Cylindrical Bunch with Elliptical Cross Section', BD-03/002, 29/04/2003.

15. M. Ferrario, et al. : 'Recent Advances and Novel Ideas for High Brightness Electron Beam Production Based on Photo-Injectors', BD-03/003, 05/05/2003.

16. J. Rosenzweig et al.: 'Re-Examination of the Working Point for the SPARC Injector and SASE FEL', BD-03/004, 20/06/2003.

17. M. Boscolo, et al., 'Status of the Low-Energy Emittance Measurement Simulations for the SPARC Project', BD-03/005, 28/07/2003.

18. D. Alesini, C. Vaccarezza: 'Longitudinal and Transverse Phase Space Characterization', BD-03/006, 25/11/2003.

19. M. Biagini et al., 'Sparc Injector Working Point Optimization', BD-03/007, 25/11/2003.

20. C. Ronsivalle: 'Study of the Tolerances and Sensitivity to Errors in the SPARC High Brightness Photo-Injector', BD-03/008, 03/12/2003.

21. A. Bacci, M. Migliorati, L. Palumbo, B. Spataro: 'An X-Band Structure for a Longitudinal Emittance Correction at SPARC', RF-03/001, 06/05/2003, LNF-03/008(R).

22. D. Alesini, A. Bacci, M. Migliorati, A. Mostacci, L. Palumbo, B. Spataro: 'Studies on a Bi-Periodic X-Band Structure for SPARC', RF-03/002, 25/08/2003, LNF-03-013(R).

YEAR 2003 FRASCATI PUBLICATIONS

Available at www.lnf.infn.it

1 – Frascati Physics Series

Volume XXXII
19th International Conference on x–ray and Inner–Shell Processes
A. Bianconi, A. Marcelli, N.L. Saini
Università di Roma La Sapienza June 24–28, 2002
ISBN 88–86409–39–07

Volume XXXI
FrontierScience 2002
Charm, Beauty and CP, First International Workshop on FrontierScience
L. Benussi, R. de Sangro, F.L. Fabbri, P. Valente
Frascati, October 6–11 2002
ISBN 88–86409–37–0

Volume XXX – Special Issue
Les Rencontres de Physique de la Vallée d'Aoste –
Results and Perspectives in Particle Physics
M. Greco
La Thuile, Aosta Valley, March 9–15, 2003
ISBN 88–86409–39–9

Volume XXIX – Suppl.
Workshop on Radiation Dosimetry: Basic Technologies,
Medical Applications, Environmental Applications
Ed. A. Zanini
Rome (Italy), February 5–6, 2002
ISBN 88–86409–36–2

2 – LNF–Frascati Reports

LNF–03–01 (P)
A. Cardelli, G. Cibin, M. Benfatto, S. Della Longa, M.F. Brigatti, A. Marcelli
A crystal chemical investigation of Cr substitution in muscovite by XANES spectroscopy
Submitted to Physics and Chemistry of Minerals

LNF–03–02 (IR)
Irina Titkova, Mikhail Zobov, Sultan Dabagov
Syncrotron Radiation from DAΦNE Bending Magnet and Wiggler

LNF–03–03 (P)
G. Mazzitelli, P. Valente
Commissioning of the DAΦNE Beam Test Facility
Submitted to Nucl. Instr. & Meth. A

LNF–03–04 (NT)
A. Marcelli (Coordinator), P. Calvani, P. Roy, D. Moss, L. Degiorgi, M.J. Tobin, U. Schade, K. Hinrichs, A. Mondini, L. Quaroni, A. Cupane, G. Onori, E. Burattini, M. Chesters, G. Menestrina, E. Goormaghtigh, P. Mariani, J. Breton, D. Naumann, M. Manfait, J. Susini, W.E. Smith, S.M. Doglia, M. Colombatti, B. Lendl, A. Barth, I. Anastassopoulou, M. Lankosz, P. Rich, S. Fisher
Biological Applications of Synchrotron Infrared Spectroscopy in Europe – BASIE

LNF–03–05 (P)
P. Migliozzi, F. Terranova
Next Generation Long Baseline Experiments on the Path to Leptonic CP Violation
Submitted to Physics Letters B

LNF–03–06 (P)
M. Ferrario, M. Boscolo, V. Fusco, C. Vaccarezza,C. Ronsivalle, J. B. Rosenzweig, L. Serafini
Recent Advances and Novel Ideas for High Brightness Electron Beam Production Based on Photo–Injectors

LNF–03–07 (IR)
Alessandro Balla, Matteo Beretta, Federico Bertino, Maurizio Carletti, Paolo Ciambrone, Giovanni Corradi, Giulietto Felici, Maurizio Gatta, Giovanni Paoluzzi, Giuseppe Papalino, Massimo Santoni
LHCb Muon Off–Detector Eectronics: The IB System

LNF–03–08 (R)
A. Bacci, M. Migliorati, L. Palumbo, B. Spataro
An X–Band Structure For a Longitudinal Emittance Correction at SPARC

LNF–03–09 (P)
S. Bianco, F.L.Fabbri, D.Benson, I.Bigi
A Cicerone for the Physics of Charm
Published on La Rivista del Nuovo Cimento Vol. 26, Serie 4 n. 7–8 (2003)

LNF–03–10 (IR)
AA.VV.
Annnual Report 2002

LNF–03–11 (Thesis)
D. Alesini
Beam Control and Manipulation with Microwave Devices in Particle Accelerators
(Tesi di Dottorato)

LNF–03–12 (P)
Accelerator Division
Papers presented at PAC 2003
Presented at the:2003 Particle Accelerator Conference (PAC 2003), Portland, Oregon, May 12–16, 2003

LNF–03–13 (R)
D. Alesini, A. Bacci, M. Migliorati, A. Mostacci, L. Palumbo and B. Spataro
Studies on a Bi–periodic X–band Structure for SPARC

LNF–03–14 (P)
B. Spataro, D. Brandt, D. Li, M. Migliorati, A.Mostacci, L.Palumbo, F. Ruggiero, L.Vos
On Trapped Modes in the LHC Recombination Chambers: Numerical and Experimental Results
Published on Nuclear Instruments and Methods in Physics Research A 517 (2004) 19–27

LNF–03–15 (IR)
L. Benussi et al.
Results of Long–Term Position Monitoring by Means of Fiber Bragg Grating Sensors for the BTeV Detector

LNF–03–16 (P)
O.V. Mikhin, S.B. Dabagov, V.D. Gelver, A.V. Priladyshev
Novel High Flux X–Ray Source: A Laboratory Synchrotron
Submitted to Applied Physics Letters

LNF–03–17(NT)
Franco Brasolin, Angelo Veloce
Test di Configurabilta' e Prestazioni del Router Juniper

LNF–03–18 (P)
P.L. Frabetti, S. Bianco et al.
On the Narrow Dip Structure at 1.9~GeV/c^2 in Diffractive Photoproduction
Submitted to Phys. Lett. B

LNF–03–19 (P)
F. Terranova
Peak Finding Through Scan Statistics
Submitted to Nuclear Instruments and Methods in Physics Research Sec. A

LNF–03/20 (P)
R.M. Godbole A. Grau G. Pancheri and Y.N. Srivastava
Photon Total Cross–Sections
Talk presented by G. Pancheri at PHOTON–2003, International Meeting on Structure and Interactions of the Photon Frascati, Italy, April 7–11, 2003

LNF–03/21 (P)
F. Celani, A. Spallone, E. Righi, G. Trenta, C. Catena, G. D'agostaro, P. Quercia, V. Andreassi, P. Marini, V. Di Stefano, M. Nakamura, A. Mancini, P. G. Sona, F. Fontana, L. Gamberale, D. Garbelli, F. Falcioni, M. Marchesini, E. Novaro, U. Mastromatteo
Thermal and Isotopic Anomalies when Pd Cathodes are Electrolyzed in Electrolytes Containing Th–Hg Salts Dissolved at Micromolar Concentration in C2H5OD/D2O Mixtures
Presented at the 10th International Conference on Cold Fusion, 2003, Cambridge

LNF–03/22 (P)
J. M. Link, P. M. Yager, J. C. Anjos, I. Bediaga, C. Gobel, A. A. Machado, J. Magnin, A. Massafferri, J. M. de Miranda I. M. Pepe E. Polycarpo, A. C. dos Reis, S. Carrillo, E. Casimiro, E. Cuautle A. Sanchez–Hernandez, C. Uribe, F. Vazque, L. Agostino, L. Cinquini, J. P. Cumalat, B. O'Reilly, I. Segoni, M. Wahl, J. N. Butler, H. W. K. Cheung, G. Chiodini, I. Gaines, P. H. Garbincius, L. A. Garren, E. Gottschalk, P. H. Kasper, A. E. Kreymer, R. Kutschke, M. Wang, L. Benussi, M. Bertani, S. Bianco, F. L. Fabbri, A. Zallo, M. Reyes, C. Cawlfield, D. Y. Kim, A. Rahimi, J. Wiss, R. Gardner, A. Kryemadhi, Y. S. Chung, J. S. Kang, B. R. Ko, J. W. Kwak, K. B. Lee, K. Cho, H. Park, G. Alimonti, S. Barberis, M. Boschini, A. Cerutti, P. D'Angelo, M. Di Corato, P. Dini, L. Edera, S. Erba, M. Giammarchi P. Inzani, F. Leveraro, S. Malvezzi, D. Menasce, M. Mezzadri, L. Moroni, D. Pedrini, C. Pontoglio, F. Prelz, M. Rovere, S. Sala, T. F. Davenport III, V. Arena, G. Boca, G. Bonomi, G. Gianini, G. Liguori, M. M. Merlo, D. Pantea, D. Lopes Pegna, S. P. Ratti, C. Riccardi, P. Vitulo, H. Hernandez, A. M. Lopez, E. Luiggi, H. Mendez, A. Paris, J. E. Ramirez, Y. Zhang, J. R. Wilson, T. Handler, R. Mitchell, D. Engh, M. Hosack, W. E. Johns, M. Nehring, P. D. Sheldon, K. Stenson, E. W. Vaandering, M. Webster, M. Sheaff
Measurement of Masses and Widths of Excited Charm Mesons D_2 and Evidence for Broad States
Accepted by Phys. Lett. B

LNF–03/23(P)
M. Agnello, G. Beer, L. Benussi, M. Bertani, S. Bianco, E. Botta, T. Bressani, L. Busso, D. Calvo, P. Camerini, P. Cerello, B. Dalena, F. De Mori, G. D'Erasmo, D. Di Santo, F. L. Fabbri, D. Faso, A. Feliciello, A. Filippi, V. Filippini, E.M. Fiore, H. Fujioka, P. Gianotti, N. Grion, A. Krasnoperov, V. Lucherini, S. Marcello, T. Maruta, N. Mirfakhrai, O. Morra, A. Olin, E. Pace, M. Palomba, A. Pantaleo, A. Panzarasa, V. Paticchio, S. Piano, F. Pompili, R. Rui, G. Simonetti, H. So, S. Tomassini, R. Wheadon, A. Zenoni (FINUDA Collaboration)
First results from the FINUDA experiment at DAΦNE
Proc. VIII International Conference on Hypernuclear & Strange Particle Physics, Jefferson Lab., Newport News, Virginia, October 14–18, 2003

3 – INFN Reports

INFN/AE–03/01
Elvio Di Salvo
The Transversity Function and Doule Spin Azimuthal Asymmetry in Semi–Inclusive Pion Leptoproduction

INFN/AE–03/02
Ernesto Amato, Lucrezia Auditore, Renato C. Barnà,Vincenzo D'Amico, Domenico De Pasquale, Antonio Italiano, Antonio Trifirò, Marina Trimarchi
Response of an Underwater Cherenkov Detector to Supernova Neutrinos

INFN/AE–03/03
Osvaldo Catalano, Piero Vallania, Didier Lebrun, Patrick Stassi, Mario Pimenta, Catarina Espirito Santo
ULTRA –Uv Light Transmission and Reflection in the Atmosphere Technical Report. A Supporting Experiment for the EUSO Project

INFN/AE–03/04
C. Braggio, G. Bressi, G. Carugno, C. Del Noce, V. Dodonov, A. Lombardi, A. Palmieri, G. Ruoso, D. Zanello
MIR, a Feasibility Study for a Measurement of the Dynamical Casimir Effect

INFN/AE–03/05
G. Collazuol, A. Guglielmi
Monte Carlo Simulation of the SPS WANF Neutrino Flux

INFN/AE–03/06
G. Barichello, A. De Min, D. Gibin, A. Guglielmi, M. Laveder, A. Menegolli, M. Mezzetto
The HARP TOF–WALL Electronics and Trigger Logic

INFN/BE–03/01
M. Alderighi, A. Anzalone, L. Auditore, N. Arena, R. Bassini, C. Boiano, S. Brambilla, G. Cardella, S. Cavallaro, M. D'Andrea, E. DeFilippo, E. Geraci, D. Ghilardi, C. Gilardi, F. Giustolisi, A. Grzeszczuk, P. Guazzoni, E. Laguidara, G. Lanzanò, G. Lanzalone, D. Nicotra, P. Opichal, T. Paduszynski, A. Pagano, M. Papa, S. Pirrone, G. Politi, F. Porto, E. Rosato, S. Russof, G. Saccà, M. Sassi, G. Sechi, A. Trifirò, M. Trimarchi, S. Urso, M. Vigilante, L. Zetta
Preliminary Tests of Digital Pulse Shape Acquisition from Chimera CsI(Tl) Scintillators

INFN/BE–03/02
Simone Cialdi and Ilario Boscolo
A Laser Pulse Shaper for the Low Emittance Radiofrequency SPARC Electron Gun

INFN/BE–03/03
Simone Cialdi, Ilario Boscolo Alessandro Flacco
Features of a Phase–only Shaper Relative to a Long Rectangular Ultraviolet Pulse

INFN/FM–03/01
D. Doria, A. Lorusso and V. Nassisi
Movable Faraday Cup Measurements for Ion Beams Characterization

INFN/TC–03/01
E. Cisbani, S. Colilli, F. Cusanno, R. Fratoni, F. Garibaldi, F. Giuliani, M. Gricia, M. Iodice, M. Lucentini, A. Mostarda, L. Pierangeli, F. Santavenere, P. Veneroni
Sistema di Deposizione di CsI in Camera di Evaporazione ad Alto Vuoto per Fotoconvertitori di un Rivelatore RICH

INFN/TC–03/02
Flavia Groppi, Claudio Birattari, Mauro Bonardi, Luigi Gini, Mario Gallorini, Enrico Rizzio, Enrico Sabbioni, Enzo Menapace, Dolores Arginelli, Alberto Ghioni and Hae Song Mainardi
Cyclotron Production of High Specific Activity Radiochemical Forms of Vanadium, Manganese and Tallium for Metallo–Toxicological Studies

INFN/TC–03/03
M. Bozzo, S. Cuneo, K. Eggert, M. Macrì, M. Oriunno, R. Puppo
Preliminary Design of TOTEM T1 Telescopes Mechanical Support Structures

INFN/TC–03/04
Domenico Diacono
Installazione, Configurazione e Test di un Cluster di PC per Calcolo Parallelo e Seriale con Software Open–Source

INFN/TC–03/05
F. Broggi
Fault Considerations and Effects of Shorts in the Barrel Toroid Coil System

INFN/TC–03/06
G. Castiglioni, M. Castoldi, R. Cereseto, S. Cuneo, F. Mora, R. Puppo, L. Vigiani
Design and Manufacturing of Composite Spherical Mirrors for the GRAAL Cerenkov Particle Detector

INFN/TC–03/07
Stefano Zani, Riccardo Veraldi, Franco Brasolin, Angelo Veloce, Mario Masciarelli, Claudio Soprano, Fulvia Costa
Nota tecnica sul possibile utilizzo di Firewall nell' INFN

INFN/TC–03/08

S. Gammino, G. Ciavola, L. Torrisi, L. Andò, L. Celona, M. Maggiore, S. Manciagli, M. Presti, C. Percolla, E. Calzona, V. Vinciguerra, S. Dobrescu, L. Schacter, A. Drentje, K. Stiebing

Electron Donors And Their Role On The Performance of Microwave Discharge and Electron Cyclotron Resonance Ion Sources

INFN/TC–03/09

Paolo Pierini, Editor – Contributors: D. Barni, P. Michelato, L. Monaco, M. Novati, R. Paulon, P. Pierini, D. Sertore (INFN–Milano–LAS), C. Pagani (University of Milano and INFN–Milano–LASA, R. Ferdinand, H. Safa, S. Palanque (CEA/Saclay), J. L. Biarrotte, C. Commeaux, T. Junquera, A. C. Mueller, A. Tkatchenko (CNRS/Orsay), L. Burgazzi (ENEA), Y. Jongen, D. Vandeplassche (IBA)

Potential for Reliability Improvement and Cost Optimazion of LINAC and Cyclotron Accelerators

Contractual deliverable D57 of EC contract FIKW–CT–2001–00179 (FP5), subjected to final approval by the Contract Consortium

INFN/TC–03/10

V. Nasssi, F. Belloni, D. Doria, A. Lorusso

A Voltage Generator by Trasmission Lines

INFN/TC–03/11

V. Nassisi, F. Belloni, D. Doria, A. Lorusso

Theory and Realization of a New CurrentPulse Compression Circuit

INFN/TC–03/12

Ricci Pier Paolo per TIER1 Staff

Utilizzo del Software CASTOR al TIER1 CNAF

INFN/TC–03/13

M. Ameri, F. Cadoux, R. Cereseto, G. Corti, S. Cuneo, P. Musico, A. Petrolini, P. Pollovio, F. Pratolongo, F. Siccardi, A. Vinci

R&D Mechanical Studies of the Photon Detector Microcells and Modules for the EUSO Experiment

INFN/TC–03/14

C. Arnaboldi, A.Fascilla, Mark W. Lund, G.Pessina

The Study of the Noise of Silicon JFET Transistors in a Wide Temperature Range

INFN/TC–03/15

Daniela Bortolotti, Paolo Mazzanti, Franco Semeria

PROGETTO CONDOR: Installazione Automatica del Software

INFN/TC–03/16

L. Auditore, R.C. Barnà, D. De Pasquale, A. Italiano, A. Trifirò, M. Trimarchi

The 5 MeV Electron Linac for Radiation Processing in Messina

INFN/TC–03/17
Ombretta Pinazza, Alessandro Brunengo, Enrico M.V. Fasanelli, Enrico Mazzoni, Claudio Soprano, Riccardo Veraldi, Stefano Zan
Studio Preliminare di VPN per l'INFN

INFN/TC–03/18
Peter Couvares, Paolo Mazzanti, Daniela Bortolotti, Franco Semeria
Condor and the Bologna Batch System

INFN/TC–03/19
Ricci Pier Paolo, Stefano Zani
Sistemi Storage su Disco Utilizzati al TIER1 CNAF

Glossary

These are the acronyms used in each status report to describe personnel qualifications other than Staff Physicist:

Art. 15	Term Contract (Technician)
Art. 23	Term Contract (Scientist)
Ass.	Associated Scientist
Ass. Ric.	Research Associate
Bors.	Fellowship holder
Bors. PD	Post–Doc Fellow
Bors. UE	European Community Fellow
Dott.	Graduate Student
Laur.	Undergraduate Student
Osp.	Guest Scientist
Perfez.	Post–Laurea Student
Resp.	Local Spokesperson
Resp. Naz.	National Spokesperson
Specializ.	Post–Laurea Student
Tecn.	Technician